THE MOBILITY OF PETROLEUM HYDROCARBONS IN ATHABASCA OIL SANDS TAILINGS

A Thesis Submitted to the College of

Graduate Studies and Research

In Partial Fulfillment of the Requirements

For the Degree of Master of Science

In the Department of Civil and Geological Engineering

University of Saskatchewan

Saskatoon

By

Heather Anne Brickner

PERMISSION TO USE

In presenting this thesis in partial fulfilment of the requirements for a Postgraduate degree from the University of Saskatchewan, I agree that the Libraries of this University may make it freely available for inspection. I further agree that permission for copying of this thesis in any manner, in whole or in part, for scholarly purposes may be granted by the professor or professors who supervised my thesis work or, in their absence, by the Head of the Department or the Dean of the College in which my thesis work was done. It is understood that any copying or publication or use of this thesis or parts thereof for financial gain shall not be allowed without my written permission. It is also understood that due recognition shall be given to me and to the University of Saskatchewan in any scholarly use which may be made of any material in my thesis.

Requests for permission to copy or to make other use of material in this thesis in whole or part should be addressed to:

Head of the Department of Civil Engineering

University of Saskatchewan

Saskatoon, Saskatchewan, Canada, S7N 5A9

ABSTRACT

Several oil sands tailings from Suncor Energy Inc. were analysed with respect to the mobility and solubility of the petroleum hydrocarbon (PHC) contaminants. At sites where oil sands tailings materials have been disposed of and are covered with a growing medium, the PHCs from the tailings may slowly migrate into the reclamation cover, increasing their availability to the plants in the cover system, which could be detrimental to the development and establishment of the plant cover system.

This study characterized the PHC content of the tailings and quantified the desorption and diffusion coefficients for F2 and F3 fraction PHCs. All tailings materials collected from Suncor were characterized for initial PHC content. Desorption coefficients were experimentally determined using batch tests for 9 tailings materials (MFT, LG MFT, PT MFT, Tailings Sand, P4 UB Surface, P4 UB Auger, 2:1 CT, 4:1 CT and 6:1 CT). The experimental results from the batch tests were fitted to a Langmuir hyperbolic isotherm model. Diffusion coefficients were determined by fitting the experimental results from a radial diffusion 1-dimensional experiment to a Finite Difference Model. Diffusion coefficients for F2 and F3 Fraction PHCs were developed for 7 tailings materials (MFT, LG MFT, PT MFT, Tailings Sand, 2:1 CT, 4:1 CT and 6:1 CT). The diffusion coefficients (D*) and the Langmuir desorption constants (Ŭ and ɓ) developed from these experiments are included in Table A.1 below.

Table A.1: Desorption and diffusion coefficients of F2 and F3 fraction PHC from selected Suncor oil sands tailings materials.

Tailings Material	F2 Diffusion Coefficient D* ($x10^{-6}$) (cm^2/s)	F3 Diffusion Coefficient D* ($x10^{-6}$) (cm^2/s)	F2 Fraction Desorption Constants		F3 Fraction Desorption Constants	
			Ŭ (L/mg)	ƀ (mg/kg)	Ŭ (L/mg)	ƀ (mg/kg)
2:1 SFR CT	0.025	0.042	136	4010	114	18700
4:1 SFR CT	0.170	0.220	4210	3040	32.8	12400
6:1 SFR CT	0.490	0.670	115	1530	81.4	6540
MFT	0.022	0.020	62.1	10250	285	44600
LG MFT	1.10	0.530	72.3	5330	36.5	20200
PT MFT	0.405	0.330	50.7	5320	92.8	20000
P4 UB Surface	n/a	n/a	689	952	288	5820
P4 UB Auger	n/a	n/a	935	736	11800	3830
Tailings Sand	0.130	0.045	204000	35.8	398	519

The desorption coefficients resulting from this study are similar to those reported for the desorption of asphaltene, which is one of the components in oil sands tailings. The Langmuir isotherm model was found to be the best fit for the experimental desorption data; the Langmuir isotherm model is commonly used in sorption isotherms of organic chemicals.

The results of the radial diffusion experiments agree with diffusion rates found by other researchers in similar porous media. More research may be needed to verify both of these preliminary results for the desorptive and diffusive transport of F2 and F3 PHC fractions in tailings. Tailings composition will continue to change as new technologies for fines settling and bitumen extraction are developed. The diffusion of PHCs from these new materials will need to be examined as it is probable that these changes will affect the transport and mobility of the contaminants.

ACKNOWLEDGMENT S

I would like to thank my supervisor Dr. Ian Fleming for his help and support throughout my graduate studies and the completion of this thesis. I would also like to express my thanks to the committee members, Dr. Lee Barbour, Dr. Malcolm Reeves and Dr. Won Jae Chang.

I would like to thank Suncor Energy Inc. for providing the funding for this project, and to Christine Daly at Suncor for her help and support in completing this research.

I would also like to thank Dr. John Headley and Kerry Peru at the National Hydrologic Research Centre (NHRC), for their help and suggestions; a special thank you to Dr. Jinglong Du for his help with laboratory work, hydrocarbon extractions and gas chromatography results at NHRC.

Thanks also goes to Doug Fisher in the Environment Lab for his help with the analytical work I completed at the University of Saskatchewan. I would also like to acknowledge the encouragement and support I received from Stephen P. West and Jay Cooper.

To my parents, grandparents and siblings, thanks for listening when my husband was tired of hearing about my thesis; your love and support throughout my life have helped me get where I am today (a special thanks to my sister for all the math help!). Lastly, and perhaps most importantly, I would like to thank my husband Clint, who has always been supportive, encouraging, and especially patient in this long journey.

TABLE OF CONTENTS

PERMISSION TO USE i
ABSTRACT ii
ACKNOWLEDGMENTS iv
LIST OF TABLES ix
LIST OF FIGURES x
LIST OF ABBREVIATIONS xiv
1 INTRODUCTION 1
1.1 Background 1
1.2 Athabasca Oil Sands 2
1.3 Research Objective 4
1.4 Scope 5
2 LITERATURE REVIEW 1
2.1 Petroleum Hydrocarbons 1
2.1.1 Chemical Structure 3
2.1.2 PHC Composition in the Oil Sands 5
2.2 Contaminant Transport 6
2.3 Sorption Theory 8
2.4 Sorption Isotherms 10
2.4.1 Linear Sorption Isotherm 10
2.4.2 Langmuir Sorption Isotherm 11
2.4.3 Freundlich Sorption Isotherm 13
2.5 Sorption of Organics 14
2.5.1 Sorption Hysteresis 15
2.5.2 Sorption Kinetics 16

2.5.3 Temperature Dependence 17
2.5.4 Solids Effect 18
2.5.5 Solubility, Hydrophobicity and Cosolvency 20
2.5.6 Other Effects on Sorption of Organics 22
2.6 Laboratory Tests to Determine Sorption Coefficients 25
2.6.1 Batch Equilibrium Method 25
2.6.2 Flow-Through Methods 26
2.6.3 Diffusion Methods 27
2.7 Diffusion Theory 28
2.7.1 Fickôs First Law 30
2.7.2 Fickôs Second Law 32
2.8 Diffusion of Organics 32
2.8.1 Effect of Temperature 33
2.8.2 Effect of Saline Conditions 33
2.8.4 Straining and the Effect of Molecular Size 34
2.8.5 Other Effects on Diffusion 34
2.9 Determining Diffusion Coefficients 35
2.9.1 Column Methods 35
2.9.2 Reservoir Methods 37
2.9.3 Radial Diffusion Method 39
2.10 Summary 40
3 MATERIALS AND METHODS 41
3.1 Sample Collection 41
3.2 Description of Oil Sands Tailings 44
3.3 Characterization of Tailings 46

3.3.1 Hydrocarbon Analysis 46
3.3.2 Loss on Ignition 49
3.3.3 Water Content 50
3.3.4 Porewater Hydrocarbon Concentration 50
3.4 Characterization of Oil Sands Process Water 53
3.5 Petroleum Hydrocarbon Desorption 53
3.5.1 General Experimental Procedure, Phases 1 ï 3 55
3.5.2 Experimental Procedure, Phases 3D 60
3.5.3 Desorption Isotherm Modelling 61
3.6 Radial Diffusion of Petroleum Hydrocarbons 62
3.6.1 Experimental Procedure 64
3.6.2 Modelling Methodology 68
4 RESULTS AND DISCUSSION 71
4.1 Tailings Characterization 71
4.1.1 Petroleum Hydrocarbon Content 71
4.1.2 Loss on Ignition 74
4.1.3 Relationship between PHC Content and LOI 78
4.1.4 Solids and Water Content 80
4.2 Process Water Characterization 81
4.2.1 Basic Ionic Analysis 82
4.2.2 Petroleum Hydrocarbon Content of Process Water 85
4.3 Desorption of PHC from Oil Sands Tailings 86
4.3.1 Effect of Temperature on Desorption 88
4.3.2 Effect of Solution Mixture on Desorption 89
4.3.3 Percent PHC in Solution 92

4.3.4 Desorption Isotherms 94
4.3.5 Isotherm Summary 100
4.3.6 Solubility Limits 102
4.3.7 Desorption Isotherm Discussion 105
4.3.8 Summary 112

4.4 Diffusive Transport of PHCs in Oil Sands Tailings 113

4.4.1 Composite Tailings Diffusion Model 116
4.4.2 Mature Fine Tailings Diffusion Model 118
4.4.3 Tailings Sand Diffusion Model 120
4.4.4 Sensitivity Analysis 121
4.4.5 Diffusion Discussion 124
4.4.6 Summary 130

5 CONCLUSIONS & RECOMMENDATIONS 132

5.1 Conclusions 132

5.2 Implications for Design 136

5.3 Recommendations 137

REFERENCES 139
APPENDIX A 151
APPENDIX B 162
APPENDIX C 179
APPENDIX D 202
APPENDIX E 215

LIST OF TABLES

Table 1.1: Analysis completed for the 12 tailings materials. 7

Table 2.1: Hydrocarbon Classification (Fetter 1999) 3

Table 2.2: Effective diffusion coefficients for organic compounds through clay or clay liners 33

Table 4.1: Extractable Hydrocarbons (in mg/kg and percent of total PHC) of Athabasca Oil Sands Tailings 72

Table 4.2: Loss on ignition results for Athabasca Oil Sands Tailings at 550ºC. 76

Table 4.3: Percent difference and ratio between %PHC and average LOI 79

Table 4.4: Gravimetric Water Content, Total Water Content and Solids Content of Tailings. All results are given in percent (%). 81

Table 4.5: Ionic analysis of five Athabasca oil sands site waters: Process Water, 12m CT Pond, North Sustainability Pond and South Sustainability Pond 83

Table 4.6: Petroleum hydrocarbon concentration in Suncor mine site process water, shown by hydrocarbon fraction. 86

Table 4.7: Percent of Total F2 Fraction PHCs in Solution 93

Table 4.8: Percent of Total F3 Fraction PHCs in Solution 93

Table 4.9: Langmuir desorption constants Ŭ(binding energy constant) and ɓ (maximum ion sorption) for F2 PHC fraction of 9 oil sands tailings. 95

Table 4.10: Langmuir desorption constants Ŭ(binding energy constant) and ɓ (maximum ion sorption) for F3 PHC fraction of 9 oil sands tailings. 96

Table 4.11: Solubility values for F2 and F3 PHCs from literature 105

Table 4.12: Diffusion coefficients (cm^2/s), initial tailings porewater (PW) concentration and Root-Mean-Square-Error (RMSE) values for the F2 PHC fraction of Athabasca oil sands tailings. 115

Table 4.13: Diffusion coefficients (cm^2/s), initial tailings porewater (PW) concentration and Root-Mean-Square-Error (RMSE) values for the F3 PHC fraction of Athabasca oil sands tailings. 115

LIST OF FIGURES

Figure 1.1: The Athabasca Oil Sands in Alberta (Caughill et al. 1993) _____ 3

Figure 2.1: Examples of asphaltene molecular structure, showing the aromatic rings with alkane chains (Akbarzadeh et al. 2007). _____ 5

Figure 2.2: A diagram of the sorption process on a soil or sediment particle, adapted from Limousin et al. (2007). Scenario A shows the adsorption process, with a decrease in aqueous concentration and an increase in sorbed mass at equilibrium. Scenario B shows the desorption process in which the sorbed solute moves from the surface of the particle to the aqueous phase at equilibrium. Sorption is determined by measuring the initial and final aqueous concentration C. 9

Figure 2.3: Linear sorption isotherm, showing the straight line relationship between the aqueous solute concentration, C, versus mass of sorbed solute, S (Fetter 1999). _____ 11

Figure 2.4: Langmuir sorption isotherm, showing the mathematical relationship between S and C (Fetter 1999). _____ 12

Figure 2.5: Langmuir sorption isotherm showing the linear C/S versus C plot (Fetter 1999), from which the two sorption coefficients Ŭand ɓ can be determined. _____ 13

Figure 2.6: Freundlich sorption isotherm, showing the mathematical relationship between S and C (Fetter 1999). _____ 13

Figure 2.7: Freundlich sorption isotherm showing the log-log relationship between S and C (Fetter 1999), from which the two sorption coefficients K and N can be determined. _____ 14

Figure 2.8: Diffusion cell processes, after Shackelford and Daniel (1991): (a) self-diffusion, (b) tracer diffusion, (c) salt diffusion, and (d) counter-diffusion. _____ 29

Figure 2.9: The concept of effective length in diffusive transport through a porous media/soil, from Shackelford and Daniel (1991). _____ 30

Figure 2.10: Diffusion methods: column method set-up (a) constant source concentration, and (b) decreasing source concentration, after Shackelford (1991). _____ 36

Figure 2.11: Diffusion methods: reservoir method set-up (a) Double reservoir with decreasing source concentration and (b) Single reservoir method for both decreasing and constant source concentration, after Shackelford (1991). _____ 38

Figure 2.12: Cross section of the radial diffusion cell apparatus, adapted from van der Kamp (1996). Either the solution can have an initial concentration of zero which increases with time (with a spiked soil/sediment), or the reservoir can have an initial concentration of C_o which decreases with time. To obtain true 1-dimensional diffusion, the central reservoir should extend to the bottom of the soil. _____ 39

Figure 3.1: A small sample of tailings sands taken from one of Suncorôs stockpiles. There is very little bitumen present in the sand. _____ 43

Figure 3.2: Barley growing from some polymer-treated mature fine tailings (MFT). _____ 43

Figure 3.3: The porewater extraction squeezing apparatus set-up. Clockwise from top left are the completed design, one of the constructed cells, and the base of the cell showing the sampling ports (Pratt and Fonstad, 2011). _____ 52

Figure 3.4: Pore water extraction apparatus (Pratt and Fonstad, 2011). _____ 52

Figure 3.5: Desorption experiment flowchart, showing all phases of the procedure. _____ 55

Figure 3.6: Phase 1 desorption samples in the temperature control chamber _____ 57

Figure 3.7: Cross-sectional, profile and plan views of the radial diffusion cells. The tube diameter is 3 inches (76.2 mm). The pail used is a 4.55-litre HDPE pail with a snap-on lid.__ 65

Figure 4.1: Petroleum hydrocarbon content of Athabasca oil sands tailings; F2, F3 and F4+ fractions. _____ 74

Figure 4.2: Loss on ignition of Athabasca oil sands tailings at 550ºC._____ 76

Figure 4.3: Incremental temperature loss on ignition (in percent) for Athabasca oil sands tailings, showing both (a) average LOI values, and (b) normalized by the 550ºC LOI value of each tailings. _____ 77

Figure 4.4: Comparison of percent petroleum hydrocarbon to loss on ignition for Athabasca oil sands tailings. _____ 80

Figure 4.5: Aqueous concentration of major ions in Athabasca Oil Sands Process Water (OSPW), 12m CT Pond water (12m CT), North Sustainability Pond (NSP) water and South Sustainability Pond water (SSP). _____ 84

Figure 4.6: Comparison of Suncor minesite Process Water results from ALS laboratories and the University of Saskatchewan laboratory. Results are considered statistically the same when the slope of the dotted trendline reaches 1:1. _____ 85

Figure 4.7: Chromatogram for desorption sample A1-10 _____ 87

Figure 4.8: The effect of temperature on the desorption of petroleum hydrocarbons from Plant 4 Upper Beach auger and surface oil sands tailings samples. The results for 1ºC and 20ºC for both materials are shown. _____ 89

Figure 4.9: Three different solution mixtures for the desorption of total petroleum hydrocarbons from (a) Plant 4 Upper Beach surface oil sands tailings samples and (b) Plant 4 Upper Beach auger oil sands tailings samples. The results for undiluted process water, 1:1 process water de-ionized water mix and pure de-ionized water are shown. Error bars of plus/minus 10 percent are included. _____ 91

Figure 4.10: Percent of PHC in solution, broken down by PHC fraction._____ 92

Figure 4.11: Desorption experiment results for Plant 4 Upper Beach Tailings in de-ionized water. Samples of the tailings were collected at the surface and from a depth of 1.5m (auger samples). _____ 97

Figure 4.12: Desorption Langmuir model for Plant 4 Upper Beach Tailings in de-ionized water. Samples of the tailings were collected at the surface and from a depth of 1.5m (auger samples). 98

Figure 4.13: Desorption Isotherm for Plant 4 Upper Beach Tailings in de-ionized water. Samples of the tailings were collected at the surface and from a depth of 1.5m (auger samples). 99

Figure 4.14: Aqueous concentration of (a) F2 fraction and (b) F3 fraction PHCs in de-ionized water for Plant 4 Upper Beach surface and auger samples. The aqueous concentration is plotted against the total mass of F2 and F3 fraction PHC present in the solid tailings sample. 103

Figure 4.15: Radial diffusion of (a) F2 fraction and (b) F3 fraction PHCs from composite tailings into de-ionized water. 117

Figure 4.16: Radial diffusion of (a) F2 fraction and (b) F3 fraction PHCs from 3 different MFTs into de-ionized water. 119

Figure 4.17: Radial diffusion of F2 and F3 fraction PHCs from saturated tailings sand into de-ionized water. 120

Figure 4.18: Varying D* values for the 2:1 SFR CT F2 Fraction results. The best fit D* value of 2.50 x 10-8 cm^2/s was varied by half an order of magnitude above and below the best fit value. The GC model results are shown as individual square data points. 121

Figure 4.19: Varying Langmuir adsorption coefficients Ŭ(L/mgPHC) and ɓ (mgPHC / kgSOIL) for the 2:1 SFR CT F2 Fraction results. The best fit Ŭand ɓ values of were varied by two orders of magnitude above and below the best fit values. The GC model results are shown as individual square data points. 122

Figure 4.20: The F2 fraction PHC concentration for the PT MFT at three different radius values. There is little difference in the porewater concentration of F2 fraction PHCs at both values for r of 7.84cm and 9.86cm. 123

Figure 4.21: The F2 fraction PHC concentration in the tailings on Day 5 of the radial diffusion experiment for the 2:1 CT. This graph demonstrates that there is diffusion occurring at more than one value of ɑr in the model. 124

Figure 5.1: Conceptual cover system design, with 3m of 2:1 SFR CT capped with a monolithic fine-grained soil. 137

Figure D.1: Desorption experiment results for 2:1 SFR, 4:1 SFR and 6:1 SFR Composite Tailings in de-ionized water 203

Figure D.2: Desorption Langmuir model for 2:1 SFR, 4:1 SFR and 6:1 SFR Composite Tailings in de-ionized water 204

Figure D.3: Desorption Isotherm for 2:1 SFR, 4:1 SFR and 6:1 SFR Composite Tailings in de-ionized water 205

Figure D.4: Desorption experiment results for 2:1 SFR, 4:1 SFR and 6:1 SFR Composite Tailings in de-ionized water 206

Figure D.5: Desorption Langmuir model for 2:1 SFR, 4:1 SFR and 6:1 SFR Composite Tailings in de-ionized water 207

Figure D.6: Desorption Isotherm for Mature Fine Tailings in de-ionized water 208

Figure D.7: Desorption experiment results for Plant 4 Upper Beach Tailings in de-ionized water. Samples of the tailings were collected at the surface and from a depth of 1.5m (auger samples). 209

Figure D.8: Desorption Langmuir model for Plant 4 Upper Beach Tailings in de-ionized water. Samples of the tailings were collected at the surface and from a depth of 1.5m (auger samples). 210

Figure D.9: Desorption Isotherm for Plant 4 Upper Beach Tailings in de-ionized water. Samples of the tailings were collected at the surface and from a depth of 1.5m (auger samples). 211

Figure D.10: Desorption experiment results for Tailings Sand in de-ionized water. 212

Figure D.11: Desorption Langmuir model for Tailings Sand in de-ionized water. 213

Figure D.12: Desorption Isotherm for Tailings Sand in de-ionized water. 214

Figure E.1: Aqueous concentration of PHCs in de-ionized water for Composite Tailings samples after 12 days. The aqueous concentration is plotted against the total mass of PHCs present in the solid tailings sample. 216

Figure E.2: Aqueous concentration of PHCs in de-ionized water for Mature Fine Tailings samples after 12 days. The aqueous concentration is plotted against the total mass of PHCs present in the solid tailings sample. 217

Figure E.3: Aqueous concentration of PHCs in de-ionized water for Plant 4 Upper Beach surface and auger samples after 12 days. The aqueous concentration is plotted against the total mass of PHCs present in the solid tailings sample. 218

Figure E.4: Aqueous concentration of PHCs in de-ionized water for Tailings Sand samples after 12 days. The aqueous concentration is plotted against the total mass of PHCs present in the solid tailings sample. 219

LIST OF ABBREVIATIONS

PHC	Petroleum Hydrocarbons
MFT	Mature Fine Tailings
PT MFT	Polymer-Treated Mature Fine Tailings
LG MFT	Lime/Gypsum Mature Fine Tailings
SFR CT	Sands to Fines Ratio for Composite Tailings
SSP	South Sustainability Pond
NSP	North Sustainability Pond
P4UB	Plant 4 Upper Beach tailings
P4LB	Plant 4 Lower Beach tailings
OSPW	Oil sands process water
CCME	Canadian Council of Ministers of the Environment
NHRC	National Hydrologic Research Centre
BTEX	The PHCs benzene, toluene, ethylbenzene, xylenes
F1	PHC fraction with carbon numbers nC6 to nC10, minus BTEX
F2	PHC fraction with carbon numbers nC10 to nC16
F3	PHC fraction with carbon numbers nC16 to nC34

F4	PHC fraction with carbon numbers nC34 to nC50
F4G	Gravimetric heavy hydrocarbon
LOI	Loss on ignition (%)
M_T	Total mass of the sample (water content)
M_s	Mass of the soil portion of the sample (water content)
M_w	Mass of the water in the sample (water content)
S	Mass of solute sorbed onto the solid surface, per mass of solid (mg/kg)
C	Concentration of solute in aqueous solution (mg/L)
K_D	Desorption coefficient (L/kg)
Ŭ	Langmuir adsorption constant related to binding energy (L/mg)
ɓ	Langmuir isotherm coefficient, maximum amount of solute that can be absorbed by the solid (mg/kg)
N	Freundlich sorption isotherm constant
K	Freundlich sorption isotherm constant
D*	Effective Diffusion Coefficient
r	Radius of the diffusion cell (m)
RMSE	Root-mean-square-error method, to determine the best fit to modeled data

PAH	Polycyclic aromatic hydrocarbon
DOC	Dissolved organic carbon
K_{ow}	Octanol/water partition coefficient
FDM	Finite Difference Method

1 INTRODUCTION

1.1 Background

The Oil Sands developments, located in northern Alberta, produce several waste streams in the process of removing the bitumen from the sand; the waste streams are referred to as tailings, and are a combination of sand, clay and silt fines, chemical additives and process water, as well as any bitumen remaining after the extraction procedure (MacKinnon et. al 2005). Tailings are stored in large ñtailings pondsò, or more formally tailings impoundment areas, at the mine sites, with the final stage of their storage involving tailings dewatering and subsequent revegetation using a cover system. Establishment of vegetation on these reclaimed sites is important, as it keeps the cover system in place and reduces dusting, limits the water reaching the dewatered tailings and reduces erosion at the site.

Suncor Energy Inc. (Suncor) has several tailings materials requiring analysis with respect to the mobility and solubility of the petroleum hydrocarbon (PHC) contaminants. Suncor is specifically concerned with the mobility of the PHCs present in their tailings materials. At sites where tailings materials have been disposed of and are reclaimed and covered with a growing medium, the PHCs from the tailings may slowly migrate into the reclamation cover, increasing their availability to the plants in the cover system. Plants are able to utilize some PHCs as a source of organic carbon, but could be detrimental to the development and establishment of the plant cover system.

1.2 Athabasca Oil Sands

The Athabasca oil sands, located in northern Alberta near Fort McMurray, are one of the worldôs largest known oil reserves (Fedorak et al. 2002). Suncorôs mine site is located a few kilometers north of Fort McMurray, Alberta, shown on the map in Figure 1.1, which also shows the extent of the Athabasca deposit.

The geology of the deposit is briefly described as a quartz sand-fines grade soil, with bitumen and PHC gases present in the pore spaces of the mineral grains. The Athabasca oil sands ore consists of 5 percent water, 11 percent bitumen, 12 percent fines (such as clay and silt) and 72 percent sand per unit mass (Caughill et al. 1993). In 2005 the production rate from the oil sands reached more than 1 million barrels of oil per day (Siddique et.al., 2008). As of 2000, approximately 3 cubic metres of water were needed for the extraction of a oil from one cubic metre of oil sand, producing about 4 cubic metres of waste (Holowenko et al. 2000).

The hydrocarbons are extracted from the oil sands using a caustic hot water process, which was first developed in 1932 by Karl Clark (Clark and Pasternack 1932). Hot water and chemical dispersants are combined with the raw bitumen ore, which results in a sand-water stream, a water-fines-bitumen stream and a bitumen froth. The bitumen is skimmed from the froth, and removed from the water-fines-bitumen stream via air flotation. The sand-water and water-fines-bitumen streams make up the tailings stream

(Caughill et al. 1993), which is a slurry comprised of sand, clay, organics, residual PHCs and process water (Fedorak et al. 2002).

Figure 1.1: The Athabasca Oil Sands in Alberta (Caughill et al. 1993)

The oil sands operators do not release any of the tailings (waste) streams from their leased land, incorporating a zero emissions policy (Fedorak et al. 2002). The waste streams are piped into large settling ponds, or tailings ponds, where the solids in the tailings are allowed to settle (Holowenko et.al., 2000) while the process water is reused in the hot water extraction process (Fedorak et al. 2002).

1.3 Research Objective

The objective of this study is to evaluate the mobility of PHCs in various tailings materials. More specifically, this study was aimed at quantifying the desorption and diffusion coefficients for various petroleum hydrocarbons fractions in several tailings materials from the Suncor oil sands mine site. These coefficients will allow calculations or models to be carried out to determine the rate at which the petroleum hydrocarbons can be expected to migrate from the dewatered tailings into the cover soil of a remediated site.

This study provides an in-depth look at nine tailings materials from the Suncor mine site in northern Alberta. The mobility of petroleum hydrocarbons is a concern for the reclamation activities over dewatered tailings, as the migration of these contaminants into the growing medium can affect the establishment and growth of the cover system. The general objectives of this study were to better define the quantity and mobility of PHC

contaminants in the tailings. The study can be further divided into three separate but related areas:

- Characterization of the petroleum hydrocarbons (PHCs) present in each tailings material, and in the process water collected from the mine site;
- Measurement of the desorption of PHCs from the tailings into water, which is hypothesized to be the main transport media for the contaminants; and
- Measurement of the diffusion of PHCs through the tailings.

Both desorption and diffusion are likely to be the main processes for contaminant migration from the tailings into the cover system. The system has very little flow of water, so neither advection nor mechanical dispersion are expected to contribute significantly to contaminant transport.

1.4 Scope

The scope of this study includes the characterization of the PHCs in the tailings using gas chromatography. There are twelve different tailings materials from various areas of the Suncor site that are included in the study, however not all tailings materials were included in each experiment. The tailings materials whose composition were evaluated include:

- Two samples of Plant 4 Upper Beach (P4 UB) dewatered tailings, which were

collected on site. Samples from the surface (P4 UB surface) and at a depth of 1.5m (P4 UB auger) are included in this study. These tailings are from the Plant 4 process, which is an older bitumen extraction method no longer used by Suncor.

- A sample from Plant 4 Beach Lower Beach (P4 LB), another dewatered tailings on site.
- Tailings Sand, which is dewatered tailings from the sand-water stream of the hot water bitumen extraction process.
- 3 samples of Mature Fine Tailings (MFT), which is the waste from the water-fines-bitumen stream of the extraction process. MFT is a mixture of water, silt and clay fines, residual bitumen and chemical additives. MFT, dried MFT with gypsum and lime additives (Lime-gypsum MFT), and MFT with polymer additives (Polymer-treated MFT) were the three types of MFT evaluated.
- 3 different consolidated tailings (CT) were evaluated. CT is a mixture of tailings sand and MFT at different solids to fines ratios (SFR). 2:1, 4:1 and 6:1 SFR CT were considered in this study.
- *In situ* samples from two reclaimed CT wetlands/ponds were also included, from a 4 m CT Wetland and 12 m CT Pond.

The three consolidated tailings (CT) samples were manufactured at bench scale by CanMET, but have all the same sand to fines ratios as those CT materials produced at Suncor. To ensure the manufactured CT samples are comparable to the samples on site, samples from two different CT ponds, the 4 m CT Wetland and the 12 m CT Pond, were collected for comparison with the manufactured CT samples.

A breakdown of the analysis conducted in this study on each of these 12 tailings is included in Table 1.1 below.

Table 1.1: Analysis completed for the 12 tailings materials.

Tailings Material	PHC Characterization	Bench Scale Desorption	Radial Diffusion
MFT	✓	✓	✓
LG MFT	✓	✓	✓
PT MFT	✓	✓	✓
Tailings Sand	✓	✓	✓
P4 UB Surface	✓	✓	
P4 UB Auger	✓	✓	
P4 LB	✓	✓	
2:1 CT	✓	✓	✓
4:1 CT	✓	✓	✓
6:1 CT	✓	✓	✓
4m CT Pond	✓		
12m CT Pond	✓		

This thesis includes three main chapters, an introductory chapter and one short conclusion and recommendation chapter, which is presented in Chapter 5. The literature relevant to the mobility of PHCs through tailings is discussed in Chapter 2, methods applied in this study are discussed in Chapter 3 and experimental results are presented in Chapter 4. Analytical data, mathematical derivations and more detailed experimental methods are included in the appendices.

2 LITERATURE REVIEW

The mobility of aqueous phase hydrocarbons is dependent on two major mechanisms: diffusion and adsorption (Donuahue et al. 1999). Both diffusion and sorption theory were applied in this study. Background theory for both sorption and diffusion is discussed. This includes the Langmuir hyperbolic model of sorption isotherms, as well as factors affecting sorption of organic contaminants and the hysteresis of adsorption and desorption. Experimental and predictive methods of determining sorption coefficients, along with the presentation of current work in the field of hydrocarbon sorption, are also examined. Diffusion theory will also be included, which will cover methods for the prediction of diffusion coefficients, and approaches to determining diffusion coefficients through experiments.

2.1 Petroleum Hydrocarbons

Hydrocarbons are organic chemicals, comprised solely of hydrogen and carbon. They can have a number of configurations, including chains and rings. Because of their great diversity and complexity, especially as the carbon number increases, only a very small number have been identified (Hutzinger 1980). Petroleum hydrocarbons (PHCs) are one of the main components in crude oil and on average, petroleum contains 70 percent hydrocarbons by mass (Petrov 1987). The main PHC components of crude oil are: 25 percent alkanes (or saturates), 50 percent cycloalkanes (also referred to as naphthalenes), 17 percent aromatics and 8 percent asphaltics (Fetter 1999). The PHCs present in crude

oil become increasingly complex molecules as the size and carbon number of the molecule increases.

Hydrocarbons are classed as either aliphatics (also referred to as saturates), which have either branched or chain structure types, or aromatics, which have at least one benzene ring. Benzene rings consist of 6 carbon atoms bonded with alternating double bonds (Fetter 1999). Crude oil is often separated into the following classes based on molecular weight, solubility and polarity: saturates, aromatics, resins and asphaltenes, collectively referred to as SARA (Akbarzadeh 2007, Rahimi and Gentzis 2006).

The Canadian Council of the Ministers of the Environment (CCME) have classified PHCs into four main hydrocarbon fractions, plus BTEX (benzene, toluene, ethylbenzene, xylenes), based on their carbon number from gas chromatography analysis. The CCME PHC classification system was used for the purposes of this research; the fractions are defined as follows (CCME 2001):

a) F1 fraction, carbon numbers C6 to C10, minus the BTEX.
b) F2 fraction, carbon numbers C10 to C16.
c) F3 fraction, carbon numbers C16 to C34.
d) F4 fraction, carbon numbers C34 to C50 determined by GC analysis. If the gravimetric heavy hydrocarbons are also analysed (F4G), then the greater of these two numbers is the F4 fraction.

2.1.1 Chemical Structure

Hydrocarbons are chain molecules which are primarily made up of hydrogen and carbon atoms. They can vary from simple chains, to more complex rings and chains of rings (Yong and Rao 1991). Other components in PHCs include sulphur, oxygen or nitrogen containing compounds, and heavy metals (Rahimi and Gentzis 2006). The important PHCs present in gasoline, diesel and kerosene are alkanes, aromatics and polycyclic hydrocarbons (Yong and Rao 1991). The main components of crude oil are alkanes, cycloalkanes, aromatics and asphaltics (Fetter 1999). A summary of the basic hydrocarbon classification is presented in Table 2.1 below.

Table 2.1: Hydrocarbon Classification (Fetter 1999)

Hydrocarbon Class	Structure Type	Carbon Bond Type	Other names	Examples		
Aliphatics						
Alkanes	Straight or branched chain	Single	saturated hydrocarbons, paraffins, saturates	Methane, propane, hexane, ethane	CH_3 ï CH_3	*Ethane*
Alkenes	Straight or branched chain	Double	unsaturated hydrocarbons, olefins	1-Butene, ethene	$CH_2 = CH_2$	*Ethene*
Alkynes	Straight or branched chain	Triple	Acetylenes	Ethyne	HC ∫ CH	*Ethyne*
Aromatics	Contains a Benzene ring	Any, but contains at least one benzene ring		Polycyclic Aromatic Hydrocarbons, polychlorinated biphenyls (PCBs)		*Benzene* C_6H_6

Alkanes, which are also referred to as saturates (Akbarzadeh et al. 2007), include paraffins, which are hydrocarbons with straight or branched chains of carbon atoms saturated with hydrogen (Rahimi and Gentzis 2006) and cycloalkanes, which are hydrocarbons with ring structures. Some examples of alkanes include pentane, hexane, cyclepentane and cyclohexane (Yong and Rao 1993).

Aromatics and naphthenes are hydrocarbons with a central 6-sided benzene carbon ring structure. Naphthenes are saturated hydrocarbons, having at least one central ring structure. Branches, side chains or paraffinitic side chains are often present (Rahimi and Gentzis 2006, Yong and Rao 1993).

The two other components of the SARA classification are resins and asphaltenes. Resins are defined by their solubility in n-alkanes and their insolubility in propane. They are nonvolatile hydrocarbons, similar to asphaltenes. Asphaltenes are the heaviest component of the SARA classification, and like resins, they are also a solubility class. Asphaltenes are insoluble in n-alkanes (i.e. aliphatics) and soluble in aromatics such as toluene (Akbarzadeh et al. 2007, Rahimi and Gentzis 2006). Asphaltenes consist of a large central ring structure, which could contain up to 20 aromatic rings, and have several branched side chain structures. They are very complex and have a high molecular weight. They are often polar due to the presence of heteroatoms, such as heavy metals, in the central ring structure (Akbarzedeh et al. 2007). Asphaltenes are also known to

aggregate with other asphaltene molecules, thought to be propagated by the polarity of the compounds (Akbarzadeh et al. 2007, Rahimi and Gentzis 2006). Some possible molecular structures of asphaltenes are shown in Figure 2.1 below.

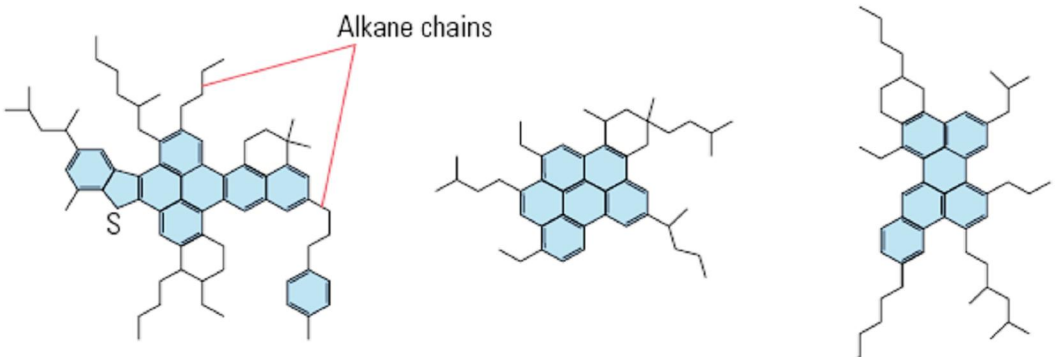

Figure 2.1: Examples of asphaltene molecular structure, showing the aromatic rings with alkane chains (Akbarzadeh et al. 2007).

2.1.2 PHC Composition in the Oil Sands

The oil sands are composed of bitumen, mineral content and water, with bitumen content ranging between 0 and 19 percent by weight (Chalaturnyk et al. 2002). Oil sands tailings materials contain residual hydrocarbons which remain after the bitumen extraction process. The waste stream from the oil sands extraction process consists of sand, fines as clay, water, some organics and some residual hydrocarbons that were not removed during processing (Holowenko et al. 2000). Of the four groups of PHCs present in petroleum, it is the presence of asphaltenes that has the most impact on the physical properties of both bitumen and other heavy oils (Rahimi and Gentzis 2006). Suncor has reported average bitumen recovery efficiencies between 90 and 92 percent for oil sands containing 12 percent bitumen (Chalaturnyk et al. 2002), meaning that a significant amount of bitumen, including asphaltenes, remains present in the tailings stream.

2.2 Contaminant Transport

Contaminant transport is the movement of solutes through porewater. The contaminant transport equation can be modified to include many different components of transport. The five main processes affecting contaminant transport are advection, dispersion, diffusion, sorption and retardation through chemical reactions. The three transport processes are advection, dispersion and diffusion, while sorption and reactions are retardation processes (Fetter 1999).

Advection is defined as the transport of particles dissolved in the porewater and subject to movement at the average seepage velocity, v_s. Dispersion is the natural mixing that occurs in the moving porewater due to the non-uniform velocity profile of the flow-path, referred to as mechanical dispersion. Diffusion is dependent on concentration gradients, and is the movement of solutes from areas of higher concentration to areas of lower concentration, and is a much more important process when there is no flow in the system. In groundwater systems, diffusion and dispersion cannot be separated when there is any flow, and the combined effect is referred to as hydrodynamic dispersion (Fetter 1999). The hydrodynamic dispersion coefficient is defined as follows:

$$D_L = \alpha_L v_i + D^* \qquad \text{[Equation 2.1]}$$

Where D_L is the hydrodynamic dispersion coefficient in the longitudinal direction, α_L is the longitudinal dynamic dispersivity, v_i is the average linear velocity in the *i*-direction and D* is the effective diffusion coefficient (Fetter 1999).

The two retardation processes, sorption and reactions, can have a significant impact on the rate of contaminant migration. Reactions may include precipitation of compounds from solution, biodegradation, abiotic degradation and radioactive decay (Fetter 1999). Sorption has previously been defined as occurring when solutes partition from the aqueous phase to the solid phase by accumulating on the surface of a soil or sediment (Fetter 1999).

The contaminant transport for one dimensional transport is found in Equation 2.2 below (Fetter 1999), which includes terms for advection, dispersion, sorption and reaction (from left to right in the equation).

$$\frac{\partial C}{\partial t} = D_L \frac{\partial^2 C}{\partial x^2} - v_s \frac{\partial C}{\partial x} - \frac{\rho_d}{\theta} \frac{\partial C^*}{\partial t} + \left(\frac{\partial C}{\partial t} \right)_{rxn} \qquad \text{[Equation 2.2]}$$

Where C is the aqueous concentration of the solute, t is time, D_L is the longitudinal dispersion coefficient, v_s is the average seepage velocity, ρ_d is the bulk density of the porous media, θ is the volumetric water content of the porous media and *rxn* refers to the chemical reactions (Fetter 1999). A derivation of the 1-D equation for diffusion-sorption is found in Appendix A.

2.3 Sorption Theory

Adsorption and desorption, collectively referred to as sorption, of organics from soil surfaces is one of the most important processes in contaminant transport. Adsorption is an important retardation process, occurring when solutes partition from the aqueous phase to the solid phase by accumulating on the surface of a soil or sediment (Fetter 1999). Desorption is the release of the sorbed particles from the surface of soils back to the aqueous phase, which also has an effect on their availability and mobility. The amount of contaminants retained on soils and sediments affects the transport processes occurring in the soil (Sparks 2003).

There are three main categories of sorption: physical, chemical and electrostatic (Delle Site 2001). The physical category includes adsorption and absorption; adsorption occurs when a solute partitions to the solid phase and attaches to the surface of a soil or sediment; desorption is the opposite process. Absorption occurs when a particle can diffuse into the pore spaces of the soil or sediment and attach to an inner surface. Electrostatic interactions, also referred to as ion exchange, occurs when oppositely charges particles and soil or sediment surfaces are attracted and held together with electrostatic energy (Fetter 1999), involving ion-ion and ion-dipole attractions between the molecules (Delle Site 2001), including weak London-van der Waals forces which increase with increasing molecular weight (ten Hulscher and Cornelissen 1996). When the solute is integrated into the soil or sediment surface through a chemical reaction, and bonded by either a hydrogen bond or a covalent bond (Delle Site 2001), the process is

referred to as chemisorption (Fetter 1999, ten Hulscher and Cornelissen 1996). Desorption is the reverse of these processes, the release of the sorbate from the soil or sediment into the aqueous phase. The adsorption and desorption processes are shown in Figure 2.2 below in Scenarios A and B respectively, adapted from Limousin et al. (2007).

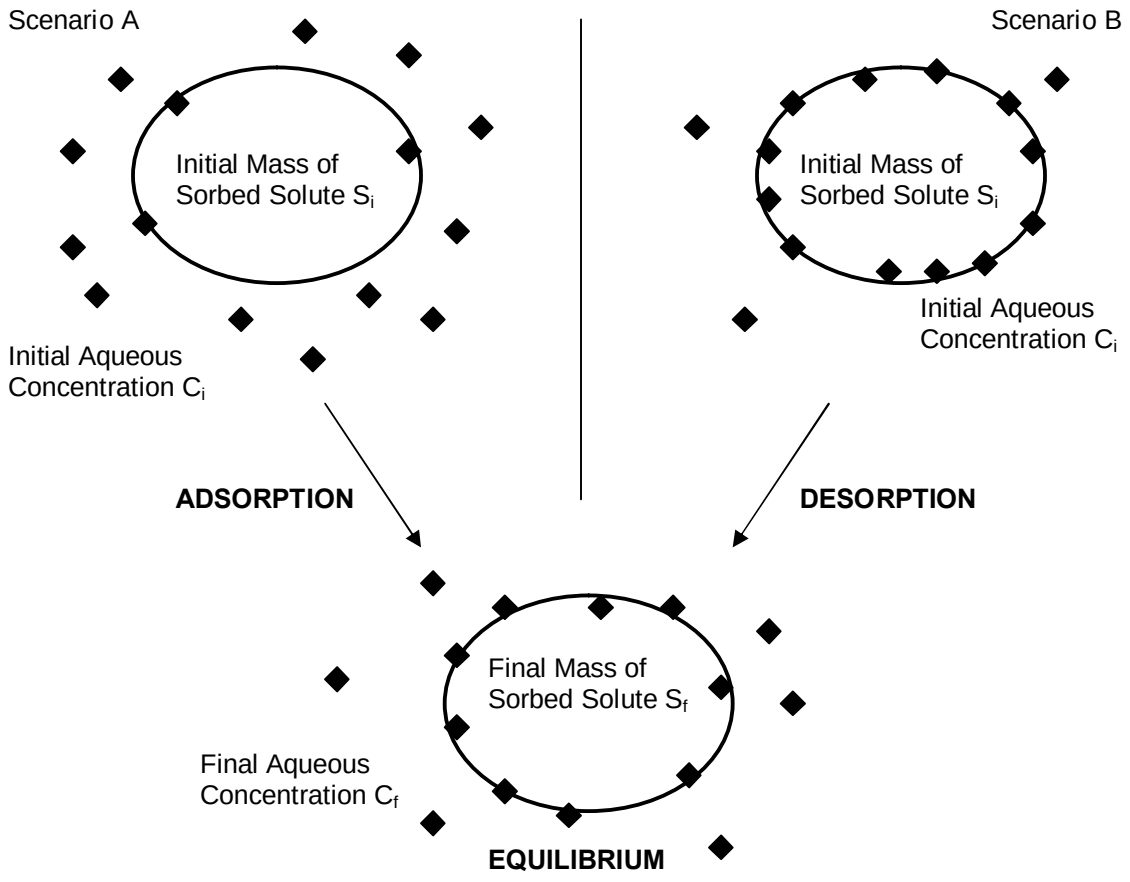

Figure 2.2: A diagram of the sorption process on a soil or sediment particle, adapted from Limousin et al. (2007). Scenario A shows the adsorption process, with a decrease in aqueous concentration and an increase in sorbed mass at equilibrium. Scenario B shows the desorption process in which the sorbed solute moves from the surface of the particle to the aqueous phase at equilibrium. Sorption is determined by measuring the initial and final aqueous concentration C.

2.4 Sorption Isotherms

The adsorption isotherm is the relationship between the amount of solute in concentration and the amount that has sorbed to the mineral surface (Limousin et al. 2007). Adsorption and desorption in an aqueous-soil system can be experimentally determined using a batch test method. The relative quantities of sorbate sorbed on the sediment and solute dissolved in the aqueous solution are measured once the system reaches equilibrium (Fetter 1999). This information is plotted using an adsorption isotherm, which describes the partitioning relationship of the sorbate between the soil/sediment phase and the aqueous phase at equilibrium (Sparks 2003).

There are a number of equilibrium based sorption models used to describe the sorption of solutes onto soils and sediments from these experimental results. The linear, Langmuir and Freundlich isotherms will be discussed here. These mathematical representations of isotherms are widely used in organic chemistry to model the results of batch sorption tests or more generally to describe sorption phenomena (Sparks 2003).

2.4.1 Linear Sorption Isotherm

The linear sorption isotherm is the simplest model, used when there is a direct linear relationship between the aqueous and the sorbed concentration of the solute, with the distribution coefficient K_d simply the slope of the line (Fetter 1999). The equation is shown below in Figure 2.3.

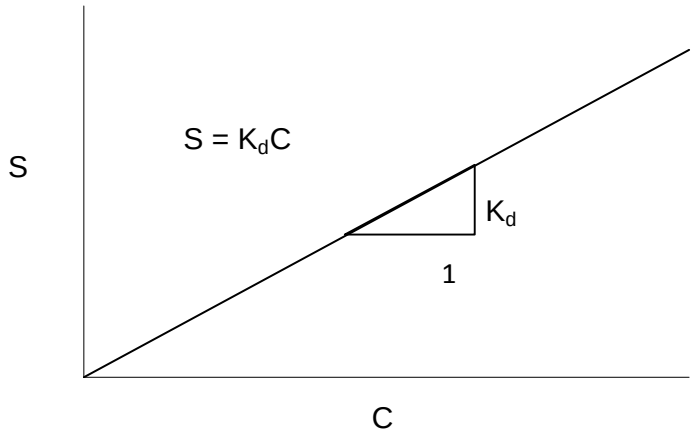

Figure 2.3: Linear sorption isotherm, showing the straight line relationship between the aqueous solute concentration, C, versus mass of sorbed solute, S (Fetter 1999).

S is mass of the sorbed solute per dry unit weight of soil in mg/kg, C is the concentration of aqueous solute in mg/L and K_d is the sorption coefficient in mL/g (Fetter 1999).

2.4.2 Langmuir Sorption Isotherm

The Langmuir sorption isotherm was developed in 1918 by Irving Langmuir to describe the adsorption relationship of gas molecules on planar surfaces. It has since been adopted for the sorption of solutes to soils and sediments by Fried and Shapiro in 1956, and is now widely used in modelling sorption to soils and sediments (Sparks 2003). The Langmuir isotherm is best used with low aqueous concentrations and the model has the following assumptions (Sparks 2003, Limousin et al. 2007):

- A fixed number of sites are available for adsorption; sites assumed to be identical with the capacity for one molecule (i.e. monolayer adsorption only);

- Adsorption is a reversible process;
- The molecules do not move laterally on the surface of the adsorbate; and,
- The sorption surface is homogeneous and the adsorbate behaves ideally, with no interaction between particles.

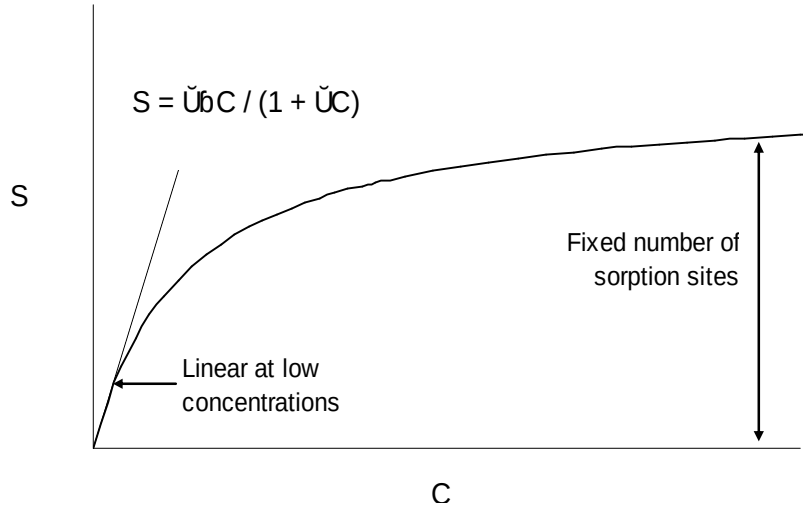

Figure 2.4: Langmuir sorption isotherm, showing the mathematical relationship between S and C (Fetter 1999).

The relationship between S and C is shown in Figure 2.4 (above). The adsorption coefficients Ŭ and ɓ can be determined by converting the S versus C graph into a linear relationship by plotting C/S versus C. The coefficient ɓ, the maximum ion sorption, can be determined from the slope of the line and the coefficient Ŭ, the binding energy constant, can be determined from the inverse of the y-intercept, as shown in Figure 2.5 below (Sparks 2003, Fetter 1999).

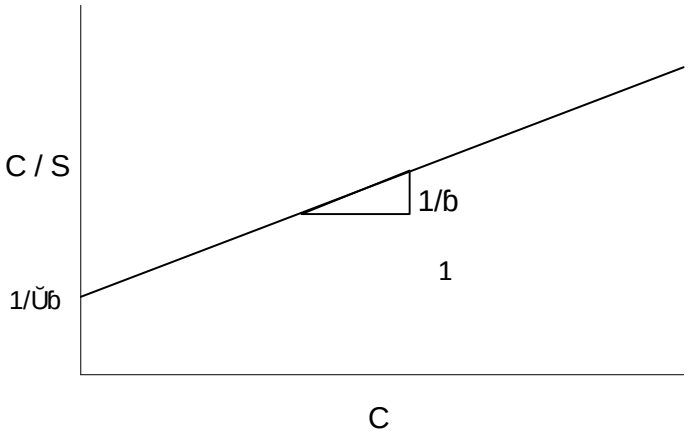

Figure 2.5: Langmuir sorption isotherm showing the linear C/S versus C plot (Fetter 1999), from which the two sorption coefficients Ŭ and ƀ can be determined.

2.4.3 Freundlich Sorption Isotherm

Another isotherm developed to describe the sorption of gas phase and solute adsorption is the Freundlich sorption isotherm (Sparks 2003).

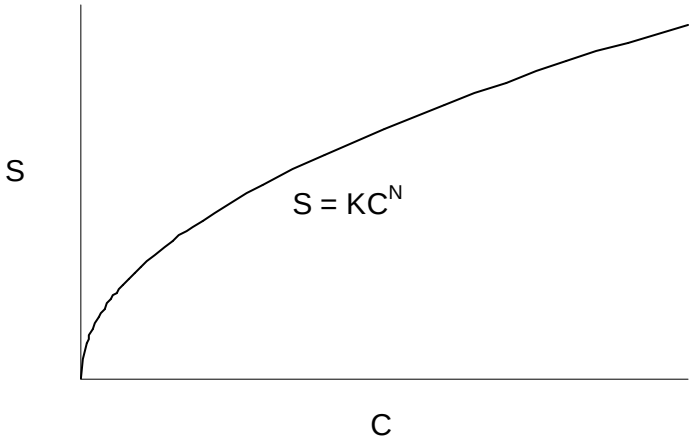

Figure 2.6: Freundlich sorption isotherm, showing the mathematical relationship between S and C (Fetter 1999).

The power-function relationship between S and C is shown in Figure 2.6 on the previous page. This relationship can be made linear by plotting the logarithm of S and C, as shown in Figure 2.7 below. The coefficients N and K can then be determined from the slope and the y-intercept of the logarithmic plot (Fetter 1999, Limousin et al. 2007). The Freundlich isotherm does not reach a final sorbed concentration plateau (Limousin et al. 2007), and the isotherm is usually determined empirically from experimental data instead of the mechanistic approach used in the Langmuir isotherm. When using the Freundlich model, the isotherm should extrapolated beyond the limits of the experimental data, as the number of sorption sites is not limited (Fetter 1999).

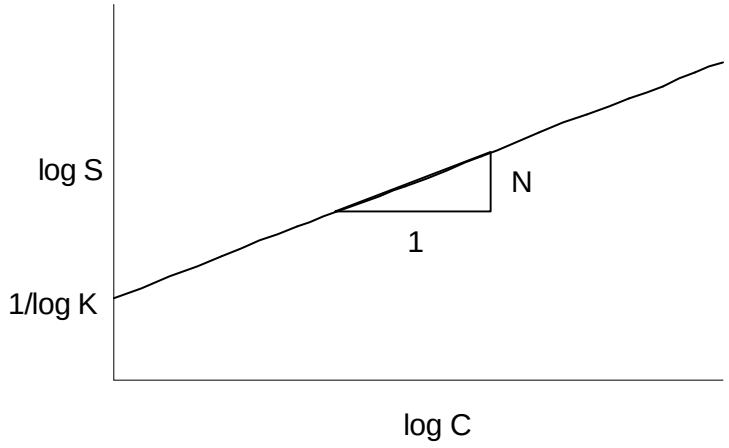

Figure 2.7: Freundlich sorption isotherm showing the log-log relationship between S and C (Fetter 1999), from which the two sorption coefficients K and N can be determined.

2.5 Sorption of Organics

The sorption of any chemical species can be a complex process, but is often regarded as occurring instantaneously (Fetter 1999). The sorption of organics is poorly understood,

and the mobility of petroleum hydrocarbons, including the desorption of tailings PHCs into water, is not well documented in the literature. However, many studies have been completed on the sorption and desorption of hydrophobic organic compounds. Temperature, solute effects, sorption hysteresis or non-singularity, sorption kinetics, solids effect, salting out, steric hindrance, water to solids ratio, steric hindrance and sorbate effects all affect the sorption-desorption process for organics. There is only a limited amount of information available specifically relating to the sorption of PHCs, so the sorption of organics in general is discussed in terms of the published literature.

2.5.1 Sorption Hysteresis

In the adsorption and desorption process for soils or sediment, it is common for the ratio of organics in solution to be different during sorption and desorption. This effect known as hysteresis, and is also referred to as non-singularity (Delle Site 2001). Sorption and desorption are not always equal processes, resulting from the irreversible sorption of some of the organic solids. Studies on the sorption/desorption of organic compounds have concluded that a percentage of the sorbate was irreversibly bound to the soil or sediment (Morrissey and Grismer 1999, Kan et al. 1998), including the desorption of asphaltenes (Dubey and Waxman 1991). By modelling the sorption process with two phases, sorption-desorption hysteresis was effectively explained by a ñrapid phaseò sorption followed by a ñslower phaseò diffusive sorption (Delle Site 2001).

Although sorption hysteresis is a naturally occurring phenomena, in some instances the effects are enhanced because of the experimental design. Huang et al. (1998) identified three experimental conditions that could possibly result in artificial adsorption-desorption hysteresis: (a) the sorption process does not reach true equilibrium, (b) any losses to apparatus components are not accounted for, or (c) the solids effect, which is thought to be due to partitioning of the solute to dissolved or colloidal organic matter. Huang et al. (1998) designed experiments that removed these conditions, and found that sorption hysteresis was still present, although to a smaller degree. The solids effect is discussed in further detail in Subsection 2.5.4.

2.5.2 Sorption Kinetics

The inequality of the sorption-desorption process as has already been discussed, but the desorption rate is also a non-uniform process. It has been found that there is a two-phase desorption relationship, with an initial ñfastò release of sorbent, which can take hours to days, followed by a second much longer ñslowò phase, which can take days to months to reach equilibrium (Huang et al. 1998, Hsieh et al. 2010, Ball and Roberts 1991, Wu and Gshwend 1988, Pignatello and Xing 1996, Cornelissen et al. 1997, Delle Site 2001). In addition, a significant portion of the sorbate can be irreversibly bound to the soil or sediment (Morrissey and Grismer 1999, Huang et al. 1998, Kan et al. 1998, Braida et al. 2002), in some cases up to 70 percent of the sorbed mass (Morrissey and Grismer 1999).

A possible explanation for the slow fraction of the two-phase relationship is slow diffusion of the sorbate within the soil particles, while the fast release is of those sorbed particles on the outside surface of the soil or sediment (Cornelissen et al. 1997). A relationship also exists between the hydrophobicity of the sorbed compound and the slow fraction desorption; the slow fraction increases with increasing hydrophobicity (Cornelissen et al. 1997).

2.5.3 Temperature Dependence

The sorption process can be affected as the temperature changes; studies have found that the sorption coefficient decreases as the temperature increases for organic compounds whose solubility also increases with temperature (Delle Site 2001, ten Hulcher and Cornelissen 1996). As both sorption coefficients and solubility are temperature-dependent, the observed effect on sorption coefficients in experimental results is a shared solubility-sorption effect (Delle Site 2001).

The slow sorption phase has been found to be strongly dependent on increasing temperature (ten Hulscher and Cornelissen 1996, Cornelissen 1997), while in studies where the observed sorption had a shorter equilibration time, the sorption appeared to be only weakly affected by the temperature (ten Hulscher and Cornelissen 1996). The strength of the sorption bond between the sorbate and the soil or sediment surface also plays a role in temperature dependence; weaker bonding forces between sorbate and the

solid surface resulted in less temperature dependence, due to the sorption enthalpyôs lower equilibrium (ten Hulscher and Cornelissen 1996).

In a study of the adsorption of asphaltenes on metals by Alboudwarej et al. (2005), it was found that the adsorption of asphaltene decreased as the temperature increased; adsorption at 60ºC and room temperature were compared in the study. Alboudwarej theorized that the decrease was likely due to a decrease in molar mass of the asphaltenes; however, the adsorption results were within the range of data scatter. Cornelissen et al. (1997) studied the effect of temperature on the adsorption and desorption from sediment of some chlorobenzenes, polychlorinated biphenyls (PCBs) and polycyclic aromatic hydrocarbons (PAHs). The study concluded that the rate constants of slow desorption after equilibrium were not significantly different at 20ºC or 65ºC, but they increased strongly with increasing temperature for the slow desorption phase.

2.5.4 Solids Effect

The ratio between water (the solvent) and the sorbent soil or sediment is another factor that affects adsorption-desorption, often referred to as the ñsolids effectò. A high ratio of water to contaminant in the system has been shown to increase the initial desorption rate constant (Hsieh et al. 2010). Several studies have concluded that different water-to-sorbent ratios in the same system (i.e. same solution and sorbent) will result in varying adsorption constants (Chang and Wang 2002).

Theoretically, the ratio between the soil or sediment and the water should have no effect on the actual value of the adsorption coefficient. However, a number of studies have found that there was a nonlinear relationship between adsorption and the solids/solution ratio and that adsorption decreased at lower concentrations of solids (Limousin et al. 2007). Some possible explanations for the solids effect have been proposed, but no single theory has explained it completely (Delle Site 2001). The volume occupied by suspended solids and the aggregation of these same suspended particles are the two main reasons proposed to explain this behaviour (Limousin et al. 2007). Three other proposed explanations are (a) an increase of available sorption sites due to the dispersion of soil aggregates in batch testing experiments; (b) an increase in the organic matter released from the sorbent; or (c) interaction between the dissolved aqueous particles (Delle Site 2001).

Generally, it is best to choose a soil/solution ratio that is representative of natural soil/solution conditions. However, this is not always a practicable choice, especially when using batch experiments or highly absorbent materials. It is recommended that the solids/solution ratio for experiments consider both natural conditions, the adsorbed/desorbed material and constraints presented by the chosen experimental method (Limousin et al. 2007).

2.5.5 Solubility, Hydrophobicity and Cosolvency

Solubility is an important factor when determining the mobility of a particular contaminant. One of the main mechanisms in the spread of a pollutant through a soil system is via the hydrologic cycle. The solubility of organic substances is very important, as the more soluble a species, the more mobile it will be in the environment (Fetter 1999). The solubility of a particular species is also one of the factors governing how rapidly a site can become contaminated (Page et al. 2000).

Petroleum hydrocarbons have very low solubilities, which decrease with increasing molecular size increases; PHC solubility is also related to their molar fraction. Empirical relationships have been developed to calculate hydrocarbon solubility in water, of both heavy and lighter PHCs (Nadim et al. 1999) using Equation 2.3 (light PHCs) or Equation 2.4 (heavy PHCs). Equation 2.3 was developed by Schwartzenbach et al. (1993) and Equation 2.4 was developed by Peters (1993) for room temperature solid state PHCs.

$$X_w = \frac{\gamma_{org.mix} X_{org.mix}}{\gamma_w} \qquad \text{[Equation 2.3]}$$

Where X_w is the mole fraction solubility of PHCs, $X_{org.mix}$ is the mole fraction of PHCs in mixture (e.g. mole fraction of toluene in gasoline), γ_w is the pure phase aqueous solubility of PHCs and $\gamma_{org.mix}$ is the activity coefficient (Nadim et al. 1999).

$$C_i = X_i S_i \left(f_L / f_S \right)_{pure(i)}$$ [Equation 2.4]

Where C is the aqueous solubility of compound i, X is the mole fraction of compound i, S_i is the aqueous solubility of the compound and f_L and f_S are the solid and liquid phase fugacities of the sub-cooled compound (Nadim et al. 1999).

Solubility is also related the hydrophobicity of a compound. Hydrophobicity (derived from Greek for ñfear of waterò) refers to the phenomenon that occurs when non-polar compounds are repelled by water. Many organic chemicals are non-polar, and also hydrophobic, being more attracted to other non-polar compounds and solvents, as well as the hydrophobic portion of the soil or sediment (Limousin et al. 2007). The hydrophobicity of a compound is quantitatively represented by the octanol-water partitioning coefficent (K_{ow}) which is defined as the ratio of the mass concentration which will dissolve in a non-polar solvent (octanol) relative to the concentration dissolved in the polar solvent water. The higher the value of this partitioning coefficient, the more hydrophobic the compound. K_{ow} for organic compounds ranges from 10,000 to 1,000,000 (Andrews et al. 2004). The log of the partition coefficient is often used to describe a compoundôs affinity to adsorb to a soil or sediment surface. Log K_{ow} has also been found to be proportional with the compoundôs molecular weight, while having an inverse relationship to its aqueous solubility (USEPA 2009).

The cosolvency effect occurs when more than one organic compound are dissolved in an aqueous solution; one of the compounds will affect the effective solubility of the other compound. Cosolvency has been shown to strongly affect the mobility of PHCs and other organic compounds (Corseuil et al. 2004, Poulsen et al. 1992, Nkedi-Kizza et al. 1985). For example, Corseuil et al. (2004) observed relatively higher concentrations of hydrophobic PAHs in natural groundwater mixed with 10 percent ethanol (by volume) than when compared to PAH concentrations in groundwater alone. This demonstrated that the presence of the ethanol increased the solubility of the hydrophobic PAHs.

The aqueous solubility of benzene, toluene, *o*-xylene, naphthalene and phenanthrene were found to increase from between 29 to 230 percent when the ethanol volume fraction was increased to 20 percent showing that there is a strong cosolvency effect for these hydrophobic PAHs (Corseuil et al. 2004). Myrand et al. (1992) concluded that cosolvent concentrations would have to be greater than 1 percent for there to be any measurable cosolvent effects on hydrophobic organic compounds.

2.5.6 Other Effects on Sorption of Organics

There are many other effects on the sorption of organics, including solute effects, salting out, steric hindrance and the hydrophobicity of non-polar compounds. These effects will be discussed briefly.

The type of solute and sorbent both have an effect on the sorption process. In his review paper, Delle Site (2001) found several examples of solute and sorbent effects. In a study on the sorption of lindane that used several solvents, it was found that lindane sorbed more effectively from water than from the organic solvents, which included ethanol; the study proposed that this was due at least in part to the increased solubility of the lindane in the organic solvents. Another study of the sorption of several organic compounds, including lindane and naphthalene, concluded that it was the organic matter fraction of the soil or sediment that had the most influence on the sorption properties of the soil (Delle Site 2001).

Salting out is another observed phenomena in solutions with high concentrations of electrolytes or salts. The salts may in fact be causing dissolved non-electrolytes to precipitate from solution, or reducing their capacity to dissolve into an aqueous solution (Grover and Ryall 2004; Shah and Tiwari 1981). Dissolved salts cause the water molecules to aggregate around the salt molecules preferentially, effectively preventing them from acting as solvents for other molecules in the solution (Shah and Tiwari 1981). The least soluble of the dissolved materials precipitates from the solution first (Grover and Ryall 2004). It is likely that hydrophobic organic compounds would be some of the first to precipitate; the presence of salts is also known to affect the sorption of organic chemicals, such as naphthenic acids (Janfada et al. 2006), naphthalene monosulfonate and naphthalene disulfonate (Li and SenGupta 2004) and nitroaromatic herbicides (Martins and Mermoud 1998).

Large hydrophobic organic compounds have decreased mobility at the molecular level, an effect known as steric hindrance; larger particles have been observed to reach sorption equilibrium at a slower rate compared to similar smaller organic particles (Wu and Gschwend 1986). Zhu et al. (2008) concluded that in the sorption of neutral organic compounds, steric hindrance may negatively affect the sorption capacity of smectitic clays.

Hydrophobicity, which was previously discussed in Section 2.1.3 for organic compounds, is also a factor of sorption capacity (Hsieh et al. 2010). Organic compounds with greater hydrophobicity have been found to have slower uptake rates into sediments (Karickhoff 1980; Wu and Gschwend 1986) and large molecules that can interact simultaneously at multiple points can be more difficult to desorb (Pignatello and Xing, 1996). Physical sorption between organic compounds and the soil surface are often relatively weak bonds, but their strength can be increased as the hydrophobicity of the sorbing organic increases because the organic is both attracted to the solid surface and repelled from the solution (Delle Site 2001). This bonding mechanism has also been termed ñhydrophobic bondingò, and is defined as the combination of London-van der Waals bonding and the repulsive force from the solution, which is direct result of the large entropy change between the sediment and the solvent (ten Hulscher and Cornelissen 1996).

2.6 Laboratory Tests to Determine Sorption Coefficients

Generally a batch-type experiment is used to determine the adsorption or desorption isotherm, but other methods have also been successfully applied. Although there are many other types of adsorption-desorption experiment designs, only three will be discussed here: batch equilibrium methods, flow-through methods and diffusion cell methods.

2.6.1 Batch Equilibrium Method

The basic and simplest method to determine sorption coefficients is the batch equilibrium method, which has been used in many different studies on the sorption of organics. Each of the batch tests will yield one point on the sorption isotherm. A known mass of sorbent (usually soil or sediment) is placed in a vial. For adsorption batch tests, a known volume of solution is added to the vial; the concentration of the solution is also known. The vial is generally placed in a shaker, and is agitated until sorption equilibrium is reached. The suspension is then centrifuged, and the liquid is separated from the soil/sediment. The final concentration of the solute is analysed, from which the sorbed concentration of solute can be calculated (Delle Site 2001, Myrand et al. 1992, Limousin et al. 2007), and adsorption isotherms can be developed.

There are a number of disadvantages and sources or error inherent in this method. Disadvantages are present in both the soil to solution ratio and the continuous shaking of

the samples. The soil to solution ratio used in batch experiments is generally both too high when compared to conditions in natural water bodies, and too low compared to natural porous media, such as aquifers (Limousin et al. 2007), or in the case of this study, tailings deposits. Continuous shaking over long periods of time may also have a detrimental effect on results; the shaking may cause the soil/sediment particles to break down, or lead to side reactions between the sorbent and aqueous solution (Limousin et al. 2007). Sources of error include losses through chemical degradation of volatilization of the solutes, the water/sorbent ratio, or allowing insufficient time for the sample to reach true equilibrium (Delle Site 2001). It has been concluded that when used for preliminary results, the batch test method is sufficient (Limousin et al. 2007).

2.6.2 Flow-Through Methods

Flow-through methods are also used to determine the sorption coefficient, K_d (Delle Site 2001, Limousin et al. 2007). The flow-through method uses column containing a known amount of sorbent/soil, through which water containing a known concentration of the sorbate is pumped from an inlet at the base of the column. When the concentration at the inlet and outlet is equal, the system has reached equilibrium (Delle Site 2001, Limousin et al. 2007). Once it has reached equilibrium, the column can also be used for desorption experiments (Delle Site 2001). K_d can be determined using relationship in Equation 2.5 below (Delle Site 2001).

$$K_d = \frac{\left[\left(m_i - m_0\right)/m_s\right]}{C} \qquad \text{[Equation 2.5]}$$

Where m_i is the total mass (g) of the sorbate in solution at the inlet; m_0 is the total mass (g) of the sorbate in solution at the outlet; m_s is the mass (g) of sorbent in column; and C is the concentration of the sorbate at equilibrium (g/cm^3).

A major advantage over the batch tests is that the sorption kinetics are much easier to study (Limousin et al. 2007). There are several sources of error that must be taken into account, including colloidal transport, the possible development of preferential flowpaths, slow sorption kinetics, transport of colloids in the solution and the possible presence of immobile water in the sorbent (Limousin et al. 2007). It is suggested that various conditions be tested, such as several injected concentrations and flow rates (Limousin et al. 2007). When compared with batch equilibrium experiment results, flow through experiment yields comparable results (Delle Site 2001).

2.6.3 Diffusion Methods

Conventional diffusion methods for determining adsorption coefficients assume a linear inverse relationship between the apparent diffusion coefficient and the adsorption coefficient, K_d. The apparent diffusion coefficient is dependent on the distance to the first contaminated soil/sediment layer, and the time it took for this layer to become contaminated with the sorbent. Diffusion is a very slow process and these measurements may be difficult to obtain due to this fact (Delle Site 2001).

A modified diffusion batch method, using much smaller samples, was successfully employed by Zhang et al. (1998) to determine sorption coefficients for benzene. The study compared the results of conventional batch test methods to the diffusion batch method, concluding that while the K_d values obtained were similar, the results from the diffusion tests had reduced variability. The test method was recommended for sorption experiments using volatile organic compounds.

2.7 Diffusion Theory

Diffusion is the movement of dissolved solutes from areas of higher concentration to areas of lower concentration, and occurs whenever there are concentration gradients present (Fetter 1999, Shackelford and Daniel 1991). There are four types of diffusion, which is illustrated in Figure 2.8 below (Shackelford and Daniel 1991, Shackelford 1991).

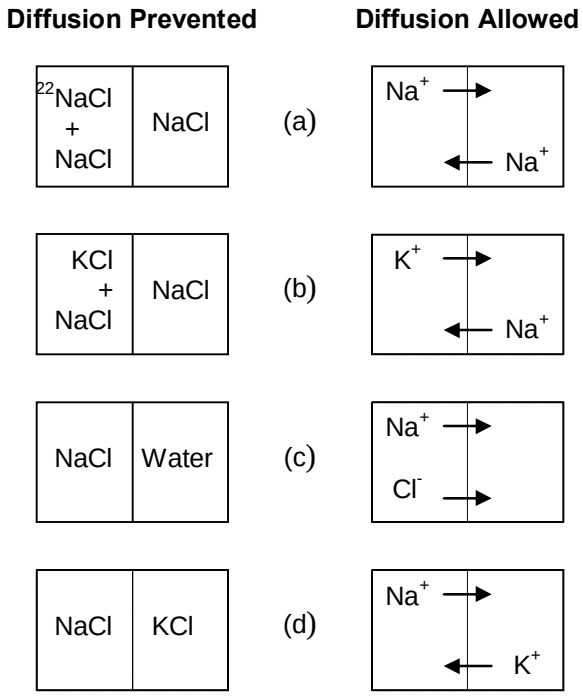

Figure 2.8: Diffusion cell processes, after Shackelford and Daniel (1991): (a) self-diffusion, (b) tracer diffusion, (c) salt diffusion, and (d) counter-diffusion.

Self diffusion in (a) is the random movement of NaCl molecules between two half-cells, which in reality could not be measured. A small amount of Na 22 isotope is added, which is then measured, yielding the ñself-diffusion coefficientò. Tracer diffusion in (b) is the same as self diffusion, except a different chemical species is added to one of the half-cells, in this case K^+, which can be traced. The third type of diffusion is salt diffusion, shown in (c), where both the Na^+ and Cl^- molecules migrate to the half-cell containing water only. The last type of diffusion is counter-diffusion or inter-diffusion, shown in (d), where Na^+ and K^+ diffuse in opposite directions from two half cells containing equal concentration of the salts KCl and NaCl (Shackelford and Daniel 1991).

2.7.1 Fick's First Law

The one-dimensional steady-state diffusive flux of solutes in a free aqueous solution is defined by Fickôs first law in Equation 2.6 below, where F is the mass flux of solute per unit area per unit time, D_0 is the diffusion coefficient in aqueous solution (or ñfree solutionò diffusion coefficient), C is the concentration of the solute and *dC/dx* is the concentration gradient (Fetter 1999, Shackelford and Daniel 1991).

$$F = -D_0 \frac{\partial C}{\partial x} \qquad \text{[Equation 2.6]}$$

In saturated soil systems, the chemical species undergoing diffusion moves much more slowly than through an aqueous solution. The dissolved species has a much longer and more tortuous pathway around the soil particles, which is illustrated in Figure 2.9 below as effective length, L_e (Shackelford and Daniel 1991).

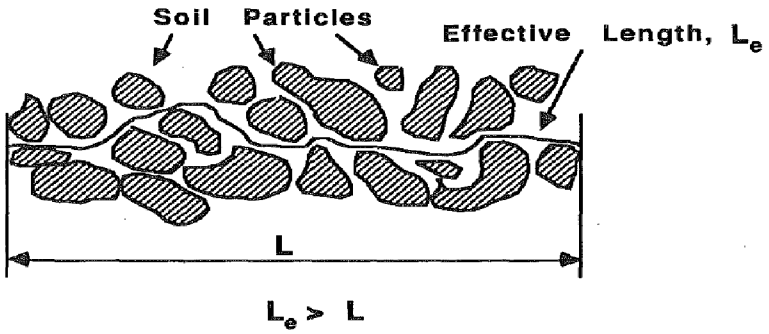

Figure 2.9: The concept of effective length in diffusive transport through a porous media/soil, from Shackelford and Daniel (1991).

In porous media, the cross-sectional area for flow is reduced because of the presence of the soil particles. To account for this, the volumetric water content, θ, is incorporated into the diffusion equation (Shackelford and Daniel 1991):

$$F = -D_0 \theta \frac{\partial C}{\partial x} \qquad \text{[Equation 2.7]}$$

The volumetric water content, θ, is related to the porosity, n, of the soil through the relationship $\theta = nS_r$. Under fully saturated conditions, the degree of saturation S_r is equal to 1, and the volumetric water content is equal to the porosity. Other factors also affect the diffusion, which are combined into an "apparent tortuosity factor" τ_a (Shackelford and Daniel 1991) or simply "tortuosity" τ (Fetter 1999). Since the tortuosity cannot be measured separately, it is combined with the free solution diffusion coefficient as the effective diffusion coefficient, $D^* = D_0\tau$. Fick's first law for fully saturated one-dimensional diffusion in porous media is thus (Shackelford 1991):

$$F = -nD^* \frac{\partial C}{\partial x} \qquad \text{[Equation 2.8]}$$

Where F is the mass flux, n is the porosity of the porous media, D* is the effective diffusion coefficient, x is the distance and C is the concentration of the solute.

2.7.2 Fick's Second Law

Fick's second law defines time-dependent transient diffusion. For saturated porous media, assuming the same tortuosity and volumetric water content, the transient diffusion equation is (Shackelford and Daniel 1991):

$$\frac{\partial C}{\partial t} = D^* \frac{\partial^2 C}{\partial x^2} \qquad \text{[Equation 2.9]}$$

The derivation of Equation 2.7 from Cartesian to Polar (i.e. radial) coordinates is included in Appendix A.

2.8 Diffusion of Organics

The diffusion of tailings PHCs into water is not well documented in the literature. In fact, the diffusive transport of most organic contaminants is not well known, and generally it is compared with the transport of inorganic contaminants (Shackelford 1991). The diffusion of some hydrophobic organic compounds in aqueous systems has been studied, and those results will be reviewed. Factors affecting the diffusion of these organics include the effect of temperature on diffusion rates, the cosolvency of organics, the straining effect, saline conditions, the overall inorganic chemistry of the system and the hydrophobicity/solubility of the organic compounds.

The D* values from studies on the diffusion of organic compounds through clay in included below in Table 2.2.

Table 2.2: Effective diffusion coefficients for organic compounds through clay or clay liners

Organic Compound	D^*x10^{-6} (cm^2/s)	Reference
Benzene through clay liner	1.57	Headley et al. 2001
Benzene through clay	0.11	Myrand et al. 1992
Toluene through clay	0.04	Myrand et al. 1992
Chlorobenzene through clay	0.03	Myrand et al. 1992
DOC through clay	0.90	Hendry et al. 2003
Cl Ė through saturated silt	9.00	Rowe and Badv 1991
Cl Ė through clayey silt till	5.70	Rowe and Badv 1991
Cl Ė through saturated sand	9.80	Rowe and Badv 1991

2.8.1 Effect of Temperature

It was found that the molecular diffusivity of various organic compounds decreased with decreasing temperature (Gustafson and Dickhut 1994, Barone et al., 1992, Donahue et al. 1999), including PAHs (Gustafson and Dickhut 1994) and benzene (Donahue et al. 1999). The decreasing diffusion rates may be due in part to the decrease in aqueous solubility and to the increase in adsorption observed as temperature decreases (Donahue et al. 1999).

2.8.2 Effect of Saline Conditions

Gustafson and Dickhut (1994) found that there was no measurable effect on the diffusion coefficient for PAHs in saline (i.e. marine) water. Conductivity was measured for the

first 3 days of each diffusion cell experiment, which provided and relative value of total dissolved solids in the reservoir, including salts. Higher salinity was not been found to affect diffusion in the study by Gustafson and Dickhut (1994), and salinity effects were not included in the scope of the experiments described in this thesis.

2.8.4 Straining and the Effect of Molecular Size

The mobility and transport of colloids in suspension can be inhibited by the size of the pore openings in the porous media, such as soil or tailings, an effect known as straining (Hendry et al. 2003). The aqueous diffusion rate of PAHs has been found to decrease with increasing molecular size (Gustafson and Dickhut 1994). Dunnivant et al. (1992) concluded that straining did not affect the diffusion of DOC through aquifer material, although Sawatsky et al. (1997) found that differences between predicted and observed diffusion coefficients for 1-napthol and naphthalene were due to restrictive pore spaces.

2.8.5 Other Effects on Diffusion

The diffusion rate of organic compounds can be affected by several other factors. The materials used in the diffusion cell construction, inorganic chemistry of the system and hydrophobicity/solubility all affect diffusion rates.

It was found that as the aqueous solubility of a volatile organic compound decreased, the effective diffusion coefficient decreased as well (Kim et al. 2001). The materials used in

the diffusion cell may also have an effect on the diffusion rate. Stainless steel components have been found to sorb hydrophobic organic compounds, resulting in significant effects on the diffusion rate (Voice et al., 1983, Barone et al., 1992). Itakura et al. (2003) used control tests to determine any diffusion losses, and concluded that any losses to the stainless steel components were not significant. Headspace development has also been reported to affect the diffusion results, as it could introduce error through movement of hydrophobic volatiles to from the aqueous to the gaseous phase (Itakura et al. 2003).

2.9 Determining Diffusion Coefficients

There are many experimental methods that can be used to determine diffusion coefficients. Steady-state methods use Fickôs first law (discussed in Section 2.7.1), while transient methods use Fickôs second law (discussed in Section 2.7.2) when there is no flow, or a version of the contaminant transport equation (see Equation 2.2) when there is advective flow, to experimentally determine the diffusion coefficient (Shackelford 1991). Steady-state methods are not included in this section; three types of transient methods will be discussed: column methods, reservoir methods and the radial diffusion cell method.

2.9.1 Column Methods

Column diffusion cells consist of a soil layer and a source reservoir. For constant source concentration, the flow of water is established through the sediment. Once the flow

reaches a steady state, the water is replaced with a solution of known concentration. The concentration of the contaminant in the effluent is measured over time. For decreasing source concentration column studies, there is no flow through the column. The soil is first saturated with water, and then the source reservoir is filled with a spiked solution of known concentration. After a set duration of time, the soil is removed from the column and sectioned to determine the concentration of the contaminant as a function of depth (Shackelford 1991). Both the constant source concentration and decreasing source concentration set-ups are shown in Figure 2.10 below.

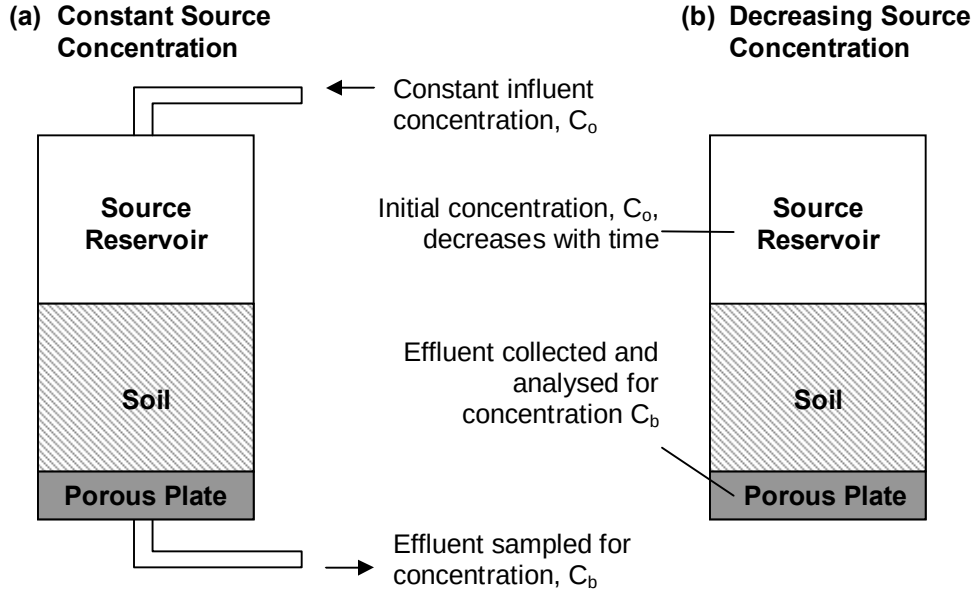

Figure 2.10: Diffusion methods: column method set-up (a) constant source concentration, and (b) decreasing source concentration, after Shackelford (1991).

The column method has been used successfully in many studies, including the diffusion of benzene, trichloroethylene, toluene and chlorobenzene into unweathered

glaciolacustrine clay (Myrand et al. 1992) and the diffusion of various salt solutions (calcium chloride, sodium chloride and potassium chloride) into a clayey soil (Rowe et al. 1988). There are two main advantages to the column method: it has been widely used in research and is well understood, and is also useful for scenarios where advective-diffusive transport is present (Shackelford 1991). However, the effective diffusion coefficient contains both the hydrodynamic dispersion and diffusive components. When using this method, the seepage velocity must remain small enough that the dispersion effects can be ignored, which will increase the length of the test (Shackelford 1991).

2.9.2 Reservoir Methods

Another commonly used diffusion cell set up is the reservoir method. There are two basic types of reservoirs methods: double cell and single cell. The double cell method includes an initial concentration reservoir (decreasing with time), a soil sample and a second reservoir from which the effluent is collected. This set up establishes diffusive transport through the soil without any advection (Rowe et al. 1988, Shackelford 1991). The single reservoir method removes the second cell, and the source reservoir can either be maintained at a constant concentration or have a concentration decreasing with time (Shackelford 1991). A schematic showing both the single reservoir and double reservoir set ups is included in Figure 2.11 below.

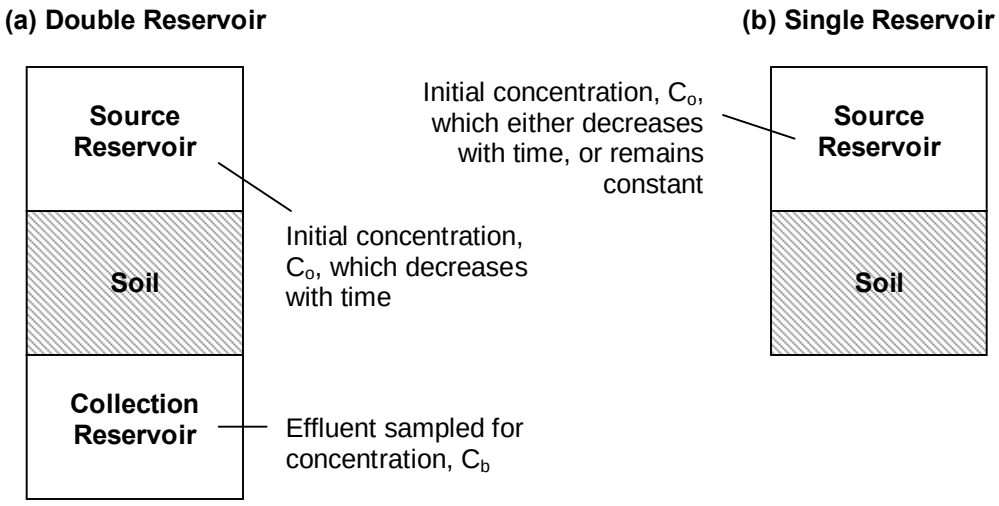

Figure 2.11: Diffusion methods: reservoir method set-up (a) Double reservoir with decreasing source concentration and (b) Single reservoir method for both decreasing and constant source concentration, after Shackelford (1991).

Unlike with the flow-through methods, with the single or double reservoir method the seepage velocity is zero and the effective diffusion coefficient obtained does not have a dispersion component. In this method, since contaminant transport relies solely on diffusion, the duration of the test is much longer than with the flow-through method (Shackelford 1991). In the single reservoir method, the hydrodynamic dispersion component is also absent, however since the diffusion distance is lower, the single reservoir test can be much shorter than the double reservoir (Shackelford 1991). Both methods have been successfully used to measure tritium diffusion into lake sediment (Van Rees et al. 1991) with both a spiked reservoir and a spiked sediment.

2.9.3 Radial Diffusion Method

Radial diffusion methods are not as common in the literature as the reservoir and column methods. The set up is shown in Figure 2.12 below, with a central reservoir of water surrounded by the soil sample. Either the water or the soil can be spiked, with the changes in concentration in the reservoir measured over time (van der Kamp et al. 1996).

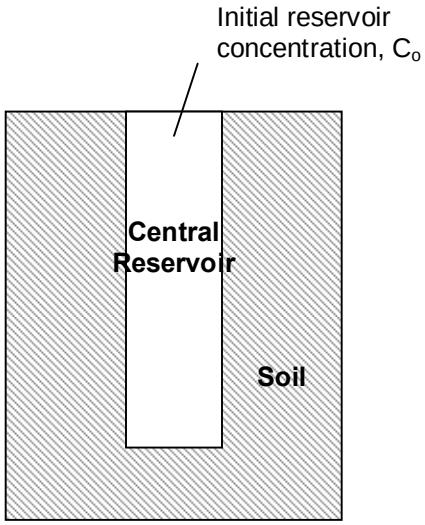

Figure 2.12: Cross section of the radial diffusion cell apparatus, adapted from van der Kamp (1996). Either the solution can have an initial concentration of zero which increases with time (with a spiked soil/sediment), or the reservoir can have an initial concentration of C_o which decreases with time. To obtain true 1-dimensional diffusion, the central reservoir should extend to the bottom of the soil.

The radial diffusion method offers several advantages when studying the diffusive properties of porous media. The geometry of the system allows for the diffusion of the contaminant to occur radially instead of simply one direction through the soil. This decreases the diffusive pathways of the contaminant, and can significantly reduce the duration of the testing period (van der Kamp et al. 1996, Novakowski et al. 1996).

2.10 Summary

In summary, there is little information available on the diffusion and sorption/desorption of PHCs. However, the contaminant transport of organics to natural soils and sediments is well documented. The overall equation that describes the contaminant transport in saturated porous media is found in Equation 2.2, and the derivation of the diffusion-sorption transport is included in Appendix A.

The sorption process is affected by a number of factors, including hysteresis, sorption kinetics, temperature, solids effect, steric hindrance, salting out and hydrophobicity. The sorption coefficient can be measured experimentally, most commonly with the batch test. Sorption isotherms, the relationship between the sorbed mass and dissolved concentration of the sorbate, are empirically derived. Three sorption isotherm models were discussed, including linear, Langmuir and Freundlich. The Langmuir and Freundlich isotherm models are most commonly used in the sorption/desorption of organics.

Steady state diffusion and transient diffusion are described by Fickôs first and second laws, respectively. The diffusive transport of organics through saturated media is affected by a number of factors, including temperature, cosolvency, saline conditions, molecular straining, hydrophobicity, and the inorganic chemistry of the system. Diffusion can be measured experimentally using many methods; column methods, reservoir methods and radial diffusion methods were discussed.

3 MATERIALS AND METHODS

This chapter describes the methods used in the analysis of hydrocarbon mobility from the tailings. For each of the various tailings materials, some or all of the following procedures were carried out:

- Analysis of PHCs in tailings;
- Petroleum hydrocarbon desorption tests; and
- Radial diffusion tests to evaluate the diffusive mobility of PHCs.

In addition, the chemistry of the oil sands process water (OSPW) was evaluated.

Both the experimental procedures and modelling methodology used for the desorption and radial diffusion of the PHCs are discussed. Complete detailed methodologies for each procedure are included in Appendix B.

3.1 Sample Collection

Samples were collected from the Suncor Energy Ltd. mine site north of Fort McMurray, Alberta, in August 2008. Several different types of tailings from the different waste streams and levels of treatment were collected. The tailings samples included tailings sand, Mature Fine Tailings (MFT), Lime-gypsum treated MFT, Polymer treated MFT, and tailings from the area known as Plant 4 Upper Beach. The Plant 4 Upper Beach tailings is waste from a process that is no longer used at Suncor Energy Inc., and samples

were collected from ground surface and at a depth of 1.5m. The tailings sand contains very little hydrocarbon content, as is shown in Figure 3.1. The PT MFT is shown in Figure 3.2.

The only samples that were not collected on site were the composite tailings (CT) samples, which were made for this project at bench scale at CanMET and shipped to the university. The CT samples were mixed at three different sands to fines ratios.

All the samples were collected, shipped and stored in large 20L HDPE pails with airtight lids to prevent moisture from escaping. The tailings were also stored at 1ºC in an environmental control chamber at the university lab.

The following figures are photographs of selected samples collected from the Suncor site: tailings sand in Figure 3.1 and polymer-treated MFT in Figure 3.2. Through the initial visual inspection, the tailings sand appeared to have very little bitumen in it. The polymer-treated MFT appeared to have significantly more residual PHCs present, but was still able to maintain the growth of some barley.

Figure 3.1: A small sample of tailings sands taken from one of Suncor's stockpiles. There is very little bitumen present in the sand.

Figure 3.2: Barley growing from some polymer-treated mature fine tailings (MFT).

3.2 Description of Oil Sands Tailings

The tailings materials analyzed in this study were tailings from the Suncor Energy Inc. (Suncor) mine site in Fort McMurray, Alberta. There were initially 9 different types of tailings material produced and collected at the mine site, with three other tailings mixes produced in small quantities for this project by CanmetENERGY. There were four main types of tailings collected for analysis: tailings sand, mature fine tailings, Plant 4 Beach tailings and composite tailings. In addition, samples of the mineôs process water, which is recycled from the tailings impoundment system, were collected for analysis.

Tailings sand is largely sand mixed with a small amount of residual petroleum hydrocarbon. It results from the treatment of the raw oil sands with hot water, which effectively forces the sand to separate from the oil and drop out. Tailings sand is collected and stored in large piles in the tailings disposal area. The tailings are dewatered until they can be reclaimed (Masliyah et al. 2004). It is hoped that the concentration of oil in this sand is low enough that it can be used in the reclamation process without being detrimental to revegetation.

The Mature Fine Tailings (MFT) are a product of the secondary treatment of the oil sands, and are mostly comprised of fines and liquid effluent. MFT is deposited in the tailings ponds at the mine site, which allows the fines to settle out from the liquid effluent. Three types of MFT were collected from the site: pure MFT with no additives,

MFT with a mixture of lime and gypsum (lime-gypsum or LG MFT) and MFT treated with a polymer additive (polymer-treated or PT MFT).

Plant 4 Beach is comprised of tailings from a process that is no longer used at the mine. It is anticipated that this site can be capped and revegetated in the near future. Three samples of Plant 4 Beach tailings were collected for this study. Plant 4 Upper Beach tailings were sampled from the surface (P4 UB Surface) and another sample of Plant 4 Upper Beach tailings was taken from an augered hole at depth of 1.5m below the surface (P4 UB Auger). A Plant 4 Lower Beach (P4 LB) tailings sample was also collected by Suncor personnel and is evaluated in the study.

Composite Tailings (CT) are a combination of tailings sand and MFT, which is produced on site to decrease the amount of time needed for the fines to separate from the liquid effluent. Suncor has several constructed wetlands made from these composite tailings at their site as part of their reclamation program. Two of the wetlands were sampled for CT, from the 12m CT Pond and the 4m CT Wetland.

Composite tailings are mixed at various sands-to-fines ratios (SFR) by Suncor. Three different mixes were produced by CanmetENERGY to determine if a change in this ratio could significantly affect the mobility of the petroleum hydrocarbons. CT samples with sands-to-fines ratios of 2:1, 4:1 and 6:1 were used in this study. The water content, loss

on ignition, and petroleum hydrocarbon characterization was determined for each of the twelve tailings materials.

Four water samples were also collected from site for a basic ionic analysis. Approximately 30 years ago, two ponds were constructed and filled with mature fine tailings to aid with settling time estimations of the tailings. These ponds were called the North and South Sustainability Ponds. Water from these two ponds, as well as from the 12m CT Pond, was collected for analysis. The process water collected from the tailings ponds was also evaluated for basic chemical parameters and petroleum hydrocarbon content.

3.3 Characterization of Tailings

A detailed characterization of the oil sands tailings was completed, which included both physical and chemical analyses as well as measurement of water content. PHC analysis was completed for each tailings material, in both the supernatant (porewater) and the solid phase of the tailings. Porewater was extracted from the tailings using a compression system and analysed for PHC content. Loss on ignition, which gives an indication of a soilôs overall organic content was also analysed for the tailings.

3.3.1 Hydrocarbon Analysis

Samples of solid and liquid phase material were required for the PHC analysis. In the cases of the tailings with higher water contents, which were more of a slurry than a solid,

it was necessary to remove some of the liquid before the samples could be sent to the lab for analysis.

During the extraction of bitumen from the ore, not all of the bitumen is separated from the sand. At Suncor, naphtha, which acts as a solvent, is added to the slurry during the processing of the bitumen froth to help separate water and solids from the froth (Masliyah et al. 2004). Residual petroleum hydrocarbons, along with varying amounts of other additives used during the extraction process, including naphtha, remain in the tailings materials. Characterizing the amount of petroleum hydrocarbons present in the tailings materials was an important first step to gaining an understanding of the mobility of PHCs in the tailings materials.

Each tailings was analysed for BTEX (benzene, toluene, ethylbenzene and xylenes) and carbon numbers C6 to C50+ using gas chromatography/mass spectrometry (GCMS). Samples were sent to Exova, an external laboratory located in Calgary, Alberta. Since very few PHCs have been individually characterized, the hydrocarbons are divided into fractions based on the number of carbon fractions present in each molecule, in accordance with CCME (2008). The PHC extraction and GCMS analysis follow the method outlined in the CCMEôs *Reference Method for the Canada-Wide Standard for Petroleum Hydrocarbons in Soil – Tier 1 Method* (2001), which are briefly described as follows.

The hydrocarbon analysis varies slightly between C6 to C10 and C10 to C50 hydrocarbons, although both analyses require the use of gas chromatography with flame ionization detector. For C6 to C10, including the BTEX fraction, methanol extraction is used. The soil containing the hydrocarbon is combined with methanol at a ratio of approximately 2:1, the vial is shaken for an hour, and the resulting solution is recovered to be analysed in the GC (CCME 2001).

For C10 to C50 hydrocarbon analysis, the hydrocarbon must first be extracted from the soil particles using a soxhlet extraction apparatus, using 50:50 n-hexane:acetone, for 16 to 24 hours. The water in this extract must be removed using silica gel column cleanup and a 50:50 hexane:DCM (dichloromethane) solvent. Once this cleaned up sample has been reduced to 2mL in a rotovap, it is stored in a GC vial in preparation of gas chromatography with flame ionization analysis (CCME 2001). For the extraction of hydrocarbons from aqueous solution, the soxhlet extraction is not required.

A more detailed method for the extraction of PHCs from soil used in this study and methodology from the external laboratory is included in Appendix B, detailed in both Method B.4 and B.5.

3.3.2 Loss on Ignition

Loss on ignition (LOI) is a simple method to determine total organic content of a given soil, presented in percent. Loss on ignition provides an estimation of organic content and is most useful for determining the organic content of sandy soils. Soils containing high percentages of clay or silt particles may fracture at high temperatures, resulting in the loss of some structural water (Rowell 1994). In this study, the majority of the organic content in the tailings is composed of PHCs, so the loss on ignition provides an indication as to the percent PHC that is present in each tailings material. Loss on ignition was compared to total PHC concentration from the GC analysis for each tailings material to see how much of a correlation there was between total organic content and total PHC concentration.

The loss on ignition was determined using a standard method described in D.L. Rowellôs *Soil Science: Methods and Applications* (1994). Tailings samples oven-dried at 105ºC were ground with a mortar and pestle to ensure an even consistency and a minimum of 5 grams of oven-dried tailings was placed in a small ceramic crucible. Oven-dried weight was recorded and the samples were then placed in a furnace at 550ºC for a minimum of 4 hours. Samples were cooled in a desiccator and then weighed to determine the amount of mass lost in the furnace. A detailed loss on ignition procedure is included in Appendix B.

3.3.3 Water Content

Water content was determined for each of the tailings materials using the standard ASTM method D2216-10, *Standard Test Methods for Laboratory Determination of Water (Moisture) Content of Soil and Rock by Mass* (ASTM, 2010). Tailings samples were placed in aluminum pans of known mass and the wet sample mass was recorded. The pans were placed in a 100ºC to 120ºC oven for several days, until the mass of the sample became constant. The mass of the dried tailings (m_D) was recorded and the geotechnical (dry mass) water content was determined using the relationship in Equation 3.1. The water content of each tailings sample was done in triplicate to ensure accuracy of results.

$$w = \frac{m_w}{m_D} \qquad \text{[Equation 3.1]}$$

w = water content

m_w = mass of water lost (g)

m_D = mass of dried soil (g)

3.3.4 Porewater Hydrocarbon Concentration

Some of the tailings materials were not saturated when they were collected from the Suncor mine, including the tailings sand and lime-gypsum MFT. However, for the radial diffusion experiment, it was necessary to have all the materials saturated to avoid ñpreferential diffusionò through a partially saturated soil matrix. Determining the initial sorbed and aqueous PHC concentrations for each of the tailings materials was also required for the modelling and analysis of the radial diffusion experiment.

Porewater was extracted from the tailings using two different methods. A number of the tailings materials had a higher water content, and almost had the consistency of a slurry. These samples were centrifuged to remove any suspended fines and the resulting supernatant was decanted and sent for GC analysis at the external laboratory. The same GC method was used as described in Section 3.2.1. Centrifugation is a good technique for the extraction of pore water that will be analysed for nonionic organic chemicals (Ankley and Schubauer-Berigan, 1994), such as PHCs.

The porewater from the remaining samples was extracted using a compression porewater extraction apparatus, such as those described by Böttcher et al. (1996) and Jahnke (1988). The details of the apparatus used for the extraction of porewater from the tailings are described by Pratt and Fonstad (2011) and the system is shown in Figures 3.3 and 3.4.

Porewater from the tailings sand, Plant 4 Upper Beach, PT MFT, LG MFT and the 6:1 SFR CT porewater were extracted using this method. The sample container (compression cell) is shown in Figure 3.4 below, and the entire porewater extraction set up is shown in Figure 3.5. Saturated tailings were placed in the compression cell, and then placed in the compression apparatus. The compression was allowed to continue for several hours, and the porewater was collected in a sterile syringe from the collection ports in the bottom of the compression cell.

Figure 3.3: The porewater extraction squeezing apparatus set-up. Clockwise from top left are the completed design, one of the constructed cells, and the base of the cell showing the sampling ports (Pratt and Fonstad, 2011).

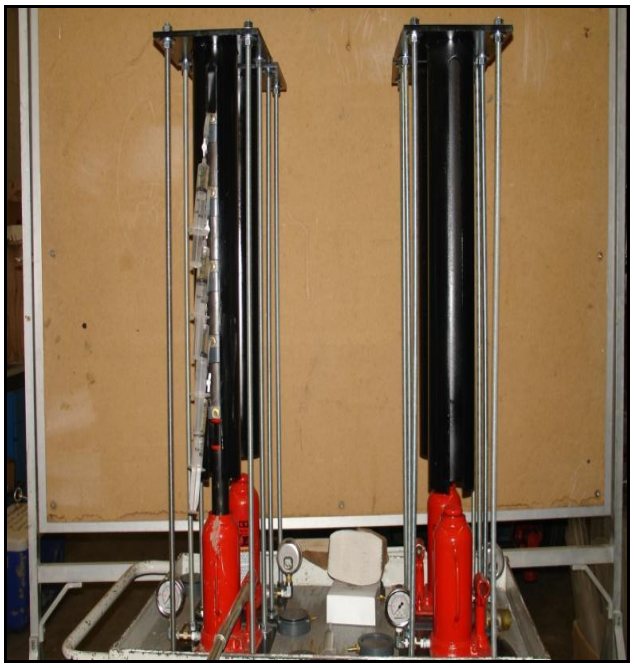

Figure 3.4: Pore water extraction apparatus (Pratt and Fonstad, 2011).

3.4 Characterization of Oil Sands Process Water

The oil sands process water (OSPW) was analysed for PHC content as well as other dissolved ions. PHC analysis was completed at an external laboratory, and ion analysis was completed internally using a spectrophotometer, digital titrator and a flame photometer. Detailed methodology for all tests is included in Appendix B.

The OSPW was analysed for C11 to C50+ at Exova, an external laboratory, using gas chromatography/mass spectrometry (GCMS) methods, as described in Section 3.2.1. Complete laboratory methodology from the external laboratory is included in Appendix B (Method B.5). Dissolved ion analysis was completed for a number of water samples collected from the Suncor minesite. Most of the dissolved ion analysis of the OSPW was completed internally using the DR/4000 Hach Spectrophotometer and the Hach Digital Titrator, Model 16900. Potassium and sodium were analysed using a flame photometer. Each analysis was performed in triplicate. An ion balance was calculated for each of the four water samples to determine if all the major dissolved ions had been accounted for.

3.5 Petroleum Hydrocarbon Desorption

There is no prior research on the desorption of petroleum hydrocarbons from OST materials. Accordingly, in an effort to identify potential factors that might affect the results, a series of trials were completed. In this way, the potential was decreased that the data results reflect artifacts of the experimental design. Such factors evaluated to define

the parameters of the procedure included sample size, temperature and duration of the experiment. Once these factors had been evaluated from the initial data, the experiment for the remaining tailings materials could be conducted.

The procedure used in this study involved three distinct phases, and one additional phase, which was an extension of Phase 3. Figure 3.5 on the following page shows the experiment flow chart, and shows all phases of the experiment. For simplicity, only two of the nine OSTôs were used for the initial two-phase experimental design. The results from these first two phases were then used to determine the best procedure with the remaining seven tailings materials. For the subsequent Phase 3, the remaining tailings materials were used. This section outlines the general procedure used in all phases of the desorption experiment.

Since the testing methodology for PHCs in soil and water required individual sub-samples to be sacrificed at various times, a number of duplicates were used if more than one sampling event was required. In Phase 3 of the experiment, duplicate samples were used to compare the difference in PHC concentrations between the duplicate samples. Detailed methodologies are included in Appendix B for the testing carried out for the Phases 1 to 3C and 3D.

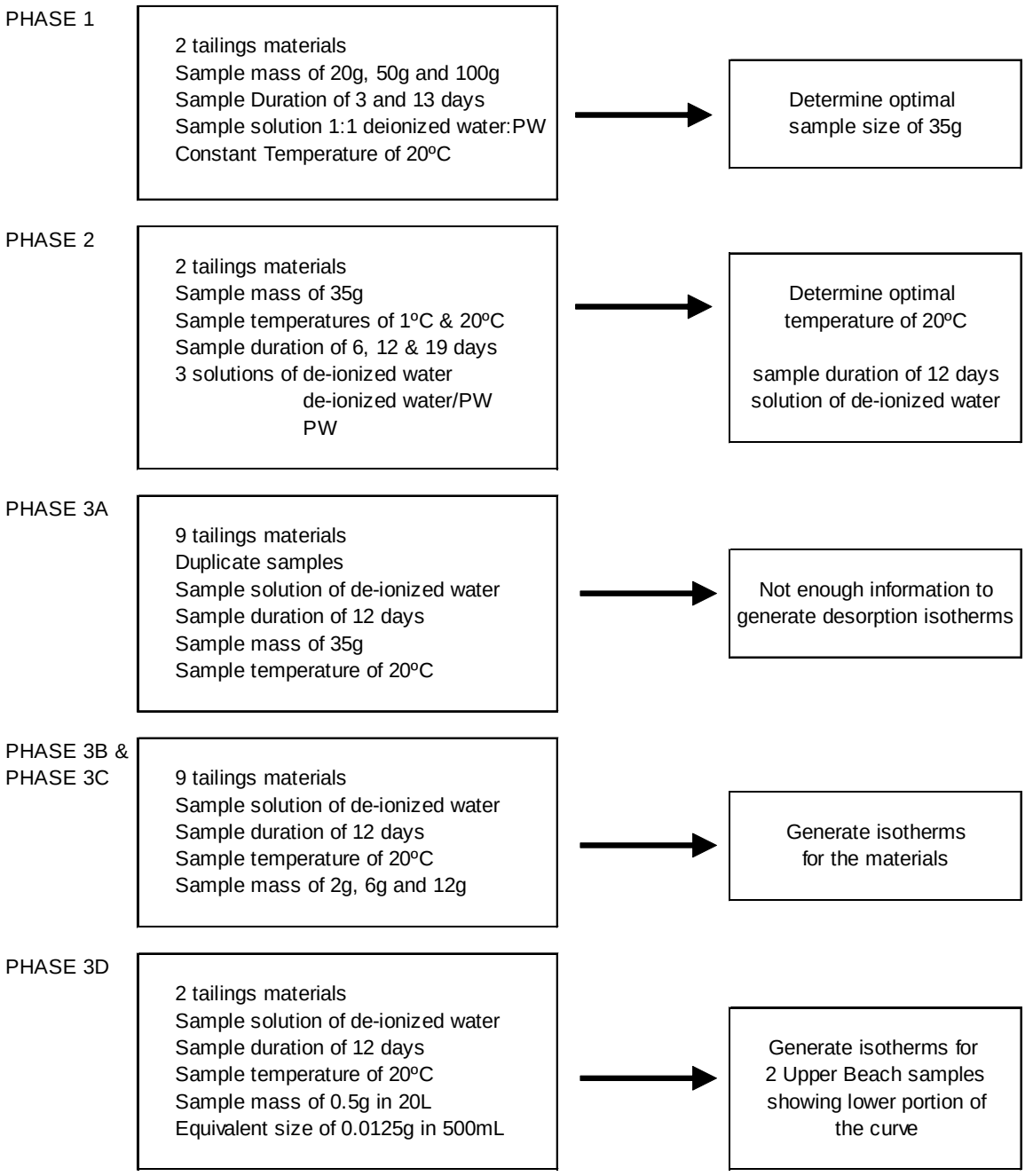

Figure 3.5: Desorption experiment flowchart, showing all phases of the procedure.

3.5.1 General Experimental Procedure, Phases 1 – 3

The desorption of PHCs from the tailings was measured using a batch experiment method, with each sample providing one data point. It is designed to be cost-effective

and reproducible, using 500mL amber glass jars to reduce the adsorption of organics onto the sides of the container. All jars used in the experiment were pre-sterilized and shipped directly from VWR International. A measured amount of wet tailings was added to the sample jar, which was then filled with a solution of varying amounts of de-ionized water or OSPW from the mine site.

In the procedure, the mass of tailings added was identified as a dry weight. However, wet tailings were added to the batch tests, equivalent to a dry weight of tailings and calculated from the measured water content. The following relationship was used to determine the equivalent mass of wet tailings to be added to the samples.

$$Mass\ of\ wet\ tailings = \frac{Mass\ dry\ tailings}{Solid\ content} \qquad \text{[Equation 3.2]}$$

The container was then carefully filled with a solution of OSPW and/or de-ionized water, ensuring that there was no headspace to reduce the possibility of PHC volatilization. Jars were sealed with a Teflon-lined twist on cap, and shaken by hand 2 times per day to facilitate even distribution of the solid suspension through the liquid. Prior to the extraction of the liquid, samples were centrifuged to remove any remaining suspended particles. A clean syringe was used to extract the supernatant from the sample containers, which was analysed for PHC content at a commercial lab. A detailed desorption

methodology for the experiment is included in Appendix B, methods B.4 and B.5. Figure 3.6 below shows some of the prepared samples in the temperature control chamber.

Figure 3.6: Phase 1 desorption samples in the temperature control chamber

a) Phase 1

Phase 1, the initial phase of the experiment, used only two tailings materials, Plant 4 Upper Beach (P4UB) surface sample and P4UB auger sample. The goal was to determine the required desorption time and the optimum sample mass (by dry weight of tailings) to be used in subsequent tests. Three initial sample masses of 20g, 50g and 100g were selected to try and determine the best sample mass for the ensuing phases. Six desorption samples were set up for each of the different tailings materials, with replicates of the 6 samples used to determine the effect of contact time in the solution, for a total

number of 12 samples. Only one solute was used for this phase of testing, a 1:1 de-ionized water/OSPW mix. The samples were kept at a controlled 20ºC temperature for the duration of the experiment.

The desorption experiment was designed such that each separate sample provided one data point, and was sacrificed at a specific time. In Phase 1, the supernatant was sampled using a syringe at two different times, 3 days and 13 days, to try and determine the time required to reach desorption equilibrium. The supernatant was sent to an external laboratory for PHC analysis; results for BTEX and F1-F40+ were obtained for all samples. Once the supernatant was analysed for PHCs, it was determined that the sample mass of 35g (by dry weight) would be used in Phase 2 of the experiment.

b) Phase 2

In Phase 2, the same two tailings materials were used (P4UB surface and P4UB auger). The goal was to determine if there was an effect on the desorption due to moderate differences in temperature and solution mix. The optimal duration for the desorption test had not been conclusively decided from the Phase 1 results, so the experiment duration was set at 3 different time intervals: 6 days, 12 days and 19 days. The sample mass (by tailings dry weight) was set at 35g in 500mL of solution.

Two temperatures were selected, 1ºC and 20ºC. Samples were separated and placed in two temperature control chambers. Three solution mixtures of OSPW and de-ionized water were also selected, pure OSPW, pure de-ionized water and a 1:1 OSPW/de-ionized water mix. The 6-day and 12-day samples were single samples only, with a duplicate for the 19-day samples. Initially, 48 samples were set up, but 7 of the samples were not able to be analysed as the glass sample jars broke during the centrifuge process.

From the Phase 2 results, it was determined the remaining benchtop desorption tests would be conducted at 20ºC in a de-ionized water solution for 12 days. The sample mass was determined to be 35g by dry mass of tailings.

c) Phase 3A to 3C

Using the results obtained in Phases 1 and 2, the desorption of the remaining 9 tailings materials was analysed in Phase 3. All samples used de-ionized water at 20ºC for 12 days. To reduce analytical costs, duplicate tests were set up only in Phase 3A, which used the 35g sample mass. Tests were also completed for sample masses of 2g, 6g and 12g. These results were used to develop individual desorption isotherms.

3.5.2 Experimental Procedure, Phases 3D

To obtain data for the lower portion of the isotherm curves for the two upper beach samples, it was necessary to alter the procedure. Small sample masses in the batch tests, in the order of 0.5g to 2.0g, were already getting results that were very close to or at the analytical detection limits for PHCs. In order to obtain values below this detection limit, a much larger volume batch sample was used, and the resulting solute was passed through a filter to recover the desorbed PHCs from the solution.

It was necessary to increase the volume of de-ionized water solution and decrease the mass of the sample to get an equivalent sample mass of 0.0125g in 500mL. Therefore, large 20-litre HDPE pails were used instead of the 500 mL batch test jars to increase the amount of water. A sample mass of 0.5g of tailings was added to each of these 20 L vessels, to give the equivalent batch test mass-volume of 0.0125g of tailings in 500 mL. Due to the large size of the sample container, it was not possible to agitate the tailings throughout the duration of the experiment.

At the end of the 12 days, each of the two 20 L of solute were passed through 3M EmporeÊ extraction disk filters to extract any PHCs from the solution. The disk filters are specific to the extraction of oil and grease from aqueous solutions. The filter extraction was essentially a pre-concentration step for analysis of the expected very low concentration. The two filters were sent to Exova, an external laboratory, for PHC

extraction and analysis. The detailed procedure for the extraction of the hydrocarbons from the solution is included in Appendix B, method B.6.

3.5.3 Desorption Isotherm Modelling

The experimental desorption results were modeled as ñLangmuirò or hyperbolic sorption isotherms. This method was derived for use in sorption, and for the purposes of the mathematical isotherm model, it was assumed that sorption and desorption processes are completely reversible. The Langmuir method assumes that there are a finite number of sorption sites on a solid surface, or in the case of this experiment, a finite number of desorption sites from the solid surface. Equilibrium in the system is reached once all the sorption/desorption sites have been completely filled/emptied and no more solute can be sorbed/desorbed from the solution (Fetter, 1999). The Langmuir isotherm is described by the following equation:

$$\frac{C}{S} = \frac{1}{\alpha\beta} + \frac{C}{\beta} \qquad \text{[Equation 3.3]}$$

C = concentration of solute in the solution (mg/L)

S = mass of solute sorbed onto the solid surface, per mass of solid (mg/kg)

Ŭ= adsorption constant related to binding energy (L/mg)

ɓ = the maximum amount of solute that can be absorbed by the solid (mg/kg)

The value of C was determined through GCMS analysis, and the corresponding value of S was calculated from the known initial PHC content of the each of the tailings material.

The values of Ŭ and ɓ were determined with a plot of C vs. C/S. The two adsorption constants were calculated from the slope and intercept of this plot (Fetter, 1999) for each of the tailings materials. Refer to Section 2.3.2 for a full explanation of Langmuir sorption isotherm theory.

3.6 Radial Diffusion of Petroleum Hydrocarbons

The second experiment used fewer tailings materials than the desorption batch tests; the diffusion rates of 7 different tailings materials was observed. A single reservoir radial diffusion method was used to determine the diffusion coefficient. The radial diffusion was completed over a number of weeks, as only ten diffusion cells could be set up at the same time. Each of the tailings materials had three diffusion cells, for a total of 21 diffusion cells. Each of the cells was designed to provide one data point on the time versus concentration diffusion curve. Reservoir samples were collected after 3, 6 and 10 days of diffusion.

The tailings chosen for analysis were 2:1 SFR CT, 4:1 SFR CT, 6:1 SFR CT, MFT, LG MFT, PT MFT and tailings sand. Not all of the tailings were used to reduce the length of time needed to complete the experiment and analysis.

Shackelford (1991) lists several methods for completing diffusion testing in the laboratory; it is this basic method for decreasing source concentration in a single cell

reservoir that will be used in the batch testing. However, additional testing methods were consulted with respect to disturbed samples and the diffusion of volatile organic compounds.

The diffusion coefficient was determined using only the time versus concentration data for the receptor reservoir. In many diffusion single-cell tests, the soil is divided into equal parts to determine the concentration profile of the soil. However, this is difficult to do, as many of the solutes were potentially volatile and reactive, and the time to measure the concentration profile of the soil would be lengthy (Shackelford, 1991 and Myrand et al., 1992). Several of the tailings materials have a consistency closer to a slurry than a true soil, which would also make it difficult to determine a concentration profile by dividing the soil.

The time versus concentration diffusion results were modeled using a Finite Difference Method (FDM) model. The desorption isotherms and corresponding hyperbolic desorption coefficients were used in the diffusion model as the adsorption component of the contaminant transport process. The model was fitted to the experimental data by minimizing the calculated Root Mean Square Error between the data points and the model.

3.6.1 Experimental Procedure

a) Radial Diffusion

The diffusion tests were in a single cell radial diffusion reservoir using a disturbed sample of tailings. Diffusion cells were constructed with 4.55-litre HDPE pails and custom made cylindrical stainless steel mesh tubes. Three diffusion cells were constructed for each of the seven tailings materials, for a total of 21 cells, to be sampled at 3, 6 and 10 days. A detailed methodology of the construction and subsequent sampling of the diffusion cells is included in Appendix B.

Only 10 cells could be constructed at one time due to the limited number of stainless steel mesh tubes. Each diffusion cell was constructed to be one-time use only, with the entire contents of the reservoir sampled at one time. The cells were placed in a temperature control chamber at 20ºC for the duration of the experiment and conductivity was measured on a daily basis to monitor the relative rate of diffusion into the reservoir. The design of the diffusion cells is shown in Figure 3.5.

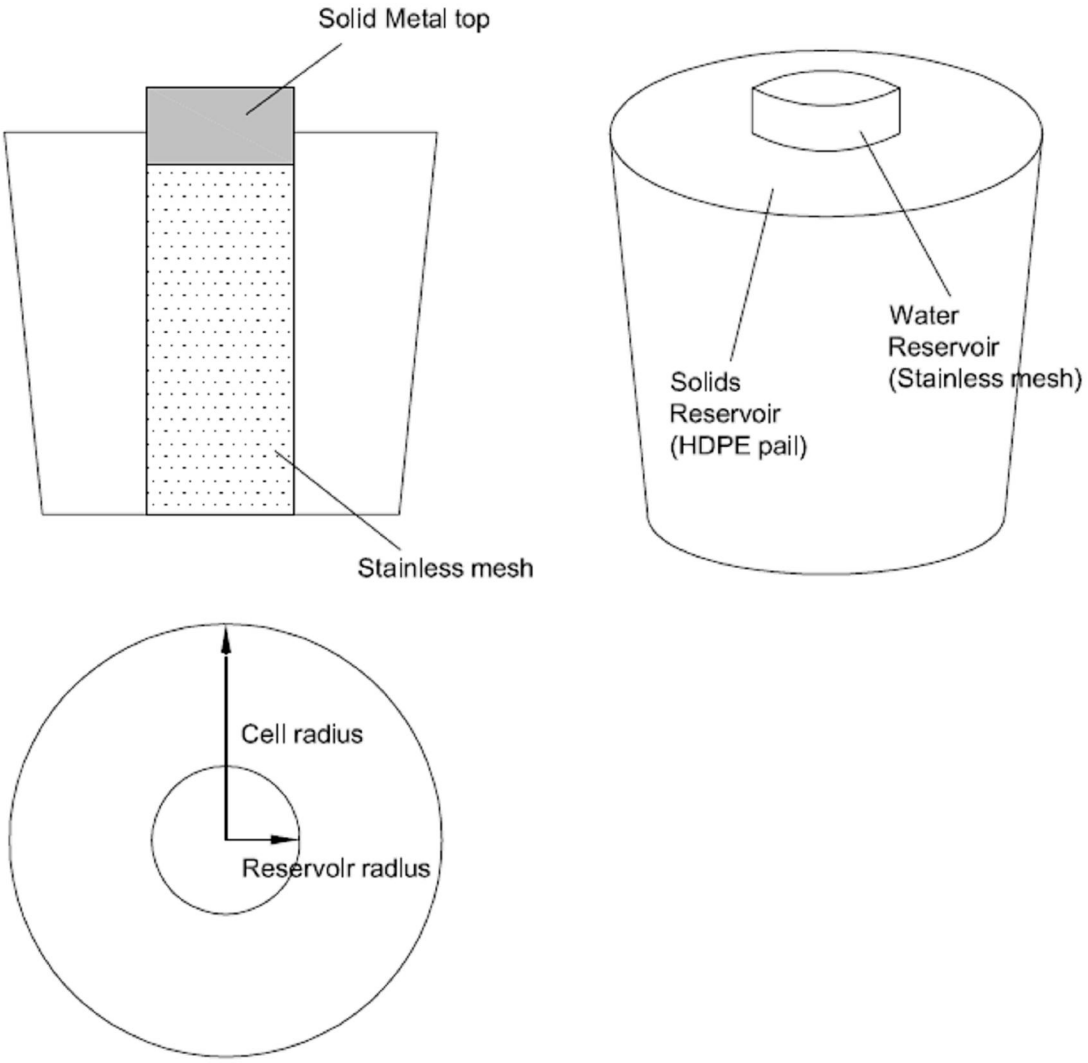

Figure 3.7: Cross-sectional, profile and plan views of the radial diffusion cells. The tube diameter is 3 inches (76.2 mm). The pail used is a 4.55-litre HDPE pail with a snap-on lid.

Porosity was determined for each of the tailings samples from the phase relationship equations shown in Equation 3.4(a) and (b) (Craig 2004).

(a) $w\, G_s = e\, S_r$ (b) $n = \dfrac{e}{1+e}$ [Equation 3.4]

w = gravimetric water content

G_s = specific gravity of the soil particles

e = void ratio (ratio of the volume of voids to the volume of solids)

S_r = degree of saturation (this is equal to 1 when a soil is fully saturated)

n = porosity (ratio of the volume of void to the total volume)

Each of the tailings samples used in the diffusion cells were fully saturated, meaning that the degree of saturation was equal to 1. The specific gravity of the soil particles was estimated to be 2.65, which is a good approximation as most clays and sands range from 2.65 to 2.75.

The porosity of each tailings material was not varied with changing r values; it was assumed to be constant throughout the tailings sample. The tailings materials were well mixed before they were placed in the diffusion cells, and the nature of the material (i.e. a by-product of oil sands ore processing) meant that the material can be considered to be homogeneous and that porosity can be assumed to be constant throughout.

b) Hydrocarbon Extraction

PHC extractions and analysis were completed internally at the National Hydrology Research Centre (NHRC) in Saskatoon, using GC analysis. Only F2 and F3 fractions were analysed at their facility. F2 and F3 fraction hydrocarbons are smaller in size than the higher fractions, and thus considered more mobile, and therefore more applicable in a

diffusion experiment. Based on the PHC characterization results of the porewater and soil, it is likely that the majority of the PHCs in the tailings are in the F2 and F3 range and not the F1, BTEX or F4 range. The mobility of PHCs is highly dependent on aqueous solubility, which has been shown to decrease in PHCs as molecular size increases (Nadim et al. 1999), which is why F4 was not analysed. Based on the low concentrations of BTEX and F1 in the PHC characterization of the tailings, it was thought that if any BTEX or F1 were present, it would be in low concentrations and would not significantly affect the measured diffusion rate. Due to the decision not to analyze either BTEX or F1, the diffusion cells were constructed with a simpler design, which included some headspace in the water reservoir.

The method for PHC extraction was based on the Canadian Council for the Ministers of the Environment (CCME) *Reference Method for the Canada-Wide Standard for Petroleum Hydrocarbons in Soil* (CCME 2001). Each sample was extracted at an NHRC laboratory using the same extraction methodology. For a detailed procedure, see the *Petroleum Hydrocarbons in Water Extraction Procedure* in Appendix B.

PHC concentrations were determined using gas chromatography at NHRC. The integral of the area between the peaks of carbon number was calculated to give concentration values for each carbon number.

3.6.2 Modelling Methodology

The radial diffusion was modeled using the 1-dimensional adsorption-diffusion equation with a Finite Difference numerical analysis in spreadsheet format. Each F2 and F3 fraction for the seven tailings was analysed separately, and a diffusion coefficient for each fraction was determined with the model. The adsorption-diffusion equation was converted from Cartesian coordinates to Polar coordinates, as the experiment was radial and could be calculated using axi-symmetric methods. The partial differential equation (PDE) for the adsorption-diffusion equation for 1-dimension in Cartesian coordinates has the form shown in Equation 3.5 (Shackelford 1991 and Fetter 1999).

$$\frac{\partial C}{\partial t} = D^{*}\left(\frac{\partial^2 C}{\partial x^2}\right) - \frac{\rho_B}{n} K_D \frac{\partial C}{\partial t} \qquad \text{[Equation 3.5]}$$

(Diffusion) (Adsorption)

Where:

C = concentration in the reservoir

D* = effective diffusion coefficient

ρ_B = bulk density of the soil

n = porosity of the soil

K_D = adsorption coefficient

x = linear distance

However, in this case the diffusion occurred radially, so the adsorption-diffusion equation must be converted to polar coordinates. The full derivation for the diffusion term is included in Appendix A. Only the diffusion term, which contains an ñxò value, must be converted. The PDE for the diffusion-adsorption in polar coordinates takes the form shown in Equation 3.6.

$$\frac{\partial C}{\partial t} = D * \left(\frac{\partial^2 C}{\partial r^2} + \frac{1}{r} \frac{\partial C}{\partial r} \right) - \frac{\rho_B}{n} K_D \frac{\partial C}{\partial t} \qquad \text{[Equation 3.6]}$$

(Diffusion) (Adsorption)

Where:

r = the length of the radius from the reservoir

Using a Finite Difference Method, the solution of the PDE can be approximated. The derivatives are effectively replaced in the PDE by finite difference approximations (LeVeque 2007), and porosity and bulk density values were determined for each of the tailings materials. The best fit Langmuir isotherm coefficients, which were determined from the desorption batch tests, were also used in the FDM. By varying the value of the effective diffusion coefficient, in this case the only unknown, and plotting the model against the experimental data, it was possible to find a best fit effective diffusion coefficient for each of the PHC fractions (F2 and F3) using the Root-Mean-Square-Error (RMSE) method .

The FDM approximation of the 1-D adsorption-diffusion PDE equation used in the diffusion-adsorption model is of the form shown in Equation 3.7:

$$C_P = C_B + \Delta t D * \left[\frac{\left(\frac{C_C - 2C_B + C_A}{\Delta r^2} + \frac{1}{r}\left(\frac{C_C - C_B}{\Delta r} \right) \right)}{1 + \frac{\rho_B}{n}\left(\frac{\alpha\beta}{1 + \alpha C_B} \right)} \right] \qquad \text{[Equation 3.7]}$$

Two boundary conditions were also defined, one at the inner reservoir, and the second at the outer boundary of the diffusion cell. Both boundary conditions are further defined in Appendix A. At the inner reservoir, a conservation of mass condition was used to determine the flux into the reservoir using Fickôs First Law (refer to section 2.7.1). Cumulative concentration could then be calculated into the reservoir. The outer boundary of the diffusion cell represents a zero-flux condition, and a reflection function can be introduced at the boundary to determine the concentration at the boundary as there is no change in concentration at the boundary with changing r-values.

4 RESULTS AND DISCUSSION

This chapter describes the results obtained from the analysis of hydrocarbon mobility from the oil sands tailings. For each of the various tailings materials, some or all of the following results are discussed:

- Characterization of the various tailings materials and the oil sands process water
- Desorption of PHCs from oil sands tailings
- Diffusive transport of PHCs in oil sands tailings

All the tailings materials were included in the initial characterization. Results from the water content/solids content, loss on ignition (LOI) and PHC characterization of the tailings materials, as well as the results of the basic ionic analysis and PHC content of OSPW, are included here. Only 9 of the tailings materials were included in the desorption batch tests, whose results include Langmuir sorption isotherms and Langmuir coefficients for each material for both the F2 and F3 PHC fractions. Diffusion coefficients were estimated for the F2 and F3 PHC fractions in 7 tailings materials.

4.1 Tailings Characterization

4.1.1 Petroleum Hydrocarbon Content

The oil sands tailings materials were analysed using gas chromatography at an external laboratory to determine the extractable hydrocarbons. A summary of the results, grouped

by CCME fraction and presented in mg of PHC per kg of dried tailings, is presented in Table 4.1. Detailed results, presented by carbon number, have been included in Appendix C. Generally, soils do not have many PHCs in the C50+ range and the CCME standards therefore do not address such PHCs, but in the case of oil sands tailings the C50+ range is significant due to the bitumen content, and this fraction has thus been included.

Table 4.1: Extractable Hydrocarbons (in mg/kg and percent of total PHC) of Athabasca Oil Sands Tailings

Tailings Material	F1 (C6-C10)		F1 (BTEX)		F2 (C10-C16)	
	mg/kg	% of total	mg/kg	% of total	mg/kg	% of total
MFT	1,540	1.51	1,510	1.48	10,900	10.7
LG MFT	n/a	n/a	n/a	n/a	5,360	11.6
PT MFT	n/a	n/a	n/a	n/a	5,160	11.6
P4 UB Surface	7	0.06	7	0.06	922	7.3
P4 UB Auger	0	0.00	0	0.00	745	9.0
P4 LB	3,050	3.23	2,790	2.96	9,930	10.5
Tailings Sand	n/a	n/a	n/a	n/a	36.0	3.3
2:1 CT	415	1.09	384	1.01	4,150	10.9
4:1 CT	205	0.74	182	0.66	3,090	11.2
6:1 CT	207	1.43	193	1.33	1,550	10.7
4m CT Pond	n/a	n/a	n/a	n/a	3,370	6.8
12m CT Pond	n/a	n/a	n/a	n/a	46.0	3.2

Table 4.1 (continued): Extractable Hydrocarbons (in mg/kg and percent of total PHC) of Athabasca Oil Sands Tailings

Tailings Material	F3 (C16-C34)		F4+ (C35-C50+)		Total PHC
	mg/kg	% of total	mg/kg	% of total	mg/kg
MFT	46,800	45.9	44,600	43.7	102,000
LG MFT	20,100	43.4	20,800	44.9	46,300
PT MFT	19,900	44.6	19,500	43.7	44,600
P4 UB Surface	5,640	44.8	6,080	48.3	12,600
P4 UB Auger	3,850	46.4	3,700	44.6	8,290
P4 LB	55,100	58.4	29,300	31.1	94,300
Tailings Sand	500	45.5	566	51.5	1,100
2:1 CT	19,200	50.4	14,700	38.6	38,100
4:1 CT	12,600	45.7	12,000	43.5	27,600
6:1 CT	6,600	45.5	6,350	43.8	14,500
4m CT Pond	23,500	47.8	22,400	45.5	49,200
12m CT Pond	1,090	75.2	316	21.8	1,450

Figure 4.1 on the following page compares the F2, F3 and F4+ fractions of the tailings materials. The results indicate that Plant 4 Lower Beach sample has the highest F3 fraction, while the MFT exhibited the highest F4+ fraction. The PHC fractions of LG MFT and PT MFT are very similar, which is not surprising since both materials are composed of similar amounts of MFT with different additives. The Plant 4 Upper Beach samples are similar as well, with differences in concentration likely due to variations of PHCs in the produced tailings. The composite tailings show a decreasing trend in PHC content from 2:1 CT to 6:1 CT, which is due to the amount of MFT added to each mixture (i.e. more MFT is in the 2:1 CT mix).

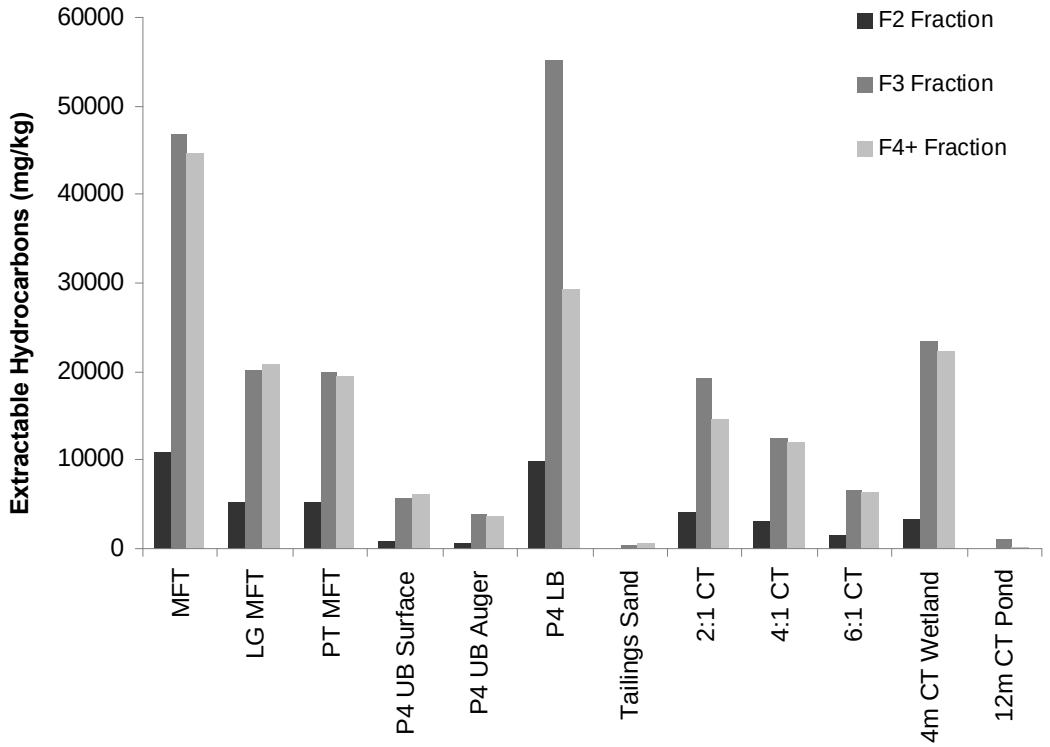

Figure 4.1: Petroleum hydrocarbon content of Athabasca oil sands tailings; F2, F3 and F4+ fractions.

4.1.2 Loss on Ignition

The loss on ignition was determined for each of the tailings materials, and an incremental LOI was also completed for most of the tailings. The results for LOI at 550ºC are shown below in Table 4.2 and in Figure 4.2, and the incremental LOI results are shown in (a) and (b) of Figure 4.3.

As with the water content, each material's LOI was measured in triplicate. The average LOI values at 550ºC are shown in Figure 4.2. Incremental LOI was also determined, with measurement of the amount of material lost taken at 80ºC, 125ºC, 250ºC, 400ºC and

550ºC. The purpose of the incremental LOI was to help determine the nature of the organic content of each tailings sample. It was determined that only one of the MFT samples would need to be evaluated in the incremental LOI. This is due to the fact that they are very similar tailings, the only difference being the addition of a polymer or a lime-gypsum mix to the original MFT.

In Figure 4.3, normalized (a) and average (b) incremental LOI results are presented; results were normalized using the 550ºC LOI value of each separate tailings material. All tailings exhibit similar organic content when normalized, as they all appear to fall within a narrow range of values, with Plant 4 Lower Beach at the upper limit and Tailings Sand at the lower limit of the LOI envelope.

Table 4.2: Loss on ignition results for Athabasca Oil Sands Tailings at 550ºC.

Material	LOI (%)
MFT	17.89
LG MFT	18.32
PT MFT	19.62
P4 Upper Beach	3.55
P4 Upper - Auger	4.21
P4 Lower Beach	42.77
Tailings Sand	0.57
2:1 SFR CT	6.99
4:1 SFR CT	7.03
6:1 SFT CT	4.18
4m CT Wetland	16.42
12m CT Pond	5.41

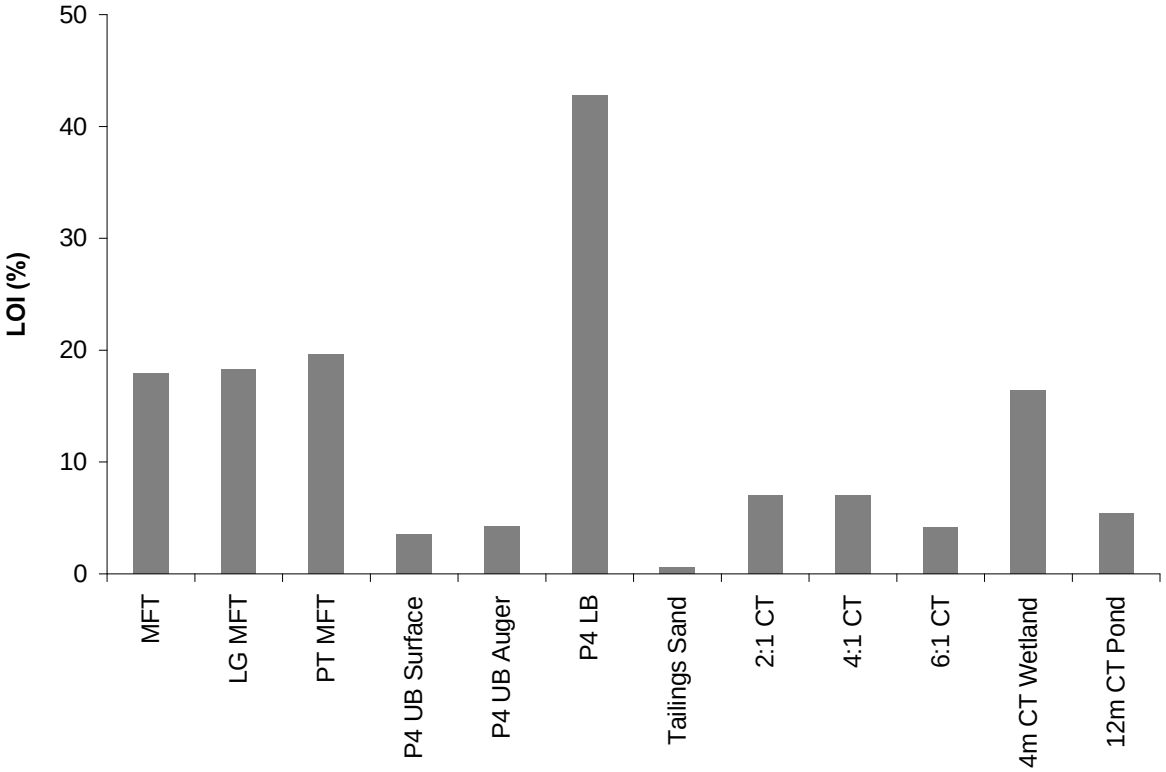

Figure 4.2: Loss on ignition of Athabasca oil sands tailings at 550ºC.

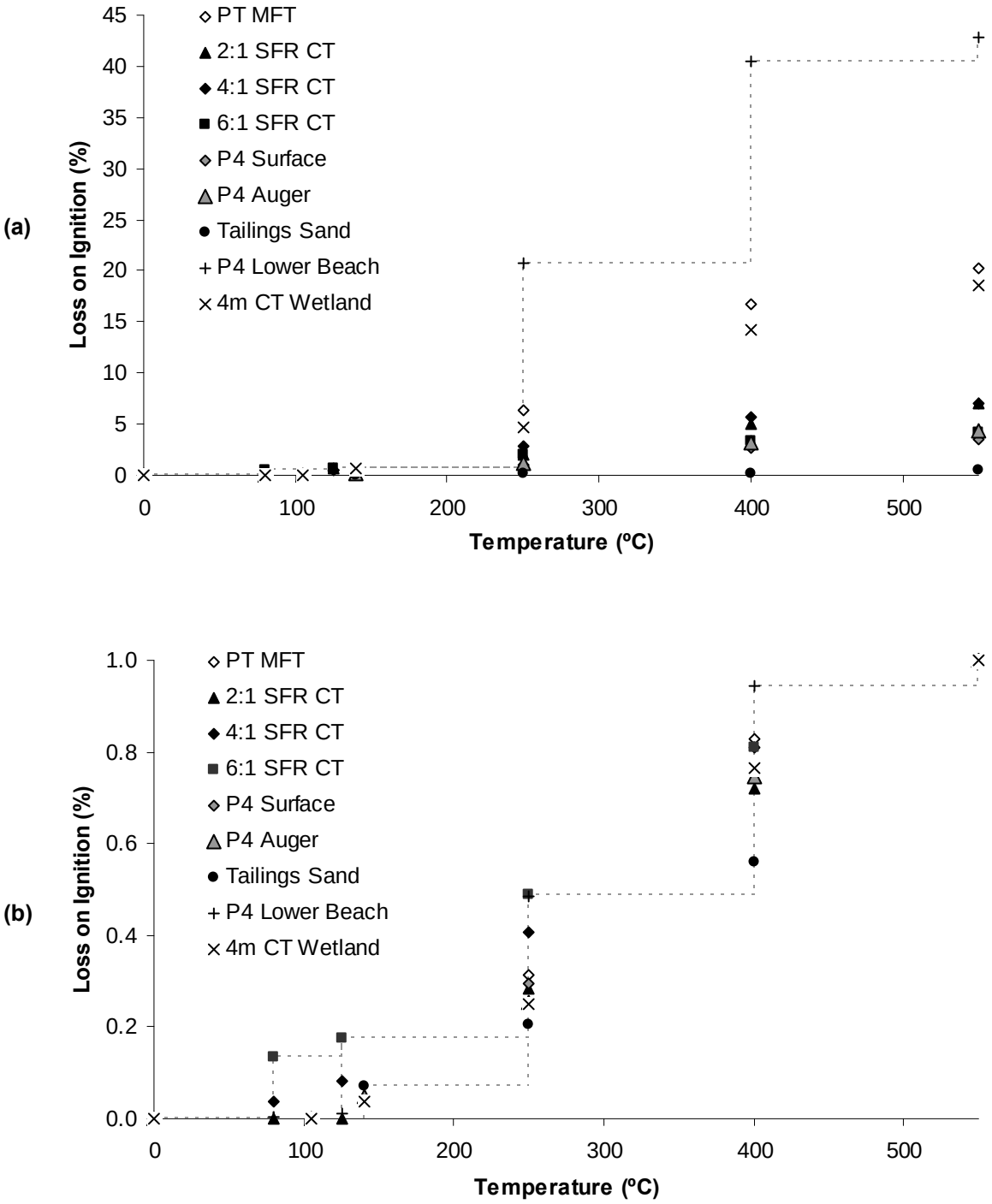

Figure 4.3: Incremental temperature loss on ignition (in percent) for Athabasca oil sands tailings, showing both (a) average LOI values, and (b) normalized by the 550ºC LOI value of each tailings.

The difference in organic content between the three MFT tailings can be attributed to volatilization and/or oxidation losses from the surface sample. The MFT materials had LOI values of 17.89, 18.32 and 19.62 for MFT, LG MFT and PT MFT, respectively. It is probable that the LG MFT and PT MFT have a slightly higher LOI because of the additives of lime-gypsum or polymer to the tailings, although this was not confirmed in this study. The tailings sand had very little visible petroleum residue, and the low LOI of 0.57 confirms that there was little organic matter present.

LOI values were measured for five CT samples, including two *in situ* samples collected from a constructed wetland and a CT pond on the Suncor mine site. The LOI for the 2:1 SFR CT, 4:1 SFR CT and 6:1 SFR CT were 6.99, 7.03 and 4.18, respectively. The 12m CT Pond sample had a very similar result of 5.41, but a value of 16.42 was measured from the 4m CT Wetland sample. The 4m CT Wetland sample was collected from sediment in a constructed wetland at the mine site. The wetland is shown in Figure 4.4 below. The LOI results indicate that there is a higher organic content present in the sample; it is most likely that this is not simply due to petroleum hydrocarbons, but also from decomposing vegetation and animal life present in the wetlands.

4.1.3 Relationship between PHC Content and LOI

The relationship between LOI values and the petroleum hydrocarbon content of each tailings material was also determined. The extractable hydrocarbon values obtained from

the analytical laboratory, in mg PHC per kg dry tailings, were converted to percent, and then compared to LOI values using percent difference (USEPA 2004).

$$\%\ Difference = \frac{|x_1 - x_2|}{(x_1 + x_2)/2} \times 100 \qquad \text{[Equation 4.1]}$$

The percent difference results are included in Table 4.3 below, along with a calculated ratio between the LOI and percent PHC values. Determining the extractable petroleum hydrocarbon content of tailings materials can be time consuming and cost-prohibitive. The calculated ratio between LOI and percent PHC could be used to estimate the PHC content of other tailings materials not included in the scope of this study. The average value of the comparison ratio (excluding the anomaly of the 12m CT Pond) is 3.5.

Table 4.3: Percent difference and ratio between %PHC and average LOI

Material	% Petroleum Hydrocarbon	Average LOI (%)	% Difference	Ratio (LOI:PHC)
MFT	10.23	17.89	54.4	1.7
LG MFT	4.63	18.32	119.4	4.0
PT MFT	4.46	19.62	126.0	4.4
P4 UB Surface	1.26	3.55	94.9	2.8
P4 UB Auger	0.83	4.21	134.2	5.1
P4 LB	9.43	42.77	127.7	4.5
Tailings Sand	0.11	0.57	134.8	5.1
2:1 CT	3.81	6.99	58.9	1.8
4:1 CT	2.77	7.03	87.0	2.5
6:1 CT	1.45	4.18	97.1	2.9
4m CT Wetland	4.92	16.42	107.8	3.3
12m CT Pond	0.15	5.41	189.5	37.2

The percent difference indicates that the LOI values and percent PHC values are quite different, so these values were plotted against each other to evaluate the correlation, as shown in Figure 4.4. The R-squared value of 0.693 indicates that the data points are fairly well represented by a linear trend line with a slope of 3.5 (LOI/PHC).

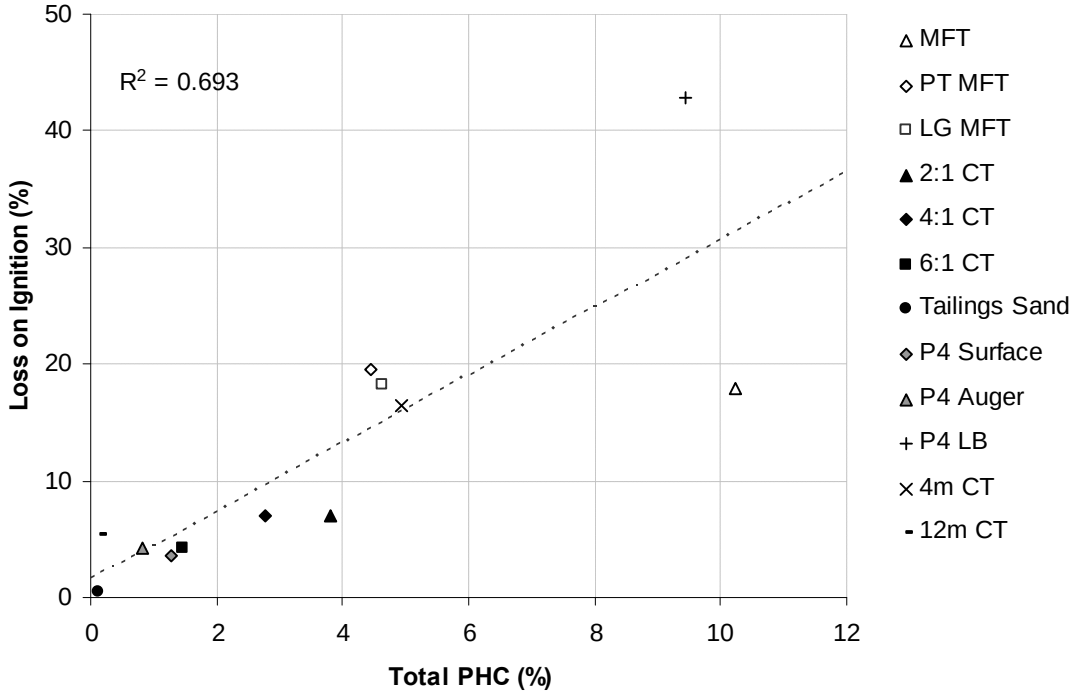

Figure 4.4: Comparison of percent petroleum hydrocarbon to loss on ignition for Athabasca oil sands tailings.

4.1.4 Solids and Water Content

Each tailings material dried in a 110-degree Celsius oven, as any mass loss at this temperature is considered to be water, in accordance with ASTM D2216-10 *Standard Test Methods for Laboratory Determination of Water (Moisture) Content of Soil and Rock by Mass* (2010). Although some of the lighter, more volatile PHC fraction may

have been lost in the drying process, the PHC characterization results indicate that it is the F2 and higher fractions that comprise the bulk of the PHC content. The gravimetric water content of each tailings material is presented in Table 4.4, as well as the total water content and the solids content. The solids content is provided because of the extremely high water content of the MFT, which can be considered a "suspended solid" and not a true soil. For precision, each material's water content was measured in triplicate.

Table 4.4: Gravimetric Water Content, Total Water Content and Solids Content of Tailings. All results are given in percent (%).

Material	Gravimetric Water Content (M_w/M_s)	Total Water Content (M_w/M_T)	Solids Content (M_s/M_T)
MFT	300.0	74.53	25.47
LG MFT	39.33	28.22	71.78
PT MFT	51.47	33.95	66.05
P4 UB Surface	1.99	1.95	98.05
P4 UB Auger	11.73	10.39	89.61
P4 LB	35.70	26.29	73.71
Tailings Sand	6.95	6.49	93.51
2:1 SFR CT	72.05	41.88	58.12
4:1 SFR CT	46.76	30.90	69.10
6:1 SFT CT	28.04	21.90	78.10
4m CT Wetland	50.22	33.42	66.58
12m CT Pond	34.91	25.87	74.13

4.2 Process Water Characterization

Water used in the bitumen extraction process from oil sands is recycled through the tailings pond system. Samples of Process Water (OSPW) were collected from the Suncor

mine site and a basic ionic analysis and PHC content characterization was completed. Water from three other sources, the 12m Composite Tailings Pond (12m CT Pond), the North Sustainability Pond (NSP) and the South Sustainability Pond (SSP), were also collected for basic ionic analysis at the university labs. The NSP and SSP are ponds that were constructed 30 years ago, and filled with MFT as a way for Suncor to try and evaluate the settlement of the MFT without additives. No inputs other than rainwater and other surface runoff have been added to the sustainability ponds.

The process water was also evaluated at an outside laboratory as a quality control check. A quality control analysis was completed to determine the accuracy of the results, which included comparison of the internal (University of Saskatchewan) and external (ALS Laboratories) results, and calculation of the ion balance from all results.

4.2.1 Basic Ionic Analysis

A basic ionic analysis was completed for four different water samples from the site. The analysis for all four waters was completed at the university, and a sample of Process Water was also sent to ALS Laboratories as a quality control check. The ion balance was calculated for each sample using the relationship in Equation 4.2 (USEPA 2004), where the concentration of cations and anions is in meq/L.

$$Ion\ Balance = \frac{\left|\sum cations - \sum anions\right|}{\sum cations + \sum anions} \times 100 \qquad \text{[Equation 4.2]}$$

The total cations and total anions in solution must be equal. The calculated ion balance helps to determine if all the major cations and anions have been included in the analysis of the water. The results of the analysis are presented in Table 4.5.

Table 4.5: Ionic analysis of five Athabasca oil sands site waters: Process Water, 12m CT Pond, North Sustainability Pond and South Sustainability Pond

Chemical Species	OSPW (U of S)	OSPW (ALS)	OSPW RPD (%)	12m CT Pond	NSP	SSP
Potassium (mg/L)	9.50	13.9	37.6	36.8	13.5	13.8
Sodium (mg/L)	521	585	11.6	521	590	412
Manganese (mg/L)	3.20	0.00	200	5.80	0.100	0.00
Total Nitrogen (mg/L)	20.3	n/a	n/a	20.2	0.200	0.300
Ferrous Iron (mg/L)	0.00	n/a	n/a	0.100	0.100	0.00
Sulphate (mg/L)	209	228	8.70	3030	614	483
Alkalinity (mg/L)	594	684	14.0	67.0	388	162
Ammonia (mg/L)	18.0	n/a	n/a	19.1	2.90	1.80
Chloride (mg/L)	207	354	52.5	538	27.7	14.8
Calcium Hardness (mg/L)	29.2	12.0	83.5	1170	65.0	48.3
Conductivity (mS/cm)	2.77	n/a	n/a	5.63	1.63	0.868
Total Hardness (mg/L)	48.8	61.0	22.2	2250	367	163
Magnesium (mg/L)	19.6	7.60	88.2	1090	302	115
Iron (mg/L)	0.00	0.400	200	0.00	0.00	0.00
Volatile Acids (mg/L)	98.3	n/a	n/a	312	219	700
Total Cations (meq/L)	25.0	27.0	n/a	68.8	33.34	21.5
Total Anions (meq/L)	29.5	33.2	n/a	143	21.53	23.8
Ion Balance (%)	0.30	15.1	n/a	10.5	14.6	8.00

The most significant concentrations present in the waters are sodium, sulphate, alkalinity, chloride, calcium hardness, total hardness and magnesium. Figure 4.5 presents the difference in these species in the various depositional areas of the minesite. The ion balance values indicate that the major ions have been included in the analysis.

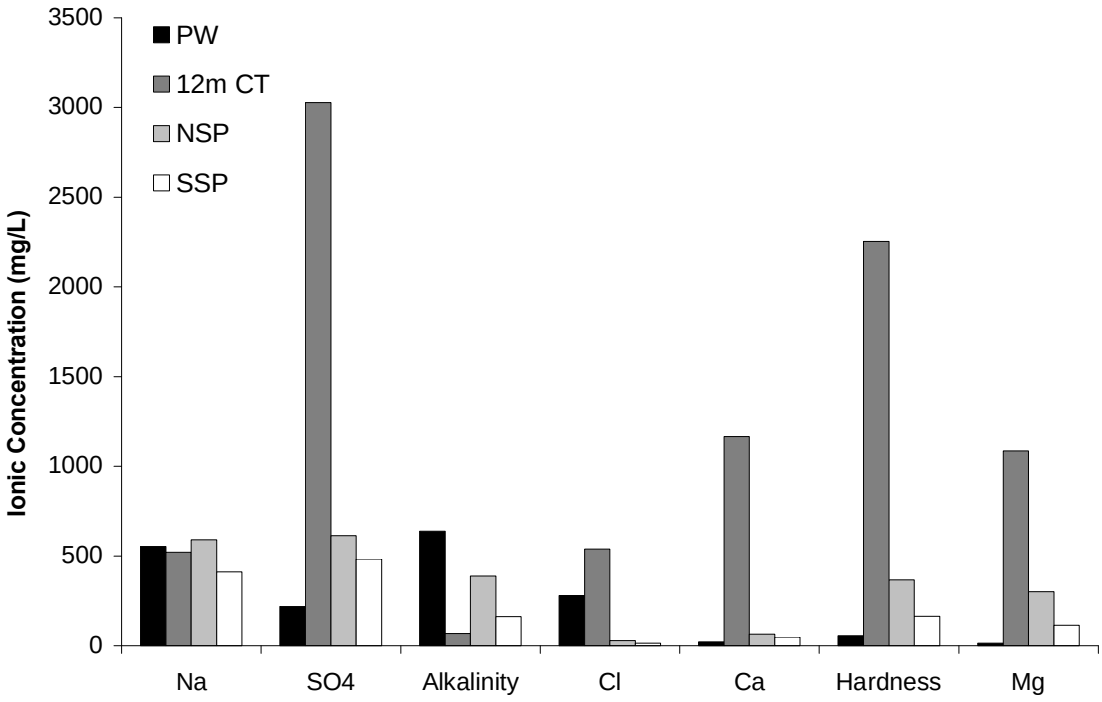

Figure 4.5: Aqueous concentration of major ions in Athabasca Oil Sands Process Water (OSPW), 12m CT Pond water (12m CT), North Sustainability Pond (NSP) water and South Sustainability Pond water (SSP).

The water sampled from the 12m CT Pond had the highest concentrations of all the major species except sodium and alkalinity, where all samples had similar sodium concentration values, but the alkalinity of the 12m CT pond was significantly lower. The results of the sustainability ponds (NSP and SSP) are less surprising, as it is expected that the amount of rainwater inflow over a period of approximately 30 years would significantly dilute ionic concentrations. The process water is continually re-circulated through the tailings ponds, while the 12m CT Pond is an isolated pond, which may also explain the difference in ionic concentrations in the water.

Figure 4.6 is a comparison of the water analysis data from ALS Laboratories and those done in-house at the university. A slope value of one indicates that both sets of data are equal, and that both sets of data are precise and accurate. The slope of the line for this data set is 0.8722, indicating that the data is slightly skewed away from the universityôs data. The R-squared value of 0.9988 indicates that the data points are well represented by the trendline. The chloride data point was not used in the trendline or the calculation of the R-squared value, but it has been included in Figure 4.6.

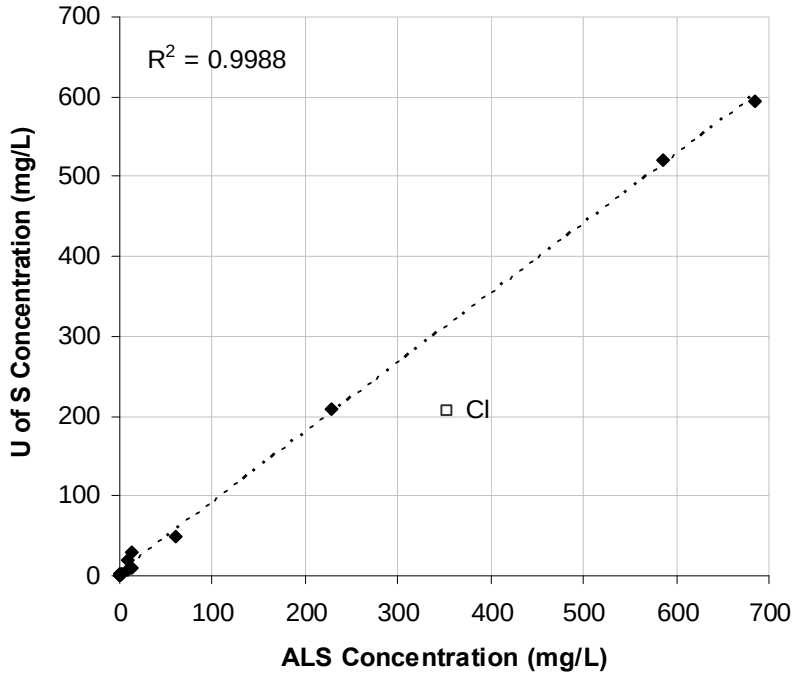

Figure 4.6: Comparison of Suncor minesite Process Water results from ALS laboratories and the University of Saskatchewan laboratory. Results are considered statistically the same when the slope of the dotted trendline reaches 1:1.

4.2.2 Petroleum Hydrocarbon Content of Process Water

The petroleum hydrocarbon content of the process water was also determined through gas chromatography at an external laboratory. The F1 fraction and BTEX fraction were both

found to be below the detectable limit of 0.2 mg/L. The F2 and F3 fractions were 0.13 mg/L and 1.0 mg/L, respectively, with no extractable hydrocarbons in the F4+ range. The extractable hydrocarbon results are summarized in Table 4.6 below. The results indicate that very little PHC concentration has accumulated in the water re-circulating through the tailings facility.

Table 4.6: Petroleum hydrocarbon concentration in Suncor mine site process water, shown by hydrocarbon fraction.

Extractable Hydrocarbons	OSPW (mg/L)
F1 C6-C10	<0.2
F1 - BTEX	<0.2
F2 (C10-C16)	0.13
F3 (C16-C34)	1
F4+ (C35-C50+)	0
TOTAL	1.13

4.3 Desorption of PHC from Oil Sands Tailings

The desorption of PHC from Athabasca oil sands tailings has not been previously studied. Preliminary testing was carried out using only two of the tailings materials in order to define the parameters of the experiment prior to conducting the remainder of the batch tests. The Plant 4 Upper Beach Surface and Plant 4 Upper Beach Auger were the two materials chosen for the initial testing, and were used as a baseline to determine the required time, temperature and amount of tailings required for subsequent tests with the remaining materials. Phases 1 and 2 of the experiment were also used to determine the effect that temperature and the solution mix had on the desorption of the two Plant 4 Upper Beach samples. The PHC content of each desorption supernatant was determined

by the external laboratory Exova (formerly Bodycote) using gas chromatography, which resulted in a chromatogram for each sample. A chromatogram for sample A1-10A is shown in Figure 4.7; analytical results for all samples can be found in Appendix C.

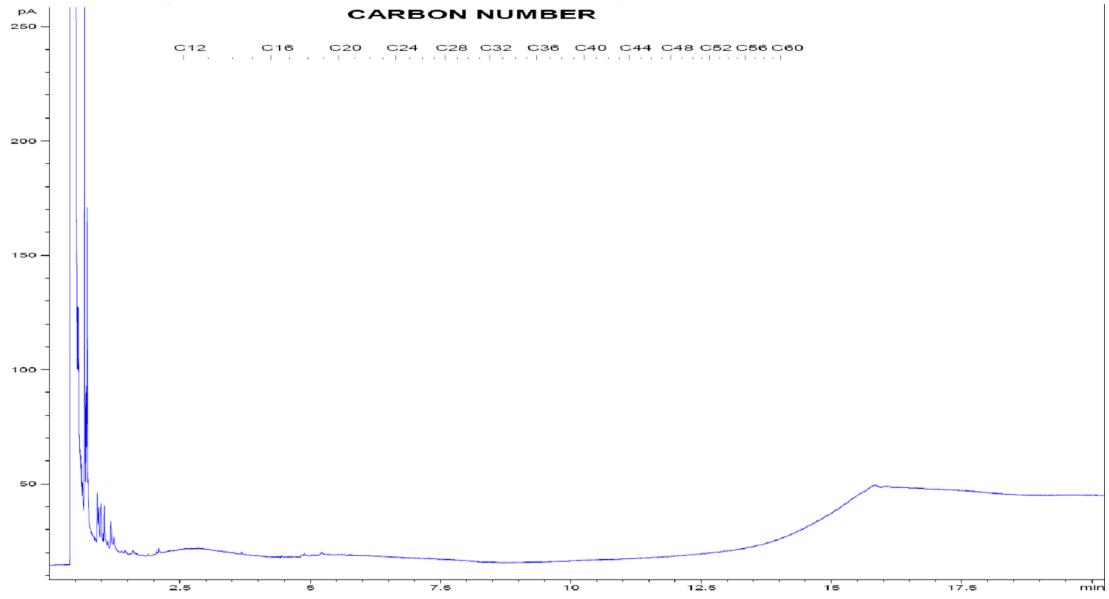

Figure 4.7: Chromatogram for desorption sample A1-10

Desorption results were from Exova, which is a Standards Council of Canada accredited laboratory. Quality control measures were conducted for all analyses completed by the lab. These included blanks and calibration checks for all groups of PHCs measured, which included mono-aromatic hydrocarbons in water, volatile PHCs in water and other extractable hydrocarbons in water (up to C40). The method of analyses used by the lab included the US EPA method 8260B/5030B and CCME Petroleum Hydrocarbons in Water method (Alberta Environment A108.0 Modified). All results passed the quality control tests performed by the lab.

4.3.1 Effect of Temperature on Desorption

In Phase 2 of the desorption experiments, the effect that a 19-degree Celsius change in temperature was examined. If there was a significant change noted between the two temperatures, it would affect how the remaining phases of the experiment were completed. The Plant 4 Upper Beach auger and surface samples were used in this batch experiment.

Half of the samples were placed in a temperature-controlled environment at 20ºC and the remaining samples were placed in a 1ºC controlled environment. The experiment proceeded for the same duration for both sets of samples. The effect of temperature on the desorption process are shown below in Figure 4.8. There is little change between the Plant 4 UB auger tailings at 1ºC and 20ºC, while the Plant 4 UB surface tailings desorption was slightly higher at 1ºC than 20ºC. From these results, it was concluded that the desorption process was not affected significantly by temperature over the time scale examined, and that provided at least 7 days was allowed for desorption, the results should be independent of temperature. The remaining tests were completed at 20ºC.

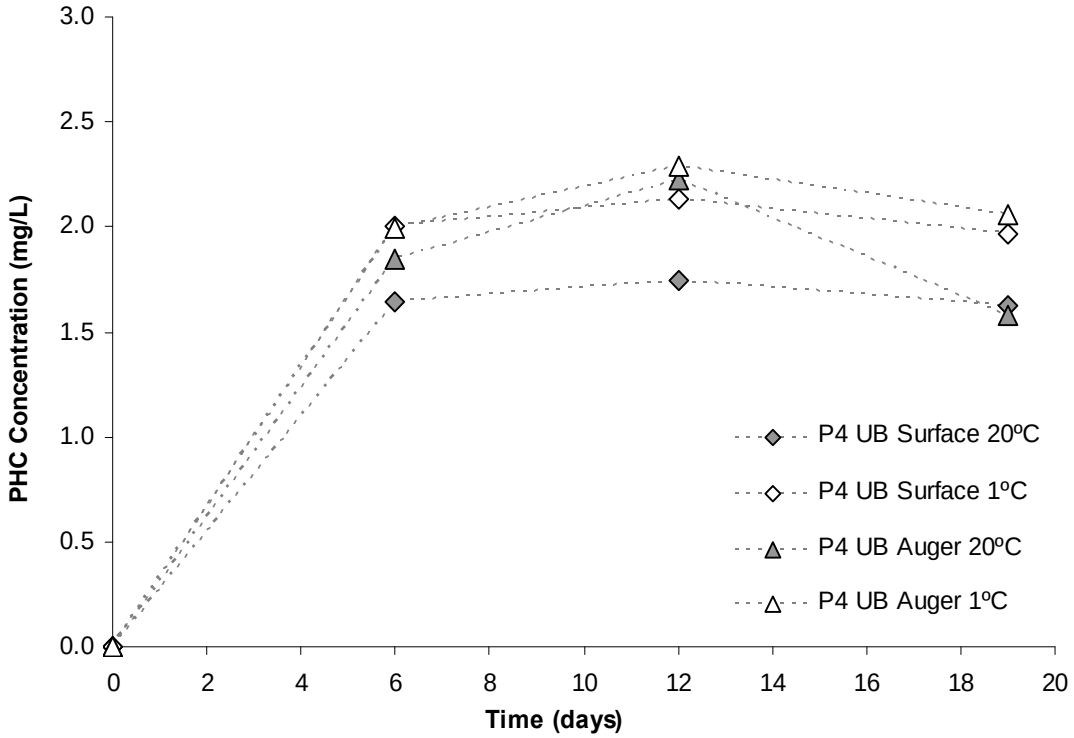

Figure 4.8: The effect of temperature on the desorption of petroleum hydrocarbons from Plant 4 Upper Beach auger and surface oil sands tailings samples. The results for 1ºC and 20ºC for both materials are shown.

4.3.2 Effect of Solution Mixture on Desorption

Phase 2 of the desorption experiment was used to determine if the solution mixture had any significant impact on the desorption of the tailings. Three different solutions with varying amounts of mine process water were used to determine if the process water had an effect on desorption. Batch tests were completed with pure de-ionized water, a 1:1 de-ionized water/process water mix, and undiluted process water.

Plant 4 UB surface tailings total PHC results are shown below in Figure 4.9(a) and Plant 4 UB auger tailings total PHC results are shown in Figure 4.9(b). In both sets of data, all

three solutions follow the same general trend, although the Plant 4 UB surface process water sample shows an increase in desorption at the end of the 20 days where the other two solution mixtures show a decrease. However, overall the solutions behaved similarly, and it was determined that for subsequent batch tests, only de-ionized water would be used.

Although the results of this batch test indicate that the use of process water does have some small effect on F2 and F3 PHC desorption, only de-ionized water was used in subsequent batch tests, based on the decision to standardize the test for the remaining phases by using replicable situations. Using de-ionized water will reduce the number of unknowns during the experiment, as concentrations of chemical species present in the process water vary in the tailings ponds themselves.

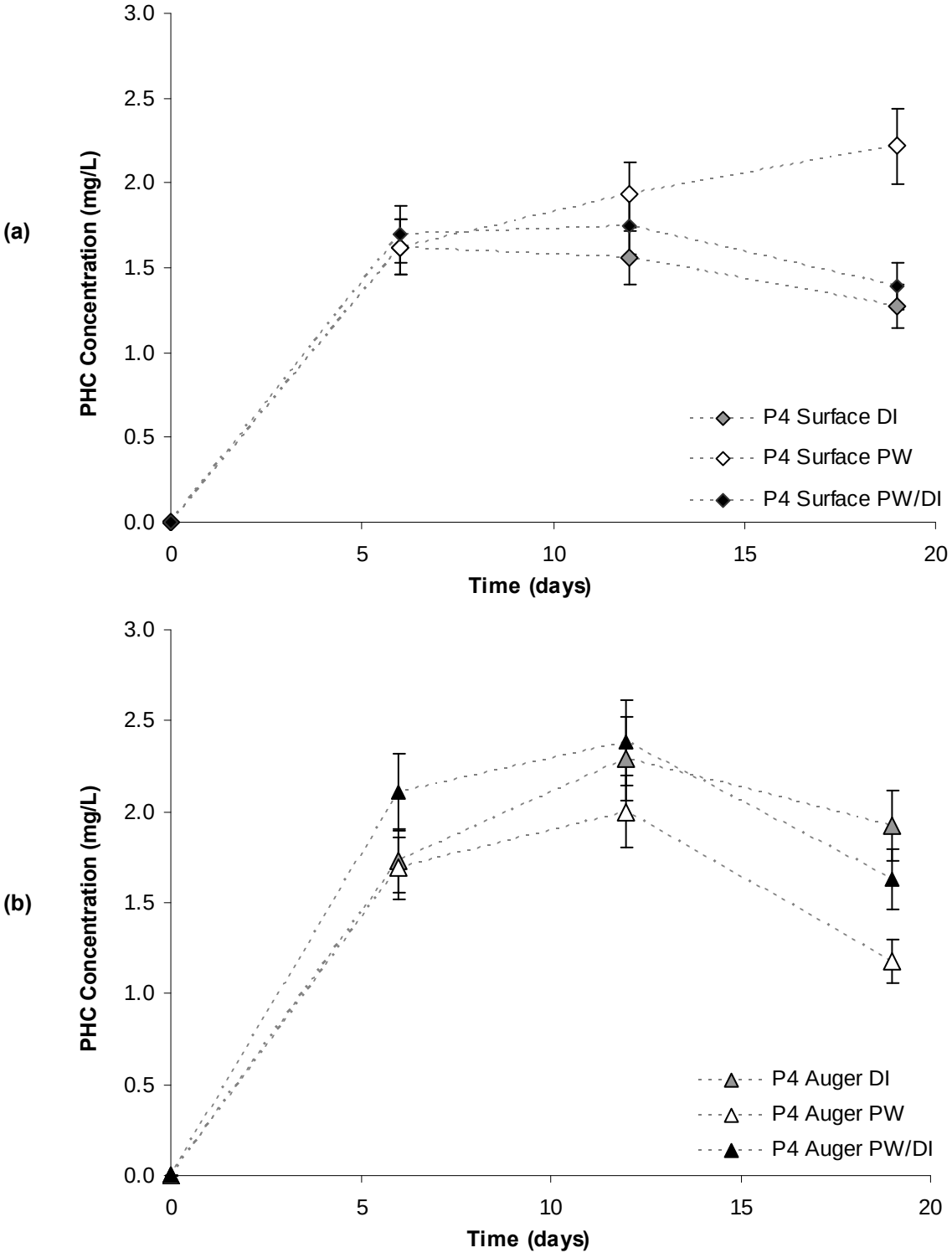

Figure 4.9: Three different solution mixtures for the desorption of total petroleum hydrocarbons from (a) Plant 4 Upper Beach surface oil sands tailings samples and (b) Plant 4 Upper Beach auger oil sands tailings samples. The results for undiluted process water, 1:1 process water de-ionized water mix and pure de-ionized water are shown. Error bars of plus/minus 10 percent are included.

4.3.3 Percent PHC in Solution

The average percent of each PHC fraction that was dissolved in aqueous solution at the end of each batch test was calculated. The percent F2 and F3 fractions are shown in Figure 4.10 below. The following relationship was used for both F2 and F3 fractions, only the F2 fraction is shown in Equation 4.3:

$$\%PHC\ in\ solution = \frac{Dissolved\ F2\ PHC}{Initial\ F2\ PHC\ in\ tailings} \times 100 \qquad \text{[Equation 4.3]}$$

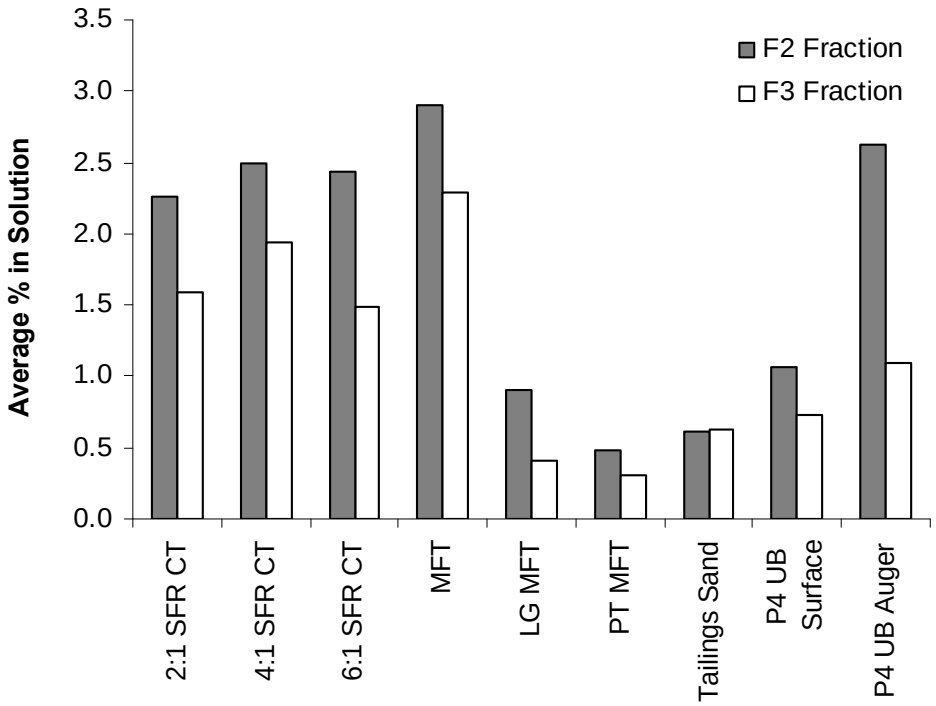

Figure 4.10: Percent of PHC in solution, broken down by PHC fraction.

For each of the tailings materials, the average F2 percentage was higher than the F3 percentage. Not surprisingly, this indicates that the smaller F2 fraction PHC molecules are able to desorb into the aqueous solution more readily, and the larger F3 fraction PHC molecules have higher stability. The percent PHC results from Phase 2 (for P4 Upper Beach samples) and Phase 3 (for all other tailings materials) are shown in Table 4.7 and 4.8 below, for F2 fraction PHCs and F3 fraction PHCs respectively.

Table 4.7: Percent of Total F2 Fraction PHCs in Solution

Material	Initial PHC in Tailings (mg)	Dissolved PHC (mg)	Avg. % F2 in Solution
2:1 SFR CT	56.84	1.55	2.26
4:1 SFR CT	42.46	1.80	2.50
6:1 SFR CT	21.26	0.37	2.44
MFT	222.4	1.96	2.91
LG MFT	109.9	0.35	0.90
PT MFT	105.8	0.27	0.47
Tailings Sand	1.09	0.004	0.61
P4 UB Surface	11.58	0.06	1.07
P4 UB Auger	9.36	0.13	2.63

Table 4.8: Percent of Total F3 Fraction PHCs in Solution

Material	Initial PHC in Tailings (mg)	Dissolved PHC (mg)	Avg. % F3 in Solution
2:1 SFR CT	264.0	5.40	1.59
4:1 SFR CT	173.0	6.12	1.94
6:1 SFR CT	90.78	1.08	1.48
MFT	958.8	6.57	2.29
LG MFT	411.6	0.58	0.41
PT MFT	408.1	0.75	0.31
Tailings Sand	15.17	0.11	0.63
P4 UB Surface	70.82	0.13	0.73
P4 UB Auger	48.40	0.24	1.09

4.3.4 Desorption Isotherms

The results of the desorption experiment for nine oil sands tailings are described by the graphs found in Figure 4.11 to Figure 4.22. The isotherms are divided by ñtypeò of tailings: composite tailings, mature fine tailings, Plant 4 Upper Beach tailings and tailings sand. Two isotherms were developed for each tailings material, an F2 fraction and an F3 fraction, as these fractions were determined to be the most abundant in the tailings characterization, and also more mobile and soluble than the higher carbon number molecules found in the F4 and F50+ carbon fractions.

For each tailings material, three sets of graphs are shown. The initial results, without any modelling are shown first, followed by the Langmuir (hyperbolic) calculation (S vs. S/C) and the final Langmuir model with the experimental results. Refer to Figures 4.11 through 4.13 for the composite tailings isotherms, Figures 4.14 through 4.16 for the MFT results, Figures 4.17 through 4.19 for the Plant 4 Upper Beach results, and Figures 4.20 through 4.22 for tailings sand results.

The Langmuir model was used to develop the isotherms by graphing the experimentally determined values of aqueous (dissolved) PHC concentration (C) against the calculated value of sorbed PHC concentration (S) divided by C. This results in a straight-line graph, which is the basis of the Langmuir relationship. Values of Ŭand ɓ are determined from the experimental data using the following hyperbolic relationship to describe the desorption of the PHCs (Fetter 1999):

$$\frac{C}{S} = \frac{1}{\alpha\beta} + \frac{C}{\beta}$$ [Equation 4.4]

C = concentration of solute in the solution (mg/L)

S = mass of solute sorbed onto the solid surface, per mass of solid (mg/kg)

Ŭ= binding energy sorption constant (L/mg)

ƀ = the maximum amount of solute that can be absorbed by the solid (mg/kg)

The Langmuir isotherm coefficients for nine oil sands tailings are summarized in Tables 4.9 and 4.10 below, along with the slope and intercept of the straight line equation. The Langmuir coefficients are presented in two different ways, with the binding energy constant Ŭ and the maximum ion sorption ƀ, and also with S_i and S_{max}. The above Equation 4.4 shows the Langmuir equation using Ŭand ƀ.

Table 4.9: Langmuir desorption constants Ŭ(binding energy constant) and ƀ (maximum ion sorption) for F2 PHC fraction of 9 oil sands tailings.

Material	Slope	Intercept	α (L/mg)	β (mg/kg)	S_i (L/kg)	S_{max} (mg/kg)
2:1 SFR CT	0.00025	0.0000018	135.74	4006.5	543845.58	4006.5
4:1 SFR CT	0.00033	0.000000078	4207.4	3042.3	12800412	3042.3
6:1 SFR CT	0.00065	0.0000057	114.60	1529.5	175275.93	1529.5
MFT	0.000098	0.0000016	62.108	10245	636273.06	10245
LG MFT	0.00019	0.0000026	72.309	5332.9	385616.46	5332.9
PT MFT	0.00019	0.0000037	50.671	5321.2	269634.00	5321.2
P4 UB Surface	0.001050	0.0000015	689.37	952.03	656297.44	952.03
P4 UB Auger	0.0014	0.0000015	935.09	735.80	688030.95	735.80
Tailings Sand	0.028	0.00000014	203531	35.807	7287733.9	35.807

Table 4.10: Langmuir desorption constants Ŭ (binding energy constant) and ƀ (maximum ion sorption) for F3 PHC fraction of 9 oil sands tailings.

Material	Slope	Intercept	α (L/mg)	β (mg/kg)	S_i (L/kg)	S_{max} (mg/kg)
2:1 SFR CT	0.000053	0.00000047	114.16	18738	2139113.4	18738
4:1 SFR CT	0.000081	0.0000025	32.769	12403	406452.49	12403
6:1 SFR CT	0.00015	0.0000019	81.425	6541.1	532609.93	6541.1
MFT	0.000022	0.000000079	285.33	44642	12737622	44642
LG MFT	0.000049	0.0000014	36.524	20202	737862.74	20202
PT MFT	0.000050	0.00000054	92.800	19992	1855216.5	19992
P4 UB Surface	0.00017	0.00000060	287.85	5819.7	1675202.0	5819.7
P4 UB Auger	0.00026	0.000000022	11793	3832.9	45201533	3832.9
Tailings Sand	0.0019	0.0000048	398.44	518.51	206591.84	518.51

A set of three isotherm graphs is included on the following pages in Figures 4.11 through 4.13, showing desorption results for the Plant 4 Upper Beach tailings samples (surface and auger) in de-ionized water for the F2 and F3 PHC fractions. The isotherm sets for all tailings materials (CT, P4UB, MFT and tailings sand) are included in Appendix D.

(a)

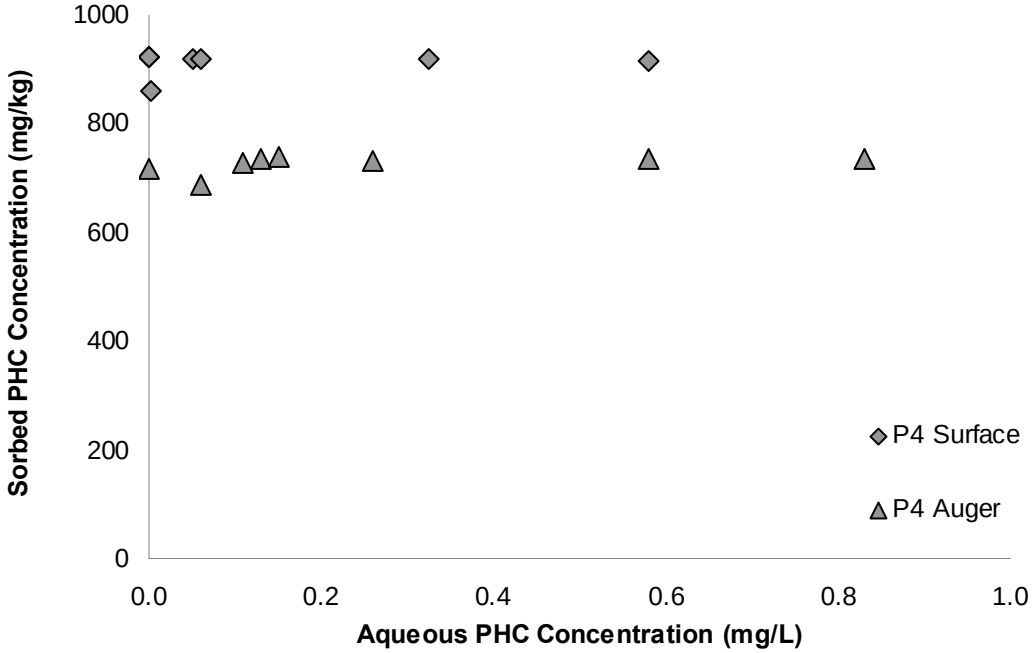

(b)

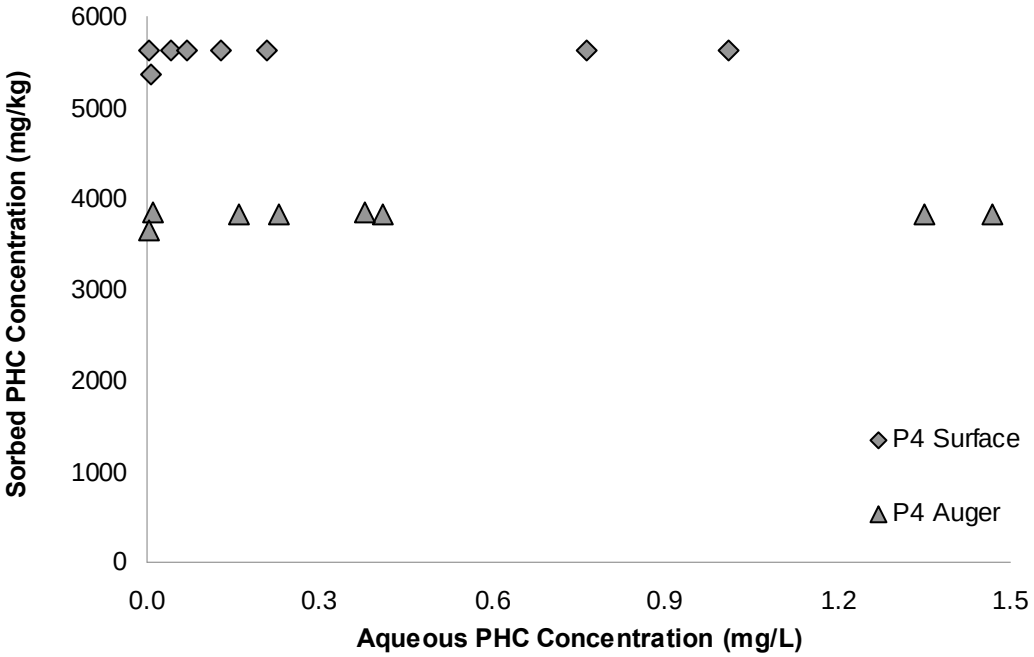

Figure 4.11: Desorption experiment results for Plant 4 Upper Beach Tailings in de-ionized water. Samples of the tailings were collected at the surface and from a depth of 1.5m (auger samples).

a) F2 PHC Fraction
b) F3 PHC Fraction

(a)

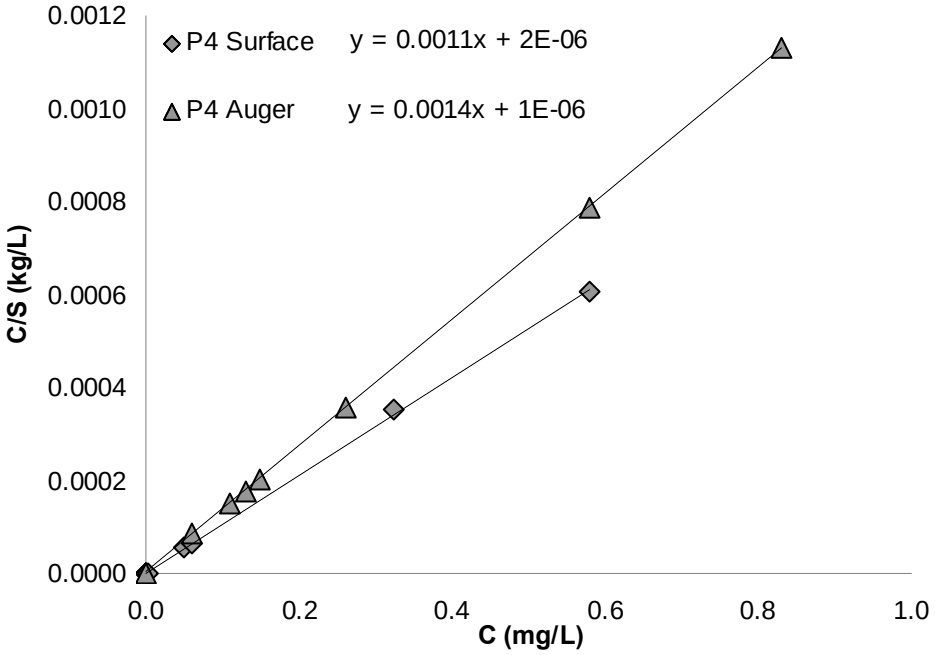

(b)

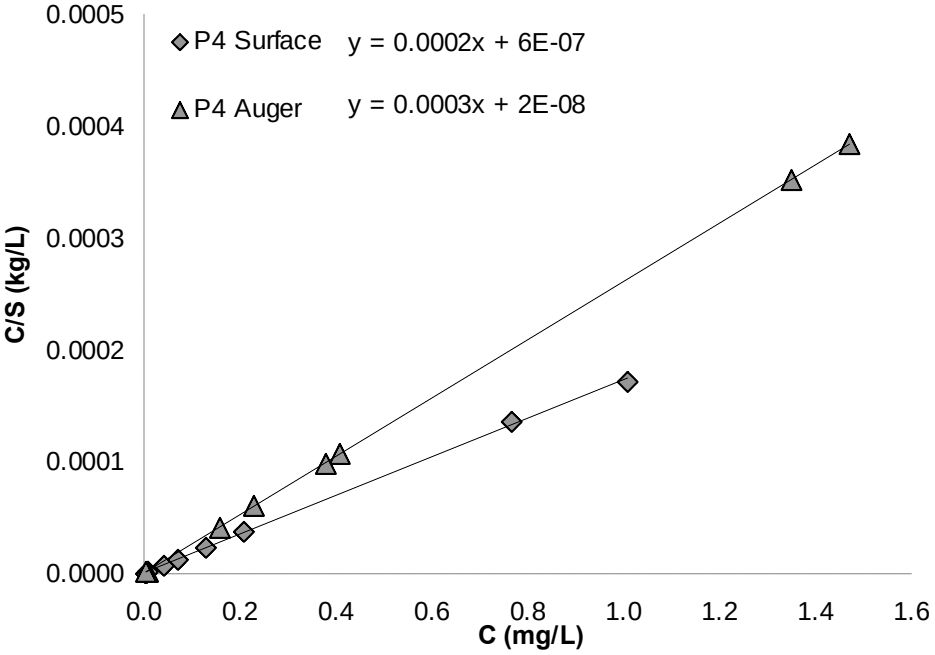

Figure 4.12: Desorption Langmuir model for Plant 4 Upper Beach Tailings in de-ionized water. Samples of the tailings were collected at the surface and from a depth of 1.5m (auger samples).

a) F2 PHC Fraction
b) F3 PHC Fraction

(a)

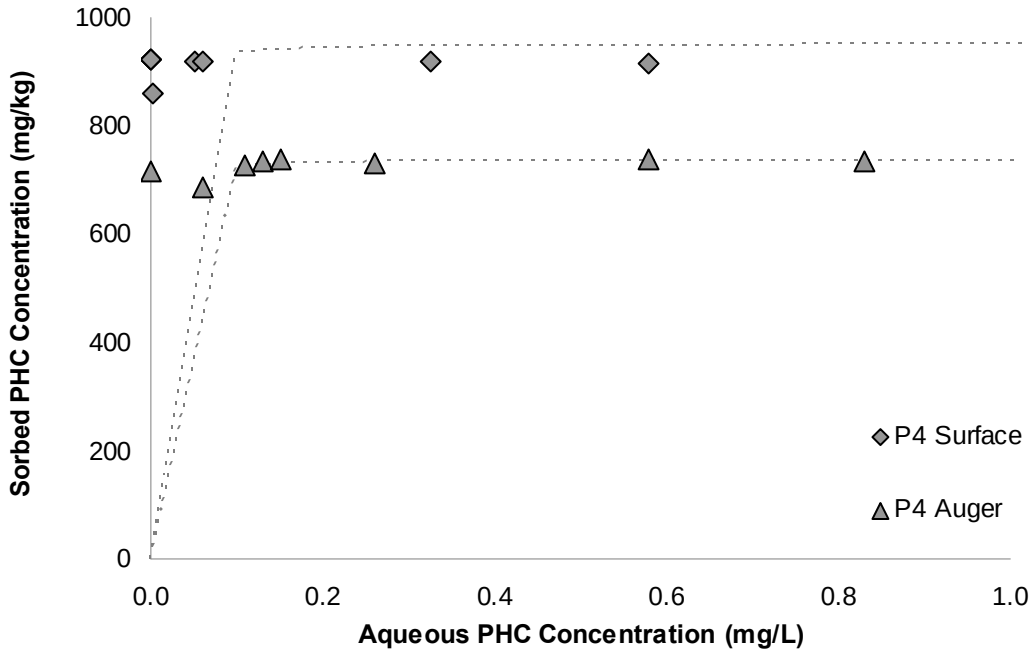

(b)

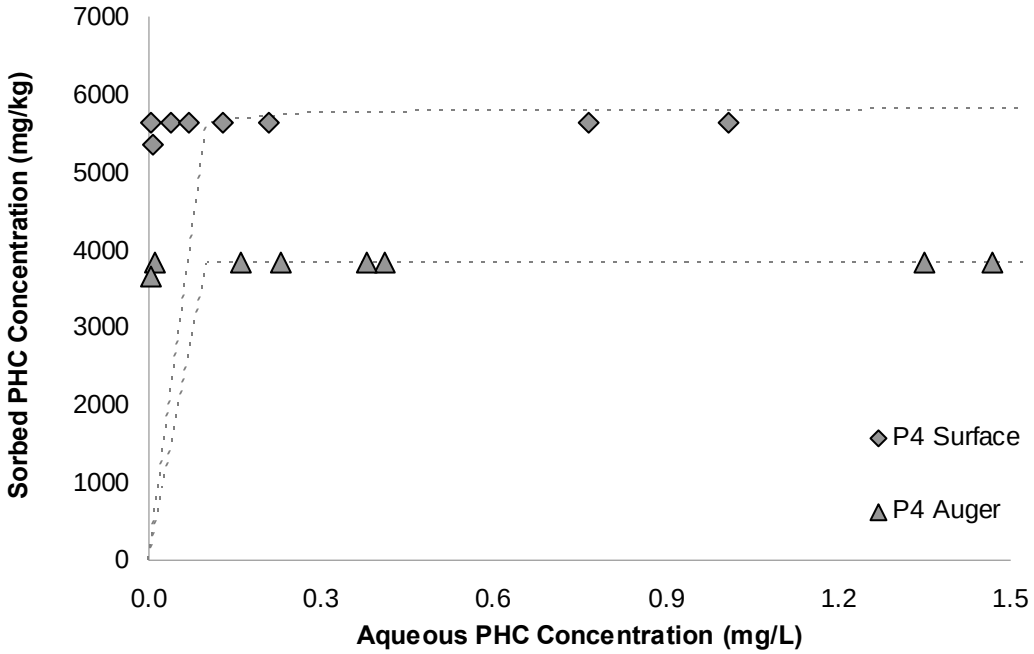

Figure 4.13: Desorption Isotherm for Plant 4 Upper Beach Tailings in de-ionized water. Samples of the tailings were collected at the surface and from a depth of 1.5m (auger samples).

a) F2 PHC Fraction
b) F3 PHC Fraction

4.3.5 Isotherm Summary

a) Composite Tailings Isotherms

2:1 CT shows the highest amount of desorption in both the F2 fraction and the F3 fraction, followed by the 4:1 CT in the middle, and the 6:1 CT with the lowest desorption. These results are as expected, given that the 2:1 CT has the highest concentration of PHCs due to the higher MFT content in the tailings mix. The F3 fraction for all tailings showed higher desorption than the F2 fraction, which could be attributed to the higher concentration of F3 in the tailings themselves. All three CT tailings display higher desorption than both the tailings sand and the Plant 4 Upper Beach samples.

b) Mature Fine Tailings Isotherms

Undiluted MFT shows the highest amount of desorption in both the F2 fraction and the F3 fraction, followed by both the LG MFT and the PT MFT. The LG MFT and PT MFT have similar results, which may indicate that the effect of the stabilization process on each material is approximately the same. These results are as expected, given that the MFT has a much higher concentration of PHCs than either of the other two materials. The F3 fraction for all three tailings showed higher desorption than the F2 fraction, which could be attributed to the higher concentration of F3 in the tailings themselves. All three MFT tailings display higher desorption than any of the other tailings tested.

c) Plant 4 Upper Beach Tailings Isotherms

The Plant 4 Upper Beach Surface tailings shows higher desorption in both the F2 fraction and the F3 fraction than the auger sample, although both sets of results are close and in the same order of magnitude. These results are as expected, given that the Surface sample has a higher PHC concentration than the auger sample. The F3 fraction for all tailings showed greater desorption than the F2 fraction, which could be attributed to the higher concentration of F3 in the tailings themselves. Some lower data points on the isothermôs curve can be seen, as these tailings had additional scaled up desorption batch tests, using 0.5g of tailings in 20-L samples of de-ionized water.

d) Tailings Sand Isotherms

The tailings sand has the lowest desorption in both the F2 fraction and the F3 fraction of any of the oil sands tailings. This is consistent with the PHC characterization, which indicated that there was very little PHC present in the tailings sand.

4.3.6 Solubility Limits

There is the possibility that the desorption data was affected by the solubility limits of F2 or F3 fraction PHCs in water. In order to ascertain whether the desorption tests measured desorption or solubility, further data analysis was completed.

An equivalent mass of PHC (for both F2 or F3 fraction) in the batch test was calculated from the mass of the tailings sample added to the container and the PHC content of each tailings material. The percent mass of PHC in each tailings material was known from the results of PHC characterization of the tailings. The relationship for the mass of PHC in the sample is shown in Equation 4.5:

$$PHC\ mass = (\%\ Tailings\ PHC)\ x\ (Mass\ tailings\ sample) \qquad \text{[Equation 4.5]}$$

The PHC mass in the sample was plotted against the measured aqueous concentration of PHC in the desorption batch test for each F2 and F3 fraction separately (the same aqueous concentration results that were used to develop the Langmuir isotherms). The PHC mass versus aqueous concentration plots for the Plant 4 Upper Beach Surface and Auger samples are shown below in Figure 4.14.

(a)

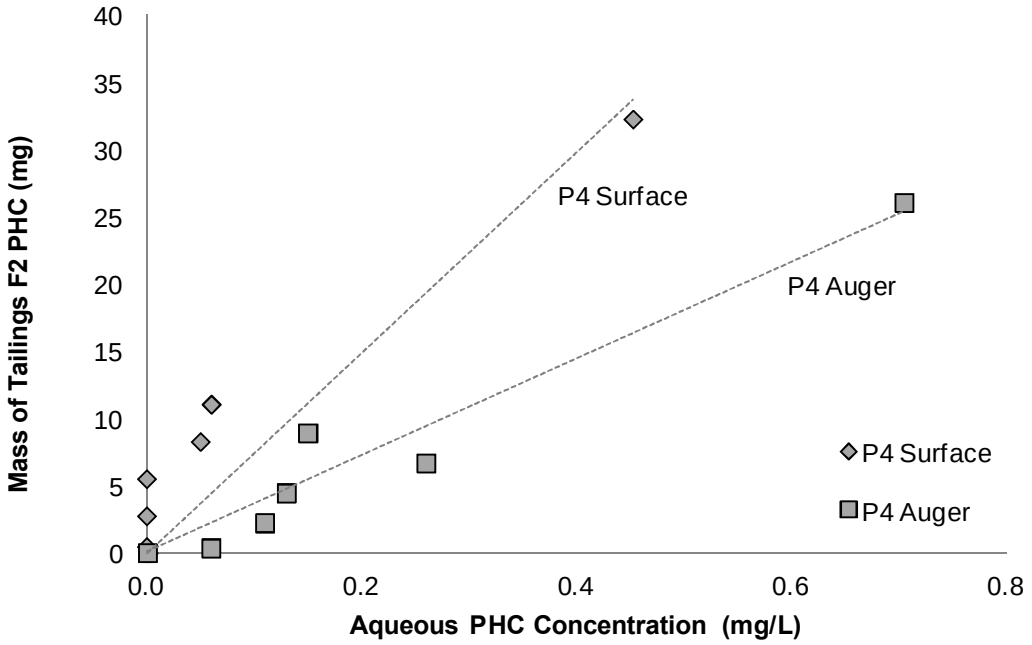

(b)

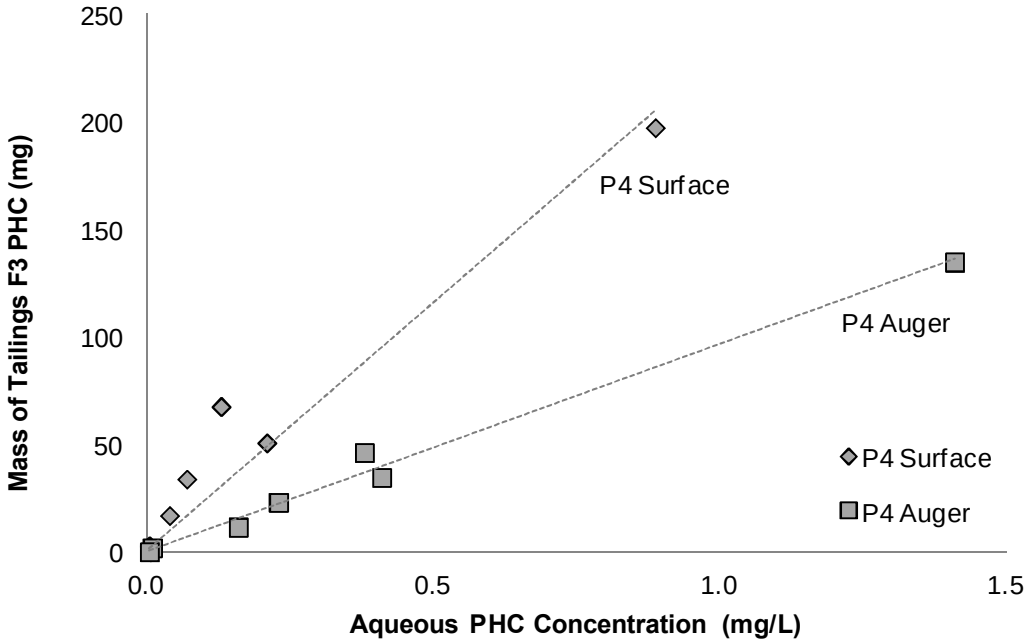

Figure 4.14: Aqueous concentration of (a) F2 fraction and (b) F3 fraction PHCs in de-ionized water for Plant 4 Upper Beach surface and auger samples. The aqueous concentration is plotted against the total mass of F2 and F3 fraction PHC present in the solid tailings sample.

If the desorption batch tests indicated that a solubility limit had been reached, there would be a trend in the aqueous concentration data showing that a plateau or saturation in dissolved PHC had been reached. The aqueous concentration values for the Plant 4 Upper Beach tailings do not indicate that a plateau in solubility was reached with the mass of tailings sample used in these batch tests. In fact, the concentration appears to be best represented with a linear trend, as shown in the graphs. If the solubility of tailings PHCs is to be quantified, further testing would be required, as determining tailings PHC solubility is outside of the scope of this research. The solubility graphs for all tailings materials have been included in Appendix E.

Aqueous concentration graphs for the remaining tailings samples (MFT, CT and tailings sand) are included in Appendix E. They show that, as with the Plant 4 Upper Beach samples, there is no discernible pattern of solubility limits with the aqueous concentration data available. Some of the tailings samples, such as the MFT, were found to have higher aqueous concentrations of PHC present, although there was no discernible trend in the data to show that a solubility limit had been reached for any other tailings materials tested.

Literature solubility values for some F2 and F3 PHCs are included in Table 4.11, which show solubilities quite a bit lower than the PHC concentrations found from the desorption experiments. One possible explanation for the higher aqueous PHC concentrations is the formation of microdroplets of PHC in the aqueous phase. The samples were shaken

twice daily to ensure the tailings were well-mixed with the de-ionized water, but the shaking may also have affected the measured aqueous concentration by including a portion of suspended PHC. However, the amount of suspended PHC was likely minimized once the batch samples were centrifuged prior to the extraction of the solute. To determine oil solubility, it would be more practicable to gently stir the sample to minimize the formation of any of these microdroplets (Chen et al. 2007), although solubility was outside of the scope of this research.

Table 4.11: Solubility values for F2 and F3 PHCs from literature

PHC	Formula or Group	Fraction	Solubility (mg/L)	Reference
Naphthalene (C10)	$C_{10}H_8$	F2	31.7	Miller and Wasik 1985
C10 - C12	aromatics	F2	25	ATSDR 1999
C12 - C16	aromatics	F2	0.65	ATSDR 1999
C10 - C12	aliphatics	F2	0.034	ATSDR 1999
C12 - C16	aliphatics	F2	0.00076	ATSDR 1999
Hexadecane (C16)	$C_{16}H_{34}$	F3	0.0063	Goral et al. 2006
Octadecane (C18)	$C_{18}H_{38}$	F3	0.0021	Goral et al. 2006
C16 - C21	aromatics	F3	0.65	ATSDR 1999
C21 - C35	aromatics	F3	0.0066	ATSDR 1999
C16 - C35	aliphatics	F3	0.0000025	ATSDR 1999
C16 - C35	aliphatics	F3	0.0000025	ATSDR 1999

4.3.7 Desorption Isotherm Discussion

There are several considerations in the desorption of PHCs and other hydrophobic organic compounds. Temperature dependence, the effect of the solution used in the batch tests (solute), sorption hysteresis, the hydrophobicity of the PHCs, steric hindrance, the water-to-sorbent ratio and salting-out are all included in this section. The use of the

Langmuir isotherm model, and the similarities to asphaltene sorption results are also discussed.

a) Temperature Dependence

The results show that for the range of temperatures evaluated in Phase 2, there was little or no effect on the desorption of F2 and F3 PHC fraction from the oil sands tailings. The results of the desorption bench tests conducted at 20ºC and 1ºC did not show temperature dependence, but this is likely due to the fact that the very slow fraction, which could take several months to measure, was not measured.

b) Effect of the Solute

Bitumen is a heavy PHC, with many high carbon number components. PHCs are also non-polar organic chemicals, and have a decreasing solubility as the carbon number and molecular mass increases (Hutzinger 1980), meaning that the BTEX and F1 fraction are much more soluble than PHCs with higher carbon numbers. The tailings characterization revealed that the majority of the PHCs present in the tailings were in fractions F2 to F5G. The PHC characterization of the tailings indicates that the PHCs present will not readily dissolving in water, or only a small amount of PHC will dissolve.

The size of organic compounds can also have an effect on the sorption behaviour of F2 and F3 fraction tailings PHCs. The fact that larger molecules have been found to desorb

more slowly may explain why a larger percent of the total F2 fraction desorbed from the tailings than the F3 fraction.

In the desorption batch tests, it was found that increasing the initial amount of tailings did not increase the aqueous concentration of PHCs substantially. The hydrophobicity of the PHCs may be one of the reasons there was only a small increase in aqueous PHC concentration.

c) Similarity to Asphaltene Desorption Results

The desorption isotherm for each oil sands tailings was best modeled using the Langmuir isotherm. Each isotherm is similarly shaped, regardless of the tailings material, and that the maximum ion sorption, ϭ, was reached at a very low aqueous PHC concentrations. The shape of the isotherm is very different from most desorption isotherms in that it reaches the maximum concentration in the solution extremely quickly. However, the shape of the isotherms are consistent with the asphaltene desorption results into toluene (instead of water), observed by Dubey and Waxman (1991). Asphaltenes are similar to bitumen, with very high hydrocarbon numbers, and are likely present in the tailings materials, as the amount of F3 and F4+ fraction PHCs indicates that heavy hydrocarbons are abundant. The order of magnitude of Dubey and Waxmanôs results is also in the same order of magnitude as those results obtained in this study, in the range of 26.0 mg/g (or 2600 mg/kg) of maximum sorbed asphaltene concentration. Maximum sorbed PHC

concentration for the tailings materials ranged from 35.81 mg/kg in tailings sand to 10245 mg/kg in MFT (refer to ɓ in Tables 4.8 and 4.9).

Given that asphaltenes are likely present in the tailings materials tested, the similarity of the desorption results in this study to the asphaltene desorption could indicate that the tailings PHCs and asphaltenes have similar transport mechanisms.

d) Use of the Langmuir Isotherm

Studies on the sorption of organic compounds have found that the use of the Langmuir type isotherm best fits their experimental data (Kan et al. 1998, Dubey and Waxman 1991; Szymula and Marczewski 2002; Marczewski and Szymula 2002). In certain cases, it was found that the Langmuir isotherm would only describe the irreversible sorption, with the reversible sorption modeled using a linear sorption relationship (Kan et al. 1998), or by using a combination of Freundlich and Langmuir isotherm models (Szymula and Marczewski 2002; Marczewski and Szymula 2002). The Langmuir type isotherm provided the best fit for the desorption data, a conclusion that is supported in the literature.

e) Sorption Hysteresis

Sorption and desorption rates play an important role in the transport of large hydrophobic organic compounds in soils and sediments (Braida et al. 2002), such as tailings PHCs.

Hysteresis is common with solid/aqueous phase of organics from sediments and soils, with distribution coefficients measured for desorption frequently reported as being significantly greater than for sorption in the same system (Huang et al. 1998). In sorption studies of organics, up to 80 percent of the solute, which includes a study on asphaltenes, has been found in to be irreversibly sorbed to the soil or sediment (Dubey and Waxman 1991; Morrissey and Grismer 1999; Kan et al. 1998). Desorption occurs at a different rate than adsorption in the same system, with large amounts of solute irreversibly bound to the sediment. The hysteresis shown in these studies indicates that the adsorption and desorption processes cannot be used interchangeably for organics, which includes PHCs. Notwithstanding this consideration, it was necessary to find a starting point in the evaluation of PHC mobility from tailings materials and these desorption results constitute a reasonable first step.

f) Sorption Kinetics

Equilibrium concentration was reached very quickly in Phases 1 and 2 of the batch tests, with the results from the 3-day samples very similar to the 13-day results in Phase 1. The 6-day, 12-day and 19-day results were also close in Phase 2. All desorption results are included in Appendix C. It is very common for the sorption of hydrophobic organic compounds to occur very quickly, and often within the first days of the experiment (Alboudwarej et al. 2005). It is likely that a significant portion of the PHCs in the tailings are irreversibly sorbed to the inorganic sediment particles, as this is quite

common with other organic compounds in soil and sediment systems (Morrissey and Grismer 1999; Huang et al. 1998; Cornelissen et al. 1997; Braida et al. 2002).

Desorption of organic compounds often occurs in two separate phases, a relatively fast phase of desorption, occurring within hours to days, and a much slower phase which can occur over a period of weeks to months. Low solubility of the hydrophobic organic compounds likely contributes to the observed two-phase desorption. The slow fraction is generally small in comparison to the fast desorption (Huang et al. 1998; Hsieh et al. 2010; Ball and Roberts 1991; Wu and Gschwend 1986; Pignatello and Xing, 1996), and is often governed by diffusion. Generally much longer time periods are required to accurately determine a K_D accounting for both fast and slow sorption (Pignatello and Xing 1996). Slow diffusion within the sediment particles is usually suggested as the mechanistic explanation for this phenomenon, and the rapid release of organic compounds has been interpreted as coming from the outer surface area of the sediment or soil, which is usually in direct contact with the aqueous solution (Cornelissen et al. 1997).

In the case of F2 and F3 PHC fraction desorption from the tailings materials, the slow fraction is not likely to have a much impact on the mobility of the oil sands PHCs, as the slower desorption phase may take weeks to months to begin to occur, and at a much slower rate than the initial ñfastò desorption.

g) Other Effects

Salting out is another observed phenomena in solutions with high concentrations of electrolytes or salts that may be impacting the desorption of F2 and F3 PHC fractions from the tailings. The presence of salts is known to affect the sorption of organic chemicals (Li and SenGupta 2004, Martins and Mermoud 1998, Janfada et al. 2006). The process water in the tailings ponds are known to be high in mono and divalent cations and anions (e.g. Na^+, K^+, Mg^{2+}, Cl^-, SO_4^{2-}, etc.) as well as salts (refer to Section 4.2). These ions and salts will remain with the tailings as they are dewatered for reclamation. The salts may be interfering and reducing the desorption rates of the PHCs from the tailings into the aqueous solution of the batch tests. Salts may be causing dissolved non-electrolytes to precipitate from solution, or reducing their capacity to dissolve into an aqueous solution (Grover and Ryall 2004; Shah and Tiwari 1981).

The ratio of de-ionized water to tailings also has an effect on desorption rates; a high ratio of water to contaminant in the system will increase the initial desorption rate constant (Hsieh et al. 2010). It has been shown that different water-to-sorbent ratios in the same system (i.e. same solution and sorbent) will result in varying adsorption constants (Chang and Wang 2002). For simplicity the ratio of solution (either water or OSPW) varied with the sample mass for all the desorption batch tests in this study, due to the requirement of eliminating the headspace to keep volatiles in the aqueous phase. For all the batch tests, regardless of the changing mass of the sample, a 500mL jar was used. Sample masses in the batch tests used to develop the isotherms ranged from 0.5g to 20g by dry weight, while the size of the jar remained at 500mL. This dilution ratio between soil and solution

may be a source of error in the results, as the volume of water decreased as the tailings source was increased. This may mean that a solubility limit could be reached more quickly with the larger samples, although the solubility analysis indicates that there was no solubility limit trend in any of the aqueous concentration data.

4.3.8 Summary

The desorption isotherms obtained from these results are very different from most desorption isotherms, in that the maximum concentration in the solution is reached rapidly. A key finding is that the shape of the desorption isotherms resulting from this study were found to be similar to those reported for the desorption of asphaltene, which is one of the components in oil sands tailings. The Langmuir isotherm model was the best fit for the experimental desorption data; the Langmuir isotherm model is commonly used in sorption isotherms of organic chemicals.

Temperature dependence has been observed in the slow fraction of desorption, but no temperature dependence was found for desorption batch tests conducted at 20ºC and 1ºC in this study. Increasing the dry mass of tailings in these batch tests (from 20 to 100 g) did not result in an increase in the aqueous PHC concentration, which is likely due to the hydrophobicity of the PHCs.

The literature regarding sorption hysteresis of organic compounds indicates that the adsorption and desorption processes are non-reversible, with a significant portion of the organic sorbed irreversibly to the soil or sediment. Desorption and adsorption of PHCs

are not equal processes, and desorption results should not be used in place of adsorption without further study.

The sorption of organics is also a kinetic process, with a ñfastò and ñslowò portion. The fast portion occurs within hours to days of the start of the sorption process, with the slower portion taking weeks to months to reach equilibrium. The slow fraction is very small when compared with the fast sorption, and it is unlikely that the slow portion will affect the mobility of the PHCs from the tailings to the topsoil.

Steric hindrance and salting out may also be affecting the desorption rates. Large molecules desorb more slowly, which explains why a larger percent of the F2 fraction desorbed from the tailings when compared to the F3 fraction. Salts may also be reducing the desorption rate of PHCs into aqueous solution. The dilution ratio of DDI water to tailings solids was not a constant for all batch tests, and is a potential source of error for the desorption results.

4.4 Diffusive Transport of PHCs in Oil Sands Tailings

The diffusive transport of PHCs from Athabasca oil sands tailings has not been previously studied. The radial diffusion experiment in this study used a porous metal mesh tube as a separator between the reservoir and tailings material. Due to time constraints, only 7 of the tailings materials were used in the diffusion experiment, and it was anticipated that the diffusivity of the remaining tailings, which have been well

characterized in this study, could be extrapolated from the results obtained for the 7 tailings materials actually tested.

The seven tailings studied in the diffusion experiment were the three composite tailings (2:1 SFR, 4:1SFR and 6:1 SFR CT), the three MFT tailings (pure MFT, PT MFT and LG MFT) and the tailings sand. Only the F2 and F3 PHC fractions were analysed in this diffusion experiment.

Once the experimental results were obtained, an approximate 1-D axisymmetric solution of the PDE was implemented using a Finite Difference Method (FDM). For each of the seven tailings, the experimental results were divided into F2 and F3 PHC fractions, and a diffusion coefficient for each fraction was determined from the FDM model (refer to Section 3.6.2 and Appendix A for details on the FDM approximation). The best fit of the FDM was determined by varying the value of D* to minimize the value of the Root-Mean-Square-Error (RMSE) between the calculated aqueous PHC concentration and the actual experimentally determined concentration.

The experimentally derived diffusion coefficients for the F2 and F3 PHC fractions of the seven tailings are summarized in Tables 4.12 and 4.13 below, along with the initial PHC concentration in the tailings porewater and the Root-Mean-Square-Error (RMSE) value,

which was used as an indicator to find the best fit between the experimental data and the model.

Table 4.12: Diffusion coefficients (cm^2/s), initial tailings porewater (PW) concentration and Root-Mean-Square-Error (RMSE) values for the F2 PHC fraction of Athabasca oil sands tailings.

Material	Initial PW Concentration (mg/L)	Diffusion Coefficient, D* ($x10^{-6}$)	RMSE (mg/L)
2:1 SFR CT	46.3	0.025	0.090
4:1 SFR CT	5.25	0.170	0.134
6:1 SFR CT	1.86	0.490	0.117
MFT	205	0.022	1.082
LG MFT	0.54	1.10	0.397
PT MFT	4.74	0.405	0.180
Tailings Sand	1.99	0.130	0.029

Table 4.13: Diffusion coefficients (cm^2/s), initial tailings porewater (PW) concentration and Root-Mean-Square-Error (RMSE) values for the F3 PHC fraction of Athabasca oil sands tailings.

Material	Initial PW Concentration (mg/L)	Diffusion Coefficient, D* ($x10^{-6}$)	RMSE (mg/L)
2:1 SFR CT	174	0.042	0.802
4:1 SFR CT	22.1	0.220	0.720
6:1 SFR CT	7.31	0.670	1.323
MFT	819	0.020	2.577
LG MFT	0.96	0.530	1.200
PT MFT	15.2	0.330	1.548
Tailings Sand	52.5	0.045	0.356

All F2 and F3 fraction diffusion coefficients are within two orders of magnitude and there is quite a bit of scatter in this diffusion data. However, these diffusion results are necessarily preliminary and represent the first attempt at characterizing the diffusion of F2 and F3 PHCs from oil sands tailings. Accordingly these diffusion coefficients have

uncertainty attached to them, and must be verified with further diffusion tests to determine reliability and minimize error.

4.4.1 Composite Tailings Diffusion Model

Radial diffusion experiments were completed with all three of the composite tailings materials. The F2 fraction PHC radial diffusion results are shown in Figure 4.15(a) and the F3 fraction PHC radial diffusion results are shown in Figure 4.15(b) below. Experimental data is presented with error bars for plus-minus twenty percent of the experimental results, which is consistent with the accuracy that can be achieved from GC analysis of hydrocarbons. All CT diffusion coefficients are within one order of magnitude.

(a)

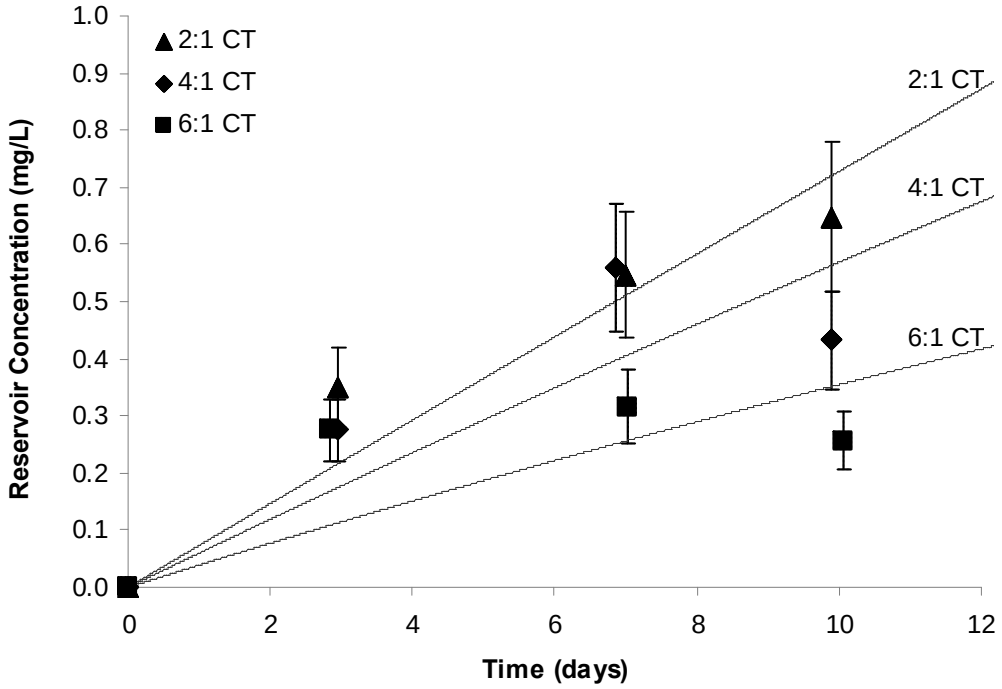

(b)

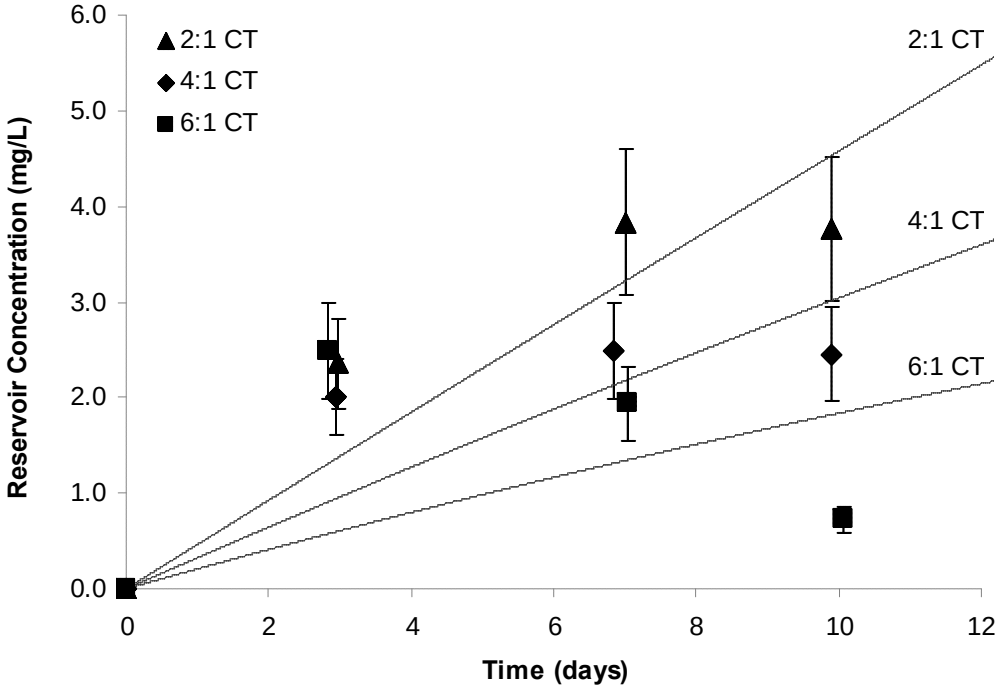

Figure 4.15: Radial diffusion of (a) F2 fraction and (b) F3 fraction PHCs from composite tailings into de-ionized water.

4.4.2 Mature Fine Tailings Diffusion Model

Radial diffusion experiments were completed with all three of the mature fine tailings materials. The F2 radial diffusion results are shown in Figure 4.16(a) and the F3 radial diffusion results are shown in Figure 4.16(b) below. Experimental data is presented with error bars for plus-minus twenty percent of the experimental results, which is consistent with the accuracy that can be achieved from GC analysis of hydrocarbons.

The results of the initial concentration of PHC in the porewater of the LG MFT were much lower than the PHC concentrations obtained from the cellôs reservoir during the 10-day diffusion experiment. These porewater results were unable to be used in the FDM model for either PHC fraction, so the porewater results from PT MFT were used to determine the diffusion coefficient (D*). As such, the D* values are not as reliable as some of the other results obtained, although they do fall within the same range and order of magnitude as the other MFT results, which indicates that the substitution of PT MFT porewater concentration was valid.

(a)

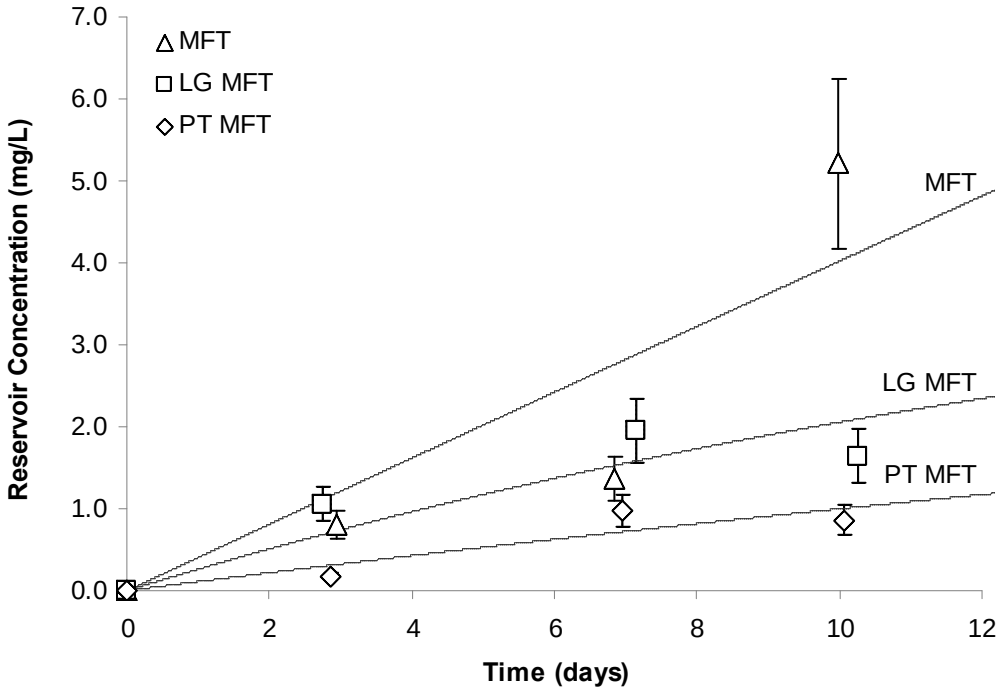

(b)

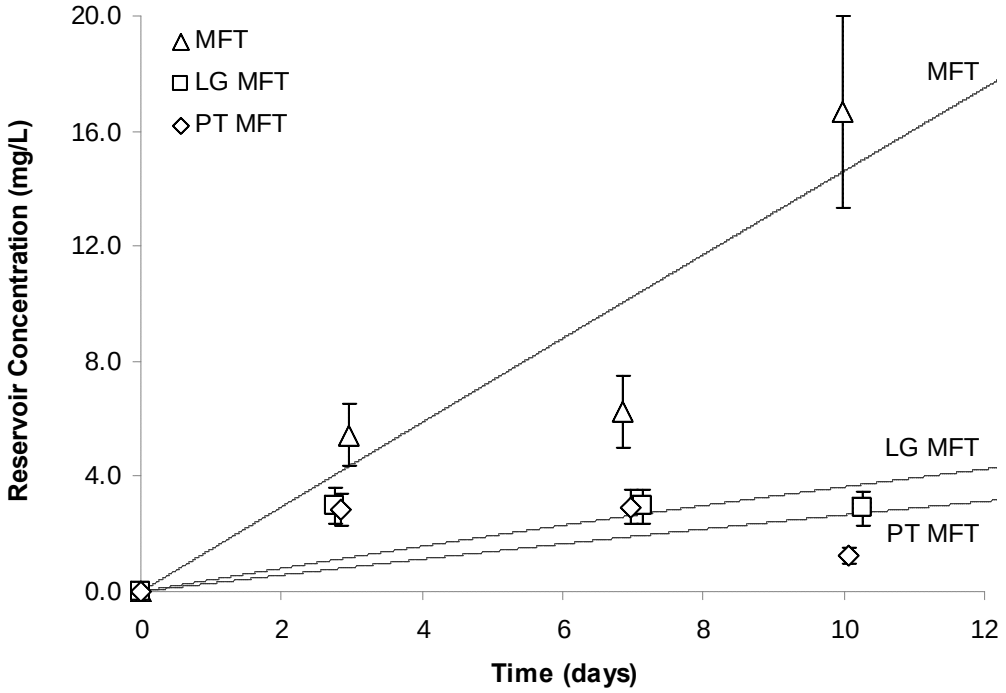

Figure 4.16: Radial diffusion of (a) F2 fraction and (b) F3 fraction PHCs from 3 different MFTs into de-ionized water.

4.4.3 Tailings Sand Diffusion Model

A radial diffusion experiment was completed for the tailings sand, which was saturated for the experiment. The F2 and F3 fraction radial diffusion results are shown in Figure 4.17 below. Experimental data is presented with error bars for plus-minus 20 percent of the experimental results, which is consistent with the accuracy that can be achieved from GC analysis of hydrocarbons.

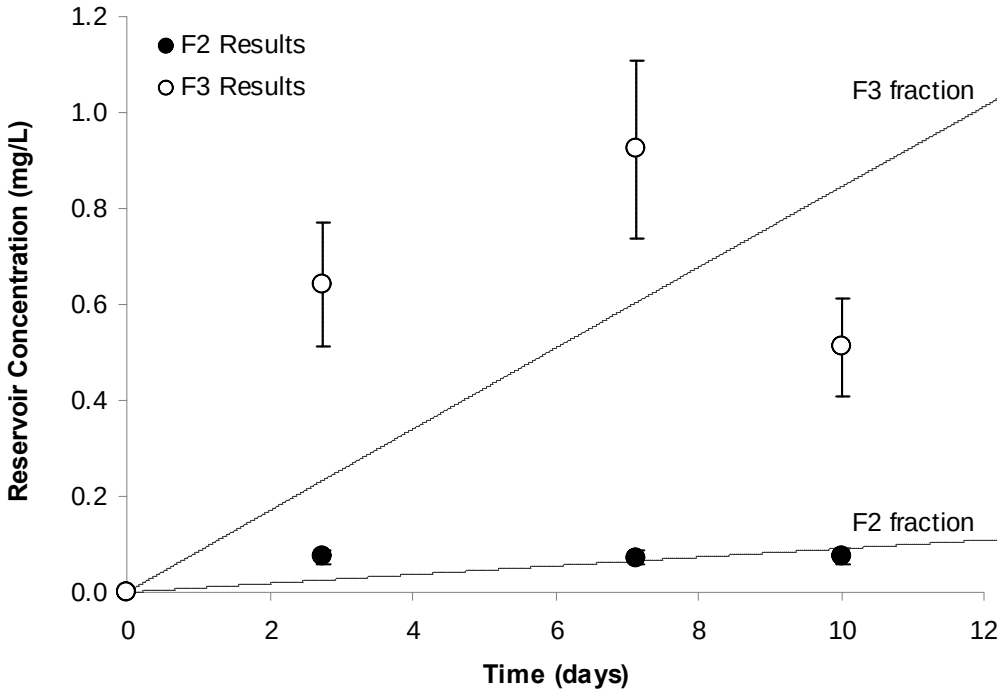

Figure 4.17: Radial diffusion of F2 and F3 fraction PHCs from saturated tailings sand into de-ionized water.

4.4.4 Sensitivity Analysis

To illustrate that the values of the adsorption and diffusion coefficients were the best fit values for the FDM model, the values of the diffusion and adsorption coefficients were varied separately in the model to determine their sensitivity to the results. Figure 4.18 below shows the deviation away from the GC model results when the diffusion coefficient D* is varied within half an order of magnitude above and below the best fit value of D*. As can be seen, there is quite a bit of variability in the model when D* is varied.

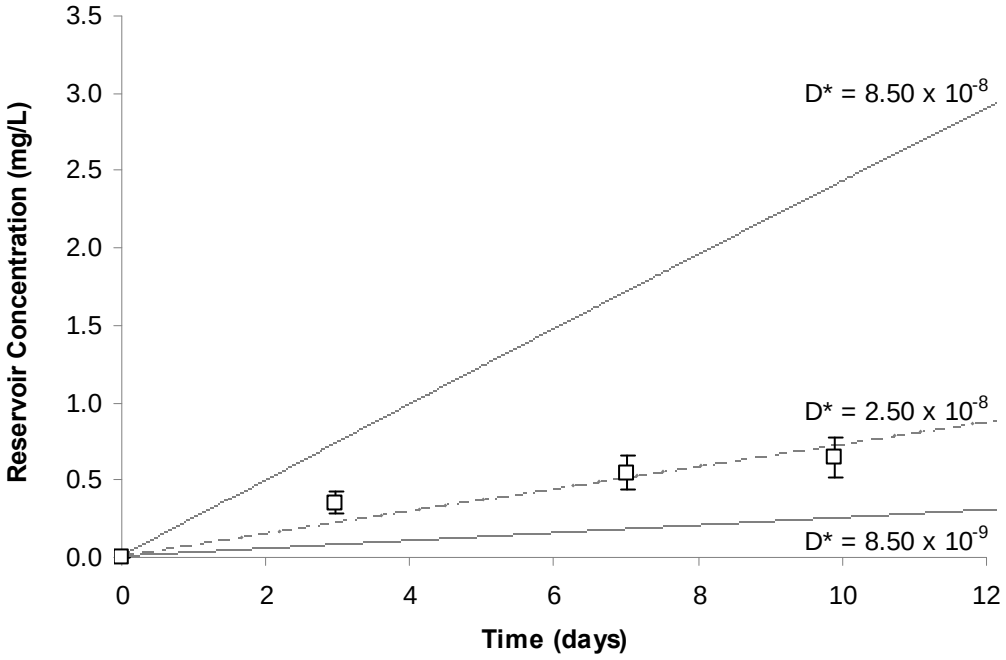

Figure 4.18: Varying D* values for the 2:1 SFR CT F2 Fraction results. The best fit D* value of 2.50 x 10-8 cm^2/s was varied by half an order of magnitude above and below the best fit value. The GC model results are shown as individual square data points.

Figure 4.19 below shows the deviation away from the GC model results when the adsorption coefficients Ŭ and ɓ are varied within two orders of magnitude above and

below the best fit value for the Langmuir adsorption coefficients. As can be seen, the adsorption coefficients have much less impact on the sensitivity of the model results than the diffusion coefficient. This indicates that it is the diffusion coefficient that is the main transport mechanism in this system.

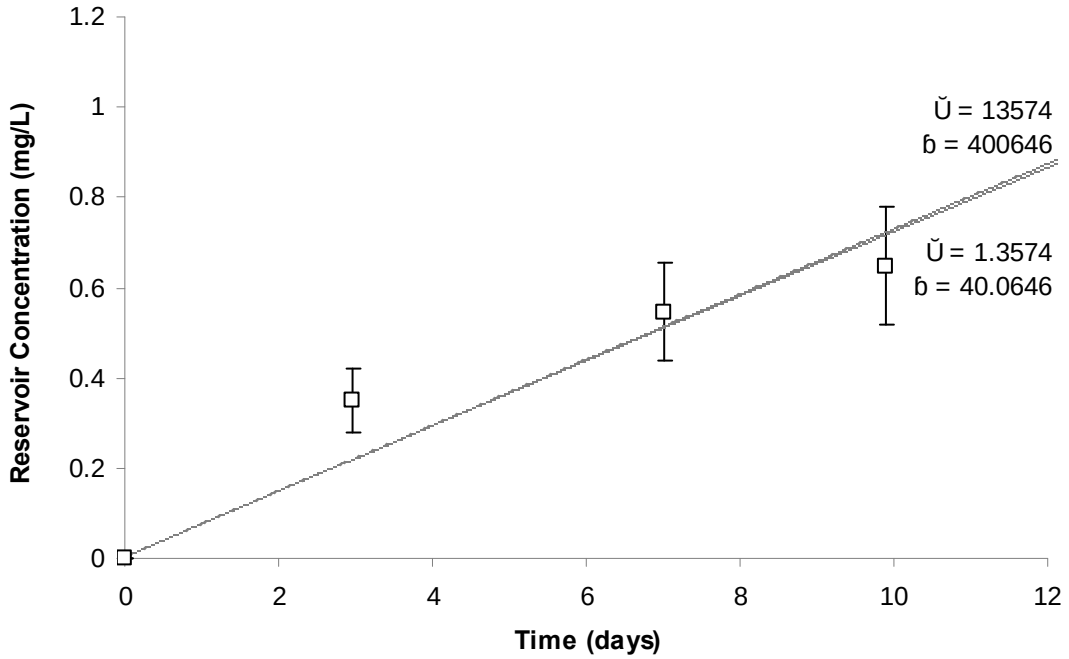

Figure 4.19: Varying Langmuir adsorption coefficients Ŭ (L/mgPHC) and ƀ (mgPHC / kgSOIL) for the 2:1 SFR CT F2 Fraction results. The best fit Ŭ and ƀ values of were varied by two orders of magnitude above and below the best fit values. The GC model results are shown as individual square data points.

To demonstrate the difference in PHC concentration throughout the tailings in the diffusion cell, the calculated F2 fraction concentration of PHCs at 3 radius values, for PT MFT, is shown in Figure 4.20 below. The concentration is shown in the central reservoir, and also at two radial distances from the central reservoir, at values of 7.84 cm and 9.86 cm. Compared to the PHC concentration in the central reservoir, the concentration in the

porewater of the PT MFT tailings is very high. It is possible that as PHCs move from the pore-spaces of the tailings into the central reservoir, other PHCs desorb from the surface of the tailings grains. From the characterization of PHCs present in the tailings materials, it is known that the PHC content in the tailings is very high, especially when compared to the PHC concentration in the porewater.

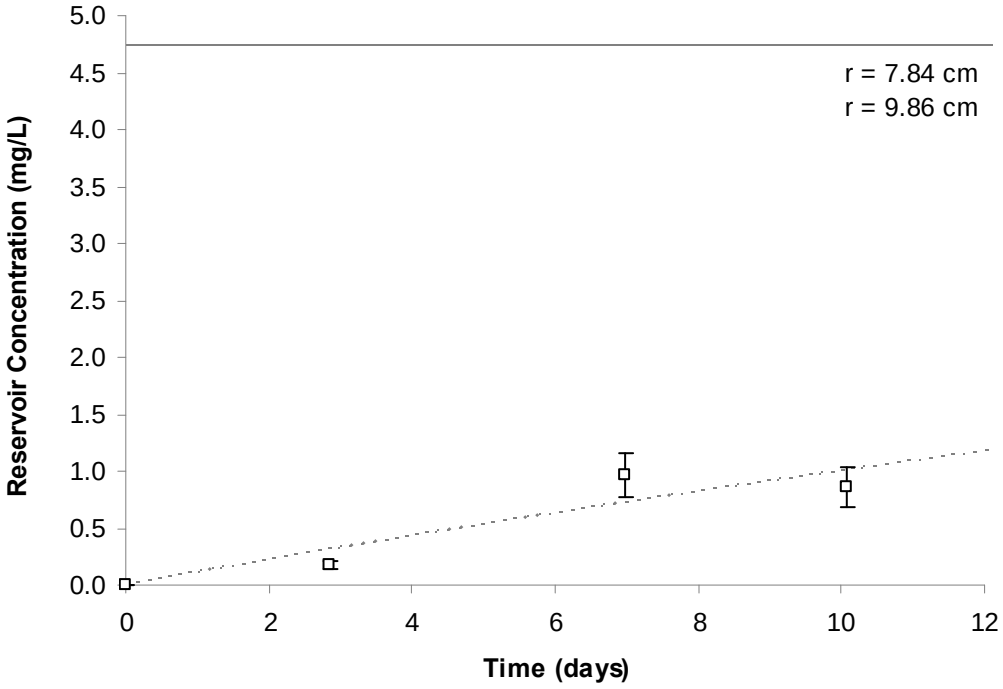

Figure 4.20: The F2 fraction PHC concentration for the PT MFT at three different radius values. There is little difference in the porewater concentration of F2 fraction PHCs at both values for r of 7.84cm and 9.86cm.

To demonstrate that the FDM is modeling diffusion, and not just an apparent effect due to the size of Δr (the incremental change in radius in the FDM model), a graph of Δr versus the concentration of F2 fraction PHC in the tailings between radius 0mm and 0.2mm is

shown in Figure 4.21 for the 2:1 CT on Day 5 of the radial diffusion experiment. Changes in concentration are shown for several values of Δr (the diamond shaped data points), which confirms the FDM model is not dependent on the value of Δr.

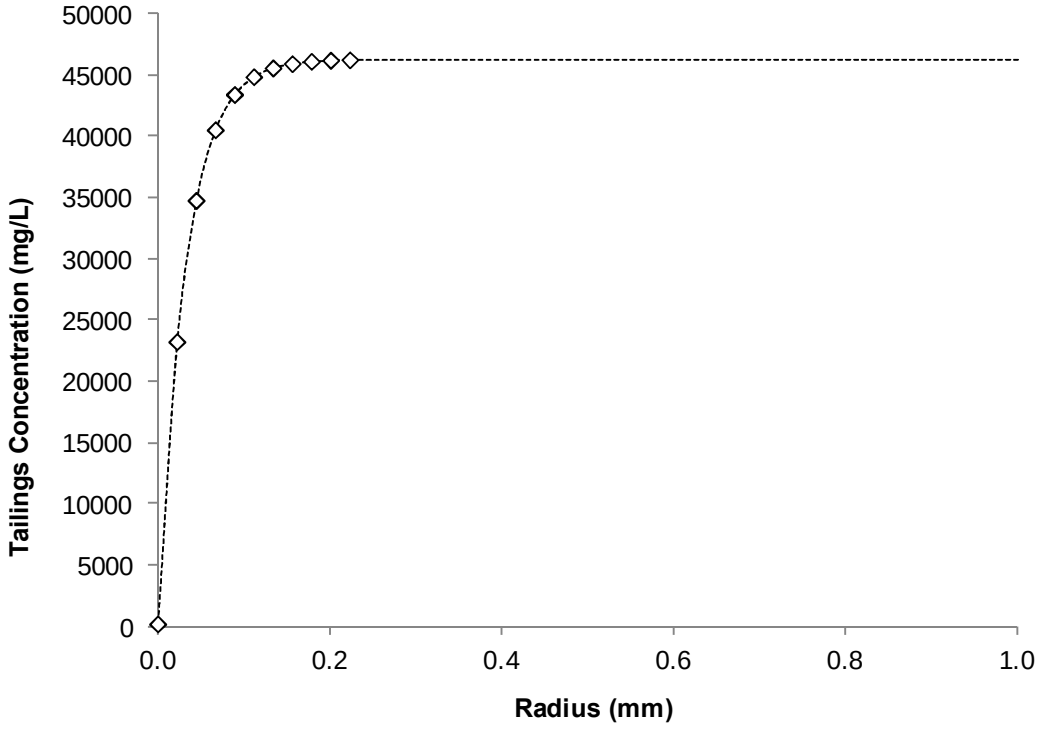

Figure 4.21: The F2 fraction PHC concentration in the tailings on Day 5 of the radial diffusion experiment for the 2:1 CT. This graph demonstrates that there is diffusion occurring at more than one value of θr in the model.

4.4.5 Diffusion Discussion

There are several considerations in the diffusion of PHCs and other hydrophobic organic compounds. The effect of temperature on diffusion rates, the cosolvency of organics, straining effect and molecular size, the effect of saline conditions, are all included in this section. A comparison of the D* results with effective diffusion coefficients of organic

compounds found in literature is also discussed, as well as the effect of the materials used in the diffusion cell construction and the hydrophobicity of the organic compounds.

a) Effect of Temperature on Diffusion

Temperature effects were not included in determining the diffusion coefficients of the oil sands tailings, however in field conditions, temperature will play an important role in both diffusion and adsorption rates, as both lower and higher temperatures as well as freezing conditions that can be expected in northern Alberta.

The diffusion coefficients discussed above were determined from tests conducted at 20ºC. It is expected that the PHCs present in the tailings material will act similarly to other hydrophobic organic compounds in porous media, which means that diffusion can be expected to decrease and adsorption increased as the temperature drops below 20ºC.

b) Cosolvency of Organics

The individual identification of each PHC present in the tailings was not possible, so the effects of cosolvency were not considered in these diffusion experiments, although co-solvency is certain to have been present in the F2 and F3 fraction PHC diffusion experiments in this research, as there are a variety of PHCs present in the tailings materials, of which a very few have been individually identified, such as benzene or toluene.

The cosolvent effect depends on the dissolved constituents from the tailings, and it is likely each tailings material will behave differently as their compositions vary. If the components of the tailings change, the diffusion rates may be affected in part by cosolvency. The presence of non-polar organic co-solvents will almost certainly increase the solubility of PHCs, which will in turn increase their diffusive mobility.

c) Effect of Saline Conditions

Oil sands process water was found to have a higher concentration of salts and alkalinity when compared with natural waters. Higher salinity in the process water has also been documented in the literature (MacKinnon et al. 2005). Gustafson and Dickhut (1994) found that there was no measurable effect on the diffusion coefficient for PAHs in saline (i.e. marine) water. Conductivity was measured for the first 3 days of each diffusion cell experiment, which provided a relative measure of diffusion of dissolved electrolytes into the reservoir, including salts. Higher salinity has not been found to affect diffusion in other studies, so there is no reason to suspect that it has affected the diffusion rate in these experiments.

d) Straining and the Effect of Molecular Size

The mobility and transport of colloids in suspension can be inhibited by the size of the pore openings in the porous media, such as soil or tailings, an effect known as straining (Hendry et al. 2003), or the molecular sieve effect. The aqueous diffusion rate of PAHs

has been found to decrease with increasing molecular size (Gustafson and Dickhut 1994). Dunnivant et al. (1992) concluded that straining did not affect the diffusion of naturally occurring dissolved organic carbon (DOC) through aquifer material, although Sawatsky et al. (1997) found that differences between predicted and observed diffusion coefficients for 1-napthol and naphthalene through clay materials were due to restrictive pore spaces. The calculated radius of naturally occurring DOC is between 1.1 and 1.25 nm (Hendry et al. 2003). The radius of typical asphaltene molecules, one of the larger components of tailings PHCs, is 1.2 to 2.4 nm (Groenzin and Mullins 1999).

The radii of the DOC are similar to the smaller of the asphaltenes, so there is likely to be little effect on the diffusion of the smaller tailings PHCs due to straining. As asphaltenes can be much as two times larger than DOC, it is more likely that the pore sizes may be a limiting diffusion factor for the higher PHC fractions in the tailings materials, particularly in the finer-grained tailings materials. The diffusion of those tailings materials exhibiting smaller pore sizes or grain sizes may be more affected, such as the three MFT and three CT tailings. The tailings sand is least likely to be affected, as it has the highest grain size of all tailings materials in this study.

e) Comparison to Literature D* values

The tailings samples collected in the field were disturbed samples, although most cannot be classified as a ñsoilò. Many of the tailings have the consistency closest to a slurry, and are approximately homogeneous, unlike natural soils. Whether testing with these types of materials would yield reasonable diffusion coefficient estimates was unknown prior to the experiment. Diffusion is dependent on several physical properties of the soil,

including porosity of the soil, and the tortuosity of the path the contaminant must take through the soil matrix (Shackelford, 1991). However, a study completed by Badv and Faridfard (2005) used disturbed sand samples in a single reservoir diffusion test. Their results showed that the measured and calculated diffusion coefficients were reasonably close.

The radial diffusion experiments yielded effective diffusion coefficients (D*) from between 0.020 x 10^{-6} cm^2/s for F3 MFT to 1.10 x 10^{-6} cm^2/s for F2 LG MFT. The D* values from other studies of the diffusion of organic compounds through clay provide similar values, or within one order of magnitude.

The majority of the tailings consisted of fine-grained materials (sand-clay-silt). The similarity between the effective diffusion coefficients from the literature and the results obtained in this study supports the idea that the diffusion of the PHCs from the tailings is similar to the movement of hydrophobic organic compounds through clay.

g) Tailings PHC as an Infinite Source

The amount of PHC present in most of the tailings indicates that it could be treated as an ñinfinite sourceò of PHC contaminant. A solubility of 6.42 mg/L for F2 fraction PHCs and 0.164 mg/L for F3 fractions was assumed, which is an estimate based on to the measured ranges of PHC solubility from ASTDR (1999). Using these values, it was

estimated that the number of pore volumes required to deplete the F2 and F3 PHC from the tailings was between approximately 14,600 and 311,000 times. This supports the assumption that the PHC in the tailings could be considered an infinite source of contaminant.

h) Effect of the Diffusion Cell Materials

The wire mesh used to separate the inner reservoir from the tailings material may also have had an effect on the diffusion rates. The stainless steel wire mesh used for the reservoir was a 165 x 800 Twill Dutch weave with a nominal retention size of 24-26 microns and a total thickness of 0.16 mm. The open area of the mesh was calculated to be 11.79%. The open area was less than the porosity for all tailings materials, which had an average value of 0.58 and ranged from 0.36 for tailings sand to 0.89 for MFT. However, the mesh was far less than 1 mm thick, the open area was greater than 10%, and water was able to pass through the mesh at a slow but steady rate when it was tested. Asphaltenes, which are one of the largest components of tailings PHCs, are between 0.0012 to 0.0024 microns (Groenzin and Mullins 1999), which is far smaller than the average nominal retention size of 25 microns. Based on this information, it is unlikely that the wire mesh was a limiting factor for the measured diffusion rates.

The stainless steel mesh tubes used in this study may also have sorbed some PHCs, and introduced some uncertainty in the D* values obtained. Headspace development may also be a source of error, although headspace is more likely to affect volatile (i.e. F1 and

BTEX) fractions of PHCs. Measuring potential losses from headspace development and materials used in apparatus were not in the scope of this study.

g) Other Effects on Diffusion

There are several other factors that may affect the diffusion rate of the tailings PHCs. The materials used in the diffusion cell construction, inorganic chemistry of the system and hydrophobicity/solubility all affect diffusion rates.

It was found that as the aqueous solubility of a volatile organic compound decreased, the effective diffusion coefficient decreased as well (Kim et al. 2001). In general, these findings support the tailings PHC results. With the exception of the composite tailings results, the F2 fraction D* values are greater than the F3; F2 fraction PHCs are smaller molecules and, as was found in the desorption experiments, more soluble than F3 fraction PHCs.

4.4.6 Summary

The diffusion coefficients resulting from this study are similar to those effective diffusion coefficients for benzene, toluene chlorobenzene and DOC through clay, listed in Table 4.12. Temperature was not likely to have affected the diffusion coefficient results from this study, although temperature effects can be expected under field conditions because a greater range in temperatures are present under field conditions, including freezing conditions. Salinity is also not likely to be affecting these results. Co-solvency depends on the dissolved constituents from the tailings, and it is likely each tailings material will

behave differently as their compositions vary. Organic co-solvents will almost certainly increase the mobility of PHCs through the tailings, as one of the most basic concepts of solubility is that like dissolves like (i.e. non-polar solutes will dissolve more readily in non-polar solvents). Straining may also be a limiting factor in diffusion rates, as the pore size openings may be smaller than some of the suspended colloids in the tailings. In general, as aqueous solubility decreases, so does diffusivity of organic compounds. This supports the tailings PHC results, as the F2 fraction D* values are greater than the F3 for most of the tailings.

The results of the radial diffusion experiments agree with diffusion rates found by other researchers in similar porous media. More research will be needed to verify these preliminary results for the diffusive transport of F2 and F3 PHC fractions in tailings. Tailings composition will continue to change as new technologies for fines settling and bitumen extraction are developed. The diffusion of PHCs from these new materials will need to be examined as it is probable that these changes will affect the transport and mobility of the contaminants.

5 CONCLUSIONS & RECOMMENDATIONS

5.1 Conclusions

The objective of this study was to determine desorption and diffusion coefficients of petroleum hydrocarbons from several tailings materials from the Suncor oil sands mine site. These coefficients will help determine the rate at which the petroleum hydrocarbons can be expected to migrate from the dewatered tailings into the cover soil of a remediated site. The following conclusions have been made from the results obtained in this study:

1) Characterization of Oil Sands Tailings

a) The results show that the MFT and CT have a much higher concentration of PHC than some of the other tailings. The amount of PHC present in the CT is directly related to the percent of fines in the tailings mix.

b) The PHC concentration results presented in this study are within +/- 20 percent of the reported number, which is not very precise. This is a very large source of potential error in the PHC results.

2) Desorption of Oil Sands Tailings

a) The Langmuir isotherm model was found to be the best fit for the desorption data from the desorption experiments. The Freundlich model was also considered, but was not found to fit the data as closely.

b) The desorption results obtained were found to be similar in shape and magnitude to the results of asphaltene desorption, which is one of the components of tailings PHCs.

c) Temperature and solution mixture were studied in the early phases of the desorption experiments. It was found that neither temperature nor solution mixture had much impact on the results (refer to Section 4.4.2). These observations are likely because the change in temperature (0ºC and 20ºC) wasnôt great enough to show any significant changes in the results. Other studies have found that organic compounds which are increasingly soluble with increasing temperature have lower K_d values at higher temperatures (Delle Site 2001).

d) The detection limit of PHCs is a limiting factor, and the error in the method for analyzing the PHC content should always be a consideration when interpreting analytical results. The lab results for PHC concentration reported in this study are within +/- 20 percent.

e) It did not appear as though the aqueous concentration data from the desorption tests had reached a solubility limit. It is possible that the aqueous concentration included microdroplets of PHC in suspension, which would have contributed to the total aqueous concentration measured, resulting in the measurement of a combined ñsuspendedò and ñdissolvedò aqueous PHC concentration.

f) Many PHCs are hydrophobic organic compounds, and are relatively insoluble in water. Their limited solubility in water directly affects the concentration of PHCs in solution, and may have been a limiting factor in the desorption coefficients.

g) The adsorption-desorption process of organic non-polar compounds is not completely reversible, resulting in sorption hysteresis. Studies have shown that there is a fraction of

the organic solute that is irreversibly bound to the soil or sediment (Dubey and Waxman 1991; Morrissey and Grismer 1999; Kan et al. 1998). However, there is less desorption than adsorption occurring, and if the assumption is that these processes are equal, there is less adsorption occurring in the model than would be occurring in a natural porous media system, and as a result the contaminant will mobilize more slowly than predicted by the model.

h) The PHCs in tailings consist of many hydrophobic organic compounds, such as benzene, toluene and asphaltenes. This is supported by the slower desorption of the larger F3 fraction molecules on a percentage basis of the total fraction.

i) The sorption kinetics of organics compounds has two fractions, a ñfastò fraction, and a much smaller ñslowò fraction. The fast fraction generally occurs within hours to days, while the slow fraction takes days to weeks and sometimes longer to reach equilibrium. Under field conditions, timescales will be much longer and the much smaller slow fraction may begin to have a small effect the contaminant transport rate of PHCs from the tailings into the topsoil cover system. However, the slow fraction is much smaller and it is likely that it will only begin to occur once vegetation has been established.

j) Organic matter in soil has a high affinity for the adsorption of non-polar organic compounds, as hydrophobic organic compounds have a preference to partition to other organic matter from the aqueous phase, including polychlorinated biphenyls (PCBs) and polycyclic aromatic hydrocarbons (PAHs) (Delle Site, 2001). The PHCs mobilizing from the tailings to the overlying topsoil are also likely to sorb onto the organic matter. This will likely reduce the bioavailability of PHCs for plant uptake. This may also be

attributed to the slow migration of hydrophobic species is believed to be attributed to their tendency to adsorb onto the soil organic matter (Barone et.al., 1992).

k) There are other potential sources of error in the desorption coefficients. The presence of dissolved salts in the tailings may have an effect on desorption rates, causing ñsalting outò. Steric hindrance may also be affecting desorption rates. Studying these effects is outside of the scope of this study.

3) Diffusion of PHCs Oil Sands Tailings

a) It was found that the diffusion coefficients of the tailings are similar the diffusion coefficients of several organic compounds through clay materials (refer to Table 4.12). The results of these radial diffusion experiments are generally in agreement with other study results for diffusion rates through similar porous media.

b) The F2 fraction was found to be more mobile than the F3 fraction, as the F2 fraction diffusion coefficients were greater than the F3 fraction coefficients. It has been found that as diffusivity decreases, aqueous solubility also decreases. The larger fraction F3 molecules have higher carbon numbers, and are likely to be less soluble than the F2 fraction, which is a possible explanation for this observation.

c) Although not all of the tailings samples were included in the diffusion tests, because the PHC content and desorption of all tailings were characterized, the diffusion results may be of use in approximating the diffusive behaviour of other tailings materials.

d) Temperature effects are not likely to affect the diffusion coefficients obtained in this study, although there are expected to be temperature effects on diffusion under field conditions. The effect of temperature on the diffusion was not in the scope of this study.

e) Cosolvency is definitely present in the pore water of the tailings materials, and in other studies has been found to affect diffusion rates. The effect of cosolvency on diffusion is outside the scope of this study.

f) Steric hindrance may also be affecting the diffusion rates, effectively decreasing the mobility of the larger molecules. This phenomenon may have more of an effect in field conditions, where the tailings are likely to consolidate. Consolidation of the tailings would also likely decrease the transportation rates of PHCs by rendering the pore sizes smaller. The effect of steric hindrance and field consolidation of tailings on diffusion rates are outside the scope of this study.

5.2 Implications for Design

The desorption and diffusion coefficients determined from this work can be used in cover system design applications, such as the simple conceptual cover system shown below in Figure 5.1. In this example, 3m of 2:1 SFR CT is capped with 1m of monolithic fine-grained soil, a growing medium likely containing a mixture of clay, silt, sand and organic material. The tailings have a nearly limitless supply of F2 and F3 PHCs, allowing the system to be modeled as a constant source concentration. The monolithic fine-grained soil is assumed to be nearly saturated in this example, and the PHC contaminants are shown to move through the entire thickness of the cover soil.

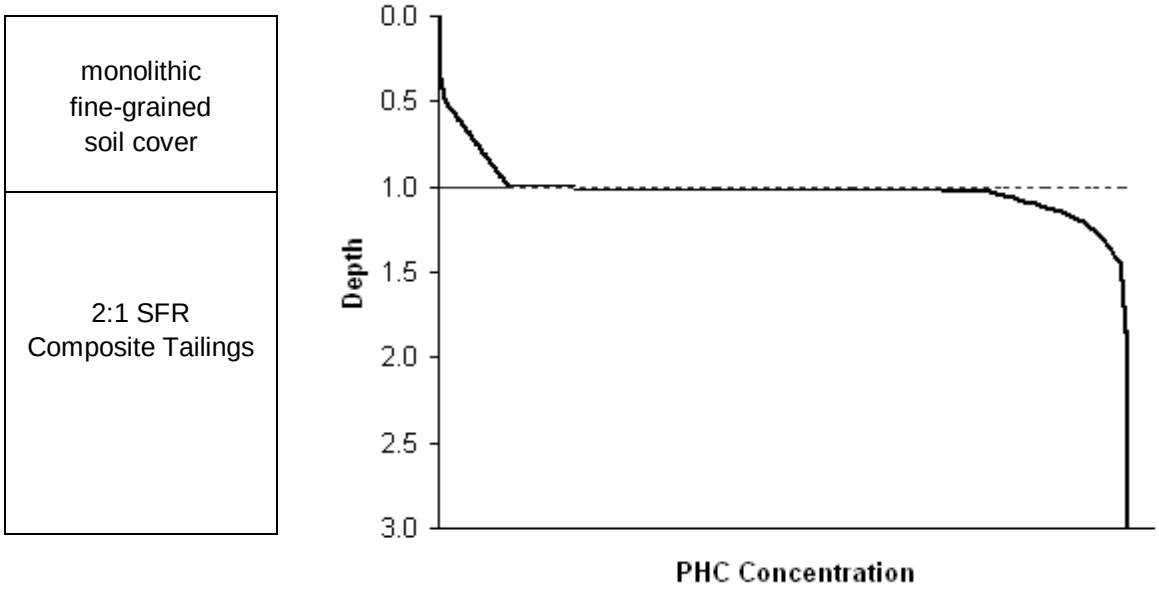

Figure 5.1: Conceptual cover system design, with 3m of 2:1 SFR CT capped with a monolithic fine-grained soil.

This example is meant to demonstrate that the tailings F2 and F3 desorption and diffusion coefficients from this work can be used to generate similar contaminant transport models once the F2 and F3 PHC fraction adsorption and diffusion coefficients are determined for that specific cover system soil. To complete this model, a number of assumptions would have to be made for the cover soil, including porosity, the diffusion coefficient and the adsorption coefficient. For this reason only a conceptual model was used to demonstrate the potential applications of the tailings PHC desorption and diffusion coefficients.

5.3 Recommendations

The following recommendations are suggested for any future work on the mobility and transport of PHCs from oil sands tailings:

1) The desorption and diffusion of oil sands tailings has not previously been studied, and it is recommended that the accuracy of these results be verified with future studies. PHC mobility is an important consideration in reclamation and revegetation efforts, as they can be toxic to vegetation in high concentrations. Some of the effects on sorption and diffusion that were discussed in this study, but outside the scope of work, should be incorporated into future work.
2) Adsorption of the tailings should be studied, as hysteresis in the adsorption-desorption processes is likely occurring.
3) Parametric studies, which would now be relatively easy to conduct, should be completed and compared to actual lab results.
4) The bench top desorption test would be is fairly simple to complete for new or other types of tailings. Estimates for the diffusion and desorption coefficients of these new materials could be extrapolated from the results obtained in this study.
5) A second type of adsorption-desorption study should be completed to verify the validity of the sorption coefficients obtained from these experiments. Flow-through column tests are one possible suggestion.
6) Adsorption/desorption and diffusion studies using the topsoil (cover soil) that will be used in the revegetation at the mine site would be useful in determining timelines for contaminant migration into those soils from the tailings. These results, in conjunction with the results from the work already completed, will provide an overall analysis of the complete system.

REFERENCES

3M Empore. 2004. Extraction Disks EPA Method 1664, Bioanalytical Technologies Project, St. Paul, Minnesota.

Akbarzadeh, K., Hammami, A., Kharrat, A., Zhang, D., Allenson, S., Creek, J., Kabir, S., Jamaluddin, A., Marshall, A.G., Rodgers, R.P., Mullins, O.C., and Solbakken, T. 2007. Asphaltenes - problematic but rich in potential, Oilfield Review, **19**(2): 22-43.

Alboudwarej, H., Pole, D., Svrcek, W.Y., and Yarranton, H.W. 2005. Adsorption of asphaltenes on metals, Industrial and Engineering Chemistry Research, **44**(15): 5585-5592.

Andrews, J.E., Brimblecombe, P., Jickells, T.D., Liss, P.S., Reid, B.J. 2004. An introduction to environmental chemistry. Blackwell Science, Malden, Mass.

ATSDR. 1999. Toxicological Profile for Total Petroleum Hydrocarbons. Agency for Toxic Substances and Disease Registry, Atlanta, GA.

ASTM Standard D2216-10, 2010. Standard test methods for laboratory determination of water (moisture) content of soil and rock by mass. ASTM International, West Conshohocken, PA. DOI: 10.1520/D2216-10, www.astm.org.

Badv, K. and Faridfard, M.R. 2005. Laboratory determination of water retention and diffusion coefficient in unsaturated sand, Water, air, and soil pollution, **161**(1-4): 25-38.

Ball, W.P. and Roberts, P.V. 1991. Long-term sorption of halogenated organic chemicals by aquifer material. 1. equilibrium, Environmental Science and Technology, **25**(7): 1223-1237.

Barone, F.S., Rowe, R.K., and Quigley, R.M. 1992. A laboratory estimation of diffusion and adsorption coefficients for several volatile organics in a natural clayey soil, Journal of contaminant hydrology, **10**(3): 225-250.

Böttcher, G., Brumsack, H., Heinrichs, H., and Pohlmann, M. 1997. A new high-pressure squeezing technique for pore fluid extraction from terrestrial soils, Water, air, and soil pollution, **94**(3-4): 289-296.

Braida, W.J., White, J.C., Zhao, D., Ferrandino, F.J., and Pignatello, J.J. 2002. Concentration-dependent kinetics of pollutant desorption from soils, Environmental Toxicology and Chemistry, **21**(12): 2573-2580.

Caughill, D.L., Morgenstern, N.R., and Scott, J.D. 1993. Geotechnics of nonsegregating oil sand tailings, Canadian Geotechnical Journal, **30**(5): 801-811.

CCME. 2008. Canada-wide standards for petroleum hydrocarbons (PHC) in soil. Canadian Council of Ministers of the Environment, Ottawa, ON.

CCME. 2001. Reference method for the Canada-wide standard for petroleum hydrocarbons in soil ï tier 1 method. Canadian Council of Ministers of the Environment, Ottawa, ON.

Chalaturnyk, R.J., Scott, J.D., and Özüm, B. 2002. Management of oil sands tailings, Petroleum Science and Technology, **20**(9-10): 1025-1046.

Chang, T.W. and Wang, M.K. 2002. Assessment of sorbent/water ratio effect on adsorption using dimensional analysis and batch experiments, Chemosphere, **48**(4): 419-426.

Clark, K. and Pasternack, D. 1932. Hot water separation of bitumen from Alberta bituminous sand, Industrial and Engineering Chemistry, **24**: 1410-1416.

Cornelissen, G., Van Noort, P.C.M., and Govers, H.A.J. 1997. Desorption kinetics of chlorobenzenes, polycyclic aromatic hydrocarbons, and polychlorinated biphenyls: Sediment extraction with Tenax® and effects of contact time and solute hydrophobicity, Environmental Toxicology and Chemistry, **16**(7): 1351-1357.

Cornelissen, G., Van Noort, P.C.M., Parsons, J.R., and Govers, H.A.J. 1997. Temperature dependence of slow adsorption and desorption kinetics of organic compounds in sediments, Environmental Science and Technology, **31**(2): 454-460.

Corseuil, H.X., Kaipper, B.I.A., and Fernandes, M. 2004. Cosolvency effect in subsurface systems contaminated with petroleum hydrocarbons and ethanol, Water research, **38**(6): 1449-1456.

Craig, R.F. 2004. Craigôs Soil Mechanics, Seventh Edition. Spon Press, New York, NY.

Delle Site, A. 2001. Factors affecting sorption of organic compounds in natural sorbent/water systems and sorption coefficients for selected pollutants. A review, Journal of Physical and Chemical Reference Data, **30**(1): 187-439.

Donahue, R.B., Barbour, S.L., and Headley, J.V. 1999. Diffusion and adsorption of benzene in Regina clay, Canadian Geotechnical Journal, **36**(3): 430-442.

Dubey, S.T. and Waxman, M.H. 1991. Asphaltene adsorption and desorption from mineral surfaces, SPE Reservoir Engineering (Society of Petroleum Engineers), **6**(3): 389-395.

Dunnivant, F.M., Jardine, P.M., Taylor, D.L., and McCarthy, J.F. 1992. Transport of naturally occurring dissolved organic carbon in laboratory columns containing aquifer material, Soil Science Society of America Journal, **56**(2): 437-444.

Fedorak, P.M., Coy, D.L., Salloum, M.J., and Dudas, M.J. 2002. Methanogenic potential of tailings samples from oil sands extraction plants, Canadian journal of microbiology, **48**(1): 21-33.

Fetter, C.W. 1999. Contaminant hydrogeology. Prentice Hall, Upper Saddle River, NJ.

Gharagheizi, F. 2012. Determination of diffusion coefficient of organic compounds in water using a simple molecular-based method, Industrial and Engineering Chemistry Research, **51**(6): 2797-2803.

Goral, M., Wisniewska-Goclowska, B., Skrzecz, A., Owczarek, I., Blazej, K., Haulait-Pirson, M.-., Hefter, G.T., Kapuku, F., Maczynska, Z., and Szafranski, A. 2006. IUPAC-NIST solubility data series. 81. hydrocarbons with water and seawater - revised and updated. part 11. C13-C36 hydrocarbons with water, Journal of Physical and Chemical Reference Data,**35**(2): 687-784.

Groenzin, H. and Mullins, O.C. 1999. Petroleum asphaltene molecular size and structure, ACS Division of Fuel Chemistry, Preprints, **44**(4): 728-732.

Grover, P.K. and Ryall, R.L. 2005. Critical appraisal of salting-out and its implications for chemical and biological sciences, Chemical reviews, **105**(1): 1-10.

Gustafson, K.E. and Dickhut, R.M. 1994. Molecular diffusivity of polycyclic aromatic hydrocarbons in aqueous solution, Journal of Chemical and Engineering Data, **39**(2): 281-285.

Headley, J.V., Boldt-Leppin, B.E.J., Haug, M.D., and Peng, J. 2001. Determination of diffusion and adsorption coefficients for volatile organics in an organophilic clay-sand-bentonite liner, Canadian Geotechnical Journal, **38**(4): 809-817.

Hendry, M.J., Ranville, J.R., Boldt-Leppin, B.E.J., and Wassenaar, L.I. 2003. Geochemical and transport properties of dissolved organic carbon in a clay-rich aquitard, Water Resources Research, **39**(7).

Holowenko, F.M., MacKinnon, M.D., and Fedorak, P.M. 2000. Methanogens and sulfate-reducing bacteria in oil sands fine tailings waste, Canadian journal of microbiology, **46**(10): 927-937.

Hsieh, P., Lee, C., and Chiu, A. 2010. Desorption kinetics of naphthalene from sediment particles: Batch and stepwise desorption approach. Water Science & Technology, **61**(4): 1011-1017.

Huang, W., Yu, H., and Weber Jr., W.J. 1998. Hysteresis in the sorption and desorption of hydrophobic organic contaminants by soils and sediments. 1. A comparative

analysis of experimental protocols, Journal of contaminant hydrology, **31**(1-2): 129-148.

Hutzinger, O. 1980. The handbook of environmental chemistry [online].

Itakura, T., Airey, D.W., and Leo, C.J. 2003. The diffusion and sorption of volatile organic compounds through kaolinitic clayey soils, Journal of contaminant hydrology, **65**(3-4): 219-243.

Jahnke, R.A. 1988. A simple, reliable, and inexpensive pore-water sampler, Limnology & Oceanography, **33**(3): 483-487.

Janfada, A., Headley, J., Peru, K., and Barbour, S. 2006. A laboratory evaluation of the sorption of oil sands naphthenic acids on organic rich soils, Journal of Environmental Science and Health - Part A Toxic/Hazardous Substances and Environmental Engineering, **41**(6): 985-997.

Kan, A.T., Fu, G., Hunter, M., Chen, W., Ward, C.H., and Tomson, M.B. 1998. Irreversible sorption of neutral hydrocarbons to sediments: Experimental observations and model predictions, Environmental Science and Technology, **32**(7): 892-902.

Karickhoff, S.W. 1980. Contaminants and Sediments: Analysis, Chemistry, and Biology.

Kim, J.Y., Edil, T.B., and Park, J.K. 2001. Volatile organic compound (VOC) transport through compacted clay, Journal of Geotechnical and Geoenvironmental Engineering, **127**(2): 126-134.

Kreyszig, E. 2006. Advanced engineering mathematics. John Wiley, Hoboken, NJ.

LeVeque, R.J. 2007. Finite difference methods for ordinary and partial differential equations: Steady-state and time-dependent problems. Society for Industrial and Applied Mathematics, Philadelphia, PA.

Li, P. and SenGupta, A.K. 2004. Sorption of hydrophobic ionizable organic compounds (HIOCs) onto polymeric ion exchangers, Reactive and Functional Polymers, **60**(1-3): 27-39.

Limousin, G., Gaudet, J., Charlet, L., Szenknect, S., Barthès, V., and Krimissa, M. 2007. Sorption isotherms: A review on physical bases, modeling and measurement, Applied Geochemistry, 22(2): 249-275.

MacKinnon, M., Kampala, G., Marsh, B., Fedorak, P., and Guigard, S. 2005. Indicators for assessing transport of oil sands process-affected waters. *In* IAHS-AISH Publication, pp. 71-80.

Marczewski, A.W. and Szymula, M. 2002. Adsorption of asphaltenes from toluene on mineral surface, Colloids and Surfaces A: Physicochemical and Engineering Aspects, **208**(1-3): 259-266.

Martins, J.M. and Mermoud, A. 1998. Sorption and degradation of four nitroaromatic herbicides in mono and multi-solute saturated/unsaturated soil batch systems, Journal of contaminant hydrology, **33**(1-2): 187-210.

Masliyah, J., Zhou, Z., Xu, Z., Czarnecki, J., and Hamza, H. 2004. Understanding water-based bitumen extraction from Athabasca oil sands, Canadian Journal of Chemical Engineering, **82**(4): 628-654.

Morrissey, F.A. and Grismer, M.E. 1999. Kinetics of volatile organic compound sorption/desorption on clay minerals, Journal of contaminant hydrology, **36**(3-4): 291-312.

Myrand, D., Gillham, R.W., Sudicky, E.A., O'Hannesin, S.F., and Johnson, R.L. 1992. Diffusion of volatile organic compounds in natural clay deposits: Laboratory tests, Journal of contaminant hydrology, **10**(2): 159-177.

Nadim, F., Hoag, G.E., Liu, S., Carley, R.J., and Zack, P. 2000. Detection and remediation of soil and aquifer systems contaminated with petroleum products: An overview, Journal of Petroleum Science and Engineering, **26**(1-4): 169-178.

Nkedi-Kizza, P., Rao, P.S.C., and Hornsby, A.G. 1985. Influence of organic cosolvents on sorption of hydrophobic organic chemicals by soils, Environmental Science and Technology, **19**(10): 975-979.

Novakowski, K.S. and Van Der Kamp, G. 2004. The radial diffusion method, 2, A semianalytical model for the determination of effective diffusion coefficients, porosity, and adsorption, Water Resour.Res. **32**(6): 1823-1830.

Page, C.A., Bonner, J.S., Sumner, P.L., and Autenrieth, R.L. 2000. Solubility of petroleum hydrocarbons in oil/water systems, Marine Chemistry, **70**(1-3): 79-87.

Peters, C.A. 1993. Coal tar dissolution in water-miscible solvents: Experimental evaluation, Environment Science Technology, **27**(13): 2831-2843.

Petrov, A.A. 1987. Petroleum hydrocarbons. Springer-Verlag, Berlin; New York.

Pignatello, J.J. and Xing, B.S. 1996. Mechanisms of slow sorption of organic chemicals to natural particles, Environmental science & technology, **30**(1): 1-11.

Poulsen, M., Lemon, L., and Barker, J. 1992. Dissolution of monoaromatic hydrocarbons into groundwater from gasoline oxygenate mixtures, Environmental science & technology, **26**(12): 2483-2489.

Pratt, D.L. and Fonstad, T.A. 2011. Groundwater Chemistry Below Mortalities Disposal Sites. Final Report: ADF Project 20070129. Saskatchewan Ministry of Agriculture.

Rahimi, P.M. and Gentzis, T. 2006. Chapter 19: The chemistry of bitumen and heavy oil processing. In Hsu, C.S., Robinson, P.R., and SpringerLink. *Practical advances in petroleum processing*. Springer Science+Business Media, Inc., New York, NY. 149-186.

Rowe, R.K., Caers, C.J., and Barone, F. 1988. Laboratory determination of diffusion and distribution coefficients of contaminants using undisturbed clayey soil. Canadian Geotechnical Journal, **25**(1): 108-118.

Rowe, R.K. and Badv, K. 1996. Chloride migration through clayey silt underlain by fine sand or silt, Journal of Geotechnical Engineering, **122**(1): 60-68.

Rowell, D.L. 1994. Soil science: Methods and applications. Longman Scientific & Technical; Wiley, Harlow, Essex; New York.

Sawatsky, N., Feng, Y., and Dudas, M.J. 1997. Diffusion of 1-naphthol and naphthalene through clay materials: Measurement of apparent exclusion of solute from the pore space, Journal of contaminant hydrology, **27**(1-2): 25-41.

Shackelford, C.D. 1991. Laboratory diffusion testing for waste disposal - A review, Journal of contaminant hydrology, **7**(3): 177-217.

Shackelford, C.D. and Daniel, D.E. 1991. Diffusion in saturated soil. 1. background, Journal of Geotechnical Engineering, **117**(3): 467-484.

Shah, D.J. and Tiwari, K.K. 1981. Effect of salt on the distribution of acetic acid between water and organic solvent, Journal of Chemical and Engineering Data, **26**(4): 375-378.

Siddique, T., Gupta, R., Fedorak, P.M., MacKinnon, M.D., and Foght, J.M. 2008. A first approximation kinetic model to predict methane generation from an oil sands tailings settling basin, Chemosphere, **72**(10): 1573-1580.

Sparks, D.L. 2003. Environmental soil chemistry. Academic, San Diego, Calif. ; London.

Suthaker, N.N. and Scott, J.D. 1996. Measurement of hydraulic conductivity in oil sand tailings slurries, Canadian Geotechnical Journal, **33**(4): 642-653.

Schwarzenbach, R.P., Gschwend, P.M., and Imboden, D.M. 1993. Environmental organic chemistry. J. Wiley, New York.

Szymula, M. and Marczewski, A.W. 2002. Adsorption of asphaltenes from toluene on typical soils of Lublin region, Applied Surface Science, **196**(1-4): 301-311.

Ten Hulscher, T.E.M. and Cornelissen, G. 1996. Effect of temperature on sorption equilibrium and sorption kinetics of organic micropollutants - A review, Chemosphere, **32**(4): 609-626.

USEPA. 2004. National Wadeable Stream Assessment: Water Chemistry Laboratory Manual. EPA841-B-04-008. U.S. Environmental Protection Agency, Office of Water and Office of Research and Development, Washington, DC.

USEPA. 2009. Glossary of technical terms: U.S. Environmental Protection Agency, access date November 22, 2012. http://www.epa.gov/oust/cat/TUMGLOSS.HTM#k

Van Der Kamp, G., Van Stempvoort, D.R., and Wassenaar, L.I. 1996. The radial diffusion method, 1, using intact cores to determine isotopic composition, chemistry, and effective porosities for groundwater in aquitards, Water Resour.Res. **32**(6): 1815-1822.

Van Rees, K.C.J., Sudicky, E.A., Suresh C Rao, P., and Ramesh Reddy, K. 1991. Evaluation of laboratory techniques for measuring diffusion coefficients in sediments, Environmental Science and Technology, **25**(9): 1605-1611.

Voice, T.C., Rice, C.P., and Weber Jr., W.J. 1983. Effect of solids concentration on the sorptive partitioning of hydrophobic pollutants in aquatic systems, Environmental Science and Technology, **17**(9): 513-518.

Wu, S. and Gschwend, P.M. 1986. Sorption kinetics of hydrophobic organic compounds to natural sediments and soils, Environmental Science and Technology, **20**(7): 717-725.

Yong, R.N. and Rao, S.M. 1991. Mechanistic evaluation of mitigation of petroleum hydrocarbon contamination by soil medium, Canadian Geotechnical Journal, **28**(1): 84-91.

Zhang, X., Barbour, S.L., and Headley, J.V. 1998. A diffusion batch method for determination of the adsorption coefficient of benzene on clay soils, Canadian Geotechnical Journal, **35**(4): 622-629.

Zhu, J., Zhu, L., Zhu, R., and Chen, B. 2008. Microstructure of organo-bentonites in water and the effect of steric hindrance on the uptake of organic compounds, Clays and Clay Minerals, **56**(2): 144-154.

APPENDIX A

Mathematical Derivations

A.1) Derivation of the Partial Differential Diffusion Equation from Cartesian to Polar Coordinates

A.2) Derivation of 1-D Diffusion-Adsorption Equation (x, r, t)

A.3) Conversion of the Diffusion-Adsorption PDE to a Finite Difference Method

A.1) Derivation of the Partial Differential Diffusion Equation from Cartesian to Polar Coordinates

This derivation is an extended version of the derivation of the partial differential equation from Cartesian to Polar coordinates, based on the method described in Kreyszigôs *Advanced Engineering Mathematics* (2006).

1. The PDE diffusion equation in Cartesian Coordinates (x, y, t):

$$\frac{\partial^2 C}{\partial t^2} = D * \left(\frac{\partial^2 C}{\partial x^2} + \frac{\partial^2 C}{\partial y^2} \right)$$

The following relationships exist between (x, y) and (r, d):

$$x = r\cos\theta$$

$$y = r\sin\theta$$

$$r^2 = x^2 + y^2$$

$$\tan\theta = \frac{y}{x}$$

2. Conversion to Polar Coordinates, x-direction

a) Using the Chain Rule:

$$\frac{\partial C}{\partial x} = \frac{\partial C}{\partial r}\frac{\partial r}{\partial x} + \frac{\partial C}{\partial \theta}\frac{\partial \theta}{\partial x}$$

b) Differentiate with respect to x:

$$\frac{\partial}{\partial x}\left(\frac{\partial C}{\partial x}\right) = \frac{\partial}{\partial x}\left(\frac{\partial C}{\partial r}\frac{\partial r}{\partial x} + \frac{\partial C}{\partial \theta}\frac{\partial \theta}{\partial x}\right)$$

c) Using the first Product Rule, and then the Chain Rule:

$$\frac{\partial}{\partial x}\left(\frac{\partial C}{\partial x}\right) = \frac{\partial}{\partial x}\left(\frac{\partial C}{\partial r}\right)\frac{\partial r}{\partial x} + \frac{\partial}{\partial x}\left(\frac{\partial r}{\partial x}\right)\frac{\partial C}{\partial r} + \frac{\partial}{\partial x}\left(\frac{\partial C}{\partial \theta}\right)\frac{\partial \theta}{\partial x} + \frac{\partial}{\partial x}\left(\frac{\partial \theta}{\partial x}\right)\frac{\partial C}{\partial \theta}$$

$$\frac{\partial^2 C}{\partial x^2} = \left(\frac{\partial^2 C}{\partial r^2}\frac{\partial r}{\partial x} + \frac{\partial^2 C}{\partial r \partial \theta}\frac{\partial \theta}{\partial x}\right)\frac{\partial r}{\partial x} + \frac{\partial C}{\partial r}\frac{\partial^2 r}{\partial x^2} + \left(\frac{\partial^2 C}{\partial \theta \partial r}\frac{\partial r}{\partial x} + \frac{\partial^2 C}{\partial \theta^2}\frac{\partial \theta}{\partial x}\right)\frac{\partial \theta}{\partial x} + \frac{\partial C}{\partial \theta}\frac{\partial^2 \theta}{\partial x^2}$$

d) First derivative of the relationship between (x, y) and r:

$$r = \sqrt{x^2 + y^2}$$

$$\frac{\partial r}{\partial x} = \frac{1}{2}\left(x^2 + y^2\right)^{-1/2}(2x) = \frac{x}{\sqrt{x^2 + y^2}} = \frac{x}{r}$$

$$\frac{\partial r}{\partial x} = \frac{x}{r}$$

e) First derivative of the relationship between (x, y) and ɖ:

$$\theta = \tan^{-1}\frac{y}{x}$$

$$\frac{\partial \theta}{\partial x} = \frac{1}{1+\left(y/x\right)^2}\left(\frac{-y}{x^2}\right) = \frac{-y}{x^2 + y^2} = \frac{-y}{r^2}$$

$$\frac{\partial \theta}{\partial x} = \frac{-y}{r^2}$$

f) Second derivative of the relationship between (x, y) and r:

$$\frac{\partial r}{\partial x} = \frac{x}{r}$$

$$\frac{\partial}{\partial x}\left(\frac{\partial r}{\partial x}\right) = \frac{\partial}{\partial x}\left(\frac{x}{r}\right) = \frac{1}{r} + x\frac{\partial}{\partial x}\left(\frac{1}{r}\right) = \frac{1}{r} + x\left(\frac{-1}{r^2}\frac{\partial r}{\partial x}\right) = \frac{1}{r} - \frac{1}{r^2}\left(\frac{x^2}{r}\right) = \frac{y^2}{r^2}$$

$$\frac{\partial^2 r}{\partial x^2} = \frac{y^2}{r^2}$$

g) Second derivative of the relationship between (x, y) and ɖ:

$$\frac{\partial \theta}{\partial x} = \frac{-y}{r^2}$$

$$\frac{\partial}{\partial x}\left(\frac{\partial \theta}{\partial x}\right) = \frac{\partial}{\partial x}\left(\frac{-y}{r^2}\right) = -y\left[\frac{\partial}{\partial x}\left(\frac{1}{r^2}\right)\right] = -y\left(\frac{-2}{r^2}\frac{\partial r}{\partial x}\right) = \frac{2y}{r^2}\left(\frac{x}{r}\right) = \frac{2xy}{r^4}$$

$$\frac{\partial^2\theta}{\partial x^2}=\frac{2xy}{r^4}$$

h) Substitute expressions from Parts d to g into the following equation from Part c:

$$\frac{\partial^2 C}{\partial x^2}=\left(\frac{\partial^2 C}{\partial r^2}\left(\frac{\partial r}{\partial x}\right)+\frac{\partial^2 C}{\partial r\partial\theta}\left(\frac{\partial\theta}{\partial x}\right)\right)\frac{\partial r}{\partial x}+\frac{\partial C}{\partial r}\left(\frac{\partial^2 r}{\partial x^2}\right)+\left(\frac{\partial^2 C}{\partial\theta\partial r}\left(\frac{\partial r}{\partial x}\right)+\frac{\partial^2 C}{\partial\theta^2}\left(\frac{\partial\theta}{\partial x}\right)\right)\frac{\partial\theta}{\partial x}+\frac{\partial C}{\partial\theta}\left(\frac{\partial^2\theta}{\partial x^2}\right)$$

$$\frac{\partial^2 C}{\partial x^2}=\left(\frac{\partial^2 C}{\partial r^2}\left(\frac{x}{r}\right)+\frac{\partial^2 C}{\partial r\partial\theta}\left(\frac{-y}{r^2}\right)\right)\frac{x}{r}+\frac{\partial C}{\partial r}\left(\frac{y^2}{r^2}\right)+\left(\frac{\partial^2 C}{\partial\theta\partial r}\left(\frac{x}{r}\right)+\frac{\partial^2 C}{\partial\theta^2}\left(\frac{-y}{r^2}\right)\right)\frac{-y}{r^2}+\frac{\partial C}{\partial\theta}\left(\frac{2xy}{r^4}\right)$$

i) Simplifying yields:

$$\frac{\partial^2 C}{\partial x^2}=\frac{\partial^2 C}{\partial r^2}\frac{x^2}{r^2}-\frac{2xy}{r^3}\frac{\partial^2 C}{\partial r\partial\theta}+\frac{y^2}{r^4}\frac{\partial^2 C}{\partial\theta^2}+\frac{2xy}{r^4}\frac{\partial C}{\partial\theta}+\frac{y^2}{r^3}\frac{\partial C}{\partial r}$$

3. Similarly, the conversion to Polar Coordinates, y-direction:

$$\frac{\partial^2 C}{\partial y^2}=\frac{\partial^2 C}{\partial r^2}\frac{y^2}{r^2}-\frac{2xy}{r^3}\frac{\partial^2 C}{\partial r\partial\theta}+\frac{x^2}{r^4}\frac{\partial^2 C}{\partial\theta^2}+\frac{2xy}{r^4}\frac{\partial C}{\partial\theta}+\frac{x^2}{r^3}\frac{\partial C}{\partial r}$$

4. Adding x and y direction together yields:

$$\frac{\partial^2 C}{\partial x^2}+\frac{\partial^2 C}{\partial y^2}=\left(\frac{\partial^2 C}{\partial r^2}\frac{x^2}{r^2}-\frac{2xy}{r^3}\frac{\partial^2 C}{\partial r\partial\theta}+\frac{y^2}{r^4}\frac{\partial^2 C}{\partial\theta^2}+\frac{2xy}{r^4}\frac{\partial C}{\partial\theta}+\frac{y^2}{r^3}\frac{\partial C}{\partial r}\right)$$

$$+\left(\frac{\partial^2 C}{\partial r^2}\frac{y^2}{r^2}-\frac{2xy}{r^3}\frac{\partial^2 C}{\partial r\partial\theta}+\frac{x^2}{r^4}\frac{\partial^2 C}{\partial\theta^2}+\frac{2xy}{r^4}\frac{\partial C}{\partial\theta}+\frac{x^2}{r^3}\frac{\partial C}{\partial r}\right)$$

$$\frac{\partial^2 C}{\partial x^2}+\frac{\partial^2 C}{\partial y^2}=\frac{\partial^2 C}{\partial r^2}+\frac{1}{r}\frac{\partial C}{\partial r}+\frac{1}{r^2}\frac{\partial^2 C}{\partial\theta^2}$$

The diffusion equation in Cartesian Coordinates from Section 1 is:

$$\frac{\partial^2 C}{\partial t^2} = D * \left(\frac{\partial^2 C}{\partial x^2} + \frac{\partial^2 C}{\partial y^2} \right)$$

Substituting the term derived in Section 4:

$$\frac{\partial^2 C}{\partial x^2} + \frac{\partial^2 C}{\partial y^2} = \left(\frac{\partial^2 C}{\partial r^2} + \frac{1}{r}\frac{\partial C}{\partial r} + \frac{1}{r^2}\frac{\partial^2 C}{\partial \theta^2} \right)$$

$$\frac{\partial^2 C}{\partial t^2} = D * \left(\frac{\partial^2 C}{\partial r^2} + \frac{1}{r}\frac{\partial C}{\partial r} + \frac{1}{r^2}\frac{\partial^2 C}{\partial \theta^2} \right)$$

In the case of the axi-symmetric radial diffusion used in this thesis, there is no change as ɗ (the angle) changes:

$$\frac{\partial C}{\partial \theta} = 0$$

The axi-symmetric radial diffusion equation then becomes:

$$\frac{\partial^2 C}{\partial t^2} = D * \left(\frac{\partial^2 C}{\partial r^2} + \frac{1}{r}\frac{\partial C}{\partial r} \right)$$

A.2) Derivation of 1-D Diffusion-Adsorption Equation (x, r, t), in Saturated Porous Media

The adsorption-diffusion equation for 1-dimension in saturated porous media can be written as follows:

$$n\frac{\partial C}{\partial t} = nD^{*}\frac{\partial^2 C}{\partial x^2} - \rho_B K_D \frac{\partial C}{\partial t}$$

(Diffusion) (Adsorption)

Where:

n = porosity (no units)

C = Concentration of solute in aqueous solution (mg/L)

Ɉ B = bulk density of the soil

K_D = adsorption coefficient (L/kg)

D* = effective diffusion coefficient

t = time (in seconds)

Using the Langmuir model, the adsorption coefficient, K_D is equal to:

$$K_D = S/C$$

$$S = \frac{\alpha\beta C}{1+\alpha C}$$

then $$K_D = \frac{\alpha\beta}{1+\alpha C}$$

Where:

S = mass of solute sorbed onto the solid surface, per mass of solid (mg/kg)

Ŭ = Langmuir adsorption constant related to binding energy (L/mg)

ɓ = Langmuir isotherm coefficient, maximum amount of solute that can be absorbed by the solid (mg/kg)

Rearranging into the diffusion-adsorption equation yields:

$$\left(1+\frac{\rho_B}{n}K_D\right)\frac{\partial C}{\partial t}=D*\frac{\partial^2 C}{\partial x^2}$$

In polar coordinates, the diffusion term becomes:

$$\frac{\partial^2 C}{\partial x^2}=\frac{\partial^2 C}{\partial r^2}+\frac{1}{r}\frac{\partial C}{\partial r}$$

Therefore, the 1-D adsorption-diffusion equation, using Langmuir sorption coefficients, can be written as follows:

$$\left(1+\frac{\rho_B}{n}\left(\frac{\alpha\beta}{1+\alpha C}\right)\right)\frac{\partial C}{\partial t}=D*\left(\frac{\partial^2 C}{\partial r^2}+\frac{1}{r}\frac{\partial C}{\partial r}\right)$$

A.3) Conversion of the Diffusion-Adsorption PDE to a Finite Difference Method

The 1-D diffusion-adsorption equation in polar coordinates was converted from a partial differential equation (PDE) to a Finite Difference Method (FDM). The FDM equation was used to model the radial diffusion of F2 and F3 PHCs in the radial diffusion experiments. Figure A.1 below shows one step of the FDM model.

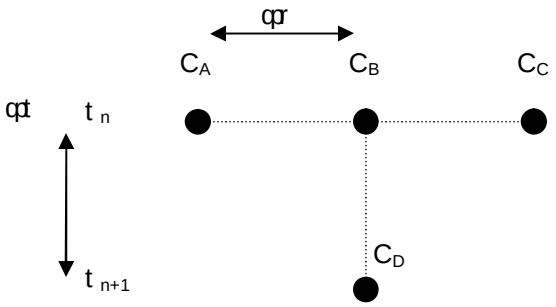

Figure A.1: Finite difference stencil for the method used in the radial diffusion analysis (adapted from LeVeque, 2007). Time steps, t, start at 0 and increase downward, and the diffusion cell radius, r, increases to the right.

1. Determination of the FDM Equation for Diffusion-Adsorption

The 1-D diffusion-adsorption equation in polar coordinates previously derived in A.2:

$$\left(1+\frac{\rho_B}{n}K_D\right)\frac{\partial C}{\partial t}=D*\left(\frac{\partial^2 C}{\partial r^2}+\frac{1}{r}\frac{\partial C}{\partial r}\right) \qquad \text{[Equation 1]}$$

Where the adsorption coefficient K_D is:

$$K_D=\frac{\alpha\beta}{1+\alpha C}$$

With the Finite Difference Method, the PDE terms can be approximated as follows:

$$\frac{\partial C}{\partial t}\approx\frac{\Delta C}{\Delta t} \quad \text{and} \quad \frac{\partial C}{\partial r}\approx\frac{\Delta C}{\Delta r} \quad \text{and} \quad \frac{\partial^2 C}{\partial r^2}\approx\frac{\Delta\left(\Delta C/\Delta r\right)}{\Delta r}$$

The approximation of ∂C/∂t can be defined using the forward difference method:

$$\frac{\Delta C}{\Delta t} = \frac{C_P - C_B}{\Delta t}$$

The approximation ∂C/∂r can be defined using one of three methods: forward difference, backward difference or central difference. For this derivation, the forward difference method was used:

$$\frac{\Delta C}{\Delta r} = \frac{C_C - C_B}{\Delta r} \quad \text{or} \quad \frac{\Delta C}{\Delta r} = \frac{C_B - C_A}{\Delta r} \quad \text{or} \quad \frac{\Delta C}{\Delta r} = \frac{C_C - C_A}{2\Delta r}$$

(Forward Difference) (Backward Difference) (Central Difference)

The approximation of $\partial^2 C / \partial t^2$ can be defined using the central difference method:

$$\frac{\Delta^2 C}{\Delta r^2} = \frac{C_C - 2C_A + C_A}{2\Delta r^2}$$

Substituting the Finite Difference Method terms into Equation 1:

$$\left(1 + \frac{\rho_B}{n}\left(\frac{\alpha\beta}{1+\alpha C}\right)\right)\frac{C_P - C_B}{\Delta t} = D * \left(\frac{C_C - 2C_B + C_A}{\Delta r^2} + \frac{1}{r}\left(\frac{C_C - C_B}{\Delta r}\right)\right)$$

Solve for the concentration at point P, C_P:

$$C_P = C_B + \Delta t D * \left[\frac{\left(\frac{C_C - 2C_B + C_A}{\Delta r^2} + \frac{1}{r}\left(\frac{C_C - C_B}{\Delta r}\right)\right)}{1 + \frac{\rho_B}{n}\left(\frac{\alpha\beta}{1 + \alpha C_B}\right)}\right]$$

2. Boundary Conditions of the FDM

Two boundary conditions were defined for this model. At the inner boundary with the central reservoir of the radial diffusion cell, a conservation of mass condition was used to determine the flux into the reservoir using Fick's First Law.

Time steps and radius steps remained small to ensure that numerical stability of the FDM model was maintained.

a) Inner Reservoir Boundary Condition

Fickôs First Law in polar coordinates:

$$F = -nD * \frac{dC}{dr}$$

Where:

F = the mass flux of solute per unit area per unit time

The dC/dr term can be approximated as follows:

$$\frac{dC}{dr} \approx \frac{\Delta C}{\Delta r}$$

And Fickôs First Law becomes:

$$F = -nD * \frac{\Delta C}{\Delta r}$$

From the Forward Difference Method, qC/qr can be represented as follows:

$$\frac{\Delta C}{\Delta r} = \frac{C_C - C_B}{\Delta r}$$

Substituting into Fickôs First Law:

$$F = -nD * \left(\frac{C_C - C_B}{\Delta r} \right)$$

Using the calculated flux term determined from the above equation, the concentration in the central reservoir was determined using the following relationship.

$$C_R = F \frac{(2\pi r)\Delta t}{\pi r^2} + C_B$$

The concentration of the central reservoir was assumed to be well mixed and was also a cumulative concentration.

b) Outer Zero-Flux Boundary Condition

The outer boundary of the diffusion cell represents a zero-flux boundary condition. Fickôs First Law is then as follows:

$$F = -nD * \frac{dC}{dr} = 0$$

Therefore, the dC/dr term at the boundary is:

$$\frac{dC}{dr} = 0$$

This dC/dr term indicates that there in no change in concentration due to a change in radius. As advection in the diffusion cell is also equal to zero, a reflection function can be introduced at the outer boundary, and the concentration at the outer boundary (or final concentration), C_f, is equal to the concentration at the previous r-vale:

$$C_f = C_{f-1}$$

APPENDIX B

Experiment Methodologies & Analytical Methods

Method B.1) Determining Organic Content of Soil Procedure for Incremental Loss on Ignition

Method B.2) Desorption of PHC from Oil Sands Tailings Experimental Procedure

Method B.3) Radial Diffusion of PHC from Oil Sands Tailings Experimental Procedure

Method B.4) Petroleum Hydrocarbons in Water Extraction Procedure

Method B.5) CCME Hydrocarbon Sample Analysis

Method B.6) Empore Disc Hydrocarbon Extraction Method

Method B.1 Determining Organic Content of Soil Procedure for Incremental Loss on Ignition

This procedure was used to determine the total organic content in each of the tailings materials. Water content must be known for each material used in the experiment, oven dried soil must be used for this procedure.

This method is based on a loss on ignition method in Rowellôs *Soil Science: Methods and Applications.*

Materials & Equipment:

- Small crucible (1 per sample)
- Laboratory furnace, capable of heating to 550ºC
- Balance
- Desiccator
- Mortar and pestle, suitable for geotechnical laboratory use.

Method:

1. Dry the soil at 80ºC until all the water is evaporated and there is no more change in soil mass.

2. Record the tare of the porcelain crucible.

3. Place between 5g and 10g of dried soil in a tared porcelain crucible, ensuring the soil have an even consistency. If it does not, it may be necessary to grind the soil with a mortar and pestle.

4. Record the initial ñoven-driedò mass of the sample.

5. Place in the furnace at 80ºC for a minimum of 4 hours. Remove the sample using tongs and place in a dessicator until it has cooled. Record the change in mass (mass LOI).

6. Repeat step 5 four more times, at 125ºC, 250ºC, 400ºC and 550ºC.

7. Calculate the loss on ignition with the following relationship:

$$\text{LOI (\%)} = (\text{Mass LOI} / \text{Initial ñoven-driedò mass}) \times 100\%$$

Method B.2 Desorption of PHC from Oil Sands Tailings Experimental Procedure

This procedure was used for Phases 1 through 3C. Water content must be known for each material used in the experiment. Do not use dried soil for this procedure

Materials & Equipment:

- 500mL sterilized amber glass jar with Teflon-lined lid
- Balance
- 60mL plastic syringe with 14-gauge needle
- De-ionized water or other aqueous solution (e.g. oil sands process water)
- Centrifuge capable of holding the 500mL glass jars

Method:

1. Determine the desired size of the soil sample by dry weight. Various dry weights were used to determine the desorption isotherm.

2. Using known water content data, calculate the equivalent mass of wet soil required.

3. Weigh out the calculated amount of soil on the balance and place it in the amber jar.

4. Fill the jar completely with de-ionized water or other aqueous solution. Ensure that there is no headspace, as any air in the jar could pull volatiles from the solution.

5. Shake the jar for approximately 1 minute, until the soil sample is completed saturated. Some air may have been trapped in the soil, so if necessary, carefully remove the lid and fill the jar again with de-ionized water.

6. Place the jar in a temperature controlled chamber. Shake vigorously for approximately 1 minute on a daily basis to ensure proper mixing of the soil and water and to try and to keep fines in suspension. An automatic shaker may also be used.

7. On day 12 of the experiment, centrifuge the sample at 1000 rpm for 15 minutes to ensure that there are no more fines in suspension.

8. Carefully remove the supernatant solution from the sample jar using the large syringe and place it in a clean sample jar.

9. PHCs can be extracted from the water using the procedure outlined in the *Petroleum Hydrocarbons in Water Extraction Procedure,* also found in Appendix B, or they can be sent to an external lab for analysis.

10. A minimum of 250mL of supernatant is required to complete the analysis, with additional supernatant for F1 and BTEX analysis.

Method B.3 Radial Diffusion of PHC from Oil Sands Tailings Experimental Procedure

This procedure was used for all the oil sands tailings, with the exception of Plant 4 Lower Beach. Water content must be known for each material used in the experiment. Do not use dried soil for this procedure.

This experiment is designed with diffusion cells that are sampled one time. Each tailings material must be done in triplicate, and sampled at different times over the 2-week period.

Materials & Equipment:

- Balance
- Dichloromethane (DCM)
- Silicone (waterproof), safe for use with oil and grease
- De-ionized water
- Heavy duty 5-Litre HDPE plastic pail and lid
- Large rubber stopper
- Utility knife
- 3-inch diameter fine metal mesh tube (see schematic on the following page)
- Cylindrical plastic sleeve, to fit inside the metal mesh tube.
- 500mL sterilized amber glass jar with Teflon-lined lid
- Silicone tubing with plastic clamp
- Laboratory vacuum source
- Conductivity meter

Method:

1. Rinse metal mesh tube with DCM to ensure any residual oil or grease is removed. Allow to dry overnight in the fume hood.

2. Silicone around the welded base of the metal mesh tube to ensure that it is sealed. Allow to dry overnight.

3. Wash the cylindrical plastic sleeve, HDPE pail and lid with laboratory grade detergent, allow to dry completely.

4. Using the utility knife, cut a hole in the centre of the pail lid of the same diameter as the metal mesh tube.

5. Place the metal mesh tube in the center of the pail. Place a clean cylindrical plastic sleeve inside the tube.

6. Cover the top of the tube and pack tailings around the outside of the tube, being careful to ensure none gets into the tube. If the tailings material is not fully saturated, add known amounts of de-ionized water to the tailings using the following steps:

    - Record the tare of a clean 5-litre pail. Fill it will unsaturated tailings and record the mass of the tailings.
    - Add water to the tailings until it is saturated (i.e. water can be seen at the top of the tailings), recording the mass of water added.
    - Calculate the new water content of the tailings based on the recorded changes in mass.
    - When using this tailings material in the radial diffusion cells, ensure that the new water content is maintained across all the samples by adding the equivalent amount of de-ionized water, using the water content equation:

        water content = mass water / mass dry soil

7. Fill the tube with de-ionized water to the same level as the tailings and remove the plastic sleeve to start the diffusion process.

8. Put a bead of silicone around the inside rim of the pail lid. Place the lid on the pail and silicone around the hole where the tube goes through the lid.

9. Place a rubber stopper over the top of the tube to minimize evaporation.

10. Construct two more diffusion cells using steps 1 to 9 until each tailings material has three identical cells.

11. Place the diffusion cells in a temperature-controlled chamber. Measure and record conductivity on a daily basis.

12. Sample the cells at three discrete times during the 2-week period (e.g.

13. The water is sampled by re-inserting the plastic sleeve into the mesh tube and sample the water into the amber glass jar, using the silicone tubing and vacuum source.

14. Sampled water should be refrigerated until PHC extraction can be completed, no more than 1 week from the sample date.

15. PHCs can be extracted from the water using the procedure outlined in the *Petroleum Hydrocarbons in Water Extraction Procedure,* also found in Appendix B, or they can be sent to an external lab for analysis.

16. A minimum 250mL sample is required to complete the analysis.

NOTE: Some of the tailings materials had noxious odours, so the use of a respirator is recommended when constructing the diffusion cells. It was not necessary when measuring conductivity or sampling the diffusion cells.

Method B.4 Petroleum Hydrocarbons in Water Extraction Procedure

Based on CCMEôs *Reference Method for the Canada-wide Standard for PHCs in Soil* (2001)

Approximately 6 samples can be extracted at the same time, due to laboratory space. Work needs to be completed in a fume hood as both DCM and hexane are highly volatile.

Reagents (all reagents must be reagent grade or better)

- Dichloromethane (DCM)
- Hexane
- Sodium sulphate

Materials & Equipment:

- Glass separatory funnel with stand and glass cap (1 per sample)
- Round bottom flask with glass cap (1 per sample)
- Small glass column with stand (1 per sample)
- Graduated test tube (1 per sample)
- GC vial (1 per sample)
- Glass pipetter with disposable tips
- Graduated cylinders for solvents
- Glass wool
- Roto-evaporator
- Nitrogen bubbler

Method:

1. Transfer sample to separatory funnel (500mL).

2. Rinse sample container with 50mL DCM and 1mL Hexane for 30 seconds. Add rinsate to separatory funnel.

3. Extract sample by vigorous shaking for approximately 2 minutes. Place in separatory funnel stand and allow 10 minutes for phase separation.

4. Place a small amount of glass wool in a small glass column. Glass wool should be washed with DCM prior to use. Put approximately 15g of sodium sulphate in the column, and then pour extract through the column, collect in round bottom flask. Do not allow emulsion to pass into flask.

5. Repeat steps 2 through 4 for a second extraction.

6. Rinse the column with 15mL DCM to ensure all extract has passed into the flask.

7. Roto-evaporate until approximately 1mL of extract remains. Transfer to a graduated test-tube by glass pipette.

8. Triple rinse the flask with 2mL hexane, adding rinsate to graduated test tube.

9. Rinse the nitrogen bubbling tubes with hexane prior to putting them in the test tubes. Gently concentrate the extract to <1.0mL using nitrogen bubbling.

10. Transfer to GC vial and bring to 1.0mL with hexane. Cap and place in fridge. GC analysis will be completed once there are a number of samples to run.

Method B.5 CCME Hydrocarbon Sample Analysis

Sections 10 and 11 of CCMEôs *Reference Method for the Canada-Wide Standard for Petroleum Hydrocarbons in Soil – Tier 1 Method* (2001) are included as follows. The calculation sections from the standard have not been included. This is also the method used by the external laboratory.

10. SAMPLE ANALYSIS – C6 TO C10 HYDROCARBONS (F1)

10.1 Prescriptive Elements

- Use gas chromatography with flame ionization detector and 100% poly(dimethylsiloxane) low bleed chromatography columns, 15 m minimum length and 0.53 mm maximum diameter, to analyze the C6 to C10 hydrocarbons. The chromatography system must separate the nC6 peak from the solvent peak.
- Use methanol extraction to analyze the C6 to C10 hydrocarbons.
- Ensure that the soil is dispersed in the methanol.
- As light hydrocarbons are not stable in soil samples, ensure that the sample is extracted with methanol within 48 hours of sample receipt or a maximum of 7 days from sample collection.
- Toluene is the primary calibration standard for C6 to C10 hydrocarbons.
- Mandatory instrument performance criteria for C6 to C10 is that the nC6 and nC10 response factors must be within 30% of the response factor for toluene.
- Perform BTEX analysis on a second sub-sample or simultaneously, e.g., by using a column splitter to an MS detector, if volatile PHCs are suspected. Alternatively, the same extract can be used if it does not compromise the required MDLs.

10.2 Performance-based Elements

- Purge and trap is the benchmark method for C6 to C10 hydrocarbons, but other suitable methods can be substituted provided that validation data demonstrates that the substitute method provides data comparable to the benchmark method.8
- If headspace analysis is to be used as an alternative to purge and trap, consider salting the sample in the headspace unit to improve the recovery of aromatic compounds, which are known to be biased low compared to aliphatics in headspace analysis.
- It is best to minimize the quantity of methanol taken for analysis, while at the same time taking sufficient sample to achieve desired MDLs.

10.3 Reagents

- All chemicals used in the method should be ACS reagent grade or better.
- Perform calibration and retention time marking for the C6 to C10 hydrocarbons using a mixture of approximately equal weights of toluene, nC6 and nC10 dissolved in methanol.
- Products used as control standards or linearity checks should cover the applicable carbon ranges for the analysis.
- MDL determination for the C6 to C10 hydrocarbons is determined experimentally using gasoline added to clean soil.

10.4 Analysis Procedure

- Take a minimum sample size of 5 g dry weight for C6 to C10 hydrocarbons as quickly as possible while still at 4oC to avoid losing volatile components. Transfer this sample to a tared glass vial with cap, and weigh it. If BTEX is also being analyzed, it is advantageous to weigh out a second sample immediately.
- Quickly add methanol in an amount that will ensure a methanol:wet solid ratio of approximately 2:1 or greater and recap the vial. Mix the vial on a mechanical shaker for one hour. Ensure that the soil is dispersed in the methanol.
- Allow the solids to settle, recover the methanol for analysis and store a portion of the methanol at 4oC for reanalysis if required.
- Measure an appropriate volume of methanol into a purge vessel containing clean water. Purge the sample into an appropriate gas chromatograph with flame ionization detector and a 100% poly(dimethylsiloxane) column. Different volumes of methanol extract can be run to get a chromatogram in the range of the calibration curve, but the reported MDL must be adjusted accordingly.
- Integrate the area under the chromatogram from the beginning of the nC6 peak to the apex of the nC10 peak as a single peak. Ensure that baseline drift between chromatograms is accounted for during integration.

10.5 Calibration Procedure

- Perform calibration and retention time marking for the C6 to C10 hydrocarbons using a mixture of approximately equal weights of toluene, nC6 and nC10 dissolved in methanol.9
- For the C6 to C10 hydrocarbons, run a minimum of a 3-point calibration curve using toluene and a blank before analysis begins. Although calibration is based on integration of area under the chromatogram between retention time markers, the highest standard

must give a higher peak height than the highest peak height in the samples to be run. Dilute samples so that the peak height of the largest sample peak is less than the peak height of the highest calibration standard. Verify instrument calibration using reference standards procured from a second source.

- Linearity of the detector response must be established using a product such as gasoline and with the single compound calibration standards. Linearity must be within 15% in each of the calibrated carbon ranges for products and within 10% for single compounds.

- At a minimum, run a daily check of the lowest calibration standard and the midpoint calibration standard to confirm stability of the calibration curve. Rerun the calibration curve if the low standard deviates by more than 20% from the curve or if the midpoint calibration standard deviates by more than 15% from the curve.

BTEX must be analyzed separately and subtracted from the C6 to C10 hydrocarbon result to give the F1-BTEX result.

11. SAMPLE ANALYSIS – C10 TO C50 HYDROCARBONS (F2, F3 and F4)

11.1 Prescriptive Elements

- Use gas chromatography with flame ionization detector and 100% poly(dimethylsiloxane) low bleed chromatography columns, 15 m minimum length and 0.53 mm maximum diameter for analysis of the C10 to C50 hydrocarbons. The chromatography system must separate the nC10 peak from the solvent peak.

- The primary calibration standard for the C10 to C50 hydrocarbons is a mixture of approximately equal amounts of nC10, nC16 and nC34 normal hydrocarbons.

- Mandatory instrument performance criteria for C10 to C50 are that nC50 response factor must be a within 30% of the average of nC10, nC16 and nC34 response factors and the nC10, nC16 and nC34 response factors must be within 10% of each other. This performance criterion must be met by any injection system used for hydrocarbon analysis and confirmed on a daily basis.

- 100% activated silica gel must be used to clean up the C10 to C50 hydrocarbons. Use 0.6 g of 100% activated silica gel for each gram of sample taken.

11.2 Performance-based Elements

- Either split/splitless, on column or other injection methods are allowed, subject to meeting quality criteria for C50 recovery in Section 11.1.

- Soxhlet extraction apparatus is the benchmark method for the C10 to C50 hydrocarbons, but other suitable extraction methods can be substituted provided that validation data

demonstrate that the substitute method provides data comparable to the benchmark method.

- Other elements of the method, such as the rotovap, shaker apparatus and ovens, can be substituted provided that the quality control criteria listed in Section 8 are met and that validation data has been generated to support the method changes.

11.3 Reagents

- All chemicals used in the method should be reagent grade or better.
- All single compound chemical calibration standards should be pure and of the highest quality available. The nC10, nC16 and nC34 hydrocarbons are prepared in toluene. The nC50 is also prepared in toluene but is only soluble to about 15 εg/mL.
- Products used as control standards or linearity checks should cover the applicable carbon ranges for the analysis.
- MDL for the C10 to C50 hydrocarbons is determined experimentally using a weathered diesel product added to clean soil.
- Silica gel should be pure, 60 to 200 mesh and should be 100% activated by drying at >101$_{o}$C overnight and used immediately.

Option B – Silica Gel Column Cleanup

- Prepare a silica gel column for each sample. Place a small quantity of glass wool into the bottom of a glass column with an internal diameter of approximately 15 to 20 mm., then dry-pack the column with (5.0±0.2) g of 100% activated silica gel. Add about 1 cm of anhydrous sodium sulphateto the top of the silica gel. The column dimensions must be such that the bed depth of the silica gel exceeds 20 mm. Clean and wet the column by eluting at least 10 mL of 50:50 hexane:DCM through the column. Do not collect this eluant.
- Quantitatively transfer the extract onto a silica gel column.[13] Collect all further eluant from the silica column in an evaporating vessel. Allow the solvent level to drop below the top of the silica bed, and then elute the column with a minimum of 20 mL of 50:50 hexane:DCM.
- Add 1 to 2 mL of toluene if required to the recovered solvent, using a rotary evaporator or other evaporation apparatus reduce collected solvent to a volume of approximately 2 to 5 mL. Quantitatively transfer the extract to a smaller vial and concentrate further to an accurate final volume of 2 mL, or to a larger final volume if appropriate. Evaporation conditions must be demonstrated to avoid the loss of the nC10 hydrocarbon.

- If the extract is not to be chromatographed immediately, transfer the extract to a vial and store in the dark at 4$_{o}$C or less. Bring the extract back to room temperature before GC analysis.

- Integrate the area under the chromatogram from the apex of the nC10 peak to the apex of the nC16 peak, from the apex of the nC16 peak to the apex of the nC34 peak and from the apex of the nC34 peak to the apex of the nC50 peak. If the chromatogram returns to baseline by the end of the C34 fraction and no heavier material is suspected, then subsequent analyses on samples from the same site may be terminated at this point.[14] Note whether the chromatogram has returned to baseline[15] at nC50 to determine whether gravimetric heavy hydrocarbons are required. Ensure that baseline drift due to column bleed between chromatograms is accounted for during integration either by blank subtraction or by column compensation.

11.5 Calibration Procedure

- Perform calibration and retention time marking for the C10 to C50 hydrocarbons using approximately equal weights of nC10, nC16 and nC34 hydrocarbons dissolved in toluene.[16]

- A solution of nC50 in toluene is used as retention time and response factor standard for the C10 to C50 hydrocarbons.

- For the C10 to C50 hydrocarbons, run a minimum of a 3-point calibration curve using the nC10, nC16 and nC34 hydrocarbons and a blank before analysis begins. Although calibration is based on integration of area under the chromatogram between retention time markers, the highest standard must give a higher peak height than the highest peak height in the samples to be run. Dilute samples so that the peak height of the largest sample peak is less than the peak height of the highest calibration standard.

- Establish linearity of the detector response using products such as diesel or motor oil and with the single compound calibration standards. Linearity must be within 15% in each of the calibrated carbon ranges for products and within 10% for single compounds.

- At a minimum, run a daily check of the lowest calibration standard and the midpoint calibration standard to confirm stability of the calibration curve. Rerun the calibration curve if the low standard deviates by more than 20% from the curve or if the midpoint calibration standard deviates by more than 15% from the curve.

Method B.6 Empore Disk Hydrocarbon Extraction Method

*The 3M **Empore™** Extraction Disks EPA Method 1664 (3M Empore 2004), based on EPA Method 1664, is included as follows:*

Description

EPA Method 1664 Revision A (February 1999) is a performance-based method for N-Hexane Extractable Material (HEM; Oil and Grease) and Silica Gel Treated N-Hexane Extractable Material (SGT ï HEM; Non-polar Material) by Extraction and Gravimetry.

The method permits a laboratory to use alternative methods to liquid-liquid hexane extraction and concentration ñprovided that all performance specifications are met.ò (page iv of EPA Method 1664 Revision A). There is a further note on page 14 of Revision A that states, ñSolid-phase extraction (SPE) may be used at the discretion of the discharger/generator and its laboratory.ò This method summary is a step-by-step guide for the use of EmporeÊ Oil and Grease Solid Phase Extraction Disks to replace the liquid-liquid hexane extraction technique.

STEP 1 Assemble Glassware

Assemble the filtration apparatus with the oil and grease disk. Disk must be inserted with dimpled surface down. For samples containing high concentrations of suspended solids, 90 mm disks and systems are recommended. The vacuum system should be capable of drawing a minimum of 25 inches Hg (0.85 bar) for 90 mm disk systems. *Note: Disk must be used with dimpled surface down.*

Place the waste-receiving vial in manifold; wash the extraction apparatus and the disk with n-hexane. Rinse down the sides of the glassware with hexane. Use enough solvent to completely cover the disk (20 ml for 47 mm disk and 30 ml for 90 mm disk). Apply vacuum to draw the solvent through the disk.

Repeat (for a total of two hexane washes). Allow the disk to dry under vacuum for one minute after the second wash.

Remove the waste receiving vial and dispose of the solvent according to local, state and/or federal regulations.

STEP 2 Condition Disk

Condition the disk by adding 10 mL methanol (47 mm disk) to the reservoir. Use approximately 30 mL methanol for a 90 mm disk. Use enough solvent to completely cover the disk. Draw a small amount of methanol through the disk with the vacuum; vent the system and allow the disk to soak for 60 seconds. Draw most of the remaining solvent through the disk, leaving enough methanol to cover the surface of the disk. Do not allow the disk to become dry. If the disk becomes dry at any point before sample extraction, repeat the conditioning step.

Rinse the disk with deionized water. Use 30 mL water for a 47 mm disk and 100 mL water for a 90 mm disk. Draw most of the water through, leaving enough to cover the disk surface. Do not allow the disk to become dry.

STEP 3 Extract Sample

Add the sample (pH adjusted to 2) to the reservoir and apply full vacuum. If the sample is high in suspended solids, allow the sediment to settle and decant as much liquid as possible into the reservoir before adding the sediment. Do not let the disk go dry before adding the sediment-containing portion. By extracting a majority of the liquid before adding the sediment, potential plugging problems will be minimized. Filter as quickly as the vacuum will allow. Drain as much water from the sample container as possible.

STEP 4 Dry Disk

Dry Disk under vacuum for no more than 5 minutes. Excessive drying (>5 min.) can lead to lower recoveries of more volatile fractions.

STEP 5 Elute Disk

Lift filtration assembly and insert suitable collection vial for eluate collection.

Add 10 mL hexane (30 mL for 90 mm disk) to the original sample container making sure to rinse down the sides. Replace the cover on the container and invert 2-3 times.

Transfer the hexane from inside the sample container to the disk using a disposable glass pipette. As the hexane is transferred to the disk, allow it to wash down the sides of the reservoir and then pass through the disk to ensure complete rinsing of all glassware.

Carefully apply vacuum to draw a few drops of hexane through the disk, and then stop the vacuum.

Allow the remaining hexane to soak into the disk for no more than 2 minutes. Then slowly draw the remaining solvent through the disk under vacuum to remove residual hexane and dry the disk.

Repeat steps above using a second aliquot of hexane. Wash the sides of the glass reservoir using another aliquot of 10 mL hexane. Apply vacuum and draw the entire volume of hexane through the disk.

Allow the disk to dry for approximately 5 minutes and then turn off the vacuum. The collection vial now contains three combined aliqouts of hexane.

STEP 6 Dry the Eluate

The eluate is dried using anhydrous sodium sulfate.

- Place glass wool into the bottom of a small funnel and add 5 gm sodium sulfate.
- Obtain a clean collection vial or weighing pan and record its weight. Note: *Wear gloves when handling preweighed collection vessels as oils from the skin may be transferred to the vial and affect results.*
- Pour or pipette the eluate onto the sodium sulfate and collect into the preweighed collection vessel.
- Rinse the sides of the collection vial with 5 mL hexane and add to the sodium sulfate.

Rinse the sodium sulfate with another aliquot of 5 mL hexane, allowing all the solvent to run through the sodium sulfate and into the collection vial.

STEP 7 Analyze

Evaporate hexane from the collection vessel until a constant weight is reached.

Weigh the collection vial, compare weight to the tared weight, and calculate the quantity of HEM (oil and grease residue) present in units of mg/L.

APPENDIX C

PHC Analytical Results

C.1) Characterization of Tailings

C.2) Desorption Experiment Results

C.3) Diffusion Experiment Result

C.1 Characterization of Tailings

Analytical Results, in mg/kg

Extractable Hydrocarbons	MFT	LG MFT	PT MFT	P4 UB Surface	P4 UB Auger	P4 LB	Tailings Sand
Benzene	1.05	n/a	n/a	<0.004	n/a	n/a	n/a
Toluene	3.37	n/a	n/a	0.016	n/a	n/a	n/a
Ethylbenzene	5.27	n/a	n/a	0.01	n/a	n/a	n/a
Xylenes	33.00	n/a	n/a	0.05	n/a	n/a	n/a
F1 C6-C10	1544	n/a	n/a	7	n/a	n/a	n/a
F1-BTEX	1505	n/a	n/a	7	n/a	n/a	n/a
C11	848	578	545	44	64	434	<1
C12	1418	589	574	92	79	976	<1
C13	1727	845	763	138	109	1270	3
C14	1849	1040	1050	197	153	1880	7
C15	2390	980	958	206	154	2410	10
C16	2632	1330	1270	245	186	2960	16
C17	2320	1090	1170	252	222	3210	24
C18	3103	1370	1380	310	240	3600	21
C19	2933	966	529	326	237	3570	25
C20	3432	1820	1690	349	308	3780	35
C21	2914	1430	1840	326	180	3830	29
C22	3174	1040	875	365	265	3270	35
C23	2843	1070	1470	353	218	3220	31
C24	3075	1560	1240	339	241	3280	31
C25	2645	1000	995	346	224	2830	51
C26	2232	1140	1250	278	88	3050	<1
C27	2309	1010	1170	295	159	2970	38
C28	2529	1220	991	394	461	3210	39
C29	2677	681	919	297	71	2870	9
C30	2370	1490	1610	527	276	2620	47
C31	2236	658	346	97	133	2740	12
C32	2287	1080	889	304	266	2360	33
C33	2086	549	965	319	70	2400	14
C34	1654	903	578	160	193	2320	26
C35	1706	843	796	253	129	1880	16
C36	1876	470	647	183	159	1980	27
C37	1175	652	584	229	75	1700	20
C38	2234	956	730	190	167	1770	10
C39	797	841	579	227	35	1730	36
C40	36841	139	570	179	200	1570	<1
C41	n/a	467	579	139	56	1490	18
C42	n/a	399	555	190	136	1450	18
C43	n/a	702	536	156	80	1280	12
C44	n/a	866	396	174	113	1320	20
C45	n/a	124	709	136	68	1190	18
C46	n/a	434	354	165	86	975	5
C47	n/a	450	403	113	60	1190	11

Extractable Hydrocarbons	MFT	LG MFT	PT MFT	P4 UB Surface	P4 UB Auger	P4 LB	Tailings Sand
C48	n/a	489	475	117	110	1060	12
C49	n/a	447	423	154	68	972	15
C50	n/a	396	442	130	110	969	17
C51	n/a	430	380	84	56	706	<2
C52	n/a	576	359	107	82	733	13
C53	n/a	122	370	104	61	630	12
C54	n/a	419	395	128	96	577	10
C55	n/a	514	363	96	59	583	16
C56	n/a	219	271	79	65	559	7
C57	n/a	386	523	157	71	478	10
C58	n/a	430	263	37	79	378	9
C59	n/a	1850	1940	95	338	437	54
C60+	n/a	7200	5860	2460	1140	1680	180
TOTAL	102312	46260	44569	12641	8296	94347	1102
Soil % Moisture	n/a	29.2	35.5	1.5	8.24	24.8	6.61
F1 C6-C10	1544	n/a	n/a	7	n/a	3050	n/a
F1 - BTEX	1505	n/a	n/a	7	n/a	2790	n/a
F2	10864	5362	5160	922	745	9930	36
F3	46819	20077	19907	5637	3852	55130	500
F4	44629	8675	8778	2735	1652	22526	255
C50+	n/a	12146	10724	3347	2047	6761	311
TOTAL	102312	46260	44569	12641	8296	94347	1102

Extractable Hydrocarbons	2:1 CT	4:1 CT	6:1 CT	4m CT Pond	12m CT Pond	OSPW (mg/L)
Benzene	0.24	0.457	0.319	n/a	n/a	n/a
Toluene	2.52	5.79	2.06	n/a	n/a	n/a
Ethylbenzene	4.59	3.03	2.46	n/a	n/a	n/a
Xylenes	23.8	14.2	9.46	n/a	n/a	n/a
F1 C6-C10	415	205	207	n/a	n/a	n/a
F1-BTEX	384	182	193	n/a	n/a	n/a
C11	397	245	119	3	<1	0.02
C12	618	446	225	125	<1	0.03
C13	651	456	231	383	<1	0.03
C14	764	588	260	757	7	0.03
C15	943	646	353	760	14	<0.01
C16	771	707	358	1340	25	0.02
C17	720	797	376	1320	42	0.04
C18	1693	787	416	1400	38	0.08
C19	860	632	449	1580	65	0.1
C20	1734	879	451	1510	47	0.12
C21	1072	770	454	1390	63	0.09
C22	1472	879	423	1140	53	0.1
C23	1173	949	418	2470	87	0.05
C24	1232	536	397	845	47	0.06
C25	1232	795	308	1340	70	0.15
C26	830	671	408	1480	68	0.03
C27	1042	569	352	811	76	0.03
C28	1102	786	350	1540	83	0.03
C29	772	703	330	1330	78	0.03
C30	749	636	332	1440	76	0.02
C31	1461	811	289	863	35	0.02
C32	617	566	330	1200	95	0.05
C33	652	620	271	1080	13	<0.01
C34	826	197	248	763	55	<0.01
C35	642	456	245	723	31	<0.01
C36	746	618	261	998	46	<0.01
C37	520	354	190	893	22	<0.01
C38	768	251	354	595	34	<0.01
C39	447	295	29	894	31	<0.01
C40	11610	427	196	917	25	<0.01
C41	n/a	340	176	518	24	<0.01
C42	n/a	234	159	667	15	<0.01
C43	n/a	402	179	506	16	<0.01
C44	n/a	275	152	747	15	<0.01
C45	n/a	306	119	604	16	<0.01
C46	n/a	258	159	539	10	<0.01
C47	n/a	277	100	466	8	<0.01
C48	n/a	246	153	578	8	<0.01
C49	n/a	277	132	544	5	<0.01
C50	n/a	281	123	392	4	<0.01

Extractable Hydrocarbons	2:1 CT	4:1 CT	6:1 CT	4m CT Pond	12m CT Pond	OSPW (mg/L)
C51	n/a	185	110	710	2	<0.02
C52	n/a	210	142	258	2	<0.02
C53	n/a	235	60	485	2	<0.02
C54	n/a	155	142	390	<2	<0.02
C55	n/a	201	100	241	<2	<0.02
C56	n/a	199	99	514	<2	<0.02
C57	n/a	198	120	455	<2	<0.02
C58	n/a	204	81	831	<2	<0.02
C59	n/a	199	109	1680	<2	<0.02
C60+	n/a	4900	2660	6190	<20	<0.20
TOTAL	26508	27654	14498	49205	1453	1.13
Soil % Moisture	n/a	33.7	22.5	34.3	24.3	
F1 C6-C10	415	205	207	n/a	n/a	<0.2
F1 - BTEX	384	182	193	n/a	n/a	<0.2
F2	4145	3088	1546	3368	46	0.13
F3	19240	12583	6602	23502	1091	1
F4	14733	5297	2727	10581	310	0
C50+	n/a	6686	3623	11754	6	0
TOTAL	38118	27654	14498	49205	1453	1.13

C.2 Desorption Results (mg/kg) – Phase 1

	P4 Upper Beach Surface					
Sample -->	**A1-1**	**A1-2**	**A1-3**	**A1-4**	**A1-5**	**A1-6**
Sample Day -->	3	13	3	13	3	13
Soil Mass (g) -->	20	20	20	20	20	20
Temp. (ºC) -->	20	20	50	50	100	100
Solution -->	OSPW/DDI	OSPW/DDI	OSPW/DDI	OSPW/DDI	OSPW/DDI	OSPW/DDI
Benzene	<0.001	<0.001	<0.001	<0.001	<0.001	<0.001
Toluene	<0.001	<0.001	<0.001	<0.001	<0.001	<0.001
Ethylbenzene	<0.001	0.001	0.002	0.001	<0.001	<0.001
Xylenes	0.001	0.002	<0.001	0.003	0.002	0.002
F1 C6-C10	<0.2	<0.2	<0.2	<0.2	<0.2	<0.2
F1-BTEX	<0.2	<0.2	<0.2	<0.2	<0.2	<0.2
C11	<0.01	<0.01	0.04	0.01	0.06	0.04
C12	0.01	<0.01	0.07	0.03	0.11	0.08
C13	0.02	0.02	0.07	0.04	0.12	0.09
C14	0.02	0.04	0.07	0.04	0.11	0.09
C15	0.01	0.04	0.05	0.03	0.1	0.08
C16	0.01	0.05	0.07	0.05	0.11	0.08
C17	0.02	0.06	0.09	0.07	0.14	0.09
C18	0.05	0.11	0.13	0.11	0.17	0.13
C19	0.07	0.1	0.14	0.14	0.2	0.14
C20	0.07	0.11	0.15	0.15	0.21	0.15
C21	0.07	0.08	0.13	0.11	0.18	0.11
C22	0.05	0.08	0.11	0.11	0.14	0.11
C23	0.03	0.05	0.08	0.08	0.11	0.08
C24	0.01	0.06	0.07	0.07	0.09	0.07
C25	<0.01	0.03	0.05	0.06	0.06	0.05
C26	<0.01	<0.01	0.04	0.03	0.05	0.02
C27	<0.01	0.01	0.03	0.03	0.04	0.03
C28	<0.01	<0.01	0.02	0.02	0.04	0.04
C29	<0.01	<0.01	0.02	0.02	0.03	<0.01
C30	<0.01	<0.01	0.01	0.02	0.03	0.01
C31	<0.01	<0.01	0.01	<0.01	0.02	0.01
C32	<0.01	<0.01	<0.01	<0.01	0.03	0.01
C33	<0.01	<0.01	<0.01	<0.01	0.02	<0.01
C34	<0.01	<0.01	<0.01	<0.01	0.02	<0.01
C35	<0.01	<0.01	<0.01	<0.01	0.02	<0.01
C36	<0.01	<0.01	<0.01	<0.01	0.02	<0.01
C37	<0.01	<0.01	<0.01	<0.01	0.02	<0.01
C38	<0.01	<0.01	<0.01	<0.01	0.02	<0.01
C39	<0.01	<0.01	<0.01	<0.01	<0.01	<0.01
C40+	0.01	<0.01	1.49	<0.01	0.13	<0.01
F1 C6-C10	<0.2	<0.2	<0.2	<0.2	<0.2	<0.2
F1-BTEX	<0.2	<0.2	<0.2	<0.2	<0.2	<0.2
F2 C11-C16	0.07	0.15	0.37	0.2	0.61	0.46
F3 C17-C34	0.37	0.69	1.08	1.02	1.58	1.05
F4 C35-C40+	0.01	0	1.49	0	0.21	0
Total C11-C40+	0.45	0.84	1.45	1.22	2.4	1.51

Desorption Results (mg/kg) – Phase 1

	P4 Upper Beach Auger					
Sample -->	**A1-7**	**A1-8**	**A1-9**	**A1-10**	**A1-11**	**A1-12**
Sample Day -->	3	13	3	13	3	13
Soil Mass (g) -->	20	20	20	20	20	20
Temp. (ºC) -->	20	20	50	50	100	100
Solution -->	OSPW/DDI	OSPW/DDI	OSPW/DDI	OSPW/DDI	OSPW/DDI	OSPW/DDI
Benzene	<0.001	<0.001	<0.001	<0.001	<0.001	<0.001
Toluene	0.013	0.01	0.023	0.032	0.034	0.029
Ethylbenzene	0.003	0.006	0.007	0.01	0.011	0.01
Xylenes	0.27	0.173	0.226	0.294	0.278	0.253
F1 C6-C10	0.6	0.5	0.6	0.8	0.8	0.8
F1-BTEX	0.3	0.3	0.3	0.5	0.4	0.5
C11	0.1	0.04	0.18	0.03	0.1	0.03
C12	0.08	0.01	0.15	0.01	0.1	<0.01
C13	0.07	0.05	0.12	0.03	0.08	0.02
C14	0.07	0.07	0.13	0.04	0.07	0.03
C15	0.06	0.05	0.12	0.02	0.05	0.03
C16	0.07	0.05	0.12	0.02	0.06	0.03
C17	0.07	0.04	0.12	0.02	0.05	0.02
C18	0.09	0.05	0.18	0.03	0.07	<0.01
C19	0.11	0.06	0.19	0.04	0.08	0.01
C20	0.13	0.05	0.19	0.04	0.08	<0.01
C21	0.13	0.05	0.19	0.04	0.08	<0.01
C22	0.11	0.03	0.16	0.02	0.06	<0.01
C23	0.11	<0.01	0.15	0.01	0.06	<0.01
C24	0.09	<0.01	0.13	<0.01	0.05	<0.01
C25	0.07	<0.01	0.14	<0.01	0.04	<0.01
C26	0.06	<0.01	0.08	<0.01	0.04	<0.01
C27	0.05	<0.01	0.07	<0.01	0.04	<0.01
C28	0.05	<0.01	0.08	<0.01	0.04	<0.01
C29	0.04	<0.01	0.08	<0.01	0.03	<0.01
C30	0.03	<0.01	0.05	<0.01	0.03	<0.01
C31	0.03	<0.01	0.06	<0.01	0.02	<0.01
C32	0.03	<0.01	0.07	<0.01	0.03	<0.01
C33	0.02	<0.01	0.04	<0.01	0.02	<0.01
C34	0.03	<0.01	0.04	<0.01	0.02	<0.01
C35	0.01	<0.01	0.04	<0.01	0.01	<0.01
C36	0.01	<0.01	0.02	<0.01	<0.01	<0.01
C37	0.01	<0.01	0.02	<0.01	<0.01	<0.01
C38	<0.01	<0.01	0.02	<0.01	<0.01	<0.01
C39	<0.01	<0.01	<0.01	<0.01	<0.01	<0.01
C40+	<0.01	<0.01	0.03	<0.01	<0.01	<0.01
F1 C6-C10	0.6	0.5	0.6	0.8	0.8	0.8
F1-BTEX	0.3	0.3	0.3	0.5	0.4	0.5
F2 C11-C16	0.45	0.27	0.82	0.15	0.46	0.14
F3 C17-C34	1.25	0.28	2.02	0.2	0.84	0.03
F4 C35-C40+	0.03	0	0.13	0	0.01	0
Total C11-C40+	1.73	0.55	2.97	0.35	1.31	0.17

Desorption Results (mg/kg) – Phase 2

	P4 Upper Beach Surface				
Sample -->	**A2-1**	**A2-2**	**A2-3**	**A2-5**	**A2-6**
Sample Day -->	6	12	19	6	12
Soil Mass (g) -->	35	35	35	35	35
Temp. (ºC) -->	20	20	20	20	20
Solution -->	OSPW	OSPW	OSPW	OSPW/DDI	OSPW/DDI
Benzene	<0.001	<0.001	<0.001	<0.001	<0.001
Toluene	<0.001	<0.001	<0.001	<0.001	<0.001
Ethylbenzene	0.008	0.006	0.003	0.003	0.003
Xylenes	<0.001	<0.001	0.002	<0.001	<0.001
F1 C6-C10	<0.2	<0.2	<0.2	<0.2	<0.2
F1-BTEX	<0.2	<0.2	<0.2	<0.2	<0.2
C11	0.02	0.04	<0.01	0.02	0.03
C12	0.06	0.07	0.05	0.05	0.05
C13	0.08	0.12	0.09	0.07	0.09
C14	0.1	0.17	0.13	0.08	0.14
C15	0.08	0.11	0.09	0.08	0.09
C16	0.09	0.11	0.12	0.08	0.07
C17	0.12	0.11	0.16	0.1	0.1
C18	0.17	0.17	0.19	0.14	0.11
C19	0.18	0.14	0.18	0.13	0.12
C20	0.16	0.15	0.12	0.12	0.14
C21	0.13	0.09	0.12	0.13	0.13
C22	0.12	0.09	0.09	0.07	0.09
C23	0.07	0.08	0.07	0.07	0.08
C24	0.05	0.06	0.06	0.04	0.06
C25	0.04	0.06	0.05	0.03	0.05
C26	0.02	0.07	0.02	0.02	0.04
C27	0.02	<0.01	0.02	<0.01	0.04
C28	0.01	0.04	0.02	<0.01	0.01
C29	0.01	0.02	0.02	<0.01	0.03
C30	<0.01	0.02	0.01	<0.01	0.02
C31	<0.01	0.02	<0.01	<0.01	0.03
C32	<0.01	0.02	<0.01	<0.01	0.01
C33	<0.01	0.02	<0.01	<0.01	0.02
C34	<0.01	0.01	<0.01	<0.01	0.02
C35	<0.01	0.03	<0.01	<0.01	0.01
C36	<0.01	<0.01	<0.01	<0.01	0.01
C37	<0.01	0.02	<0.01	<0.01	0.02
C38	<0.01	0.02	<0.01	<0.01	0.02
C39	<0.01	0.01	<0.01	<0.01	<0.01
C40+	0.01	0.3	<0.01	<0.01	0.34
F1 C6-C10	<0.2	<0.2	<0.2	<0.2	<0.2
F1-BTEX	<0.2	0.04	<0.2	<0.2	<0.2
F2 C11-C16	0.43	0.62	0.48	0.38	0.47
F3 C17-C34	1.10	1.17	1.13	0.85	1.10
F4 C35-C40+	0.01	0.38	0.00	0.00	0.40
Total C11-C40+	1.54	2.17	1.61	1.23	1.97

Desorption Results (mg/kg) – Phase 2

	P4 Upper Beach Surface				
Sample -->	**A2-7**	**A2-9**	**A2-10**	**A2-11**	**A2-12**
Sample Day -->	19	6	12	19	19
Soil Mass (g) -->	35	35	35	35	35
Temp. (ºC) -->	20	20	20	20	20
Solution -->	OSPW/DDI	DDI	DDI	DDI	DDI
Benzene	<0.001	<0.001	<0.001	<0.001	<0.001
Toluene	<0.001	<0.001	<0.001	<0.001	<0.001
Ethylbenzene	0.001	<0.001	<0.001	<0.001	<0.001
Xylenes	0.001	<0.001	<0.001	<0.001	<0.001
F1 C6-C10	<0.2	<0.2	<0.2	<0.2	<0.2
F1-BTEX	<0.2	<0.2	<0.2	<0.2	<0.2
C11		0.02	0.04	0.02	0.02
C12	0.02	0.06	0.07	0.03	0.04
C13	0.04	0.1	0.12	0.04	0.05
C14	0.06	0.14	0.14	0.04	0.05
C15	0.05	0.1	0.11	0.04	0.04
C16	0.07	0.1	0.1	0.06	0.05
C17	0.1	0.1	0.09	0.07	0.06
C18	0.12	0.12	0.1	0.12	0.08
C19	0.15	0.15	0.12	0.13	0.1
C20	0.12	0.16	0.13	0.14	0.12
C21	0.11	0.16	0.11	0.13	0.11
C22	0.08	0.09	0.09	0.1	0.08
C23	0.05	0.09	0.07	0.07	0.07
C24	0.04	0.06	0.05	0.07	0.06
C25	0.02	0.04	0.04	0.03	0.01
C26	0.02	<0.01	0.03	0.03	0.03
C27	0.01	<0.01	0.03	0.02	<0.01
C28	<0.01	<0.01	0.03	0.01	0.01
C29	<0.01	<0.01	0.02	<0.01	0.01
C30	<0.01	<0.01	0.02	<0.01	<0.01
C31	<0.01	<0.01	0.02	<0.01	0.01
C32	<0.01	<0.01	0.02	<0.01	<0.01
C33	<0.01	<0.01	0.02	<0.01	<0.01
C34	<0.01	<0.01	0.02	<0.01	<0.01
C35	<0.01	<0.01	0.01	<0.01	<0.01
C36	<0.01	<0.01	0.01	<0.01	<0.01
C37	<0.01	<0.01	0.02	<0.01	<0.01
C38	<0.01	<0.01	0.02	<0.01	<0.01
C39	<0.01	<0.01	0.02	<0.01	<0.01
C40+	<0.01	<0.01	0.34	<0.01	<0.01
F1 C6-C10	<0.2	<0.2	<0.2	<0.2	<0.2
F1-BTEX	<0.2	<0.2	<0.2	<0.2	<0.2
F2 C11-C16	0.24	0.52	0.58	0.23	0.25
F3 C17-C34	0.82	0.97	1.01	0.92	0.75
F4 C35-C40+	0.00	0.00	0.42	0.00	0.00
Total C11-C40+	1.06	1.49	2.01	1.15	1.00

Desorption Results (mg/kg) – Phase 2

	P4 Upper Beach Surface				
Sample -->	**A2-13**	**A2-14**	**A2-16**	**A2-17**	**A2-18**
Sample Day -->	6	12	19	6	12
Soil Mass (g) -->	35	35	35	35	35
Temp. (ºC) -->	1	1	1	1	1
Solution -->	PW	PW	PW	PW/DDI	PW/DDI
Benzene	<0.001	<0.001	<0.001	<0.001	<0.001
Toluene	<0.001	<0.001	<0.001	<0.001	<0.001
Ethylbenzene	0.004	0.004	<0.001	0.003	0.002
Xylenes	<0.001	<0.001	0.002	<0.001	<0.001
F1 C6-C10	<0.2	<0.2	<0.2	<0.2	<0.2
F1-BTEX	<0.2	<0.2	<0.2	<0.2	<0.2
C11	0.04	0.04	0.01	<0.01	0.05
C12	0.1	0.08	0.06	0.05	0.08
C13	0.14	0.15	0.09	0.08	0.13
C14	0.17	0.19	0.1	0.12	0.2
C15	0.13	0.13	0.07	0.08	0.13
C16	0.12	0.13	0.07	0.09	0.13
C17	0.15	0.13	0.11	0.11	0.13
C18	0.22	0.17	0.17	0.16	0.16
C19	0.2	0.19	0.16	0.14	0.16
C20	0.21	0.17	0.18	0.16	0.22
C21	0.22	0.15	0.15	0.11	0.16
C22	0.1	0.13	0.11	0.09	0.11
C23	0.12	0.1	0.08	0.06	0.09
C24	0.05	0.08	0.03	0.05	0.1
C25	0.04	0.06	0.01	0.01	0.05
C26	0.03	0.04	<0.01	0.01	0.03
C27	0.01	0.03	<0.01	<0.01	0.04
C28	0.01	0.02	<0.01	<0.01	0.05
C29	<0.01	0.02	<0.01	<0.01	0.02
C30	<0.01	0.02	<0.01	<0.01	0.02
C31	<0.01	0.02	<0.01	<0.01	0.02
C32	<0.01	0.01	<0.01	<0.01	0.03
C33	<0.01	0.01	<0.01	<0.01	0.03
C34	<0.01	<0.01	<0.01	<0.01	0.03
C35	<0.01	0.01	<0.01	<0.01	0.03
C36	<0.01	<0.01	<0.01	<0.01	<0.01
C37	<0.01	<0.01	<0.01	<0.01	0.04
C38	<0.01	<0.01	<0.01	<0.01	0.02
C39	<0.01	<0.01	<0.01	<0.01	0.02
C40+	<0.01	0.12	0.01	<0.01	0.29
F1 C6-C10	<0.2	<0.2	<0.2	<0.2	<0.2
F1-BTEX	<0.2	<0.2	<0.2	<0.2	<0.2
F2 C11-C16	0.7	0.72	0.4	0.42	0.72
F3 C17-C34	1.36	1.35	1	0.9	1.45
F4 C35-C40+	0	0.13	0.01	0	0.4
Total C11-C40+	2.06	2.20	1.41	1.32	2.57

Desorption Results (mg/kg) – Phase 2

	P4 Upper Beach Surface				
Sample -->	**A2-19**	**A2-21**	**A2-22**	**A2-23**	**A2-24**
Sample Day -->	19	6	12	19	19
Soil Mass (g) -->	35	35	35	35	35
Temp. (ºC) -->	1	1	1	1	1
Solution -->	PD/DDI	DDI	DDI	DDI	DDI
Benzene	<0.001	<0.001	<0.001	<0.001	<0.001
Toluene	<0.001	<0.001	<0.001	<0.001	<0.001
Ethylbenzene	<0.001	<0.001	<0.001	<0.001	<0.001
Xylenes	0.001	<0.001	<0.001	<0.001	<0.001
F1 C6-C10	<0.2	<0.2	<0.2	<0.2	<0.2
F1-BTEX	<0.2	<0.2	<0.2	<0.2	<0.2
C11	0.02	0.03	0.05	0.03	0.03
C12	0.06	0.05	0.07	0.07	0.05
C13	0.07	0.06	0.14	0.08	0.06
C14	0.07	0.08	0.17	0.07	0.07
C15	0.04	0.06	0.12	0.06	0.06
C16	0.03	0.07	0.1	0.05	0.06
C17	0.05	0.06	0.1	0.05	0.06
C18	0.11	0.09	0.11	0.07	0.09
C19	0.13	0.1	0.14	0.09	0.12
C20	0.13	0.09	0.15	0.09	0.14
C21	0.13	0.1	0.14	0.09	0.16
C22	0.08	0.07	0.11	0.06	0.07
C23	0.06	0.07	0.08	0.04	0.08
C24	0.04	0.02	0.07	0.02	0.03
C25	0.01	0.02	0.05	<0.01	0.01
C26	<0.01	0.01	0.05	<0.01	<0.01
C27	<0.01	<0.01	0.03	<0.01	<0.01
C28	<0.01	<0.01	0.03	<0.01	<0.01
C29	<0.01	<0.01	0.03	<0.01	<0.01
C30	<0.01	<0.01	0.03	<0.01	<0.01
C31	<0.01	<0.01	0.03	<0.01	<0.01
C32	<0.01	<0.01	0.03	<0.01	<0.01
C33	<0.01	<0.01	0.02	<0.01	<0.01
C34	<0.01	<0.01	0.02	<0.01	<0.01
C35	<0.01	<0.01	0.02	<0.01	<0.01
C36	<0.01	<0.01	0.03	<0.01	<0.01
C37	<0.01	<0.01	0.03	<0.01	<0.01
C38	<0.01	<0.01	0.02	<0.01	<0.01
C39	<0.01	<0.01	0.03	<0.01	<0.01
C40+	0.01	<0.01	0.53	<0.01	<0.01
F1 C6-C10	<0.2	<0.2	<0.2	<0.2	<0.2
F1-BTEX	<0.2	<0.2	<0.2	<0.2	<0.2
F2 C11-C16	0.29	0.35	0.65	0.36	0.33
F3 C17-C34	0.74	0.63	1.22	0.51	0.76
F4 C35-C40+	0.01	0	0.66	0	0
Total C11-C40+	1.04	0.98	2.53	0.87	1.09

Desorption Results (mg/kg) – Phase 2

	P4 Upper Beach Auger				
Sample -->	**A2-25**	**A2-26**	**A2-27**	**A2-29**	**A2-30**
Sample Day -->	6	12	19	6	12
Soil Mass (g) -->	35	35	35	35	35
Temp. (ºC) -->	20	20	20	20	20
Solution -->	PW	PW	PW	PW/DDI	PW/DDI
Benzene	<0.001	<0.001	<0.001	<0.001	<0.001
Toluene	0.031	0.016	0.012	0.017	0.017
Ethylbenzene	0.019	0.011	0.007	0.008	0.007
Xylenes	0.295	0.172	0.148	0.21	0.207
F1 C6-C10	0.4	0.3	<0.2	0.4	0.3
F1-BTEX	0.8	0.5	0.3	0.6	0.6
C11	0.1	0.1	0.08	0.14	0.14
C12	0.08	0.11	0.09	0.13	0.12
C13	0.09	0.16	0.09	0.12	0.18
C14	0.12	0.23	0.08	0.12	0.24
C15	0.12	0.17	0.06	0.11	0.17
C16	0.11	0.16	0.04	0.1	0.17
C17	0.13	0.13	0.05	0.11	0.14
C18	0.16	0.13	0.08	0.13	0.13
C19	0.15	0.13	0.08	0.13	0.13
C20	0.13	0.11	0.06	0.13	0.12
C21	0.1	0.07	0.04	0.08	0.07
C22	0.08	0.09	0.03	0.09	0.1
C23	0.06	0.06	0.02	0.07	0.08
C24	0.08	0.13	<0.01	0.04	0.06
C25	<0.01	<0.01	<0.01	0.04	0.06
C26	<0.01	<0.01	<0.01	0.03	0.05
C27	<0.01	0.04	<0.01	0.02	0.03
C28	<0.01	0.01	<0.01	0.03	0.03
C29	<0.01	0.02	<0.01	0.01	0.04
C30	<0.01	0.03	<0.01	0.02	0.02
C31	<0.01	0.03	<0.01	0.01	0.02
C32	<0.01	0.01	<0.01	<0.01	0.03
C33	<0.01	0.02	<0.01	<0.01	0.01
C34	<0.01	0.02	<0.01	<0.01	0.02
C35	<0.01	0.01	<0.01	<0.01	0.02
C36	<0.01	0.01	<0.01	<0.01	0.01
C37	<0.01	0.02	<0.01	<0.01	0.02
C38	<0.01	0.01	<0.01	<0.01	0.01
C39	<0.01	0.02	<0.01	<0.01	0.01
C40+	<0.01	0.29	<0.01	<0.01	0.21
F1 C6-C10	0.4	0.3	<0.2	0.4	0.3
F1-BTEX	0.8	0.5	0.3	0.6	0.6
F2 C11-C16	0.62	0.93	0.44	0.72	1.02
F3 C17-C34	0.89	1.03	0.36	0.94	1.14
F4 C35-C40+	0	0.36	0	0	0.28
Total C11-C40+	1.51	2.32	0.8	1.66	2.44

Desorption Results (mg/kg) – Phase 2

	P4 Upper Beach Auger				
Sample -->	**A2-31**	**A2-33**	**A2-34**	**A2-35**	**A2-36**
Sample Day -->	19	6	12	19	19
Soil Mass (g) -->	35	35	35	35	35
Temp. (ºC) -->	20	20	20	20	20
Solution -->	PW/DDI	DDI	DDI	DDI	DDI
Benzene	<0.001	<0.001	<0.001	<0.001	<0.001
Toluene	0.022	0.009	0.004	0.006	0.009
Ethylbenzene	0.009	0.001	0.002	0.003	0.003
Xylenes	0.265	0.123	0.109	0.165	0.177
F1 C6-C10	0.3	<0.2	0.2	<0.2	0.2
F1-BTEX	0.6	0.3	0.3	0.4	0.4
C11	0.11	0.12	0.11	0.06	0.12
C12	0.08	0.08	0.1	0.06	0.08
C13	0.09	0.06	0.15	0.09	0.08
C14	0.11	0.06	0.19	0.11	0.08
C15	0.08	0.05	0.14	0.07	0.08
C16	0.08	0.05	0.14	0.08	0.07
C17	0.11	0.06	0.12	0.1	0.11
C18	0.1	0.07	0.12	0.09	0.11
C19	0.1	0.09	0.15	0.12	0.15
C20	0.1	0.09	0.14	0.09	0.18
C21	0.07	0.08	0.14	0.1	0.12
C22	0.07	0.07	0.1	0.11	0.12
C23	0.06	0.04	0.09	0.08	0.07
C24	0.06	0.03	0.08	0.06	0.08
C25	0.03	0.02	0.1	0.05	0.05
C26	0.04	0.01	<0.01	0.06	0.05
C27	0.02	0.01	0.05	0.05	0.05
C28	0.03	0.01	0.06	0.05	0.04
C29	0.02	<0.01	0.04	0.05	0.04
C30	0.02	<0.01	0.04	0.04	0.03
C31	0.01	<0.01	0.02	0.04	0.03
C32	0.02	<0.01	0.04	0.04	0.02
C33	0.01	<0.01	0.04	0.03	0.04
C34	<0.01	<0.01	0.02	0.03	0.02
C35	<0.01	<0.01	0.03	0.03	0.02
C36	<0.01	<0.01	0.04	0.03	0.03
C37	<0.01	<0.01	0.02	0.03	0.02
C38	<0.01	<0.01	0.06	0.02	0.03
C39	<0.01	<0.01	<0.01	0.02	0.02
C40+	<0.01	<0.01	0.46	0.39	0.11
F1 C6-C10	0.3	<0.2	0.2	<0.2	0.2
F1-BTEX	0.6	0.3	0.3	0.4	0.4
F2 C11-C16	0.55	0.42	0.83	0.47	0.51
F3 C17-C34	0.87	0.58	1.35	1.19	1.31
F4 C35-C40+	0	0	0.61	0.52	0.23
Total C11-C40+	1.42	1.00	2.79	2.18	2.05

Desorption Results (mg/kg) – Phase 2

	P4 Upper Beach Auger				
Sample -->	**A2-37**	**A2-38**	**A2-39**	**A2-40**	**A2-41**
Sample Day -->	6	12	19	19	6
Soil Mass (g) -->	35	35	35	35	35
Temp. (ºC) -->	1	1	1	1	1
Solution -->	PW	PW	PW	PW	PW/DDI
Benzene	<0.001	<0.001	<0.001	<0.001	<0.001
Toluene	0.027	0.036	0.021	0.021	0.03
Ethylbenzene	0.015	0.014	0.004	0.003	0.014
Xylenes	0.22	0.288	0.293	0.31	0.251
F1 C6-C10	0.3	0.4	0.2	0.2	0.4
F1-BTEX	0.6	0.7	0.5	0.6	0.7
C11	0.1	0.11	0.11	0.14	0.13
C12	0.08	0.11	0.09	0.1	0.11
C13	0.11	0.15	0.08	0.09	0.11
C14	0.13	0.24	0.09	0.09	0.13
C15	0.11	0.17	0.07	0.08	0.09
C16	0.1	0.15	0.09	0.08	0.07
C17	0.12	0.13	0.12	0.1	0.07
C18	0.13	0.16	0.15	0.11	0.08
C19	0.15	0.17	0.22	0.17	0.1
C20	0.18	0.18	0.24	0.16	0.1
C21	0.18	0.15	0.16	0.16	0.11
C22	0.11	0.13	0.19	0.12	0.09
C23	0.05	0.11	0.13	0.11	0.07
C24	0.07	0.08	0.07	0.1	0.05
C25	0.03	0.08	0.07	0.06	0.04
C26	0.02	0.06	0.05	0.07	0.01
C27	<0.01	0.04	0.04	0.06	0.02
C28	<0.01	0.05	0.04	0.05	0.02
C29	<0.01	0.04	0.01	0.04	0.01
C30	<0.01	0.03	0.02	0.05	0.01
C31	<0.01	0.02	0.02	0.04	<0.01
C32	<0.01	0.03	0.01	0.03	0.01
C33	<0.01	0.02	0.01	0.04	<0.01
C34	<0.01	0.02	<0.01	0.03	<0.01
C35	<0.01	0.02	0.01	0.02	<0.01
C36	<0.01	0.02	0.01	0.02	<0.01
C37	<0.01	0.02	0.01	0.02	<0.01
C38	<0.01	0.01	0.02	0.02	<0.01
C39	<0.01	0.01	0.01	0.02	<0.01
C40+	<0.01	5.79	0.05	0.3	<0.01
F1 C6-C10	0.3	0.4	0.2	0.2	0.4
F1-BTEX	0.6	0.7	0.5	0.6	0.7
F2 C11-C16	0.63	0.93	0.53	0.58	0.64
F3 C17-C34	1.04	1.5	1.55	1.5	0.79
F4 C35-C40+	0	5.87	0.11	0.4	0
Total C11-C40+	1.67	8.30	2.19	2.48	1.43

Desorption Results (mg/kg) – Phase 2

	P4 Upper Beach Auger					
Sample -->	**A2-42**	**A2-43**	**A2-45**	**A2-46**	**A2-47**	**A2-48**
Sample Day -->	12	19	6	12	19	19
Soil Mass (g) -->	35	35	35	35	35	35
Temp. (ºC) -->	1	1	1	1	1	1
Solution -->	PW/DDI	PW/DDI	DDI	DDI	DDI	DDI
Benzene	<0.001	<0.001	<0.001	<0.001	<0.001	<0.001
Toluene	0.033	0.022	0.018	0.025	0.016	0.022
Ethylbenzene	0.01	0.002	0.008	0.009	0.008	0.009
Xylenes	0.28	0.332	0.196	0.248	0.201	0.311
F1 C6-C10	0.4	0.3	0.3	0.3	<0.2	0.2
F1-BTEX	0.7	0.7	0.5	0.6	0.4	0.6
C11	0.13	0.04	0.11	0.12	0.15	0.15
C12	0.08	0.03	0.07	0.06	0.12	0.13
C13	0.16	0.04	0.08	0.13	0.11	0.11
C14	0.22	0.04	0.09	0.19	0.09	0.11
C15	0.15	0.04	0.07	0.12	0.06	0.07
C16	0.16	0.04	0.07	0.12	0.06	0.05
C17	0.13	0.06	0.07	0.09	0.08	0.09
C18	0.13	0.06	0.08	0.11	0.1	0.08
C19	0.17	0.09	0.1	0.13	0.16	0.13
C20	0.15	0.08	0.12	0.12	0.18	0.12
C21	0.15	0.06	0.11	0.11	0.18	0.12
C22	0.18	0.06	0.07	0.08	0.11	0.1
C23	0.03	0.05	0.06	0.08	0.11	0.08
C24	0.1	0.03	0.04	0.04	0.08	0.05
C25	0.05	0.02	<0.01	0.05	0.07	0.05
C26	0.04	0.02	0.01	0.03	0.05	0.05
C27	0.03	0.01	0.01	0.03	0.06	0.04
C28	0.04	0.01	0.01	0.04	0.03	0.04
C29	0.02	<0.01	0.01	0.01	0.04	0.03
C30	0.03	<0.01	0.01	<0.01	0.04	0.02
C31	0.02	<0.01	<0.01	0.02	0.03	0.02
C32	0.03	<0.01	0.01	<0.01	0.02	0.02
C33	0.02	<0.01	<0.01	0.01	0.01	0.01
C34	0.02	<0.01	<0.01	0.01	<0.01	0.01
C35	0.02	<0.01	<0.01	0.01	<0.01	<0.01
C36	0.01	<0.01	<0.01	<0.01	<0.01	<0.01
C37	0.02	<0.01	<0.01	<0.01	<0.01	<0.01
C38	0.01	<0.01	<0.01	<0.01	<0.01	<0.01
C39	0.01	<0.01	<0.01	<0.01	<0.01	<0.01
C40+	0.2	<0.01	<0.01	0.22	0.01	<0.01
F1 C6-C10	0.4	0.3	0.3	0.3	<0.2	0.2
F1-BTEX	0.7	0.7	0.5	0.6	0.4	0.6
F2 C11-C16	0.9	0.23	0.49	0.74	0.59	0.62
F3 C17-C34	1.34	0.55	0.71	0.96	1.35	1.06
F4 C35-C40+	0.27	0	0	0.23	0.01	0
Total C11-C40+	2.51	0.78	1.20	1.93	1.95	1.68

Desorption Results (mg/kg) – Phase 2 Trial D

	P4 Upper Beach Surface			
Sample -->	**A2 - D1**	**A2 - D2**	**A2 - D3**	**A2 - D4**
Sample Day -->	12	12	12	12
Soil Mass (g) -->	0.5	0.5	3.0	3.0
Temp. (ºC) -->	20	20	20	20
Solution -->	DDI	DDI	DDI	DDI
Benzene	<0.001	<0.001	<0.001	<0.001
Toluene	<0.001	<0.001	<0.001	<0.001
Ethylbenzene	<0.001	<0.001	<0.001	<0.001
Xylenes	<0.001	<0.001	<0.001	<0.001
F1 C6-C10	<0.2	<0.2	<0.2	<0.2
F1-BTEX	<0.2	<0.2	<0.2	<0.2
C11	<0.01	<0.01	<0.01	<0.01
C12	<0.01	<0.01	<0.01	<0.01
C13	<0.01	<0.01	<0.01	<0.01
C14	<0.01	<0.01	<0.01	<0.01
C15	<0.01	<0.01	<0.01	<0.01
C16	<0.01	<0.01	<0.01	<0.01
C17	<0.01	<0.01	<0.01	<0.01
C18	<0.01	<0.01	<0.01	<0.01
C19	<0.01	<0.01	<0.01	0.01
C20	<0.01	<0.01	<0.01	<0.01
C21	<0.01	<0.01	<0.01	0.02
C22	<0.01	<0.01	<0.01	0.02
C23	<0.01	<0.01	<0.01	0.02
C24	<0.01	0.01	<0.01	<0.01
C25	<0.01	<0.01	<0.01	0.01
C26	<0.01	<0.01	<0.01	<0.01
C27	<0.01	<0.01	<0.01	<0.01
C28	<0.01	<0.01	<0.01	<0.01
C29	<0.01	<0.01	<0.01	<0.01
C30	<0.01	<0.01	<0.01	<0.01
C31	<0.01	<0.01	<0.01	<0.01
C32	<0.01	<0.01	<0.01	<0.01
C33	<0.01	<0.01	<0.01	<0.01
C34	<0.01	<0.01	<0.01	<0.01
C35	<0.01	<0.01	<0.01	<0.01
C36	<0.01	<0.01	<0.01	<0.01
C37	<0.01	<0.01	<0.01	<0.01
C38	<0.01	<0.01	<0.01	<0.01
C39	<0.01	<0.01	<0.01	<0.01
C40+	<0.01	<0.01	<0.01	<0.01
F1 C6-C10	<0.2	<0.2	<0.2	<0.2
F1-BTEX	<0.2	<0.2	<0.2	<0.2
F2 C11-C16	0.00	0.00	0.00	0.00
F3 C17-C34	0.00	0.01	0.00	0.08
F4 C35-C40+	0.00	0.00	0.00	0.00
Total C11-C40+	0.00	0.01	0.00	0.08

Desorption Results (mg/kg) – Phase 2 Trial D

	P4 Upper Beach Surface			
Sample -->	**A2 - D5**	**A2 - D6**	**A2 - D13**	**A2 - D14**
Sample Day -->	12	12	12	12
Soil Mass (g) -->	6.0	6.0	9.0	12.0
Temp. (ºC) -->	20	20	20	20
Solution -->	DDI	DDI	DDI	DDI
Benzene	<0.001	<0.001	<0.001	<0.001
Toluene	<0.001	<0.001	<0.001	<0.001
Ethylbenzene	<0.001	<0.001	<0.001	<0.001
Xylenes	<0.001	<0.001	<0.001	<0.001
F1 C6-C10	<0.2	<0.2	<0.2	<0.2
F1-BTEX	<0.2	<0.2	<0.2	<0.2
C11	<0.01	<0.01	<0.01	<0.01
C12	<0.01	<0.01	<0.01	<0.01
C13	<0.01	<0.01	<0.01	0.01
C14	<0.01	<0.01	0.01	0.02
C15	<0.01	<0.01	0.02	0.02
C16	<0.01	<0.01	0.02	0.01
C17	<0.01	<0.01	0.02	0.01
C18	<0.01	<0.01	0.02	0.01
C19	<0.01	<0.01	0.03	0.02
C20	0.02	<0.01	0.03	0.02
C21	0.02	<0.01	0.03	0.02
C22	0.03	<0.01	0.03	0.02
C23	0.02	<0.01	0.02	0.02
C24	0.02	<0.01	0.02	0.01
C25	<0.01	<0.01	0.01	<0.01
C26	<0.01	<0.01	<0.01	<0.01
C27	0.01	<0.01	<0.01	<0.01
C28	0.01	<0.01	<0.01	<0.01
C29	<0.01	<0.01	<0.01	<0.01
C30	0.01	<0.01	<0.01	<0.01
C31	<0.01	<0.01	<0.01	<0.01
C32	<0.01	<0.01	<0.01	<0.01
C33	<0.01	<0.01	<0.01	<0.01
C34	<0.01	<0.01	<0.01	<0.01
C35	<0.01	<0.01	<0.01	<0.01
C36	<0.01	<0.01	<0.01	<0.01
C37	<0.01	<0.01	<0.01	<0.01
C38	<0.01	<0.01	<0.01	<0.01
C39	<0.01	<0.01	<0.01	<0.01
C40+	<0.01	<0.01	<0.01	<0.01
F1 C6-C10	<0.2	<0.2	<0.2	<0.2
F1-BTEX	<0.2	<0.2	<0.2	<0.2
F2 C11-C16	0.00	0.00	0.05	0.06
F3 C17-C34	0.14	0.00	0.21	0.13
F4 C35-C40+	0.00	0.00	0.00	0.00
Total C11-C40+	0.14	0.00	0.26	0.19

Desorption Results (mg/kg) – Phase 2 Trial D

	P4 Upper Beach Auger			
Sample -->	**A2 - D7**	**A2 - D8**	**A2 - D9**	**A2 - D10**
Sample Day -->	12	12	12	12
Soil Mass (g) -->	0.5	0.5	3.0	3.0
Temp. (ºC) -->	20	20	20	20
Solution -->	DDI	DDI	DDI	DDI
Benzene	<0.001	<0.001	<0.001	<0.001
Toluene	<0.001	<0.001	<0.001	<0.001
Ethylbenzene	<0.001	<0.001	<0.001	<0.001
Xylenes	0.006	0.005	0.025	0.029
F1 C6-C10	<0.2	<0.2	<0.2	<0.2
F1-BTEX	<0.2	<0.2	<0.2	<0.2
C11	0.03	<0.01	0.05	0.03
C12	0.03	<0.01	0.02	0.02
C13	0.02	<0.01	0.02	0.02
C14	0.01	<0.01	0.02	0.02
C15	0.02	<0.01	0.01	<0.01
C16	0.01	<0.01	0.01	<0.01
C17	<0.01	<0.01	<0.01	<0.01
C18	0.01	<0.01	0.02	<0.01
C19	0.01	<0.01	0.02	<0.01
C20	<0.01	<0.01	0.03	<0.01
C21	<0.01	<0.01	0.03	0.02
C22	<0.01	<0.01	0.03	0.02
C23	<0.01	<0.01	0.02	0.01
C24	<0.01	<0.01	0.02	0.02
C25	<0.01	<0.01	0.02	0.01
C26	<0.01	<0.01	<0.01	<0.01
C27	<0.01	<0.01	<0.01	0.01
C28	<0.01	<0.01	<0.01	0.01
C29	<0.01	<0.01	<0.01	0.01
C30	<0.01	<0.01	<0.01	<0.01
C31	<0.01	<0.01	<0.01	0.01
C32	<0.01	<0.01	<0.01	0.01
C33	<0.01	<0.01	<0.01	<0.01
C34	<0.01	<0.01	<0.01	<0.01
C35	<0.01	<0.01	<0.01	<0.01
C36	<0.01	<0.01	<0.01	<0.01
C37	<0.01	<0.01	<0.01	<0.01
C38	<0.01	<0.01	<0.01	<0.01
C39	<0.01	<0.01	<0.01	<0.01
C40+	<0.01	<0.01	<0.01	<0.01
F1 C6-C10	<0.2	<0.2	<0.2	<0.2
F1-BTEX	<0.2	<0.2	<0.2	<0.2
F2 C11-C16	0.12	0.00	0.13	0.09
F3 C17-C34	0.02	0.00	0.19	0.13
F4 C35-C40+	0.00	0.00	0.00	0.00
Total C11-C40+	0.14	0.00	0.32	0.22

Desorption Results (mg/kg) – Phase 2 Trial D

	P4 Upper Beach Auger			
Sample -->	**A2 - D11**	**A2 - D12**	**A2 - D15**	**A2 - D16**
Sample Day -->	12	12	12	12
Soil Mass (g) -->	6.0	6.0	9.0	12.0
Temp. (ºC) -->	20	20	20	20
Solution -->	DDI	DDI	DDI	DDI
Benzene	<0.001	<0.001	<0.001	<0.001
Toluene	<0.001	<0.001	<0.001	<0.001
Ethylbenzene	<0.001	<0.001	<0.001	<0.001
Xylenes	0.003	0.012	<0.001	<0.001
F1 C6-C10	<0.2	<0.2	<0.2	<0.2
F1-BTEX	<0.2	<0.2	<0.2	<0.2
C11	0.04	0.04	0.09	0.07
C12	0.03	0.02	0.03	
C13	0.03	0.02	0.04	0.01
C14	0.02	0.02	0.04	0.02
C15	0.01	0.01	0.03	0.02
C16	0.01	0.01	0.03	0.03
C17	<0.01	0.01	0.02	0.02
C18	0.01	0.02	0.03	0.04
C19	0.03	0.03	0.04	0.05
C20	0.03	0.04	0.05	0.06
C21	0.04	0.04	0.06	0.07
C22	0.02	0.04	0.05	0.04
C23	0.02	0.03	0.04	0.04
C24	0.02	0.02	0.03	0.03
C25	<0.01	0.03	0.03	0.02
C26	<0.01	<0.01	0.02	0.01
C27	0.01	<0.01	0.01	<0.01
C28	0.01	<0.01	0.01	<0.01
C29	<0.01	<0.01	0.01	<0.01
C30	0.01	<0.01	0.01	<0.01
C31	<0.01	<0.01	<0.01	<0.01
C32	<0.01	<0.01	<0.01	<0.01
C33	<0.01	<0.01	<0.01	<0.01
C34	<0.01	<0.01	<0.01	<0.01
C35	<0.01	<0.01	<0.01	<0.01
C36	<0.01	<0.01	<0.01	<0.01
C37	<0.01	<0.01	<0.01	<0.01
C38	<0.01	<0.01	<0.01	<0.01
C39	<0.01	<0.01	<0.01	<0.01
C40+	<0.01	<0.01	0.02	0.01
F1 C6-C10	<0.2	<0.2	<0.2	<0.2
F1-BTEX	<0.2	<0.2	<0.2	<0.2
F2 C11-C16	0.14	0.12	0.26	0.15
F3 C17-C34	0.20	0.26	0.41	0.38
F4 C35-C40+	0.00	0.00	0.02	0.01
Total C11-C40+	0.34	0.38	0.69	0.54

Desorption Results (mg/kg) – Phase 3

	MFT			LG MFT	
Sample -->	**3A-1**	**3A-2**	**3B-1**	**3A-4**	**3B-3**
Soil Mass (g) -->	35	35	6	35	6
Sample Day -->	12	12	12	12	12
Temp. (ºC) -->	20	20	20	20	20
Solution -->	DDI	DDI	DDI	DDI	DDI
Benzene	0.033	0.032	0.006	<0.001	n/a
Toluene	0.058	0.059	0.018	<0.001	n/a
Ethylbenzene	0.045	0.049	0.019	0.001	n/a
Xylenes	0.233	0.229	0.184	0.029	n/a
F1 C6-C10	0.9	1	0.9	0.3	n/a
F1-BTEX	1.3	1.4	1.2	0.3	n/a
C11	0.09	0.09	0.91	0.04	0.18
C12	0.05	0.05	1	0.04	0.12
C13	0.05	0.05	1.23	0.05	0.18
C14	0.06	0.05	1.46	0.06	0.23
C15	0.04	0.03	1.48	0.04	0.2
C16	0.06	0.03	1.6	0.06	0.23
C17	0.04	0.04	1.61	0.04	0.19
C18	0.12	0.07	1.83	0.07	0.18
C19	0.1	0.12	1.9	0.06	0.19
C20	0.09	0.04	1.86	0.05	0.16
C21	0.1	0.06	1.68	0.03	0.15
C22	0.09	0.07	1.82	0.03	0.14
C23	0.02	0.02	1.67	0.04	0.13
C24	0.08	0.04	1.49	0.04	0.11
C25	0.04	0.03	1.34	<0.01	0.11
C26	0.05	0.02	1.44	0.02	0.09
C27	0.05	<0.01	1.26	0.03	0.06
C28	0.02	0.02	1.39	<0.01	0.07
C29	0.02	<0.01	1.34	0.01	0.07
C30	0.02	<0.01	1.24	0.02	0.08
C31	0.01	<0.01	1.07	<0.01	0.04
C32	0.02	<0.01	1.03	0.01	0.05
C33	0.02	<0.01	1.16	0.01	0.06
C34	<0.01	<0.01	1.02	<0.01	0.05
C35	0.01	<0.01	0.76	<0.01	0.02
C36	0.01	<0.01	0.88	<0.01	0.05
C37	<0.01	<0.01	0.84	<0.01	0.03
C38	<0.01	<0.01	0.7	0.02	0.04
C39	<0.01	<0.01	0.75	0.01	0.03
C40+	0.4	0.21	16.4	0.69	0.63
F1 C6-C10	0.9	1	0.9	0.3	n/a
F1-BTEX	1.3	1.4	1.2	0.3	n/a
F2 C11-C16	0.35	0.3	7.68	0.29	1.14
F3 C17-C34	0.89	0.53	26.15	0.46	1.93
F4 C35-C40+	0.42	0.21	20.33	0.72	0.8
Total C11-C40+	1.66	1.04	54.16	1.47	3.87

Desorption Results (mg/kg) – Phase 3

	PT MFT			P4 Lower Beach	
Sample -->	**3A-5**	**3A-6**	**3B-2**	**3A-11**	**3A-12**
Soil Mass (g) -->	35	35	6	35	35
Sample Day -->	12	12	12	12	12
Temp. (ºC) -->	20	20	20	20	20
Solution -->	DDI	DDI	DDI	DDI	DDI
Benzene	<0.001	0.001	n/a	0.042	0.042
Toluene	0.004	0.01	n/a	0.507	0.517
Ethylbenzene	0.007	0.013	n/a	0.038	0.037
Xylenes	0.037	0.061	n/a	0.723	0.719
F1 C6-C10	0.4	0.5	n/a	2.1	2.1
F1-BTEX	0.4	0.6	n/a	3.4	3.4
C11	0.06	0.1	0.06	0.19	0.2
C12	0.06	0.07	0.05	0.07	0.07
C13	0.07	0.09	0.08	0.07	0.07
C14	0.12	0.14	0.1	0.08	0.06
C15	0.09	0.12	0.09	0.06	0.04
C16	0.12	0.16	0.12	0.07	0.05
C17	0.14	0.15	0.09	0.05	0.04
C18	0.16	0.38	0.06	0.1	0.05
C19	0.23	0.26	0.17	0.11	0.1
C20	0.14	0.16	0.13	0.11	0.1
C21	0.07	0.19	0.08	0.11	0.05
C22	0.19	0.22	0.07	0.07	0.08
C23	0.11	0.11	0.11	0.06	0.03
C24	0.06	0.15	0.03	0.09	0.06
C25	0.07	0.09	0.05	0.04	0.04
C26	0.05	0.1	0.06	0.05	0.03
C27	0.08	0.09	0.03	0.08	0.03
C28	0.05	0.11	0.06	0.03	0.03
C29	0.04	0.06	0.04	0.06	0.03
C30	0.04	0.06	0.05	0.03	0.02
C31	0.03	0.05	0.03	0.04	0.02
C32	0.02	0.08	0.05	0.03	0.01
C33	0.03	<0.01	0.03	0.03	0.02
C34	0.02	0.07	0.04	0.02	0.02
C35	0.02	0.03	0.01	0.02	0.01
C36	0.03	0.03	0.03	0.02	0.01
C37	<0.01	0.05	0.02	0.03	0.02
C38	0.02	0.04	0.02	0.02	0.02
C39	<0.01	0.03	0.03	0.02	<0.01
C40+	0.46	1.42	0.43	0.8	0.4
F1 C6-C10	0.4	0.5	n/a	2.1	2.1
F1-BTEX	0.4	0.6	n/a	3.4	3.4
F2 C11-C16	0.52	0.68	0.5	0.54	0.49
F3 C17-C34	1.53	2.33	1.18	1.11	0.76
F4 C35-C40+	0.53	1.6	0.54	0.91	0.46
Total C11-C40+	2.58	4.61	2.22	2.56	1.71

Desorption Results (mg/kg) – Phase 3

	P4 Upper Beach Surface				P4 Upper Beach Auger			
Sample -->	**3A-7**	**3A-8**	**3D-01**	**3D-02**	**3A-9**	**3A-10**	**3D-03**	**3D-04**
Soil Mass (g) -->	35	35	0.0125	0.0125	35	35	0.0125	0.0125
Sample Day -->	12	12	12	12	12	12	12	12
Temp. (ºC) -->	20	20	20	20	20	20	20	20
Solution -->	DDI	DDI	DDI	DDI	DDI	DDI	DDI	DDI
Benzene	<0.001	<0.001	n/a	n/a	<0.001	<0.001	n/a	n/a
Toluene	<0.001	<0.001	n/a	n/a	0.005	0.005	n/a	n/a
Ethylbenzene	<0.001	<0.001	n/a	n/a	0.002	0.003	n/a	n/a
Xylenes	<0.001	<0.001	n/a	n/a	0.161	0.163	n/a	n/a
F1 C6-C10	<0.2	<0.2	n/a	n/a	0.4	0.4	n/a	n/a
F1-BTEX	<0.2	<0.2	n/a	n/a	0.5	0.6	n/a	n/a
C11	0.05	0.04	n/a	n/a	0.17	0.15	n/a	n/a
C12	0.05	0.04	n/a	n/a	0.09	0.08	n/a	n/a
C13	0.07	0.06	n/a	n/a	0.09	0.08	n/a	n/a
C14	0.08	0.06	n/a	n/a	0.1	0.09	n/a	n/a
C15	0.05	0.04	n/a	n/a	0.08	0.07	n/a	n/a
C16	0.06	0.05	n/a	n/a	0.08	0.08	n/a	n/a
C17	0.06	0.05	n/a	n/a	0.06	0.08	n/a	n/a
C18	0.1	0.08	n/a	n/a	0.18	0.13	n/a	n/a
C19	0.11	0.09	n/a	n/a	0.18	0.16	n/a	n/a
C20	0.12	0.13	n/a	n/a	0.18	0.13	n/a	n/a
C21	0.08	0.07	n/a	n/a	0.15	0.13	n/a	n/a
C22	0.09	0.04	n/a	n/a	0.17	0.17	n/a	n/a
C23	0.03	0.06	n/a	n/a	0.05	<0.01	n/a	n/a
C24	0.06	0.04	n/a	n/a	0.11	0.08	n/a	n/a
C25	0.03	0.03	n/a	n/a	0.01	0.05	n/a	n/a
C26	0.02	0.03	n/a	n/a	0.07	0.07	n/a	n/a
C27	0.05	0.01	n/a	n/a	0.08	0.08	n/a	n/a
C28	<0.01	0.02	n/a	n/a	0.04	0.02	n/a	n/a
C29	0.02	0.01	n/a	n/a	0.07	0.05	n/a	n/a
C30	0.01	0.01	n/a	n/a	0.05	0.03	n/a	n/a
C31	0.01	0.02	n/a	n/a	0.06	0.05	n/a	n/a
C32	<0.01	0.01	n/a	n/a	0.04	0.05	n/a	n/a
C33	0.01	<0.01	n/a	n/a	0.05	0.02	n/a	n/a
C34	0.01	0.02	n/a	n/a	0.04	0.05	n/a	n/a
C35	<0.01	<0.01	n/a	n/a	0.02	<0.01	n/a	n/a
C36	0.01	0.01	n/a	n/a	0.03	0.03	n/a	n/a
C37	<0.01	<0.01	n/a	n/a	0.02	0.02	n/a	n/a
C38	0.02	0.02	n/a	n/a	0.03	0.04	n/a	n/a
C39	0.01	0.01	n/a	n/a	0.04	0.02	n/a	n/a
C40+	0.06	1.03	n/a	n/a	1.11	0.69	n/a	n/a
F1 C6-C10	<0.2	<0.2	n/a	n/a	0.4	0.4	n/a	n/a
F1-BTEX	<0.2	<0.2	n/a	n/a	0.5	0.6	n/a	n/a
F2 C11-C16	0.36	0.29	0	0	0.61	0.55	0	0
F3 C17-C34	0.81	0.72	0	0	1.59	1.35	0	0
F4 C35-C40+	0.1	1.07	0	0	1.25	0.8	0	0
Total C11-C40+	1.27	2.08	0	0	3.45	2.70	0	0

C.3 Desorption Results

Material	Sample Time (days)	F2 Conc. (mg/L)	F3 Conc. (mg/L)	Total PHC Conc. (mg/L)
2:1 SFR CT	3.0	0.35	2.36	2.71
	7.0	0.55	3.83	4.38
	9.9	0.65	3.76	4.41
4:1 SFR CT	2.9	0.27	2.00	2.27
	6.9	0.56	2.49	3.05
	9.9	0.43	2.45	2.89
6:1 SFR CT	2.8	0.28	2.48	2.76
	7.0	0.32	1.94	2.26
	10.1	0.26	0.72	0.98
MFT	2.9	0.81	5.43	6.24
	6.8	1.37	6.23	7.60
	10.0	5.21	16.68	21.89
Lime-Gypsum MFT	2.8	1.06	2.99	4.05
	7.1	1.94	2.95	4.89
	10.3	1.64	2.88	4.52
Polymer-treated MFT	2.8	0.18	2.84	3.02
	7.0	0.97	2.93	3.89
	10.1	0.87	1.25	2.12
Tailings Sand	2.7	0.07	0.64	0.72
	7.1	0.07	0.92	1.00
	10.0	0.07	0.51	0.59

APPENDIX D

Desorption Isotherms

D.1) Composite Tailings F2 and F3 fraction PHC Isotherms

D.2) Mature Fine Tailings F2 and F3 fraction PHC Isotherms

D.3) Plant 4 Upper Beach Tailings F2 and F3 fraction PHC Isotherms

D.4) Tailings Sand F2 and F3 fraction PHC Isotherms

D.1 Composite Tailings F2 and F3 fraction PHC Isotherms

(a)

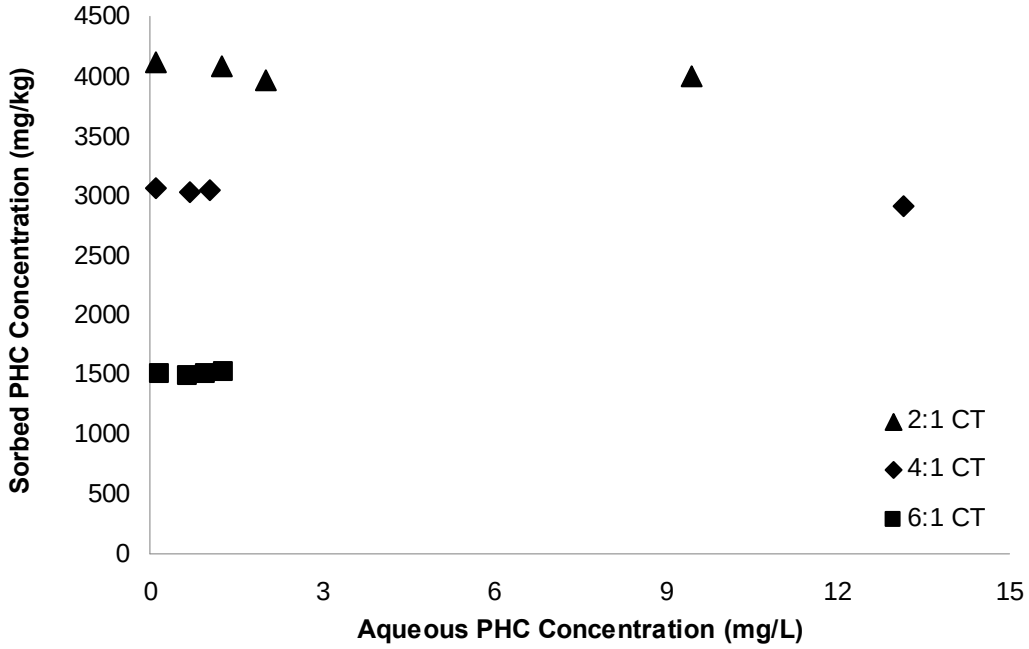

(b)

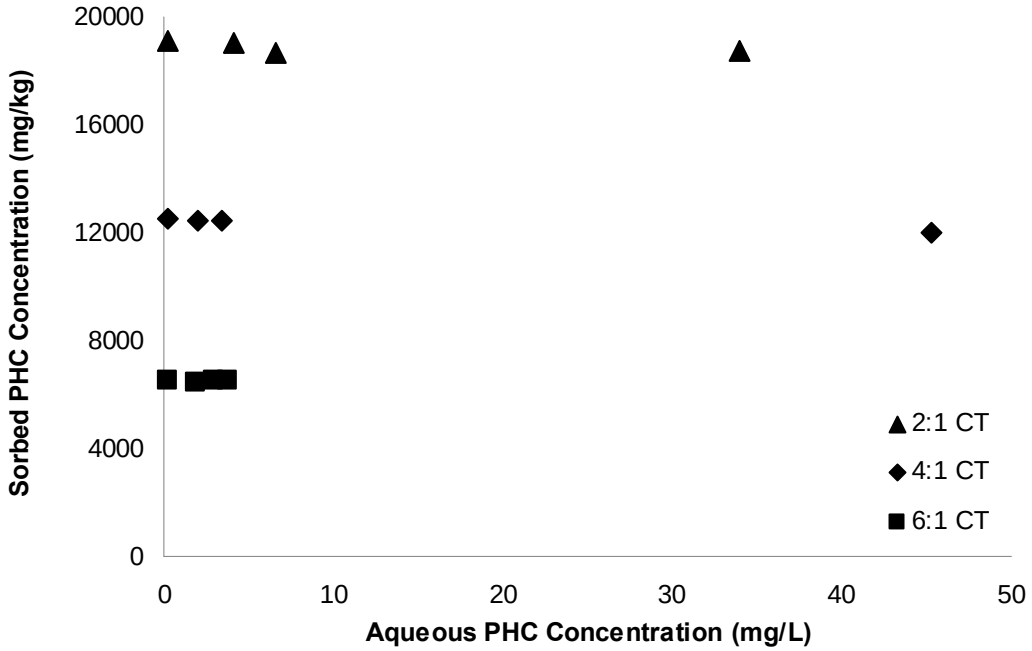

Figure D.1: Desorption experiment results for 2:1 SFR, 4:1 SFR and 6:1 SFR Composite Tailings in de-ionized water

a) F2 PHC Fraction
b) F3 PHC Fraction

(a)

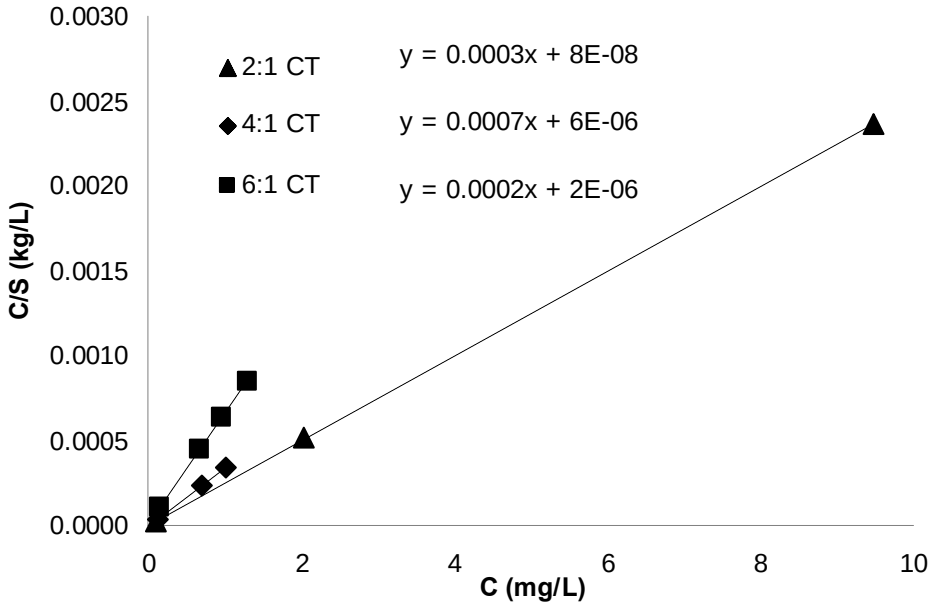

(b)

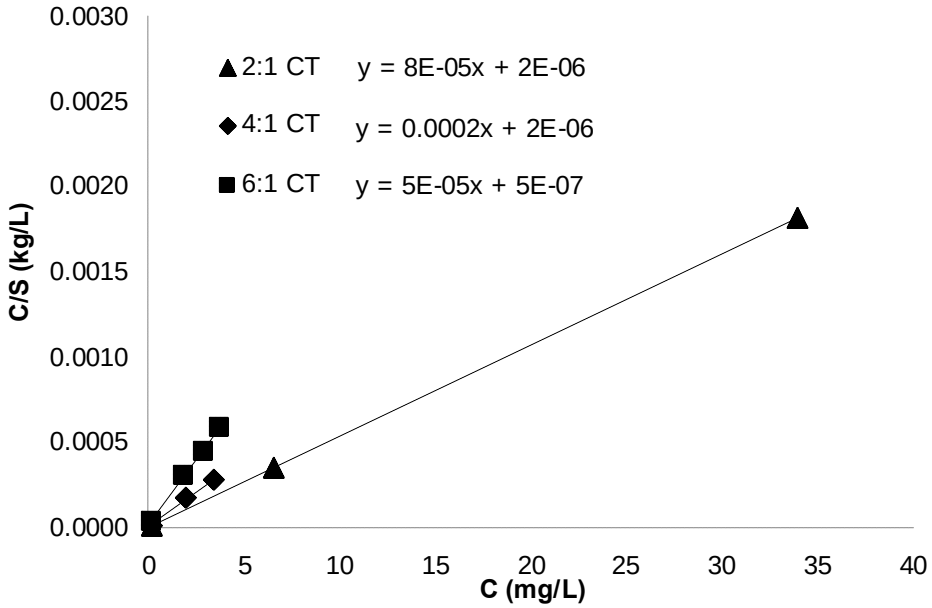

Figure D.2: Desorption Langmuir model for 2:1 SFR, 4:1 SFR and 6:1 SFR Composite Tailings in de-ionized water

a) F2 PHC Fraction
b) F3 PHC Fraction

(a)

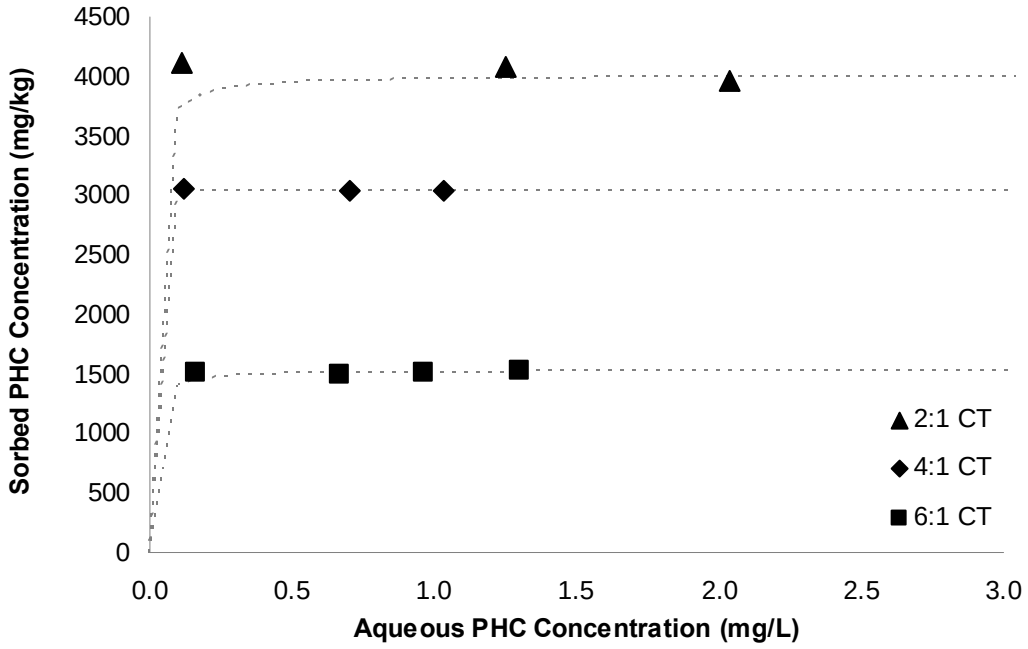

(b)

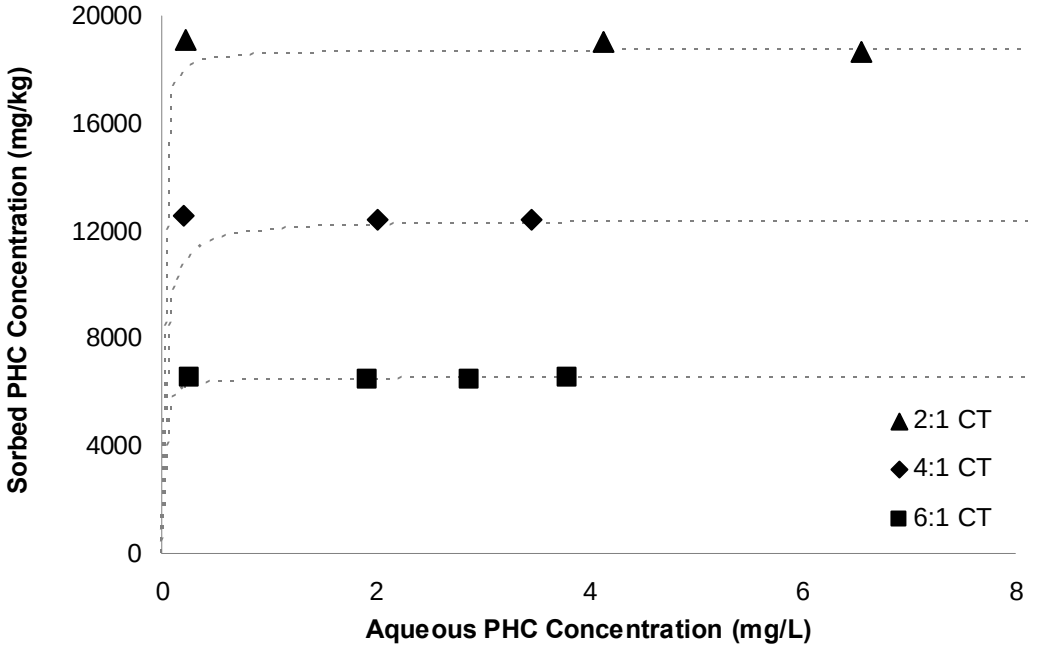

Figure D.3: Desorption Isotherm for 2:1 SFR, 4:1 SFR and 6:1 SFR Composite Tailings in de-ionized water

a) F2 PHC Fraction
b) F3 PHC Fraction

D.2 Mature Fine Tailings F2 and F3 fraction PHC Isotherms

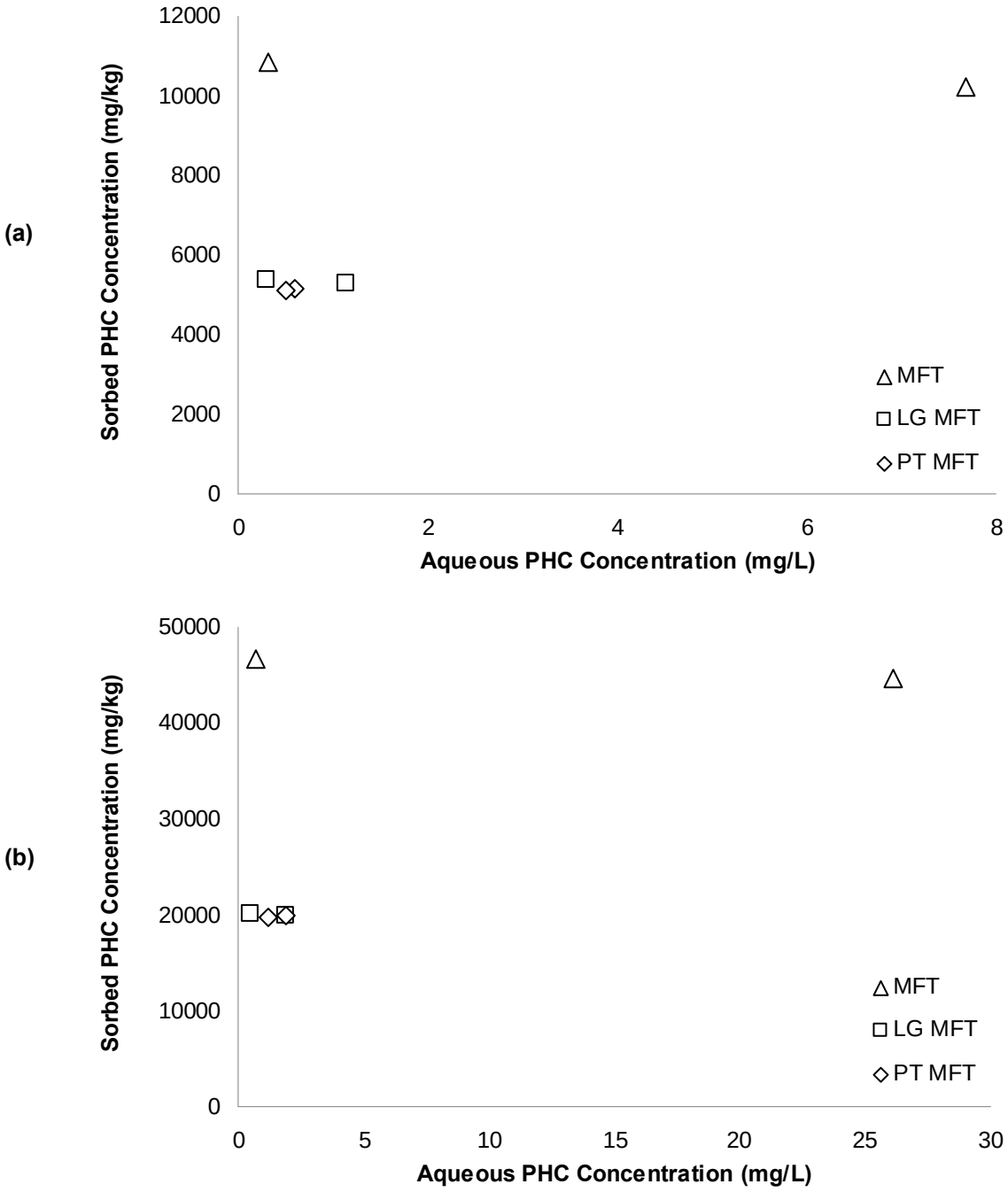

Figure D.4: Desorption experiment results for 2:1 SFR, 4:1 SFR and 6:1 SFR Composite Tailings in de-ionized water

a) F2 PHC Fraction
b) F3 PHC Fraction

(a)

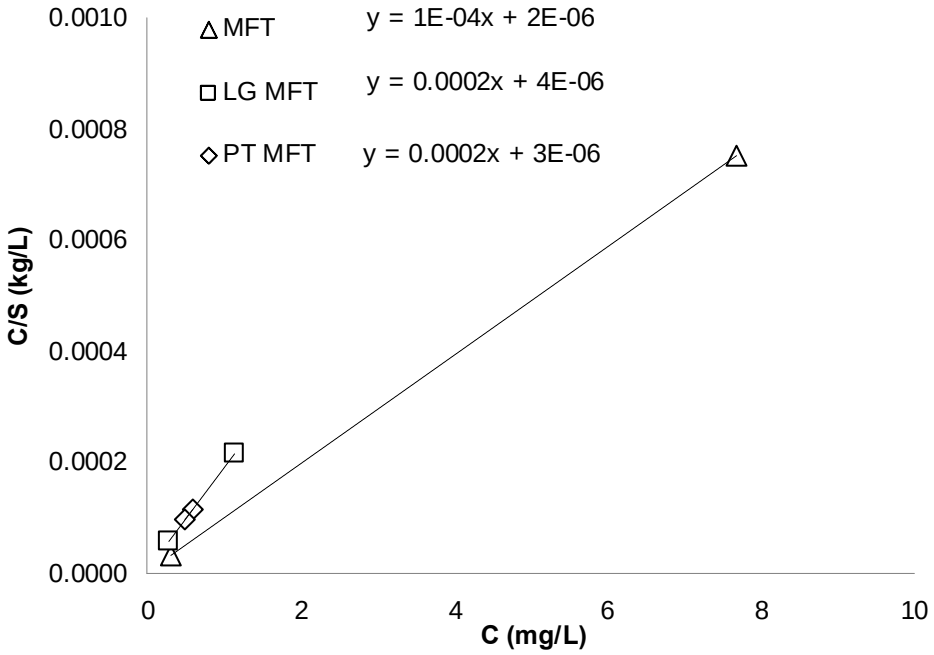

(b)

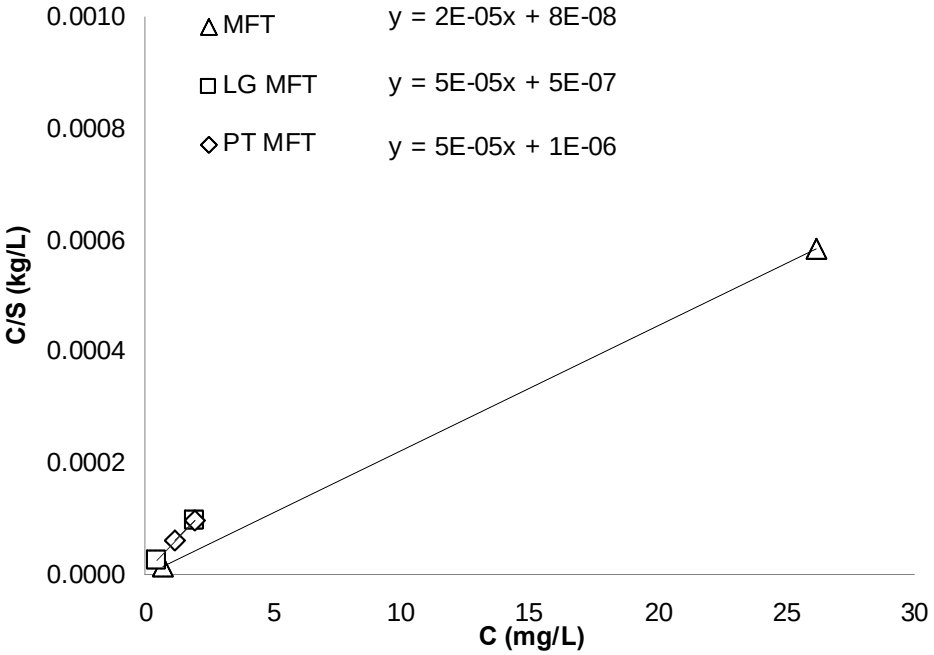

Figure D.5: Desorption Langmuir model for 2:1 SFR, 4:1 SFR and 6:1 SFR Composite Tailings in de-ionized water

a) F2 PHC Fraction
b) F3 PHC Fraction

(a)

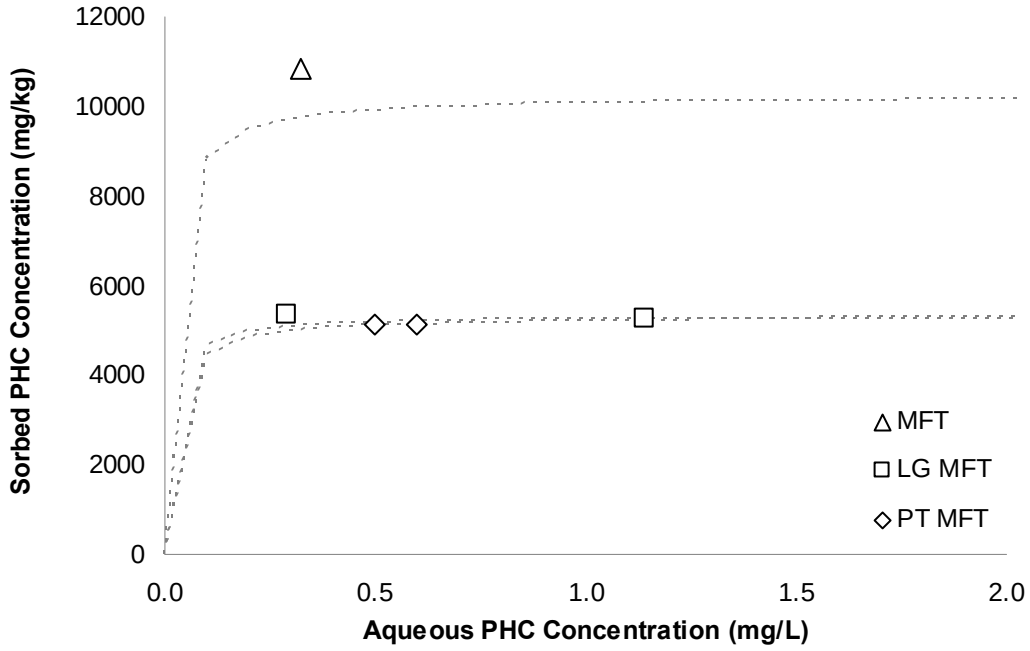

(b)

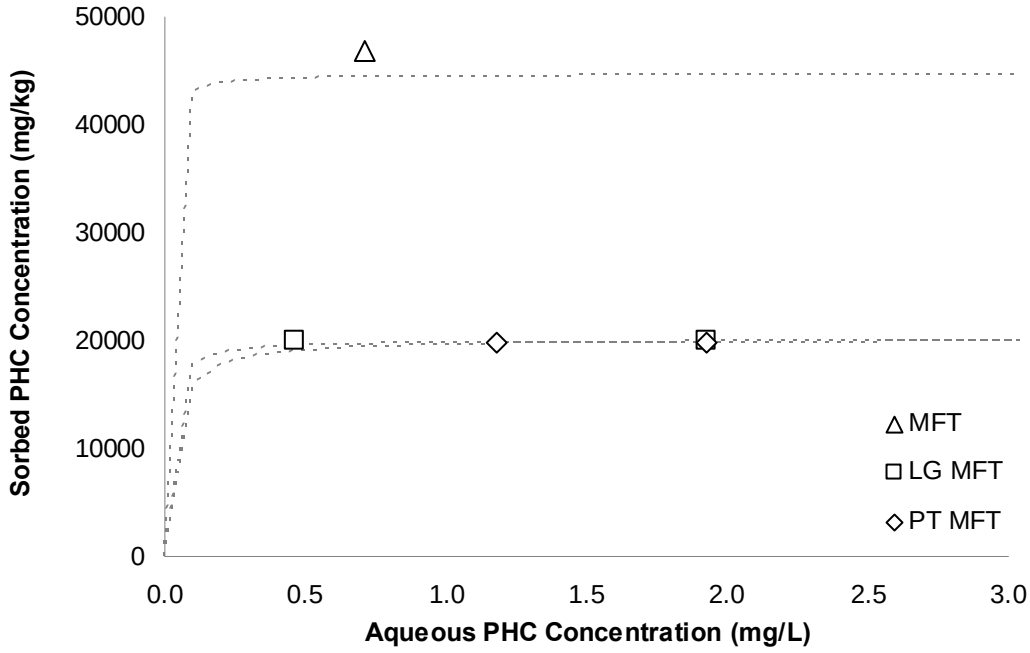

Figure D.6: Desorption Isotherm for Mature Fine Tailings in de-ionized water

a) F2 PHC Fraction
b) F3 PHC Fraction

D.3 Plant 4 Upper Beach Tailings F2 and F3 fraction PHC Isotherms

(a)

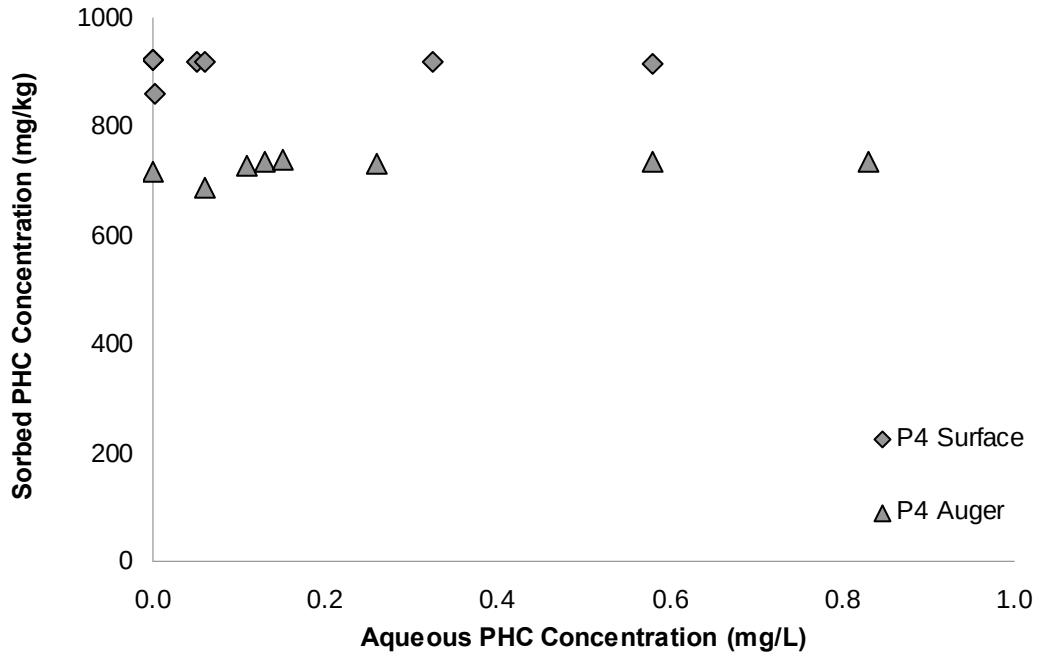

(b)

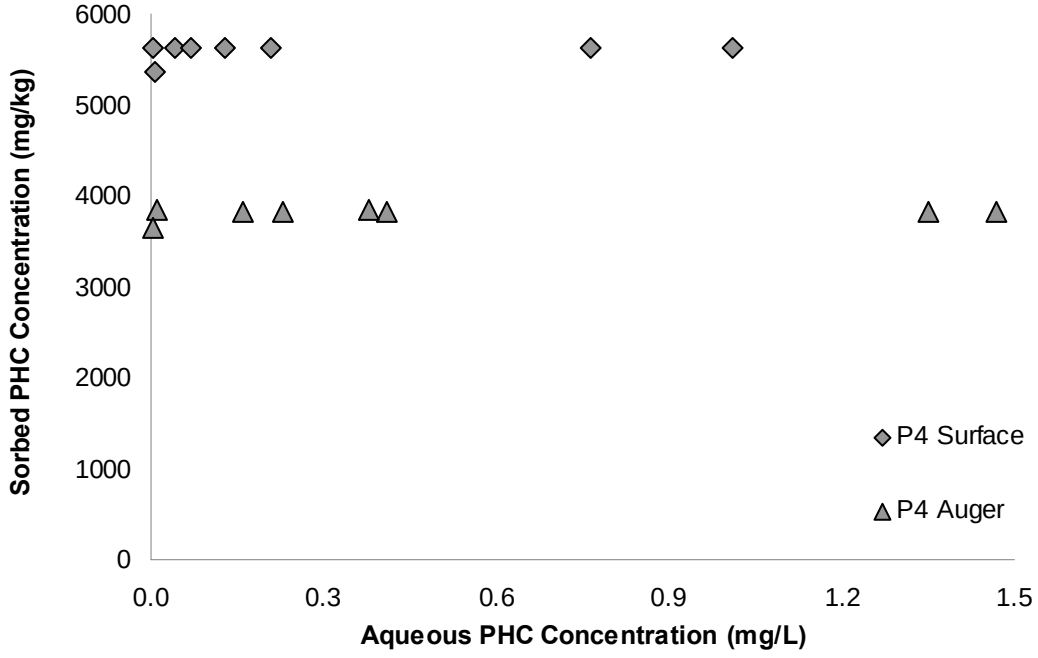

Figure D.7: Desorption experiment results for Plant 4 Upper Beach Tailings in de-ionized water. Samples of the tailings were collected at the surface and from a depth of 1.5m (auger samples).

a) F2 PHC Fraction
b) F3 PHC Fraction

(a)

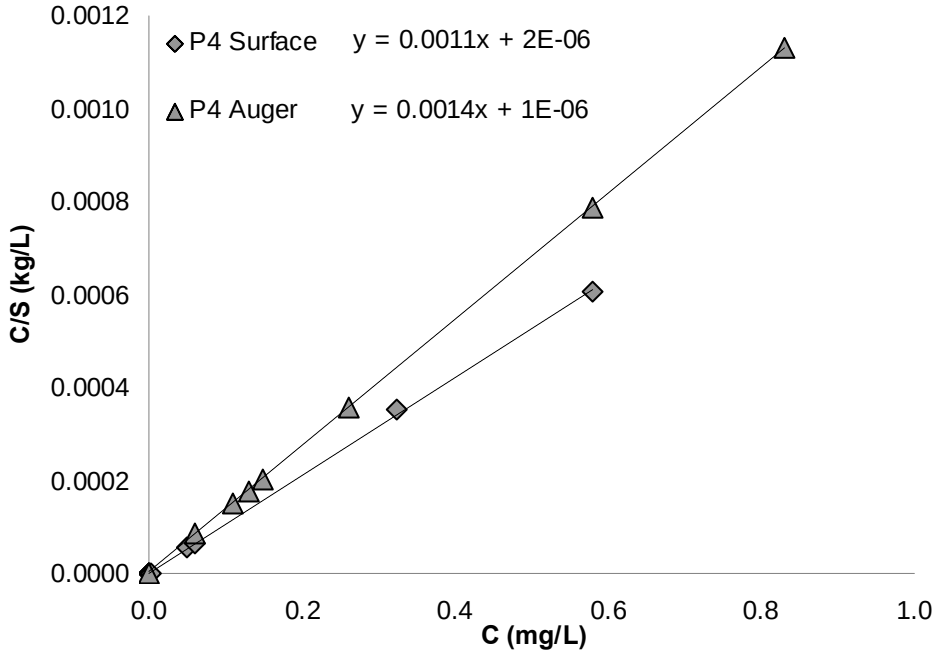

(b)

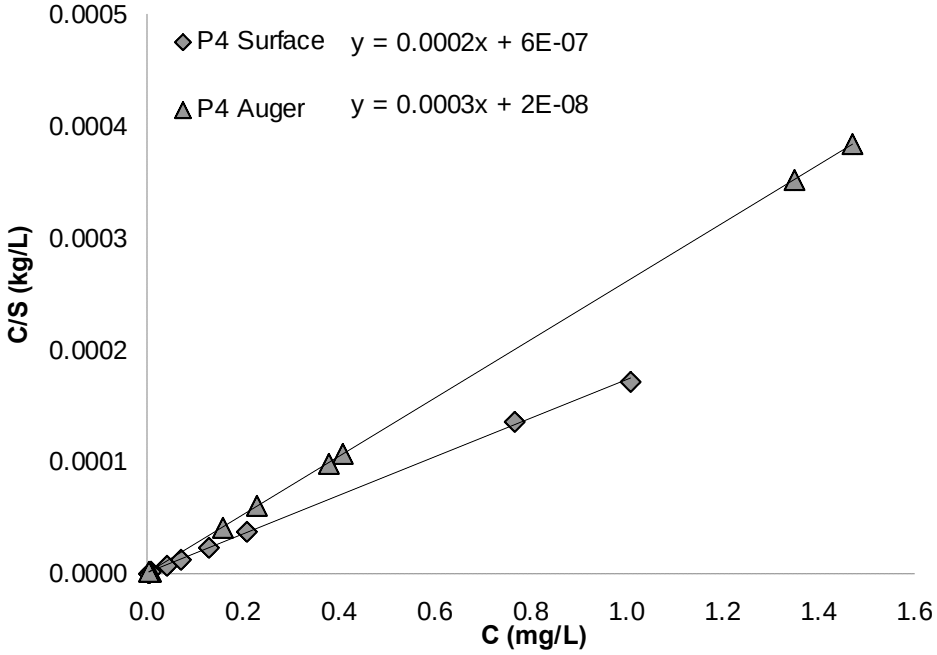

Figure D.8: Desorption Langmuir model for Plant 4 Upper Beach Tailings in de-ionized water. Samples of the tailings were collected at the surface and from a depth of 1.5m (auger samples).

a) F2 PHC Fraction
b) F3 PHC Fraction

(a)

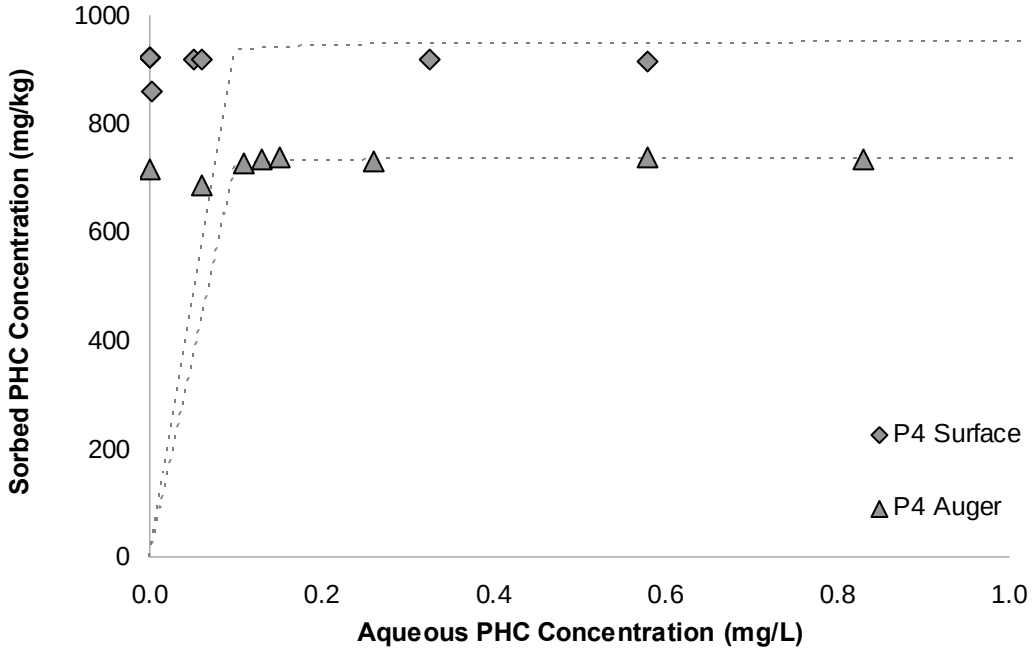

(b)

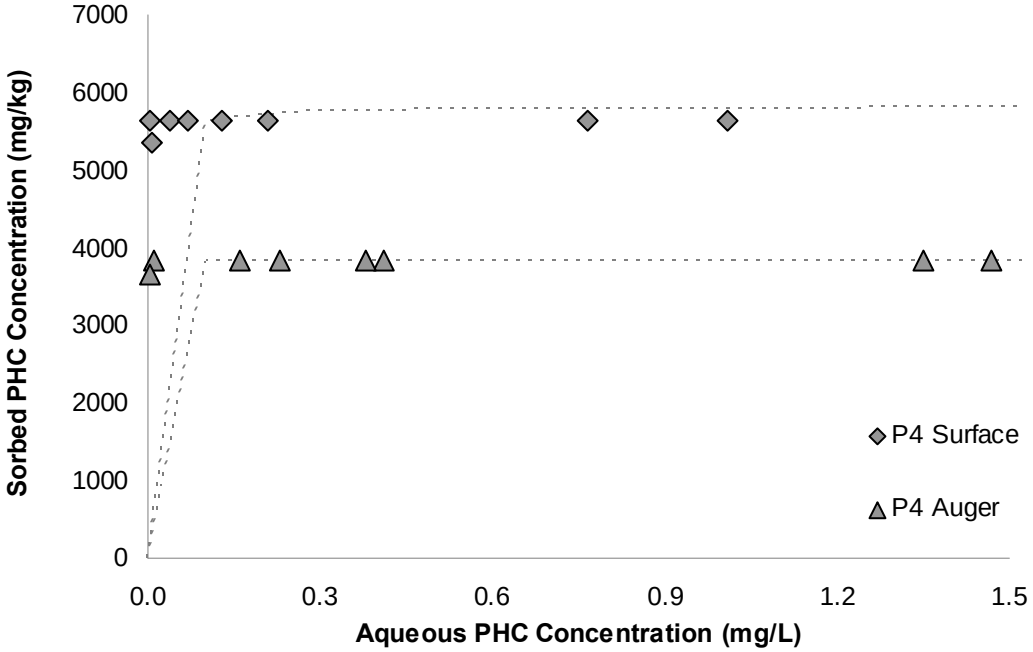

Figure D.9: Desorption Isotherm for Plant 4 Upper Beach Tailings in de-ionized water. Samples of the tailings were collected at the surface and from a depth of 1.5m (auger samples).

a) F2 PHC Fraction
b) F3 PHC Fraction

D.4 Tailings Sand F2 and F3 fraction PHC Isotherm

(a)

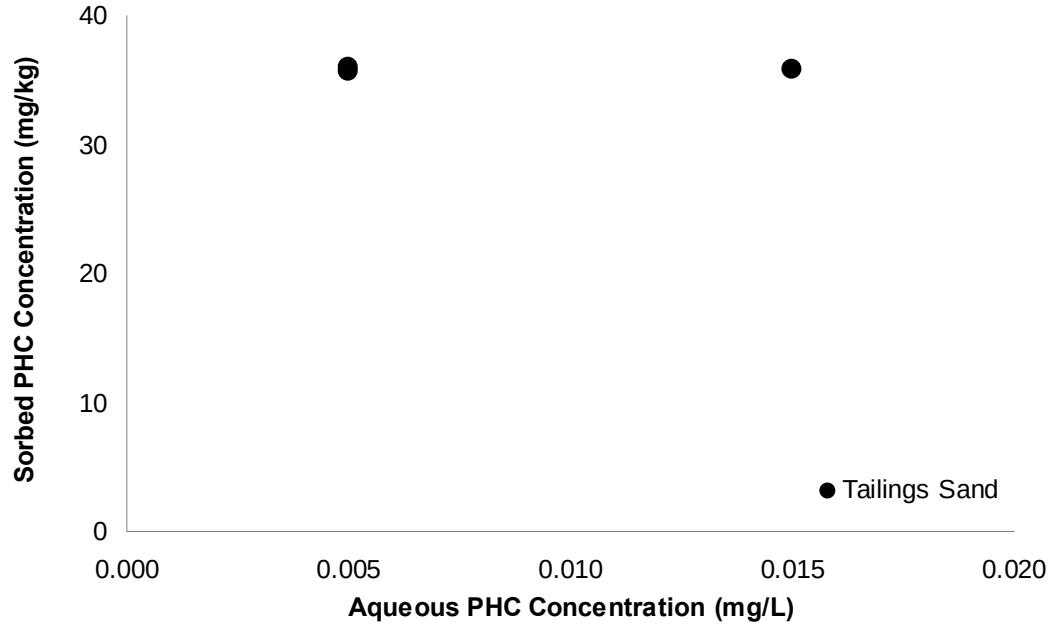

(b)

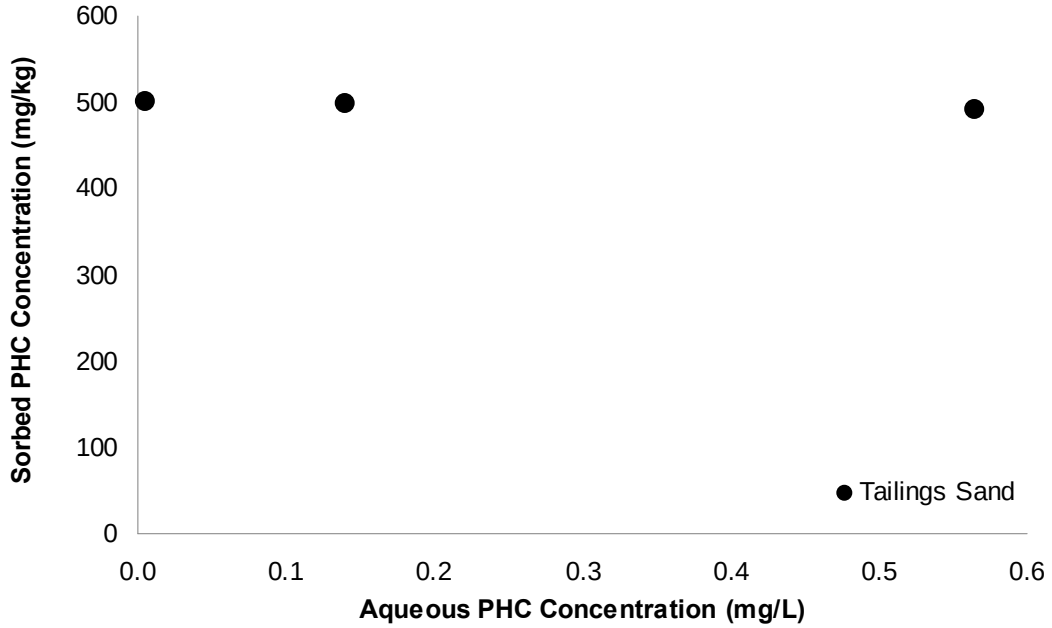

Figure D.10: Desorption experiment results for Tailings Sand in de-ionized water.

a) F2 PHC Fraction
b) F3 PHC Fraction

(a)

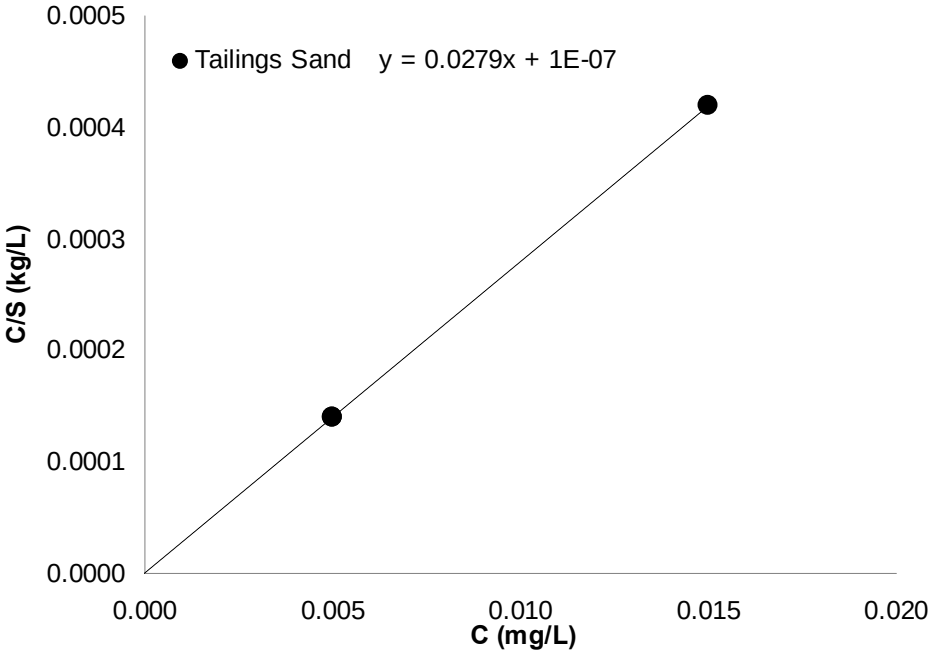

(b)

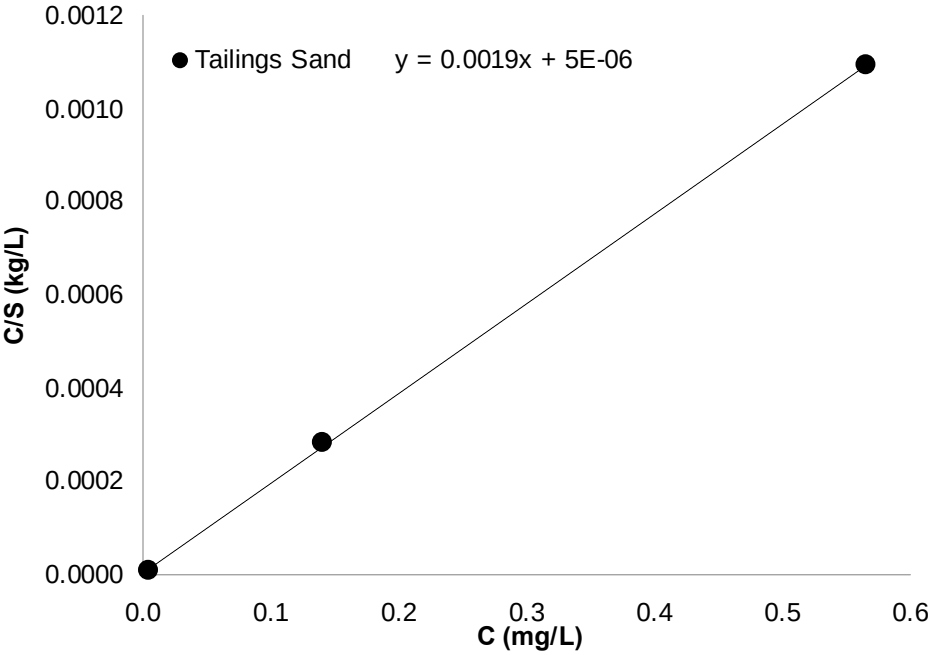

Figure D.11: Desorption Langmuir model for Tailings Sand in de-ionized water.

a) F2 PHC Fraction
b) F3 PHC Fraction

(a)

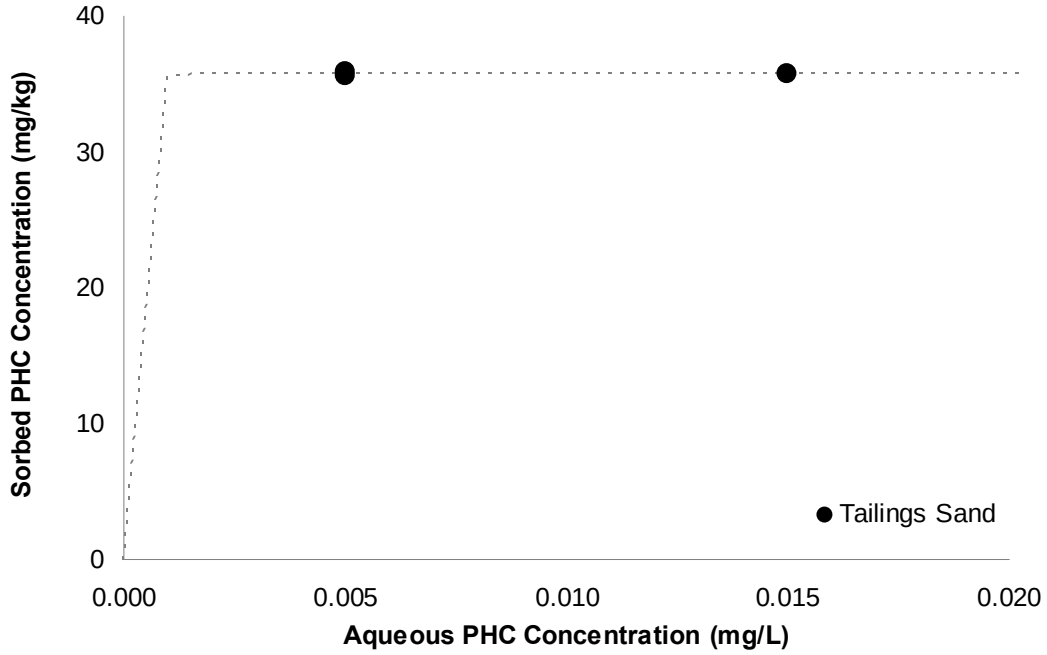

(b)

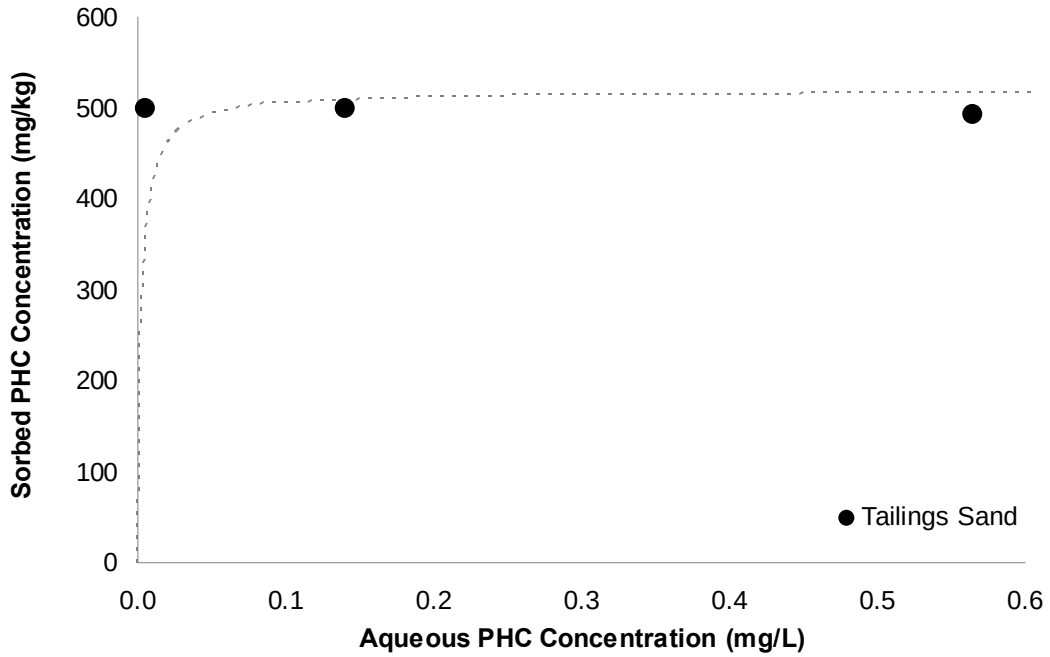

Figure D.12: Desorption Isotherm for Tailings Sand in de-ionized water.

a) F2 PHC Fraction
b) F3 PHC Fraction

APPENDIX E

Aqueous Concentrations

E.1) Composite Tailings F2 and F3 Aqueous Concentration

E.2) Mature Fine Tailings F2 and F3 Aqueous Concentration

E.3) Plant 4 Upper Beach Tailings F2 and F3 Aqueous Concentration

E.4) Tailings Sand F2 and F3 Aqueous Concentration

E.1 Composite Tailings F2 and F3 fraction PHC Aqueous Concentration

(a)

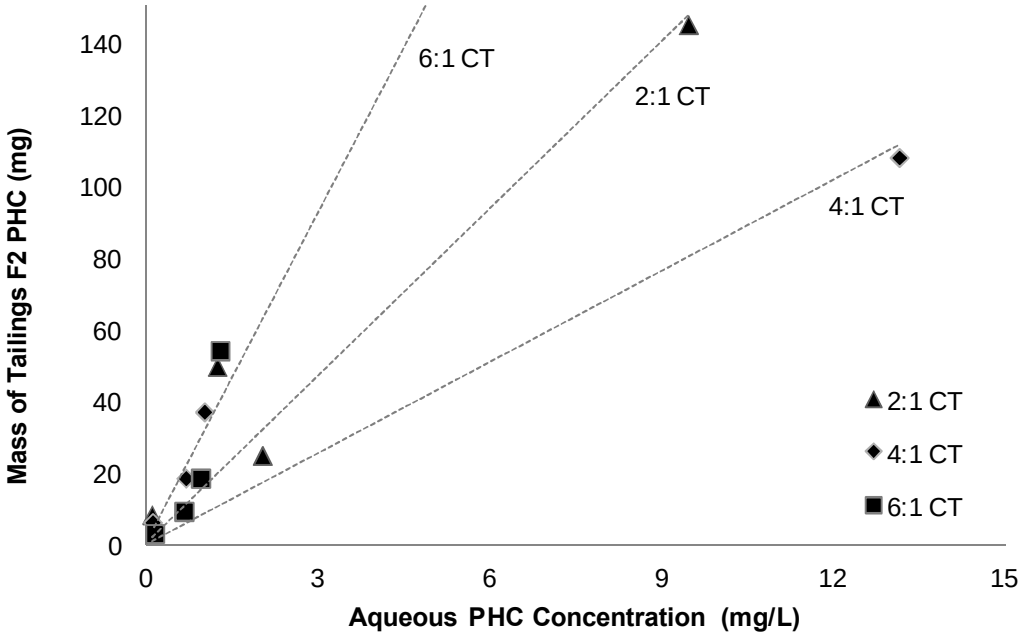

(b)

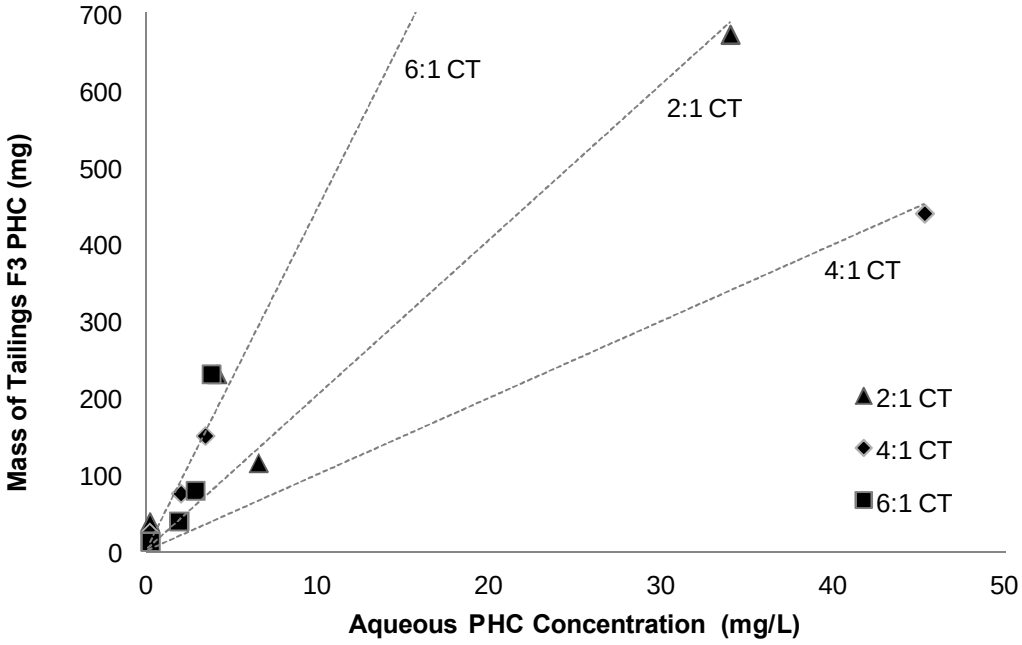

Figure E.1: Aqueous concentration of PHCs in de-ionized water for Composite Tailings samples after 12 days. The aqueous concentration is plotted against the total mass of PHCs present in the solid tailings sample.

a) F2 PHC Fraction
b) F3 PHC Fraction

E.2 Mature Fine Tailings F2 and F3 fraction PHC Aqueous Concentration

(a)

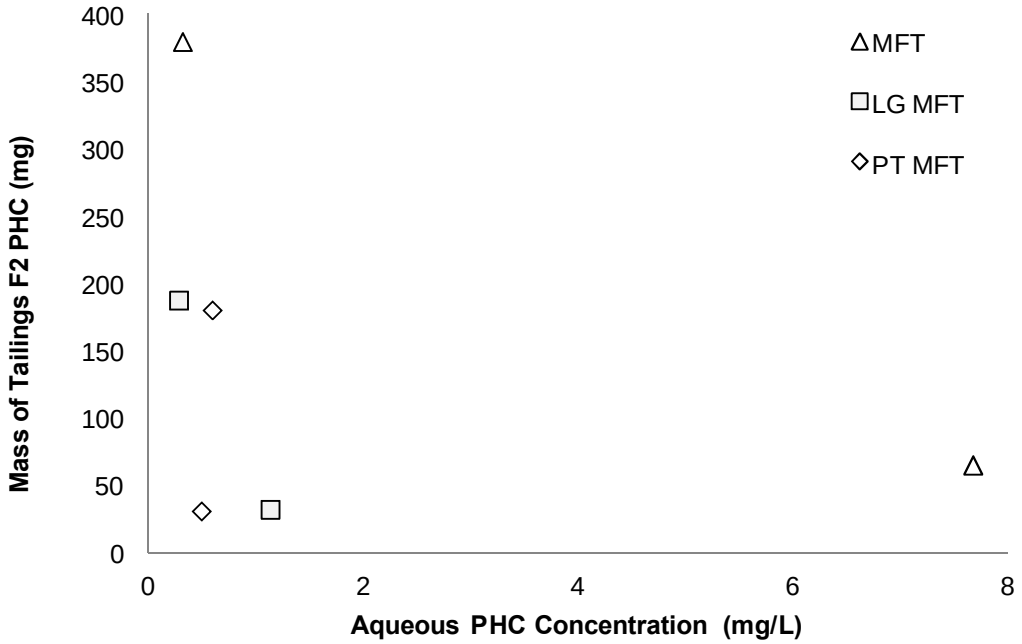

(b)

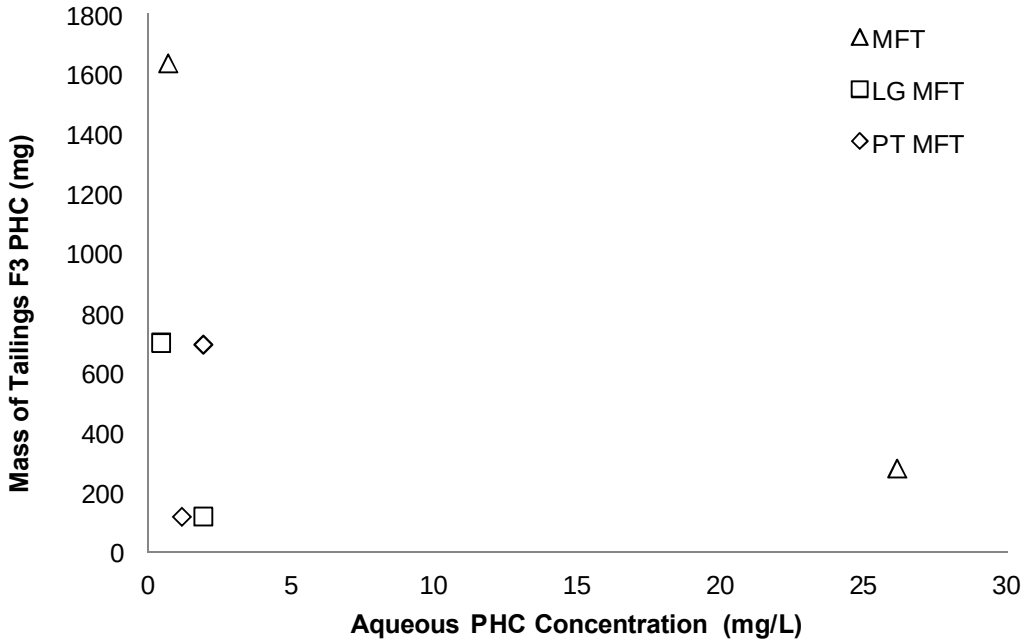

Figure E.2: Aqueous concentration of PHCs in de-ionized water for Mature Fine Tailings samples after 12 days. The aqueous concentration is plotted against the total mass of PHCs present in the solid tailings sample.

a) F2 PHC Fraction
b) F3 PHC Fraction

E.3 Plant 4 Upper Beach Tailings F2 and F3 fraction PHC Aqueous Concentration

(a)

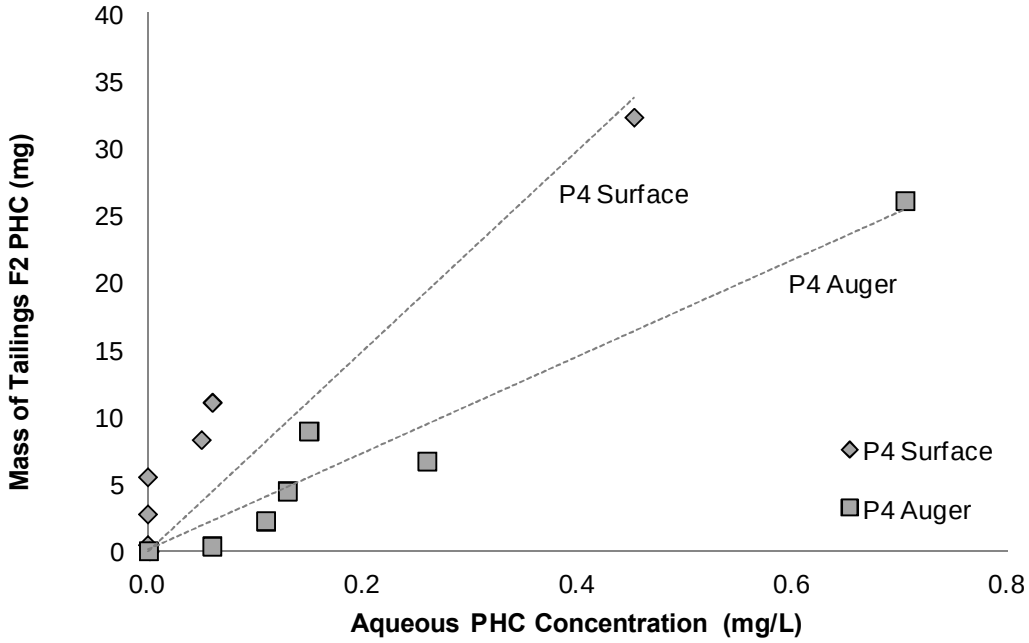

(b)

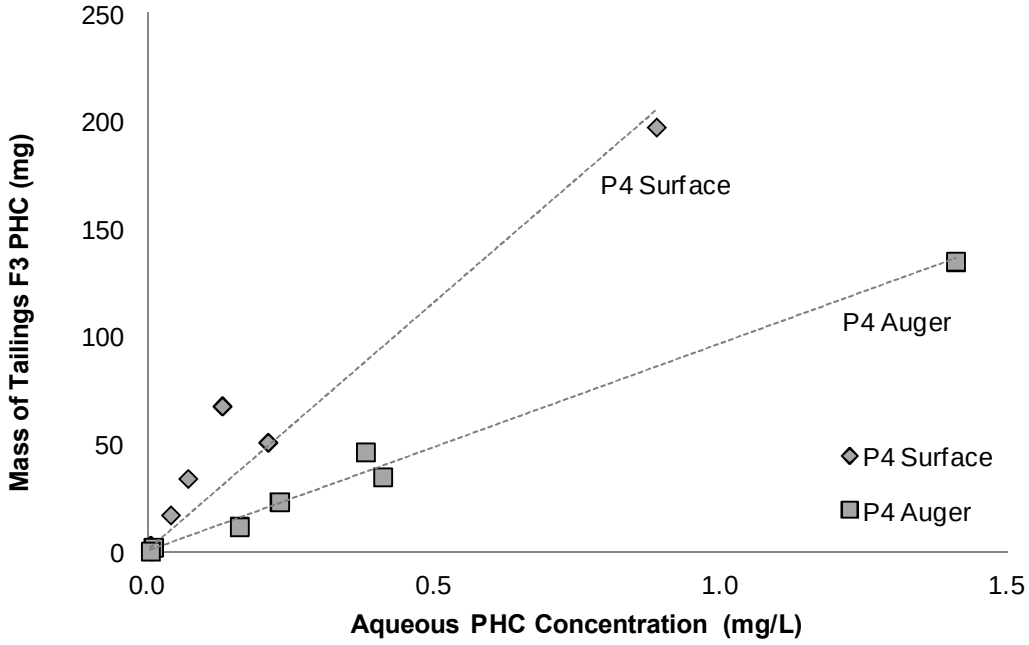

Figure E.3: Aqueous concentration of PHCs in de-ionized water for Plant 4 Upper Beach surface and auger samples after 12 days. The aqueous concentration is plotted against the total mass of PHCs present in the solid tailings sample.

a) F2 PHC Fraction
b) F3 PHC Fraction

E.4 Tailings Sand F2 and F3 fraction PHC Aqueous Concentration

(a)

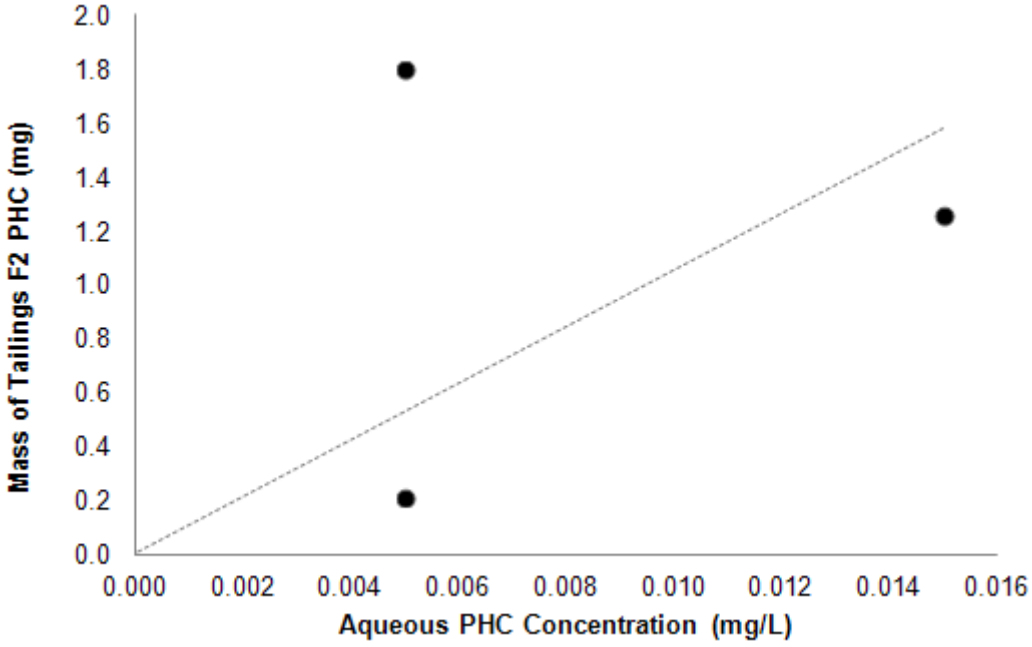

(b)

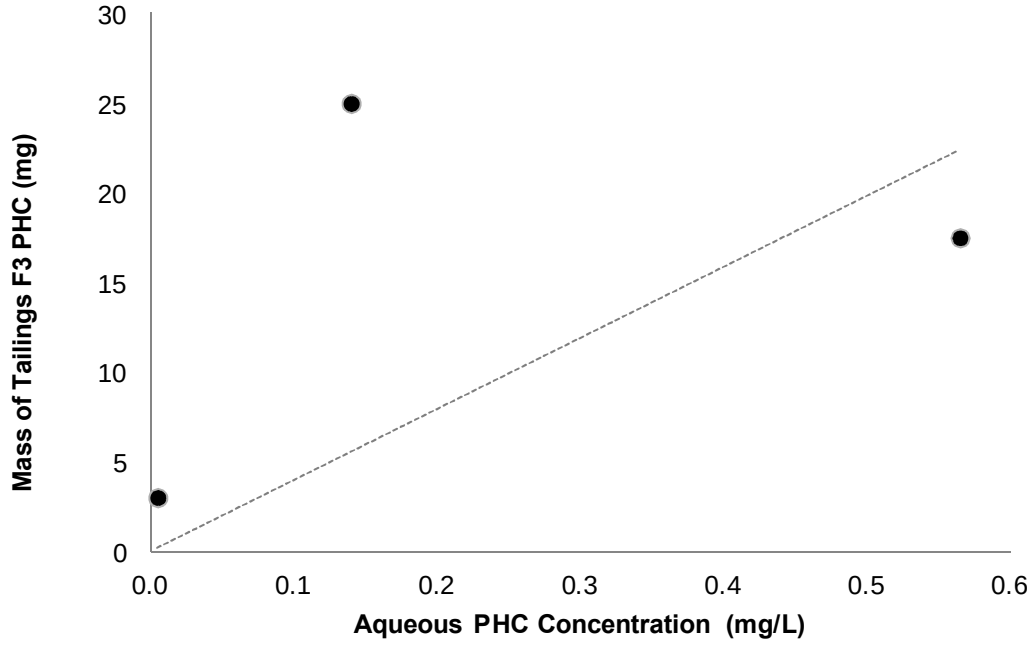

Figure E.4: Aqueous concentration of PHCs in de-ionized water for Tailings Sand samples after 12 days. The aqueous concentration is plotted against the total mass of PHCs present in the solid tailings sample.

a) F2 PHC Fraction
b) F3 PHC Fraction